UNIVERSITY
OF FLORIDA
LIBRARIES

ENGINEERING
& PHYSICS
LIBRARY

Gainesville GENESYS

Digitized by the Internet Archive
in 2013

http://archive.org/details/unitoperationsof00rich

Unit Operations of Sanitary Engineering

Unit Operations of Sanitary Engineering

LINVIL G. RICH
Professor and Head,
Department of Civil Engineering,
Clemson College

formerly

Professor of Sanitary Engineering
Illinois Institute of Technology

New York · London, John Wiley & Sons, Inc.

Copyright © 1961 by John Wiley & Sons, Inc.
All Rights Reserved.

This book or any part thereof
must not be reproduced in any form
without the written permission of the publisher.

Library of Congress Catalog Card Number: 61-15410
Printed in the United States of America

To Peggy Burton Rich for her help and understanding.

Preface

Traditionally, the scope of sanitary engineering has been confined primarily to water supply, sewerage, and general environmental sanitation. Since World War II, however, the profession has expanded to include increased responsibilities in industrial waste treatment, stream sanitation, air pollution, and radiological health. Academic institutions in an effort to keep abreast with postwar developments have added course after course to their graduate curricula, each covering a new area of sanitary engineering activities. The student, often finding it impossible to take all courses in the 9 to 12 months normally allotted to the Master of Science program, is forced prematurely into specialization at the first year graduate level. Furthermore, courses constituting these "compartmentalized" curricula are designed to include both theory and practice. Since it is impossible to do justice to both within the framework of a single course, emphasis is placed on the practice of engineering, with little attention being paid to basic principles.

As long as treatment processes remained simple and efficiencies of low order were tolerable, the sanitary engineer educated in the traditional manner functioned with reasonable effectiveness. Today, however, processes are becoming more complex and there is an increased emphasis on higher efficiencies. Empiricism can no longer be trusted. In short, the profession faces a dilemma. Sanitary engineering has out-distanced the practitioner! Obviously, if this serious and very embarrassing situation is to be resolved, drastic changes in the educational process are in order.

I believe that a solution to the problem lies in a comprehensive revision of present curricula accompanied by a reorientation of educational

objectives. Specifically, the revision would entail an integration of subject matter in fewer courses, a separation of analyses from design, and a strong emphasis on the rational approach to design. The objective would be a creative engineer who, with a modicum of experience, could function effectively in any one of several branches of sanitary engineering; one who could take a particular water or waste into the laboratory, analyze it, and then design a treatment process on the basis of the laboratory evaluation. It is to this end that this textbook has been written.

This book deals with physical processes, called unit operations, which are common to many water and waste treatment systems. By examining these operations apart from a particular application, the student is encouraged to concentrate on fundamental principles. The duplication of topic material normally encountered in "compartmentalized" curricula is avoided, and time is available to consider a larger variety of operations. The unit operations approach has been employed in chemical engineering education for years with considerable success.

The book has been written for students with a typical undergraduate background in civil engineering. Comprehension requires only an understanding of freshman chemistry, engineering physics, calculus, and elementary hydraulics. Duplication of material covered in hydraulics has been restricted to those topics with ramifications important to sanitary engineering but not falling within the scope of an elementary course. Although I teach a unit operations course at the graduate level, there is no reason why it cannot be taught to advanced undergraduates as well. The practicing engineer also may find the text helpful in a program of home study.

The material covered in this book can be presented within the scope of a four-semester hour course. Details of equipment design are discussed only briefly since several books already published treat this aspect with thoroughness and clarity. References to these sources are listed as footnotes. Furthermore, several operations of a less complex nature have been omitted to make room for those ordinarily not considered in courses in sanitary engineering but which are of growing importance in the field.

The decision as to what notation to use was difficult to make. The material included in this book was taken from sources both in hydraulic and chemical engineering. The use of mixed notations would only confuse the student. The choice, then, was between two alternatives: hydraulic notations or those of chemical engineering. The latter were chosen. I am convinced that sanitary engineering design is basically process engineering and, as such, has a future closely related to chemical engineering. The use of the standard notation in chemical engineer-

ing would serve to familiarize the student with the notation, making available to him much of the literature in the process engineering field. Such accomplishment would enable him to apply to his field tools developed in allied engineering fields.

In conclusion, it must be emphasized that this book is not a treatise. Rather, it is a textbook dealing only with one facet of sanitary engineering—the design of unit operations. Basic sanitary science, analytical procedures, and unit chemical and biological processes, although of equal importance, are not the concern of this textbook. Although empirical design is still the rule in practice, the book has been oriented toward rational design. In the words of T. R. Camp:[1]

> It is the duty of engineers . . . to place their analyses and design on as rational a basis as can be obtained. If sanitary engineers do not follow this philosophy generally, in due time the business of designing plants will be taken over by more competent experts.

The material presented herein was taken from many sources, all of which are acknowledged. I can take credit only for bringing the information together in an attempt to make it more accessible to the sanitary engineering profession.

Acknowledgment is made with thanks to the valuable assistance given by many of my students and colleagues. Special acknowledgment is made to Mr. R. O. Matthern, both student and colleague.

LINVIL G. RICH

Clemson, South Carolina
June 1961

[1] Camp, T. R., "Sedimentation and the Design of Settling Tanks," *Transactions*, ASCE, **111** (1946), 956.

Contents

Fluid Transport in Closed Conduits	**1**	1
Fluid Transport in Open Conduits	**2**	32
Mixing	**3**	60
Sedimentation	**4**	81
Flotation and Aerosol Separation	**5**	110
Flow Through Beds of Solids	**6**	136
Vacuum Filtration	**7**	159
Gas Transfer	**8**	171
Adsorption and Leaching	**9**	208
Heat Transfer	**10**	218
Evaporation	**11**	239
Psychrometry and Humidification	**12**	255
Drying	**13**	274
Appendixes		289
Index		304

1

Fluid transport in closed conduits

1-1. Introduction

Fluid transport is of great importance in sanitary engineering. This unit operation is employed in water distribution, waste water collection, and the transfer of both water and waste water from one treatment process to another. The transport of such fluids as viscous sludges and gases is a vital operation in many treatment processes.

The fundamentals of fluid statics, fluid dynamics, and flow measurements are covered thoroughly in elementary fluid mechanics textbooks. The application of these fundamentals to the transport and pumping of aqueous systems is dealt with specifically in undergraduate textbooks dealing with applied hydraulics, water supply, and sewerage. Most of the topics presented in Chapters 1 and 2 of this book are ordinarily not covered in detail (or at all) in elementary textbooks used by the sanitary engineer. Where duplication of topic material occurs, an attempt has been made to keep such duplication brief, and to use it to provide a foundation on which to develop new topics.

1-2. Systems of Units and General Definitions

Newton's law provides one of the most fundamental relationships used in fluid mechanics.

$$F = Kma \tag{1-1}$$

where F = unbalanced force acting on body
m = mass of body
a = acceleration of body in the direction of unbalanced force
K = constant

In the centimeter-gram-second (cgs) system, the constant K is dimensionless and has the value of one, the mass being expressed in grams of mass, the acceleration in centimeters per second squared, and the force in dynes. The value of K in the foot-pound-second (fps) system also is dimensionless and has a value of unity. Mass is measured in pounds of mass, the acceleration in feet per second squared, and the force in poundals. Poundals are rarely used, however. Instead, common use is made of force-units expressed in pounds of force. Equation 1-1 is equated dimensionally by arbitrarily establishing the relationship

$$K = 1/g_c \tag{1-2}$$

where g_c = Newton's law conversion factor, 32.17 (ft)(lb mass)/(lb force)(sec^2)

Whereupon Equation 1-1 becomes

$$F = \frac{ma}{g_c} \tag{1-3}$$

where F = unbalanced force, lb force
m = mass, lb mass
a = acceleration, ft/sec^2

When the acceleration a is equal to the acceleration of gravity g, the ratio g/g_c has the value of unity (at the earth's surface), and the force F becomes numerically (but not dimensionally) equal to the mass m.

The density of matter can be expressed either as mass density (mass per unit volume), as specific weight (weight per unit volume), or as specific gravity (ratio of either the mass density or specific weight of the material to the same properties of water at 39.2 °F). In several fields of engineering, common use is made of specific weight. In other fields, the expression of density is confined largely to mass density.

When dimensional consistancy dictates the use of a weight density term, the mass density modified by the ratio g/g_c is used instead. The mass densities of water and several gases are presented in Appendixes 1 and 2.

1-3. Laminar Shear Stresses

At the moment a fluid, initially at rest, begins to move inside a tube, the velocities of flow at all points in a plane normal to the axis of the tube are equal. As motion proceeds, velocity gradients are established next to the wall of the tube due to resistance forces developing at the fluid-solid interface. The portion of the fluid containing the velocity gradients forms a layer between the inside surface of the tube and a fluid core in which gradients have not yet become established. As flow continues, the layer, called the Prandtl boundary layer, grows in thickness until a point is reached where it constitutes the entire bulk of the flowing fluid, and velocity gradients extend throughout the cross section of the tube. If flow is laminar and fully developed, the velocity profile will be similar to that shown in Figure 1-1*a*.

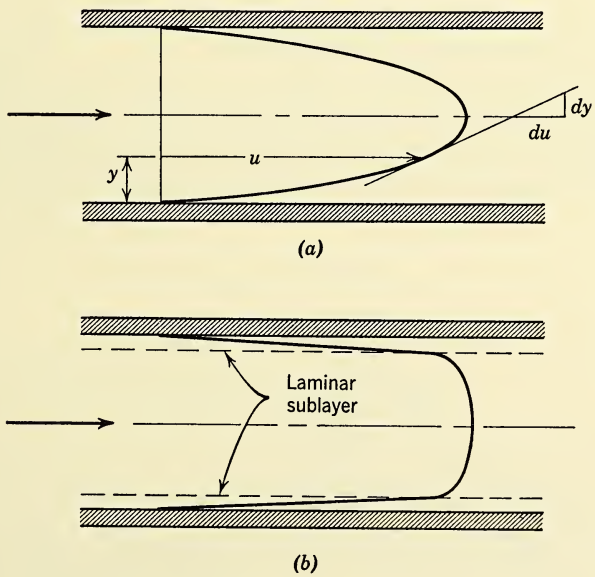

FIGURE 1-1. Velocity distribution in a pipe at a plane normal to the axis. (*a*) Velocity distribution in laminar flow. (*b*) Velocity distribution in turbulent flow.

The velocity gradients of fluids in turbulent flow form a different type of profile (Figure 1-1*b*). Although flow is turbulent, there persists at the wall of the tube a sublayer of fluid in which flow remains laminar. The laminar sublayer should not be confused with the Prandtl boundary layer which in Figure 1-1 extends completely across the tube.

The velocity gradients result in response to the relative movement between adjacent fluid layers. Since real fluids resist shear, shear stresses act (for laminar flow only) on cylindrical surfaces within the fluid. Consider Figure 1-1*a*. The local velocity at a distance y from the pipe wall is u, and the slope of the profile at that distance is the velocity gradient du/dy. The shear stress, or tractive force per unit area acting on a cylindrical surface with an axis parallel to the direction of flow is a function of the velocity gradient.

$$\tau = \psi\left(\frac{du}{dy}\right) \tag{1-4}$$

where τ = shear stress, lb force/ft^2

$\dfrac{du}{dy}$ = velocity gradient, sec^{-1}

Figure 1-2 contains curves relating shear stress to velocity gradient for several types of fluids in laminar flow.

Newtonian fluids are characterized by the fact that the shear stress is directly proportional to the velocity gradient. For conditions of laminar flow, the proportionality constant is a constant function of the viscosity and is equal to the slope of the curve relating the two variables.

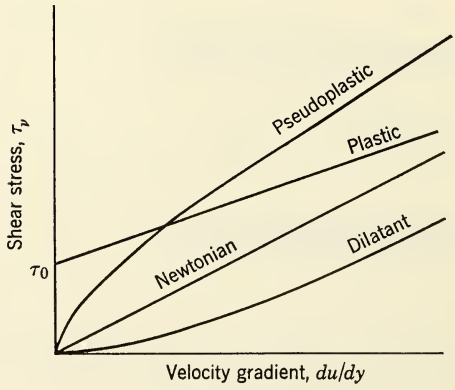

FIGURE 1-2. Fluid classification based on shear stress-velocity gradient relationships existing when flow is laminar.

For water and other fluids behaving as Newtonian fluids, Equation 1-4 becomes

$$\tau_v = \frac{\mu}{g_c}\frac{du}{dy} \tag{1-5}$$

where τ_v = shear stress resulting from viscosity, lb force/ft^2
μ = absolute or coefficient of viscosity, (lb mass)/(ft)(sec)
g_c = Newton's law conversion factor, (lb mass)(ft)/(lb force)(sec^2)

Viscosity is a measure of the resistance of a fluid to flow and varies with temperature. The absolute viscosity of water and several gases at different temperatures is given in Appendix 3. The unit of absolute viscosity in the cgs system is called the *poise* [(1 gm mass)/(cm)(sec)]. The *centipoise*, which is one one-hundredth of a poise, is often used to express viscosity. The latter term is converted to (lb mass)/(ft)(sec) by multiplication with 6.72×10^{-4}. The ratio of the absolute viscosity to the mass density of the fluid, μ/ρ, is called the kinematic viscosity, ν. In the cgs system, the kinematic viscosity is called the *stoke* (1 cm^2/sec). The *centistoke*, which is one one-hundredth of a stoke, is converted to square feet per second by multiplication with 1.075×10^{-5}.

1-4. Rheology

Plastic fluids require a minimum shear stress called the yield stress, τ_0, before velocity gradients are established. Once established, the velocity gradient increases linearly with stress. The relationship for an ideal plastic fluid is expressed mathematically as

$$\tau_v = \tau_0 + \frac{\mu_R}{g_c}\frac{du}{dy} \tag{1-6}$$

where τ_0 = yield stress, lb force/ft^2
μ_R = coefficient of rigidity, (lb mass)/(ft)(sec)

Many thick suspensions such as sewage sludges and clay slurries behave as plastic fluids.[1] In thin suspensions, the suspended particles are not in contact and the suspension will exhibit the properties of the continuous phase. When the concentration becomes sufficiently great to force the particles into contact with each other, a measurable stress

[1] Babbitt, H. E., and D. H. Caldwell, "Laminar Flow of Sludge in Pipes," *Univ. Ill. Bull.*, **319** (1939).

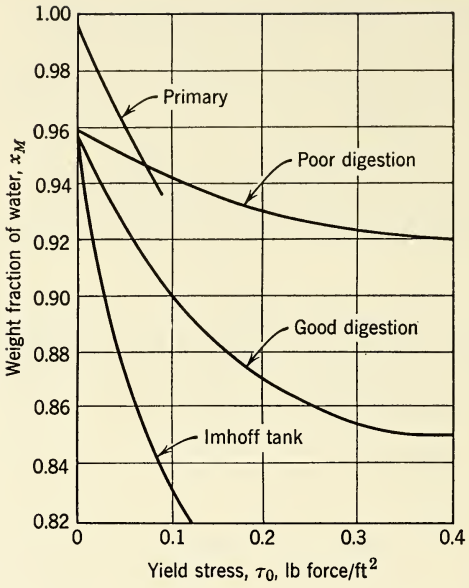

FIGURE 1-3. Variation of yield stress with moisture content of sewage sludges. [After Figure 2, Chou, T. L., "Resistance of Sewage Sludge to Flow in Pipes," *Proc. San. Engr. Div., ASCE,* Paper 1780 (Sept. 1958).]

is needed to produce relative motion within the fluid. Both the yield stress and the coefficient of rigidity increase with an increase in the concentration of suspended material.

Figures 1-3 and 1-4 are plots relating the yield stresses and coefficients of rigidity to the moisture content of several types of sewage sludges. The data on which the plots are based are limited and the individual points show considerable variation. However, the curves constructed through mean values provide a visual comparison of typical relationships. The points where the curves in Figure 1-3 intersect the moisture axis, x_{ML}, represent limiting moisture contents. With greater moisture values, the sludges lose their plasticity and behave as Newtonian fluids.

Some fluids exhibit properties that identify them as being pseudoplastic. The shear-stress–velocity-gradient curves for these fluids pass through the origin, and the increase in velocity gradient becomes progressively larger as the shear stress increases. Dilatant fluids constitute still another class. From Figure 1-2 it is seen that the curves for these fluids are inverted images of the pseudoplastic curves. Only the Newtonian fluids possess a definite viscosity. The ratio of the shear stress to the velocity gradient for fluids in other classes gives only an apparent viscosity, the value of which varies with the shear stress.

In some fluids a constant shearing stress will produce varying velocity

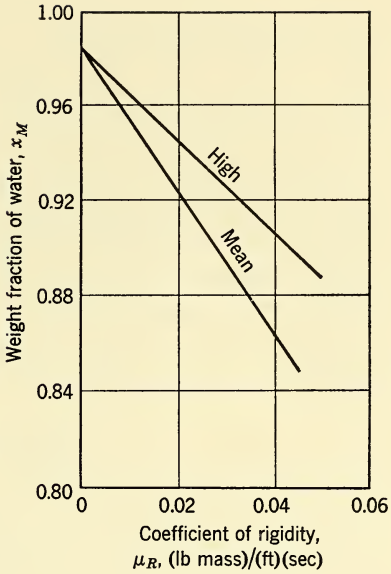

FIGURE 1-4. Variation of coefficient of rigidity with moisture content of sewage sludges. [After Figure 3, Chou, T. L., "Resistance of Sewage Sludge to Flow in Pipes," *Proc. San. Engr. Div., ASCE*, Paper 1780 (Sept. 1958).]

gradients which are time-dependent (Figure 1-5). Velocity gradients established in *thixotropic* fluids as a result of the application of a constant shearing stress increase with the time of shear. Conversely, when the shearing stress is removed, the properties of the fluid revert back to those of the fluid prior to the application of the stress. Some filter cakes and greases exhibit thixotropic properties.

Rheopectic fluids behave in a manner opposite to that of the thixotropic fluids. On the application of a constant shearing stress, fluidity decreases with time. Rheopectic properties are observed in some gypsum and bentonite suspensions in water.

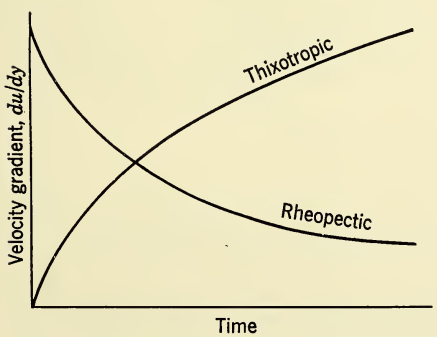

FIGURE 1-5. Effect of time on the velocity gradients produced in thixotropic and rheopectic fluids when subjected to a constant shear stress.

1-5. Turbulent Shear Stresses

The shearing stress between two fluid layers in turbulent flow is due both to viscosity and momentum exchanges taking place as a result of the movement of fluid particles from one layer to the other. Consider the situation in Figure 1-6 where two adjacent layers of a fluid in turbulent flow are moving parallel with each other along the x coordinate at velocities, the difference of which is equal to Δu_x. The total mass of the fluid particles exchanged between the two layers through area A per unit of time is equal to $\rho u_y A$. The force generated in the x direction as the result of the change in the momentum of the particles as they move from one layer to the other is

$$F_x = \frac{\rho u_y A \, \Delta u_x}{g_c} \tag{1-7}$$

and the shear stress is

$$\tau_t = \frac{\rho u_y \, \Delta u_x}{g_c} \tag{1-8}$$

where τ_t = shear stress resulting from turbulence, lb force/ft^2.

If l is taken as the average distance in the y direction in which the fluid particles are displaced before their momenta undergo change, the

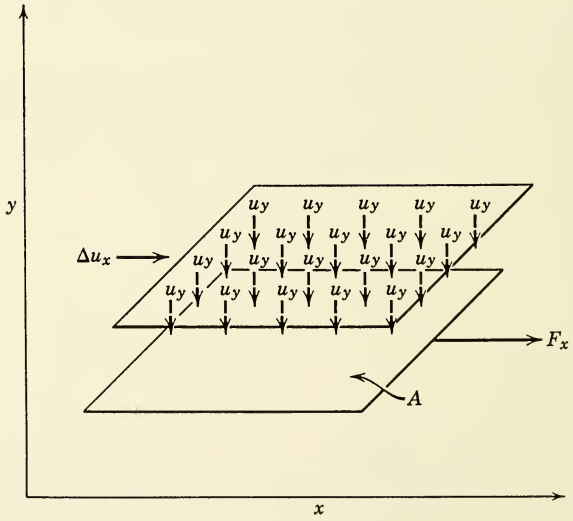

FIGURE 1-6. Momentum exchange between adjacent fluid layers.

difference in the velocities of the two layers between which the turbulent eddy travels is

$$\Delta u_x = l \frac{du}{dy} \tag{1-9}$$

where l = Prandtl mixing length.

The mass passing through any element of the fluid must remain constant with time. Therefore, according to the law of the conservation of momentum,

$$\Delta u_x = u_y \tag{1-10}$$

Equation 1-8 can now be written as

$$\tau_t = \frac{\rho}{g_c} l^2 \left(\frac{du}{dy}\right)^2 \tag{1-11}$$

Or, if

$$\eta = \rho l^2 \frac{du}{dy} \tag{1-12}$$

where η = eddy viscosity, (lb mass)/(ft)(sec), then the total shear at a point in a turbulent liquid is

$$\tau = \tau_v + \tau_t = \frac{\mu + \eta}{g_c} \frac{du}{dy} \tag{1-13}$$

The eddy viscosity is not a physical characteristic constant of the fluid like μ, but depends upon the density, the mixing length, and the velocity gradient. Since the eddy viscosity is generally much larger than the absolute viscosity, the shear stress in turbulent flow may be considerably higher than that for laminar flow. Often it is convenient to utilize a *kinematic eddy viscosity*, $e = \eta/\rho$, which is a property of the flow alone.

The Prandtl mixing length l may be computed from a relationship suggested by Von Kármán [2]

$$l = \kappa \frac{du/dy}{d^2u/dy^2} \tag{1-14}$$

where κ = universal constant in turbulent flow. The value of κ is constant regardless of the boundary configuration or the Reynolds number.

[2] Von Kármán, Th., "*Turbulence and Skin Friction*," *J. Aeronaut. Sci.*, **1**, No. 1 (1934), p. 1.

1-6. Flow in Pressure Pipes

A variety of mathematical expressions are available to the engineer for use in pipe-flow problems. Some have a rational basis whereas others have been developed empirically. The choice of equation to be used for a particular problem usually will depend on the availability of information relating to the variables employed in the equation.

Figure 1-7 is a definition sketch for the isothermal flow of an incompressible fluid through a pipe, with friction occurring but with no addition of work or heat. Using the notations in the figure, the mechanical energy equation is written as

$$\frac{g}{g_c} Z_1 + \frac{p_1}{\rho} + \frac{\overline{V}_1^2}{2g_c} = \frac{g}{g_c} Z_2 + \frac{p_2}{\rho} + \frac{\overline{V}_2^2}{2g_c} + \frac{\Delta p}{\rho} \qquad (1\text{-}15)$$

where $(g/g_c)Z$ = elevation head above arbitrary datum, (ft)(lb force)/(lb mass)
p/ρ = pressure head, (ft)(lb force)/(lb mass)
$\overline{V}^2/2g_c$ = velocity head, (ft)(lb force)/(lb mass)
$\Delta p/\rho$ = energy head loss due to friction, (ft)(lb force)/(lb mass)

The energy loss $\Delta p/\rho$ results from the conversion of mechanical energy to heat energy by friction. In an isothermal system this term repre-

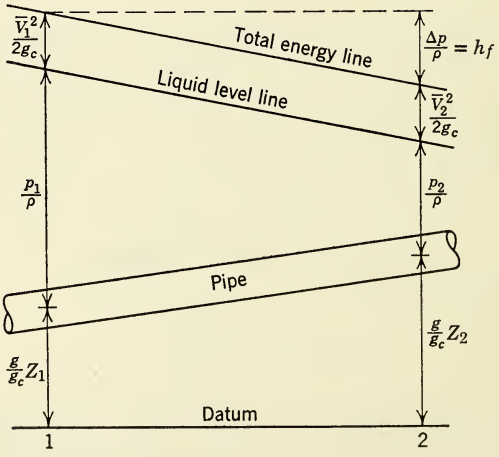

FIGURE 1-7. Notation for isothermal flow of an incompressible fluid through a pipe, with friction losses occurring but with no addition of work or heat.

sents a permanent loss in the total energy of the system. Since the notation for pressure drop due to friction, Δp, is used to indicate pressure differences caused by other factors as well, confusion is avoided through the use of the notation h_f for $\Delta p/\rho$. Pipe-flow computations commonly involve the determination of the term h_f.

Darcy-Weisbach Equation

The Darcy-Weisbach equation, often referred to as the Fanning equation, is one of the earliest rational expressions used for determining the energy loss in a liquid flowing through a pipe. The equation can be written as

$$h_f = \frac{\Delta p}{\rho} = f\left(\frac{L}{D}\right)\left(\frac{\overline{V}^2}{2g_c}\right) \tag{1-16}$$

where Δp = permanent pressure drop due to friction, lb force/ft^2
h_f = energy loss due to friction, (ft)(lb force)/(lb mass)
f = friction factor, dimensionless
ρ = mass density of liquid, lb mass/ft^3
L = length of pipe, ft
$\overline{V}$ = mean velocity of flow, ft/sec
g_c = Newton's law conversion factor, (ft)(lb mass)/(lb force)(sec^2)
D = diameter of pipe, ft

The friction factor is a function of the Reynolds number ($D\overline{V}\rho/\mu$), the roughness of the interior surface of the pipe, and the pipe diameter. The Moody diagram [3] in Figure 1-8 relates these variables with curves derived from experimental data. For Reynolds numbers up to 2000, flow is laminar, the stream lines being parallel throughout the cross section of the pipe. The friction factor is independent of pipe size and interior roughness, and is a function only of the Reynolds number. Although laminar flow can be extended beyond $N_{Re} = 2000$, this value is generally agreed to be the upper limit. Somewhere between 2000 to 4000, the flow characteristics are made unstable by transient localized turbulence, and the value of the friction factor cannot be estimated when the Reynolds number falls within this range. Above 4000, a transition zone occurs in which turbulence becomes established in the core of the flowing liquid. The Reynolds number becomes less important as the effect of pipe size and roughness becomes more pronounced.

[3] Moody, L. F., "Friction Factor for Pipe Flow," *Trans. ASME*, **66**, No. 8 (1944), p. 671.

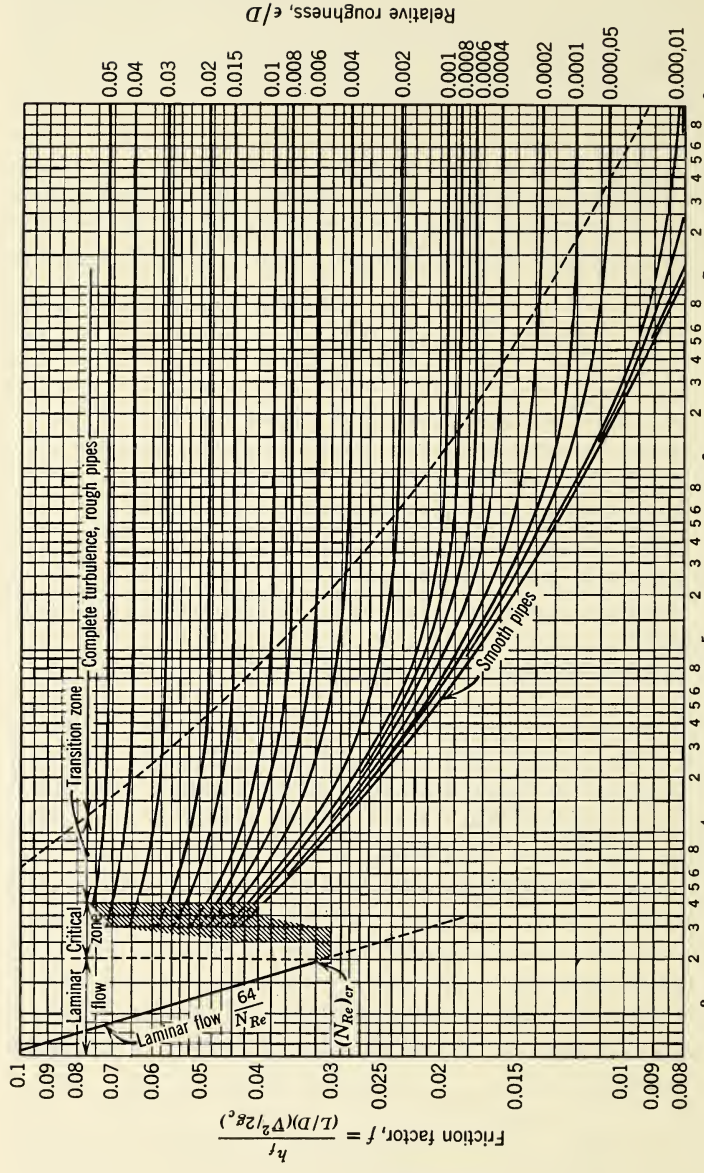

FIGURE 1-8. Moody diagram for friction in pipes. [Adapted from Moody, L. F., *Trans. ASME*, **66** (1944).]

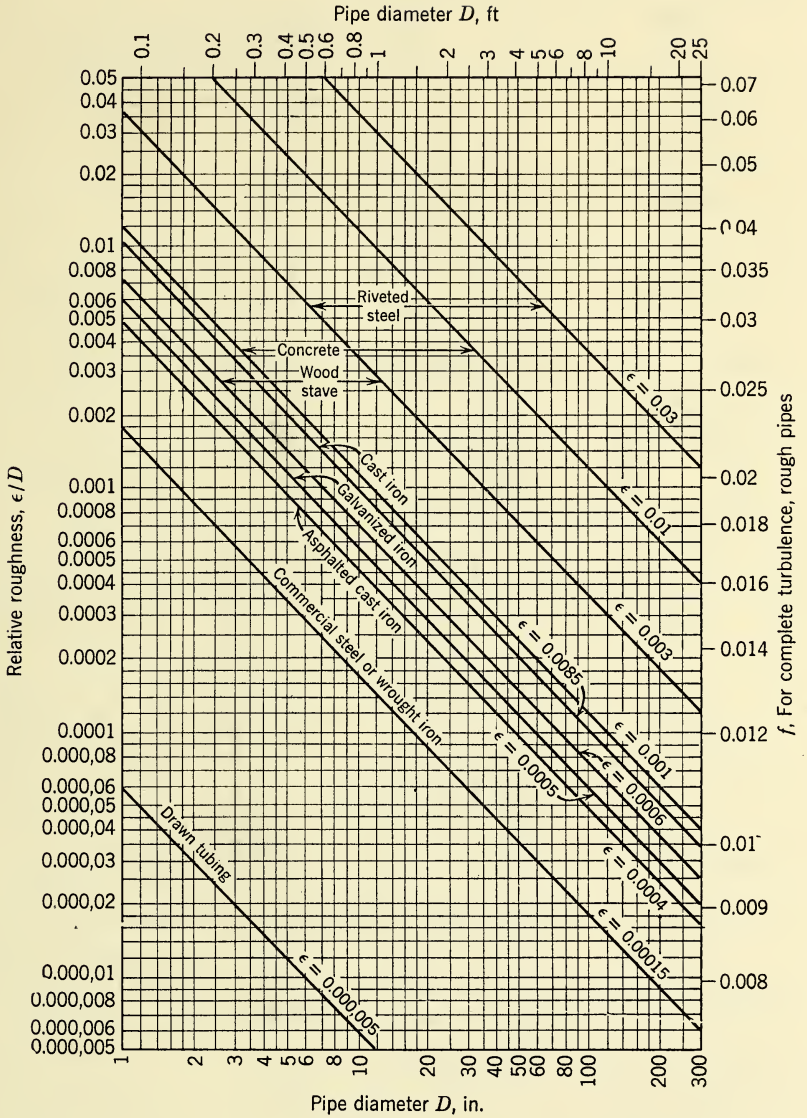

FIGURE 1-9. Relative roughness of pipes. [Adapted from Moody, L. F., *Trans. ASME*, **66** (1944).]

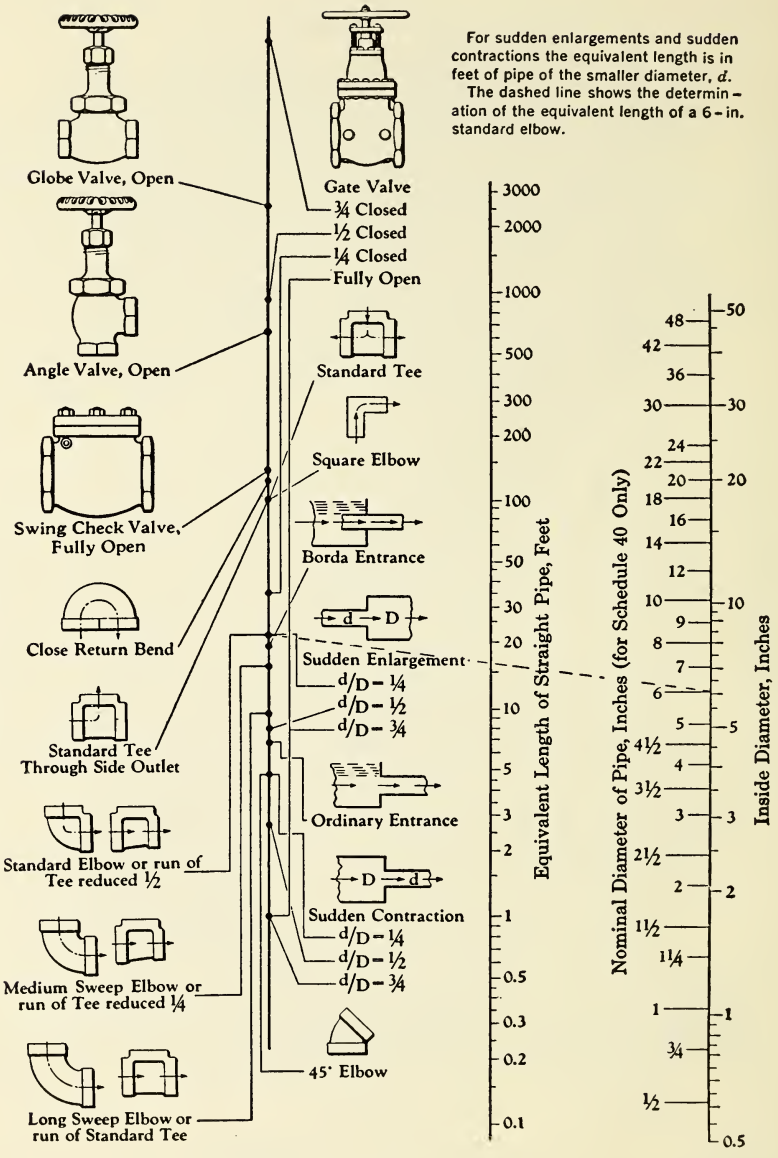

FIGURE 1-10. Equivalent lengths of valves and fittings. (*Crane Co.*)

Finally, turbulent conditions extend throughout the pipe's cross section, and a Reynolds number is reached where the friction factor is a function only of pipe diameter and roughness.

The effect of size and roughness on the friction factor is expressed in terms of the relative roughness, a ratio of the absolute roughness of the pipe ϵ to the diameter D, in feet. The absolute roughness is a somewhat arbitrary term for evaluating the roughness of the interior surface of pipes, whereas the relative roughness is a numerical designation of the effect that a given type of surface has in different sizes of pipes. Values of relative roughness for pipes of different materials are given in Figure 1-9.[4] The mass density of water at various temperatures may be found in Appendix 1.

Friction losses in valves and fittings are determined most conveniently in terms of equivalent lengths of pipe. Figure 1-10 may be used for this purpose. The values found in the figure were obtained from a manufacturer's test data, are approximate, and are applicable only to conditions of turbulent flow.

Flow equations developed for circular cross sections are often applied to cross sections of other shapes. This is done by substituting for the diameter an equivalent term which is a function of the hydraulic radius. For pipes

$$D = 4r_H \tag{1-17}$$

where r_H = hydraulic radius, ft. The hydraulic radius is the ratio

$$r_H = \frac{\text{Cross-section area}}{\text{Wetted perimeter}} \tag{1-18}$$

Use of $4r_H$ for the diameter term in Equation 1-16 is generally restricted to turbulent flow. When flow conditions are laminar, a friction factor-Reynolds number relationship different from that presented in Figure 1-8 must be employed.

Equation 1-16 can be used to compute the pressure drop due to friction in compressible fluids flowing under isothermal conditions, provided that the drop does not exceed 10 percent of the final absolute pressure. Frictional pressure drops occurring in most gas transport operations encountered by the sanitary engineer fall within this limitation, and the equation can be used with reasonable accuracy.

From the general law for gases

$$q_c = \frac{T_{Ac}p}{T_A p_c} q \tag{1-19}$$

[4] *Ibid.*

where q_c and q = volumetric rate of flow of compressed and free gases respectively, ft^3/sec

T_{Ac} and T_A = absolute temperature of compressed and free gases respectively, °R

p_c and p = pressure of compressed and free gases respectively, lb force/ft^2

also

$$\overline{V} = \frac{q_c}{S} \tag{1-20}$$

where S = cross-section area of pipe, ft^2.

In most situations where gases are transported through relatively short pipes, there is little heat loss from the system even though the conduits are unlagged. For the adiabatic compression of ideal gases,

$$\frac{T_{Ac}}{T_A} = \left(\frac{p_c}{p}\right)^{(k-1)/k} \tag{1-21}$$

where k = adiabatic compression exponent.

This expression can be used in the approximate solution of problems involving the transport of nonideal gases provided the compression ratio is not large. The exponent k is the ratio of the specific heat of the gas at constant pressure to that at constant volume. For air, the exponent is equal to 1.4.

Equations 1-19, 1-20, and 1-21 can be evaluated for the specific conditions encountered, and the appropriate substitutions can be made in Equation 1-16. The mass densities of selected gases at standard conditions are given in Appendix 2.

Hagen-Poiseuille Equation

For a Newtonian fluid in laminar flow through a circular pipe, the equilibrium force balance on a cylindrical element of fluid concentric with the pipe is (Figure 1-11)

$$\tau_r(2\pi r)L = \Delta p \pi r^2 \tag{1-22}$$

where τ_r = shear stress along the curved surface of the cylinder, lb force/ft^2

r = radius of cylinder, ft

L = length of cylinder, ft

Δp = pressure drop across length of cylinder, lb force/ft^2

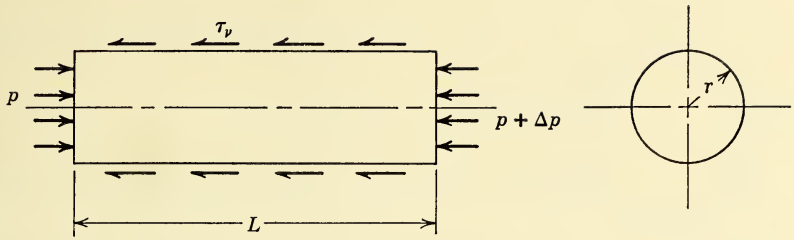

FIGURE 1-11. Forces acting on a cylindrical element of a Newtonian fluid in laminar flow through a pipe.

Solving for the shear stress, Equation 1-22 becomes

$$\tau_v = \frac{r}{2}\frac{\Delta p}{L} \tag{1-23}$$

With a change in coordinates, Equation 1-5 can be expressed as

$$\tau_v = -\frac{\mu}{g_c}\frac{du}{dr} \tag{1-24}$$

The minus sign is introduced because u decreases as r increases.

By equating Equations 1-23 and 1-24, and integrating with respect to r, an expression is obtained for the local velocity u.

$$\int \frac{du}{dr}\,dr = -\frac{g_c\,\Delta p}{2\mu L}\int r\,dr \tag{1-25}$$

$$u = -\frac{g_c\,\Delta p r^2}{4\mu L} + C \tag{1-26}$$

where C = constant of integration.

At the pipe wall $u = 0$, hence

$$C = \frac{g_c\,\Delta p r_w^{\,2}}{4\mu L} \tag{1-27}$$

where r_w = radius of pipe, ft.

Substitution of Equation 1-27 into Equation 1-26 gives

$$u = \frac{g_c\,\Delta p}{4\mu L}(r_w^{\,2} - r^2) \tag{1-28}$$

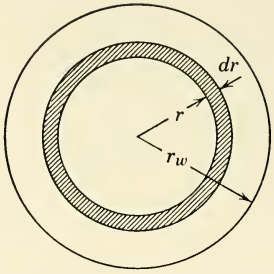

FIGURE 1-12. Ring element of pipe cross section.

The flow of fluid through the total cross section of the pipe can be formulated by integrating the product of the local velocity and the area of a ring element of the cross section (Figure 1-12).

$$q = \int u\, dS = \int_0^{r_w} \left[\frac{g_c\, \Delta p}{4\mu L}(r_w^2 - r^2)\right] 2\pi r\, dr$$

$$= \frac{\pi g_c\, \Delta p r_w^4}{8\mu L} \tag{1-29}$$

where q = volumetric rate of flow, ft^3/sec
dS = area of ring element, ft^2

By substituting the cross-section area and mean velocity of flow for q, and solving for the pressure drop,

$$\Delta p = \frac{32 L \overline{V} \mu}{g_c D^2} \tag{1-30}$$

where $\overline{V}$ = mean velocity of flow, ft/sec
D = pipe diameter, ft

When the pressure drop is due to friction

$$h_f = \frac{32 L \overline{V} \mu}{g_c D^2 \rho} \tag{1-31}$$

Equations 1-30 and 1-31 are forms of the Hagen-Poiseuille relationship and apply only to laminar flow of Newtonian fluids in circular pipes.

Sewage sludges and several types of clay slurries with moisture contents below the critical value often behave as plastic liquids. It has been shown, however, that the relationships of frictional head loss to

velocity for such materials in laminar flow through circular pipes are expressed by a modification of Equation 1-31 [5]

$$h_f = \frac{32L\overline{V}}{g_c D^2 \rho}\left(\mu_R + \frac{g_c \tau_0 D}{6\overline{V}}\right) \tag{1-32}$$

where μ_R = coefficient of rigidity, (lb mass)/(ft)(sec)
τ_0 = yield stress, lb force/ft^2

The terms enclosed in the parentheses are analogous to the absolute viscosity in Equation 1-31 and have the same dimensions. If these terms are represented by μ', then the relationship

$$N_{Re} = \frac{\overline{V} D \rho}{\mu'} = 2000 \tag{1-33}$$

can be used to determine the maximum velocity for which Equation 1-32 is applicable. Data available indicate that τ_0 and μ_R are independent of diameter and roughness of pipe. Sludge density will vary with the type of sludge and with moisture content. The variation to be expected is

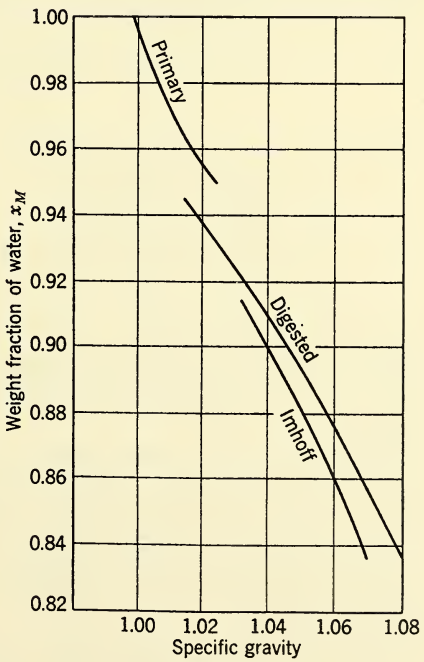

FIGURE 1-13. Variation of specific gravity with moisture content of sewage sludges. [After Figure 1, Chou, T. L., "Resistance of Sewage Sludge to Flow in Pipes," *Proc. San. Engr. Div., ASCE*, Paper 1780 (Sept. 1958).]

[5] Babbitt, H. E., and D. H. Caldwell, *loc. cit.*

indicated in Figure 1-13 where specific gravity is plotted as a function of sludge moisture.

Hazen-Williams Equation [6]

The use of the Darcy-Weisbach equation was limited for many years to laminar flow applications by the paucity of data correlating the friction factor with the roughness of the inside surface of the pipe. As a result, there came into use in hydraulic practice several exponential formulas, empirically derived from turbulent flow experiments. Most of the equations related frictional head loss in feet of water to the hydraulic radius of the conduit, length of conduit, and roughness of the interior surface. Application of the exponential equation has been confined primarily to water systems.

The Hazen-Williams equation was derived originally for turbulent flow in both pipes and open channels; but now it is more commonly used for pipe flow. The equation as generally written is

$$\overline{V} = 1.318 C_H r_H^{0.63} \left(\frac{h'_f}{L}\right)^{0.54} \tag{1-34}$$

Solving for the frictional head loss, the expression becomes:

$$h'_f = 3.03 \frac{L}{D^{1.17}} \left(\frac{\overline{V}}{C_H}\right)^{1.85} \tag{1-35}$$

where h'_f = head loss due to friction, ft of water
L = length of pipe, ft
D = diameter of pipe, ft
$\overline{V}$ = mean velocity of flow, ft/sec
C_H = Hazen-Williams coefficient

It is to be noted that $h'_f = h_f/(g/g_c)$. The slopes of both the total energy and liquid level lines in Figure 1-7 can be expressed as the ratio h'_f/L. The liquid level line is frequently referred to as the hydraulic grade line.

The value of the coefficient C_H will vary with the material of which the pipe is constructed, with the degree of deterioration of the inside surface, and, to a lesser degree, with pipe size. Values for different conduit materials are listed in Table 1-1. These values apply to water, dilute suspensions such as sewage, and sludges with moistures above the critical level.

[6] Williams, G. S., and Allen Hazen, *Hydraulic Tables*, 1st ed., John Wiley and Sons, Inc., New York (1905), with subsequent editions.

TABLE 1-1. VALUES OF THE HAZEN-WILLIAMS COEFFICIENT, C_H, FOR VARIOUS KINDS OF PIPE

Kind of Pipe	C_H
Cast iron, new	130
Cast iron, old	100
Cast iron, lined with cement or bituminous enamel	140
Steel, welded, lined with cement or bituminous enamel	140
Steel, riveted, coated with coal tar	110
Asbestos-cement	140
Concrete	120
Wood stave	120

Equation 1-35 can be used to estimate frictional head losses for the turbulent flow of plastic liquids provided the proper values of the coefficient are employed. The curve in Figure 1-14 relates the moisture content of undigested sewage sludge with values of the ratio C'_H/C_H, in which C'_H is a modified coefficient for use in the Hazen-Williams equation. Corresponding information for digested sludges in the plastic state is meager. From the available data it would appear that values of C_H for digested sewage sludges are somewhat greater than those for raw sludge. Values obtained from Figure 1-14 can be used for such sludges with a margin of safety.

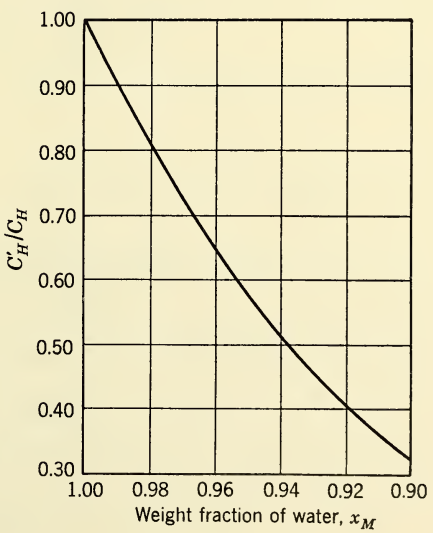

FIGURE 1-14. Variation of Hazen-Williams coefficient C_H with moisture content of undigested sewage sludge. [After Figure 4, Chou, T. L., "Resistance of Sewage Sludge to Flow in Pipes," *Proc. San. Engr. Div., ASCE,* Paper 1780 (Sept. 1958).]

The solution of Equations 1-34 and 1-35 is facilitated by the use of the alignment chart in Appendix 4. Here the head loss is expressed in feet per 1000 ft of pipe.

EXAMPLE 1-1

Estimate the frictional head loss when 800 ft^3/min of free air flows through 600 ft of 8-in. asphalted cast-iron pipe under a pressure of 6 psig. Assume the temperature of the free air to be 60 °F.

Solution

1. Compute the absolute temperature of the compressed air (Equation 1-21).

$$T_{Ac} = 520\left(\frac{20.7}{14.7}\right)^{(1.4-1)/1.4} = 574\ °R$$

2. Compute the flow of compressed air (Equation 1-19).

$$q_c = \frac{574}{520} \times \frac{14.7}{20.7}\, 13.33 = 10.45\ ft^3/sec$$

3. Compute the flow velocity (Equation 1-20).

$$\overline{V} = \frac{q_c}{S} = \frac{10.45 \times 4}{\pi(0.667)^2} = 29.9\ ft/sec$$

4. From Appendix 2,

$$\rho = 0.0808\,\frac{492}{574} \times \frac{20.7}{14.7} = 0.0975\ lb/ft^3$$

and from Appendix 3,

$$\mu = 0.0194 \times 6.72 \times 10^{-4} = 13 \times 10^{-6}\ (lb)/(sec)(ft)$$

5. Compute the Reynolds number

$$N_{Re} = \frac{29.9 \times 0.667 \times 0.0975}{13 \times 10^{-6}} = 1.5 \times 10^5$$

6. From Figure 1-9, for 8-in. asphalted cast-iron pipe,

$$\epsilon/D = 0.0006$$

7. From Figure 1-8, for $N_{Re} = 1.5 \times 10^5$ and $\epsilon/D = 0.0006$,

$$f = 0.02$$

8. Compute the frictional head loss (Equation 1-16).

$$h_f = \frac{0.02 \times 600(29.9)^2}{2 \times 32.2 \times 0.667} = 249 \text{ (ft)(lb force)/(lb mass)}$$

$$\Delta p = h_f \rho = 249 \times 0.0913 = 22.8 \text{ lb force/ft}^2 = 0.16 \text{ psi}$$

EXAMPLE 1-2

What will be the maximum velocity at which a digested sludge with 92 percent moisture will flow in a laminar state through a 12-in.-diameter pipe?

Solution

From Figure 1-3 it is seen that 92 percent falls below the critical moisture content for digested sludge. Therefore, the sludge will be expected to behave as a plastic liquid. Assuming that the digestion can be rated as good,

$$\tau_0 = 0.05 \text{ lb force/ft}^2 \qquad \text{(Figure 1-3)}$$

$$\mu_R = 0.023 \text{ (lb mass)/(ft)(sec)} \qquad \text{(Figure 1-4)}$$

$$\rho = 62.4 \times 1.032 = 64.4 \text{ lb mass/ft}^3 \qquad \text{(Figure 1-13)}$$

$$\mu' = \mu_R + \frac{g_c \tau_0 D}{6\overline{V}} = 0.023 + \frac{32.17 \times 0.05 \times 1}{6\overline{V}}$$

$$= \frac{0.023\overline{V} + 0.269}{\overline{V}}$$

$$N_{Re} = 2000 = \frac{\overline{V} D \rho}{\mu'} = \frac{\overline{V}^2 \times 1 \times 64.4}{0.023\overline{V} + 0.269}$$

$$\overline{V} = 3.26 \text{ ft/sec}$$

1-7. Limiting Velocities

When pumped through horizontal sections of pipe, emulsions and solid-liquid suspensions have a tendency to separate or settle out unless the velocity of flow is maintained above a minimum value. In the case of emulsions, separation of phases is prevented by keeping the velocity high enough to ensure turbulent flow ($N_{Re} \geqq 4000$). The momentum transfer accompanying this type of flow is sufficient to maintain the mixture.[7]

In the case of solid-liquid suspensions there are two velocities of importance. The *minimum velocity* is that velocity below which the

[7] Lowenstein, J. G., *Chem. Engr.*, **66** (Jan. 12, 1959), 133–135.

solids settle out freely. The velocity at which the solids are kept dispersed evenly across the pipe diameter is called the *standard velocity.* At intermediate velocities, definite concentration gradients exist in a vertical direction across the pipe.

The gravitational effect is more pronounced in causing the sedimentation of solids than it is in the separation of an emulsion. Consequently, in dealing with solid-liquid suspensions, such an effect must be considered along with that of turbulence. For nonflocculating particles with mean diameters between 0.05 and 0.5 mm (0.164×10^{-3} ft and 1.64×10^{-3} ft), these effects have been correlated with the limiting velocities to give [8]

$$N_{Fr} = K \frac{\rho_s - \rho}{\rho} N_{Re}^{0.775} \tag{1-36}$$

and

$$\frac{\overline{V}^2}{gD_p} = K \frac{\rho_s - \rho}{\rho} \left(\frac{\overline{V} D \rho_m}{\mu_m} \right)^{0.775} \tag{1-37}$$

where N_{Fr} = Froude number, a measure of the gravitational effect, dimensionless
$\overline{V}$ = minimum or standard velocity, ft/sec
D_p = mean diameter of particle; the diameter of that particle which is larger than 50 percent (by weight) of the particles, ft
D = diameter of pipe, ft
ρ = mass density of liquid, lb/ft^3
ρ_m = mean mass density of suspension, lb/ft^3
K = constant; equals 25.3×10^{-3} for the minimum velocity and 74.5×10^{-3} for the standard velocity
ρ_s = mass density of solid particles, lb/ft^3
μ_m = viscosity of the suspension; can be taken as equal to the viscosity of the liquid, (lb mass)/(ft)(sec)
g = acceleration of gravity, ft/sec^2

The mean density of the suspension can be computed from

$$\rho_m = x_v \rho_s + (1 - x_v)\rho \tag{1-38}$$

where x_v = volumetric fraction of solids in the suspension.

Solving Equation 1-37 for the velocity,

$$\overline{V} = \left(K g D_p \frac{\rho_s - \rho}{\rho} \right)^{0.816} \left(\frac{D \rho_m}{\mu_m} \right)^{0.633} \tag{1-39}$$

[8] Spells, K. E., *Trans. Inst. Chem. Engr.*, **33** (1955), 79–82.

At velocities greater than the standard velocity, the frictional head loss can be computed with the Darcy-Weisbach equation (Equation 1-16), with the use of a friction factor derived from Figure 1-8. In computing the Reynolds number, the density and viscosity are taken as those of the suspension.[9]

Between the minimum velocity and standard velocity, friction losses are considerably higher than for the pure liquid at the same velocity. For closely graded particles suspended in water, the pressure drop due to friction can be estimated with an empirical formula.[10]

$$\frac{\Delta p' - \Delta p}{\Delta p} = 121 x_v \left[\frac{gD(\rho_s - \rho)}{\overline{V}^2}\right]^{1.5} \left[\frac{u_t^2}{gD_p(\rho_s - \rho)}\right]^{0.75} \qquad (1\text{-}40)$$

where Δp = pressure drop due to friction computed for pure water flowing at a velocity $\overline{V}$

$\Delta p'$ = pressure drop due to friction in the suspension flowing at a velocity $\overline{V}$

u_t = terminal settling velocity of solid particle of diameter D_p, ft/sec

The frictional pressure drop in a suspension of solids having a wide range in particle size is best determined from experiments with the particular suspension.

EXAMPLE 1-3

A suspension of ore fines in water (10 percent by volume) is to be pumped through a horizontal pipe 6-in. in diameter. The particles have a specific gravity of 2 and a mean diameter of 0.2 mm. If the water has a density of 62.3 lb/ft^3 and a viscosity of 1 cp, how high a velocity must be maintained to keep the particles evenly dispersed throughout the suspension?

Solution

1. Calculate mean density of the suspension (Equation 1-38).

$$\rho_m = 0.10(2 \times 62.3) + 0.90 \times 62.3 = 68.53 \text{ lb/ft}^3$$

2. Compute standard velocity (Equation 1-39).

$$\overline{V} = (74.5 \times 10^{-3} \times 32.17 \times 6.56 \times 10^{-4} \times 1)^{0.816} \left(\frac{0.5 \times 68.53}{1 \times 6.72 \times 10^{-4}}\right)^{0.633} = 4.92 \text{ ft/sec}$$

[9] Johnstone, R. E., and M. W. Thring, *Pilot Plants, Models and Scale-Up Methods in Chemical Engineering*, McGraw-Hill Book Co., New York (1957), pp. 119–120.

[10] Durand, R., and E. Condolios, "IIme journée de l'hydraulique," *Compt. rend.*, Societé hydrotechnique de France (June 1952), p. 29.

UNIVERSITY OF FLORIDA
GENESYS LIBRARY

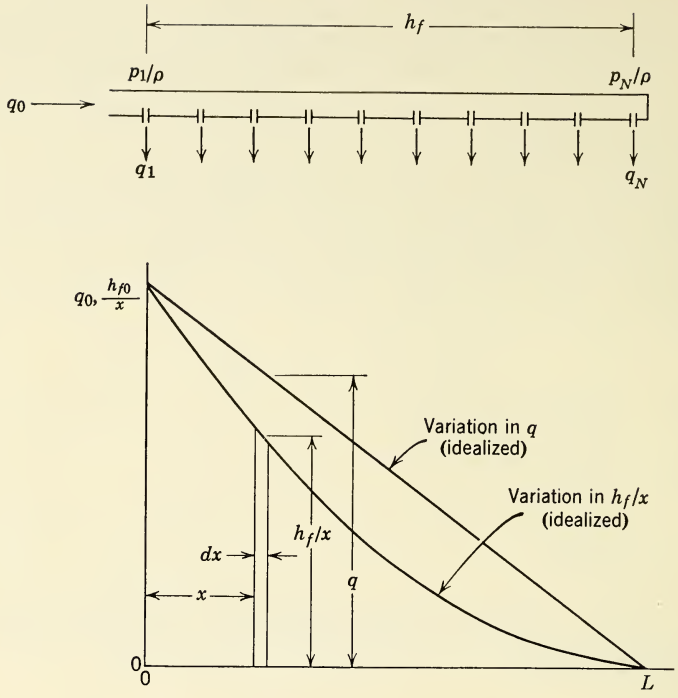

FIGURE 1-15. Frictional head loss when flow decreases uniformly. [After Figure 4, Fair, G. M., *J. Inst. Water Engrs.*, **5**, No. 2 (March 1951).]

1-8. Flow Equalization Through Multiple Outlets

The equalization of flow through multiple outlets is a problem frequently encountered in fluid transport. Precise equalization can be gained only if the frictional head losses from the common inlet to points just outside the outlets are exactly equal. An approximate equalization is often satisfactory and can be obtained simply by making the head loss across each outlet large in comparison to the head loss along the length of the conduit.

A pipe with multiple outlets is shown in Figure 1-15. The relationship between the flows through the first and last outlets is [11]

$$q_N = \gamma q_1 \tag{1-41}$$

[11] Fair, G. M., "The Hydraulics of Rapid Sand Filters," *J. Inst. Water Engrs.*, **5**, No. 2 (March 1951), 171–213.

where q_1 and q_N = volumetric rates of flow through first and last outlets respectively, ft^3/sec

γ = ratio of flow through the last outlet to that through the first

Since frictional losses occur in the pipe, p_N/ρ will be less than p_1/ρ, q_N will be less than q_1, and γ will have a value less than unity.

If the outlets are considered to be orifices [12]

$$h_{f1} = Kq_1^2 \tag{1-42}$$

and

$$h_{fN} = Kq_N^2 \tag{1-43}$$

where h_{f1} and h_{fN} = frictional head losses across first and last outlets respectively, (ft)(lb force)/(lb mass)

K = constant

Combining Equations 1-41, 1-42, and 1-43 gives

$$h_{fN} = K(\gamma q_1)^2 = \gamma^2 h_{f1} \tag{1-44}$$

Since the head loss from the entrance of the pipe to points outside all the outlets must be the same,

$$h_f + h_{fN} = h_{f1} \tag{1-45}$$

and

$$h_{fN} = h_{f1} - h_f = \gamma^2 h_{f1} \tag{1-46}$$

where h_f = frictional head loss in pipe from first to last outlet, (ft)(lb force)/(lb mass).

Therefore

$$h_f = h_{f1} - \gamma^2 h_{f1} = h_{f1}(1 - \gamma^2) \tag{1-47}$$

For any selected value of γ, the head loss in the pipe necessary to produce the flow q_N in the last outlet can be computed with Equation 1-47.

As a fluid flows through the multioutlet pipe shown in Figure 1-15, the flow rate is reduced as increments of the flow are discharged through

[12] The equation for computing the flow through an orifice can be written as

$$q = CS\sqrt{2g_c h_f}$$

where C = coefficient of discharge

S = cross-section area, ft^2

If the orifices are of the same shape and size,

$$h_f = \left(\frac{1}{2g_c C^2 S^2}\right) q^2 = Kq^2$$

successive outlets. The reduction in flow rate is accompanied by a decreasing head loss per unit length of pipe. Although flow rate and change in head loss would vary stepwise along the pipe, both are idealized in Figure 1-15 where they are represented as varying uniformly.

The head loss due to friction occurring at x distance from the inlet end of the pipe is

$$h_f = \int_0^x \frac{h_f}{x}\, dx \tag{1-48}$$

According to the Darcy-Weisbach expression (Equation 1-16), the head loss per unit length of pipe is proportional to the square of the mean flow velocity and, hence, to the square of the rate of flow

$$\frac{h_f}{x} = K'q^2 \tag{1-49}$$

where K' = constant.

If the outlets are evenly spaced along the pipe, the flow at x distance from the inlet will be

$$q = q_0 \frac{L - x}{L} \tag{1-50}$$

where q_0 = volumetric rate of flow at inlet, ft^3/sec
L = length of pipe, ft

By substituting Equations 1-49 and 1-50 in Equation 1-48 and integrating between the limits of 0 and x,

$$\begin{aligned} h_f &= \frac{K'{q_0}^2}{L^2} \int_0^x (L - x)^2\, dx \\ &= \frac{K'{q_0}^2}{L^2} \left(L^2x - Lx^2 + \frac{1}{3}x^3 \right) \\ &= K'{q_0}^2 \left(x - \frac{x^2}{L} + \frac{1}{3}\frac{x^3}{L^2} \right) \end{aligned} \tag{1-51}$$

If the flow at the inlet, q_0, were to flow the length of the pipe, i.e., if the only outlet were at the end of the pipe, the head loss per unit length of pipe would be

$$\frac{h_{f0}}{L} = K'{q_0}^2 \tag{1-52}$$

where h_{f0} = frictional head loss across pipe when flow is q_0, lb force/ft^3.

Therefore, Equation 1-51 can be written as

$$h_f = h_{f0}\left[\frac{x}{L} - \left(\frac{x}{L}\right)^2 + \frac{1}{3}\left(\frac{x}{L}\right)^3\right] \tag{1-53}$$

and for $x = L$,

$$h_f = \tfrac{1}{3}h_{f0} \tag{1-54}$$

According to Equation 1-54, the head loss across a pipe with multiple, evenly spaced outlets is approximately equal to one-third of the head loss that would result if the entrance flow were to pass through the length of the pipe.

EXAMPLE 1-4

Water at a rate of 0.4 ft^3/sec is to enter one end of a 10-ft long cast-iron pipe and be discharged through 20 identical orifices evenly spaced along the length of the pipe. The discharges through the two orifices on opposite ends are to differ no more than 1 percent from each other. Assuming the constant in Equation 1-42 to be 2×10^4, what is the diameter of the smallest pipe that can be used

Solution

1. Compute the head loss across the orifice closest to the entrance (Equation 1-42).

$$h_{f1} = 2 \times 10^4(0.4/20)^2 = 8 \text{ (ft)(lb force)/(lb mass)}$$

2. Compute the head loss across the 10-ft pipe (Equation 1-47).

$$h_f = 8(1 - 0.99^2) = 0.16 \text{ (ft)(lb force)/(lb mass)}$$

3. Compute the head loss that would occur across the pipe if 0.4 ft^3/sec were to flow the length of the pipe (Equation 1-54).

$$h_{f0} = 3 \times 0.16 = 0.48 \text{ (ft)(lb force)/(lb mass)}$$

4. Compute the pipe diameter (Equation 1-34).

$$\bar{V} = \frac{4q}{\pi D^2} = 1.318C_H\left(\frac{D}{4}\right)^{0.63}\left(\frac{h'_f}{L}\right)^{0.54}$$

$$D = \left[\frac{q}{0.431C_H\left(\frac{h'_f}{L}\right)^{0.54}}\right]^{0.38} = \left(\frac{0.4}{43.1 \times 0.195}\right)^{0.38} = 0.315 \text{ ft} = 3.78 \text{ in.}$$

Notations

a Acceleration, ft/sec^2
A Area, ft^2
C Coefficient and constant of integration
C_H Hazen-Williams coefficient; C'_H, modified coefficient
D Diameter, ft; D_p, particle diameter
e Kinematic eddy viscosity, ft^2/sec
f Friction factor, dimensionless
F Force, lb force; F_x, force acting in x direction
g Acceleration of gravity, ft/sec^2
g_c Newton's law conversion factor, 32.17 (ft)(lb mass)/(lb force)(sec^2)
h_f Permanent head loss due to friction, (ft)(lb force)/(lb mass); h_{f0}, head loss when flow is q_0; h'_f, feet of friction head loss, ft
k Adiabatic compression exponent
K, K' Constants
l Prandtl mixing length, ft
L Length, ft
m Mass, lb force
N_{Fr} Froude number, dimensionless
N_{Re} Reynolds number, dimensionless
p Pressure, lb force/ft^2; p_1, pressure at point 1; p_c, pressure of a compressed gas; p_2, pressure at point 2; Δp, pressure drop due to friction; $\Delta p'$, frictional pressure drop in a suspension; p_N, pressure at last outlet.
q Volumetric rate of flow, ft^3/sec; q_c, volumetric flow rate of compressed gas; q_1, flow rate through first outlet; q_N, flow rate through last outlet; q_0, flow rate at inlet
r Radius, ft; r_w, radius of pipe
r_H Hydraulic radius, ft
S Cross-section area, ft^2
T_A Absolute temperature, °R; T_{Ac}, absolute temperature of compressed gas
u Local velocity, ft/sec; u_y, velocity in y direction; Δu_y, difference in velocity components in y direction; Δu_x, difference in velocity components in x direction
du/dy Point velocity gradient, sec^{-1}
$\overline{V}$ Mean velocity of flow, ft/sec; $\overline{V}_1$, mean velocity at point 1; $\overline{V}_2$, mean velocity at point 2
x Distance, ft
x_M Weight fraction of water; x_{ML}, limiting moisture content
x_v Volumetric fraction of solids in suspension
y Distance from pipe wall, ft
Z Height above arbitrary datum plane, ft; Z_1, height of channel invert at point 1; Z_2, height of channel invert at point 2
γ Specific weight, lb force/ft^3
γ Ratio

ϵ Absolute roughness of surface, ft

η Eddy viscosity, (lb mass)/(ft)(sec)

κ Universal constant in turbulent flow

μ Absolute viscosity of a fluid, (lb mass)/(ft)(sec); μ_m, absolute viscosity of a suspension; μ', analogous viscosity term

μ_R Coefficient of rigidity, (lb mass)/(ft)(sec)

ν Kinematic viscosity, ft^2/sec

ρ Mass density of a fluid, lb mass/ft^3; ρ_s, mass density of a solid; ρ_m, mean mass density of a suspension

τ Shear stress, lb force/ft^2; τ_ν, shear stress resulting from viscosity; τ_t, shear stress resulting from turbulence; τ_0, shear stress at yield point

ψ Operator

2

Fluid transport in open conduits

2-1. Introduction

Open-channel flow differs from flow in pressure conduits in that a *free surface* is present in the former. Open channels of direct concern to the sanitary engineer include flumes, short weir channels, and partly filled pipes.

Flow in open channels can be either *steady* or *unsteady*, depending on whether or not the depth at a point remains constant. In addition, flow can either be *uniform* or *nonuniform*. Flow is uniform when the depth of the liquid is the same at all points along the channel and nonuniform when the depth varies.

A definition sketch is shown in Figure 2-1 for the flow of a liquid in an open channel. The energy balance can be written as

$$\frac{g}{g_c} Z_1 + \frac{g}{g_c} y_1 + \frac{\overline{V}_1^2}{2g_c} = \frac{g}{g_c} Z_2 + \frac{g}{g_c} y_2 + \frac{\overline{V}_2^2}{2g_c} + h_f \quad (2\text{-}1)$$

where $\frac{g}{g_c} y$ = depth, (ft)(lb force)/(lb mass)

h_f = frictional head loss, (ft)(lb force)/(lb mass)

As a rule, interest centers about the determination of the velocity produced by a given slope, or, conversely, about the

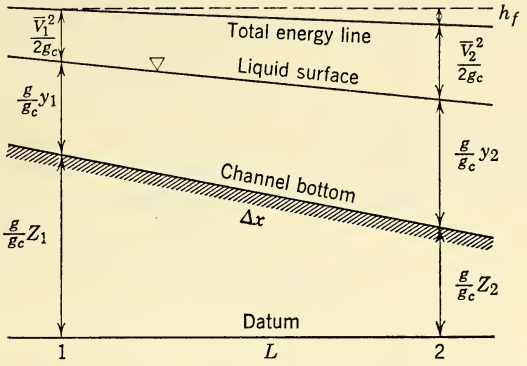

FIGURE 2-1. Notation for flow in open channels.

determination of a slope to give a desired velocity. Flow may be either laminar or turbulent.

2-2. Laminar Flow

Attention is directed to Figure 2-2. Here liquid is in laminar flow down a surface inclined at an angle α with the horizontal. The gravitational force producing flow in a layer located at the top of the liquid and

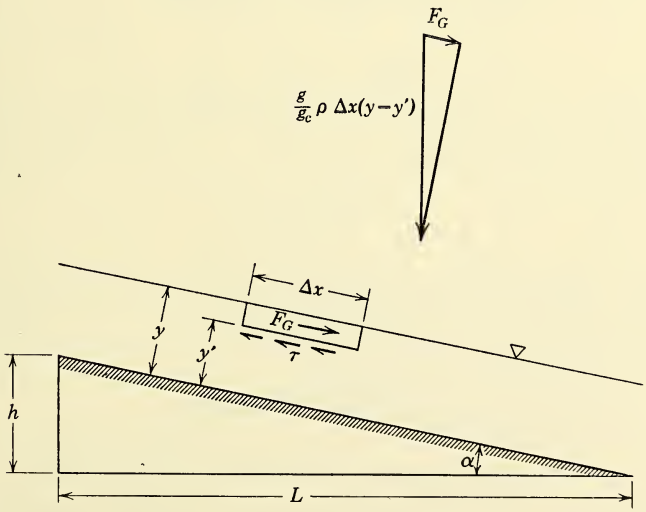

FIGURE 2-2. Flow of liquid over an inclined surface.

having a width equal to unity, a length Δx and a thickness $(y - y')$ is

$$F_G = \frac{g}{g_c} \rho \, \Delta x (y - y') \sin \alpha \tag{2-2}$$

The viscous force resisting flow is

$$F_R = \tau \, \Delta x = \frac{\mu}{g_c} \frac{du}{dy} \Delta x \tag{2-3}$$

At constant velocity the two forces are in equilibrium. Therefore,

$$\mu \frac{du}{dy} = g\rho(y - y') \sin \alpha \tag{2-4}$$

$$\int du = \frac{g\rho}{\mu} \sin \alpha \int (y - y') \, dy \tag{2-5}$$

$$u = \frac{g\rho}{\mu} \sin \alpha \left(yy' - \frac{1}{2} y'^2 \right) + \text{constant} \tag{2-6}$$

Since the velocity at the bottom of the channel is zero ($u = 0$ at $y = 0$), the constant in Equation 2-6 also is zero.

Equation 2-6 defines the flow velocity at any distance y' from the inclined surface. The volumetric flow rate per unit width of surface will be

$$q' = \int_0^y \left[\frac{g\rho}{\mu} \sin \alpha \left(yy' - \frac{1}{2} y'^2 \right) \right] dy$$

$$= \frac{g\rho}{\mu} \sin \alpha \left[\frac{yy'^2}{2} - \frac{y'^3}{6} \right]_0^y = \frac{g\rho}{3\mu} \sin \alpha \, y^3 \tag{2-7}$$

and the mean velocity of flow

$$\overline{V} = \frac{g\rho}{3\mu} \sin \alpha \, y^2 \tag{2-8}$$

where q' = volumetric flow rate per unit width of surface, ft^2/sec
$\overline{V}$ = mean flow velocity, ft/sec
g = acceleration of gravity, ft/sec^2
ρ = mass density, lb mass/ft^3
μ = absolute viscosity, (lb mass)/(ft)(sec)
y = liquid depth, ft
α = angle of inclination

Where the angle α is small, the sine function can be replaced by the ratio h/L.

Equations 2-7 and 2-8 may be applied to laminar flow in open channels provided the depth of flow is sufficiently shallow to minimize the effect of the sides on the local velocities.

As discussed in Section 1-6, flow equations developed for circular cross sections are often applied to cross sections of other shapes by using for the diameter an equivalent term, $4r_H$. By substituting the equivalent term in the Darcy-Weisbach expression (Equation 1-16) and solving for the friction factor,

$$f = \frac{8h_f r_H g}{L\overline{V}^2} \tag{2-9}$$

Experimental observations [1] have shown that for laminar flow of water in wide open channels

$$f = \frac{96}{N_{Re}} \tag{2-10}$$

where N_{Re} = Reynolds number expressed as $4r_H\overline{V}\rho/\mu$. The laminar state extends up to $N_{Re} = 4000$. Transition to fully turbulent conditions is completed at $N_{Re} = 11{,}000$.

Flow in open channels will be laminar if the cross section and velocity are extremely small or the viscosity is very high. When the liquid is water, the laminar state will be achieved only when it flows as a thin sheet across an inclined surface. Little or no information is available concerning the flow characteristics of plastic liquids in open channels.

2-3. Turbulent Flow

Figure 2-1 depicts a condition in which the flow in a rectangular channel is steady and nonuniform. According to Equation 2-1, the mechanical energy loss per unit of mass, as the liquid passes from point 1 to point 2, is

$$h_f = \frac{g}{g_c}(Z_1 - Z_2) + \frac{g}{g_c}(y_1 - y_2) + \frac{1}{2g_c}(\overline{V}_1^2 - \overline{V}_2^2) \tag{2-11}$$

The total energy lost between the two points by the liquid occupying a unit length of the channel will be

$$E_T = h_f \rho \bar{y} b \tag{2-12}$$

where b = channel width, ft

$\bar{y}$ = mean depth of liquid between points 1 and 2, ft

[1] Owen, W. M., "Laminar to Turbulent Flow in a Wide Open Channel," *Proc. ASCE*, **79**, separate No. 188 (April 1953).

The energy loss E_T is the result of the resistance offered to flow by shear stresses established along the wetted surface of the channel. The energy consumed by these stresses, as the liquid occupying a unit length of the channel flows between points 1 and 2, will be

$$E_s = \tau_w(b + 2\bar{y})\ \Delta x \tag{2-13}$$

where τ_w = average shear stress along the sides per unit of wetted area, lb force/ft^2
Δx = length of channel between points 1 and 2, ft

Disregarding any change in the internal energy of the liquid, E_T is equal to E_s,

$$\tau_w(b + 2\bar{y})\ \Delta x = h_f \rho \bar{y} b \tag{2-14}$$

and

$$\tau_w = \rho \left(\frac{b\bar{y}}{b + 2\bar{y}}\right) \frac{h_f}{\Delta x} \cong \rho \bar{r}_H \frac{h_f}{L} \tag{2-15}$$

where $\bar{r}_H$ = mean hydraulic radius of the wetted surface, ft
L = horizontal distance between points 1 and 2, ft

Where the angle at which the channel bottom makes with the horizontal is small, the term $h_f/\Delta x$ may be replaced by h_f/L. The latter term is the slope of the total energy line.

By dividing both sides of Equation 2-15 by the term $\rho\overline{V}^2/g_c$ and solving for $\overline{V}^2$

$$\overline{V}^2 = \frac{(g_c \bar{r}_H h_f)/L}{\tau_w/(\rho\overline{V}^2/g_c)} \tag{2-16}$$

When flow is turbulent, the term $\tau_w/(\rho\overline{V}^2/g_c)$ is, for all practical purposes, independent of the mean velocity.[2] However, the term is a function of the roughness of the channel surface. Experimentally, it has been found that

$$\frac{\tau_w}{\rho\overline{V}^2/g_c} = \frac{1}{16}\left(\frac{\epsilon}{4\bar{r}_H}\right)^{1/3} \tag{2-17}$$

where ϵ = absolute roughness of the surface, ft.

By substituting Equation 2-17 into Equation 2-16 and taking the square root of both sides of the latter equation,

$$\overline{V} = \left[4g_c^{1/2}\left(\frac{4}{\epsilon}\right)^{1/6}\right] \bar{r}_H^{2/3} \left(\frac{h_f}{L}\right)^{1/2} \tag{2-18}$$

[2] Coulson, J. M., and J. F. Richardson, *Chemical Engineering*, Vol. 1, McGraw-Hill Book Co., New York (1954), pp. 67–68.

Equation 2-18 is similar in form to the Manning equation,[3] a hydraulic relationship of the exponential type developed empirically for turbulent flow in open channels. The equation can be written as

$$\overline{V} = \frac{1.486}{n} \bar{r}_H^{2/3} \left(\frac{h'_f}{L}\right)^{1/2} \tag{2-19}$$

where h'_f = head loss due to friction, ft of water
n = coefficient of roughness

Values of the coefficient of roughness for different types of conduit material are listed in Table 2-1.

TABLE 2-1. VALUES OF THE ROUGHNESS COEFFICIENT n FOR DIFFERENT KINDS OF CONDUITS *

Kind of Conduit	Condition of Interior Surface			
	Best	Good	Fair	Bad
Vitrified-clay sewer pipe	0.010	0.013	0.015	0.017
Unglazed-clay drainage tile	0.011	0.012	0.014	0.017
Concrete pipe	0.012	0.013	0.015	0.016
Cement-mortar surfaces	0.011	0.012	0.013	0.015
Concrete-lined channels	0.012	0.014	0.016	0.018
Semicircular metal flumes, smooth	0.011	0.012	0.013	0.015
Semicircular metal flumes, corrugated	0.023	0.025	0.028	0.030
Wood-stave pipe	0.010	0.011	0.012	0.013

* Selected from values found in Seelye, E. E., *Data Book for Civil Engineers*, Vol. I—*Design*, John Wiley and Sons, New York (1960). Values originally compiled by R. E. Horton.

Equations 2-18 and 2-19 can be applied to the solution of problems in which liquid is in turbulent flow through sections other than rectangular. They can be used also in the solution of problems in which the conduit is closed, such as a sewer pipe, and the flow is through either a full or a partially filled section. The nomograph in Appendix 5 can be used to facilitate the use of the Manning equation in the solution of pipe-flow problems when the value of n is equal to 0.013. A chart in

[3] Manning, Robert, "Flow of Water in Open Channels and Pipes," *Trans. Inst. Civil Engr. Ireland*, **20** (1890).

Appendix 6 gives the hydraulic elements of partially filled circular sections.

In steady uniform flow, the depth and velocity remain unchanged from point to point, and the mechanical energy loss is at the expense of the potential energy only. For such flow the slope of the total energy line is parallel to both the liquid surface and the bottom of the channel.

EXAMPLE 2-1

At what depth will 80 ft^3/sec of water flow in a rectangular channel, 3 ft wide and lined with concrete, if the bottom of the channel is constructed on a slope of 7 ft in 1000 ft? Assume flow to be steady and uniform.

Solution

1. From Table 2-1, $n = 0.015$.
2. When flow is uniform, the slope of the total energy line h_f/L is equal to the slope of the channel bottom, or

$$h'_f/L = 0.007$$

3. According to Equation 2-19,

$$\overline{V} = \frac{q}{3y} = \frac{1.486}{n}\left(\frac{3y}{3+2y}\right)^{2/3}\left(\frac{h'_f}{L}\right)^{1/2}$$

$$\frac{(3y)^{5/3}}{(3+2y)^{2/3}} = \frac{0.015 \times 80}{1.486(0.007)^{1/2}} = 9.65$$

4. By trial and error

$$y = 3.2 \text{ ft}$$

2-4. Limiting Velocities

The relationship discussed in Section 1-7 for determining the limiting velocities in pressure pipes was derived empirically. A more rational expression has been developed for the determination of scouring velocities in open channels.

The maximum resistance offered to a liquid in turbulent flow by granular materials resting along the bottom of the channel can be expected to be a function of the thickness of the laminar sublayer relative to the size of the resting particles and the effective weight of the particles. If a flowing liquid is to bring about movement of the particles, then the average intensity of the tractive force along the wetted surface must at least be equal to the maximum resistance of the particles.

$$\tau'_w = \psi\left(\frac{D_p}{\delta}, \rho_s - \rho, D_p\right) \tag{2-20}$$

where τ'_w = average shear stress along wetted surface at the velocity where movement of particles is impending, lb force/ft^2
D_p = particle diameter, ft
δ = thickness of laminar sublayers, ft
ρ_s = mass density of particle, lb mass/ft^3
ρ = mass density of liquid, lb mass/ft^3

Experimentally, it has been shown that [4]

$$\frac{g_c \tau'_w}{g(\rho_s - \rho)D_p} = \phi\left(\frac{D_p}{\delta}\right) \cong K \tag{2-21}$$

where K = constant
g = acceleration of gravity, ft/sec^2
g_c = Newton's law conversion factor, (ft)(lb mass)/(lb force)(sec^2)

For materials of uniform shape and size and for fine nonuniform sand, the value of K is closely equal to 0.04. This value, in the case of the nonuniform sand, corresponds to the mean grain size.[5] The value of K for flocculent and sticky materials can be expected to be higher.

Equation 2-15 is a relationship between the tractive forces at the wetted surfaces and the frictional loss. Substituting this expression for τ'_w in Equation 2-21 and solving for h_f results in

$$h_f = \frac{gK[(\rho_s - \rho)/\rho]D_p L}{g_c \bar{r}_H} \tag{2-22}$$

The Darcy-Weisbach equation (Equation 1-16) can be modified for application to open-channel flow.

$$h_f = f \frac{L}{4\bar{r}_H} \frac{\overline{V}^2}{2g_c} \tag{2-23}$$

By equating Equations 2-22 and 2-23 and solving for $\overline{V}$,

$$\overline{V}_L = \left[\frac{8gK}{f}\left(\frac{\rho_s - \rho}{\rho}\right) D_p\right]^{1/2} \tag{2-24}$$

where $\overline{V}_L$ = limiting mean velocity of flow, ft/sec
f = friction factor, dimensionless

[4] Shields, A., "Anwendung der Aehnlichkeitsmechanik und der Turbulenzeforschung auf die Geschiebebewegung," *Mitteilungen der Preussischen Versuchsanstalt für Wasserbau und Schiffbau*, No. 26, Berlin (1936).

[5] *Paper No. 17*, U. S. Waterways Experiment Station, Vicksburg, Miss. (January 1935).

Likewise, the Manning equation (Equation 2-19) can be combined with Equation 2-22 to give

$$\overline{V}_L = \frac{1.486}{n} \bar{r}_H^{1/6} \left[K \left(\frac{\rho_s - \rho}{\rho} \right) D_p \right]^{1/2} \tag{2-25}$$

where $\bar{r}_H$ = mean hydraulic radius of channel, ft
n = coefficient of roughness

Care must be taken in selecting the proper values of f and n. If the velocity is to be kept greater than the velocity of scour, these coefficients should correspond to the surface roughness of the clean channel. At lower velocities, they should reflect the roughness imparted by the deposits.

EXAMPLE 2-2

An aqueous suspension of sand particles (sp gr = 2.65) having a mean diameter of 0.1 mm is to flow through a rectangular, concrete channel at a rate of 4 ft^3/sec. If the flow depth is to be maintained at 3 ft, how narrow must the channel be to ensure no deposition along the bottom?

Solution

1. Equation 2-25 can be written as

$$\frac{q}{S} = \frac{q}{yb} = \frac{1.486}{n} \left(\frac{yb}{b + 2y} \right)^{1/6} \left[K \left(\frac{\rho_s - \rho}{\rho} \right) D_p \right]^{1/2}$$

2. Assuming that $n = 0.015$ (Table 2-1), and that $K = 0.04$

$$\frac{4}{3b} = \frac{1.486}{0.015} \left(\frac{3b}{b + 6} \right)^{1/6} [0.04 \times 1.65(0.1 \times 3.28 \times 10^{-3})]^{1/2}$$

3. Solving for b

$$\frac{3.61b^{1.167}}{(b + 6)^{0.167}} = 7.9$$

by trial and error

$$b = 2.68 \text{ ft}$$

2-5. Specific Energy

The energy per unit mass of a liquid with respect to the bottom of the channel in which it is contained is called the *specific energy*.

$$E = \frac{g}{g_c} y + \frac{\overline{V}^2}{2g_c} \tag{2-26}$$

A plot of the specific energy E as a function of the depth y is presented in Figure 2-3. From the curve it can be seen that for a given discharge there exists a depth y_c at which the specific energy is a minimum. The velocity of flow at the critical depth is called the critical velocity $\overline{V}_c$. When for the given discharge the depth of flow is greater than the critical depth, flow conditions are said to be *tranquil*; when depths occur which are smaller than the critical depth, *rapid* flow conditions are said to prevail. For any value of specific energy except the minimum, there are two depths, called *conjugate depths*, at which flow is possible. It is to be noted that the upper leg of the curve merges with a straight line inclined 45° with the horizontal. All points along the latter represent the potential energy component of the specific energy.

If an obstruction which increases the flow depth is placed suddenly across a channel in which a liquid is flowing, a surge wave will form which

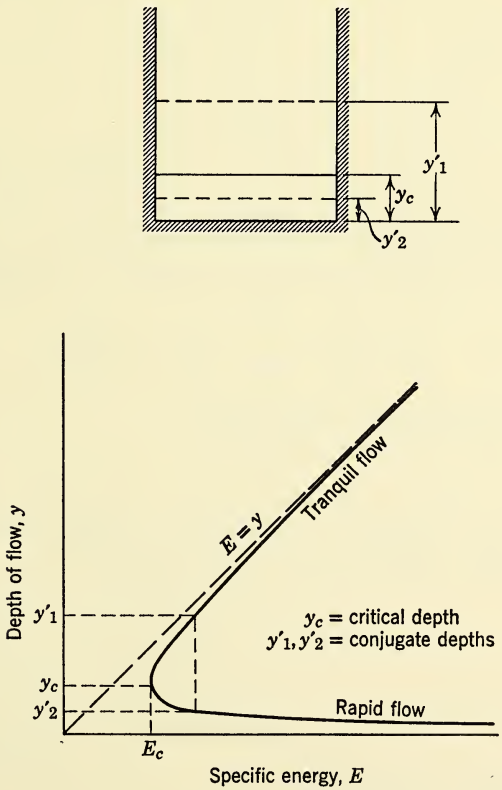

FIGURE 2-3. Specific energy as a function of depth, discharge remaining constant.

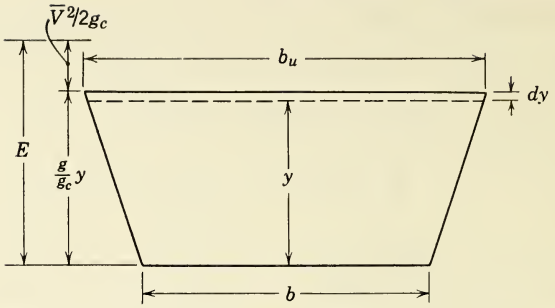

FIGURE 2-4. Specific energy of liquid flowing through a trapezoidal channel.

will tend to move upstream against the motion of the oncoming liquid. When flow is tranquil, the flow velocity is so low that a small disturbance such as a surge wave can be transmitted upstream and, thereby, change upstream conditions. Thus, flow is controlled by conditions downstream. When flow is rapid, the liquid velocity is greater than that of a surge wave, and any such disturbance formed is carried downstream. At critical flow, the velocity is equal to the velocity of a surge wave.

There is a criterion applicable to all channels which gives the relationship existing between the discharge and cross section of flow when flow conditions are critical. Attention is directed to Figure 2-4. The specific energy of the liquid flowing through the trapezoidal section is

$$E = \frac{g}{g_c} y + \frac{\overline{V}^2}{2g_c} = \frac{g}{g_c} y + \frac{q^2}{2g_c S^2} \tag{2-27}$$

where q = volumetric flow rate, ft^3/sec
S = channel cross section, ft^2

For a given discharge, the cross section at the critical depth is found when the specific energy is a minimum. By differentiating Equation 2-27 with respect to the depth y, and equating to zero,

$$\frac{dE}{dy} = \frac{g}{g_c} - \frac{q^2}{g_c S^3} \frac{dS}{dy} = 0 \tag{2-28}$$

Since at critical flow

$$q = S\overline{V}_c \tag{2-29}$$

and the change in S is given by

$$dS = b_u \, dy \tag{2-30}$$

Equation 2-28 can be written as

$$\frac{\overline{V}_c^2}{g} = \frac{S}{b_u} \tag{2-31}$$

where $\overline{V}_c$ = flow velocity at critical depth, ft/sec
b_u = top width of channel, ft

By multiplying both sides by S^2, Equation 2-31 becomes

$$\frac{q^2}{g} = \frac{S^3}{b_u} \tag{2-32}$$

When the relationship given in Equation 2-32 is obtained, flow is critical. The equation holds for any cross section, as long as the term b_u expresses the width at the top of the channel.

A more specific relationship can be developed for rectangular channels. For such channels Equation 2-32 can be expressed as

$$\frac{q^2}{g} = y_c^3 b^2 \tag{2-33}$$

or as

$$y_c = \left(\frac{q^2}{gb^2}\right)^{1/3} \tag{2-34}$$

where y_c = critical depth, ft
b = channel width, ft

Equations 2-18 and 2-19 are strictly applicable only to the solution of problems in which flow is tranquil. When flow is rapid, sizable quantities of air may become entrained in the liquid, causing both a reduction in density and an increase in volume. The Manning equation is often employed in the design of channels with steep slopes, but a modified roughness coefficient n' is substituted for the appropriate n value. The modified coefficient to be used for rectangular channels can be estimated from the following empirical relationship.[6]

$$n' = n\left\{\frac{1 + (2/b)(C\overline{V}^2/g)}{1 + (C\overline{V}^2/g)[(\overline{V}b/q) + (2/b)]}\right\}^{2/3} \tag{2-35}$$

where n = Mannings roughness coefficient
b = channel width, ft
q = volumetric rate of flow, ft^3/sec
$\overline{V}$ = mean flow velocity, ft/sec
g = acceleration of gravity, ft/sec^2
C = coefficient

[6] Hall, L. S., "Open Channel Flow at High Velocities," *Trans. ASCE*, **108** (1943), 1393–1434.

For concrete channels, the use of a value of 0.006 for C is recommended. This value is slightly larger than the average for the tests on which Equation 2-35 is based, and affords some factor of safety. The use of Equation 2-35 with Equation 2-19 requires a trial-and-error solution.

EXAMPLE 2-3

Determine the critical depth for water flowing at a rate of 4 ft^3/sec in a trapezoidal channel 2 ft wide at the bottom and with side slopes of 2:1 (vertical:horizontal).

Solution

1. From Equation 2-32,

$$\frac{S^3}{b_u} = \frac{q^2}{g} = \frac{4^2}{32.2} = 0.498$$

2. From a consideration of the geometric relationships,

$$S = y_c\left(\frac{2 + b_u}{2}\right) \qquad \text{and} \qquad b_u = 2 + y_c$$

3. Through substitution

$$\frac{(2y_c + 0.5y_c^2)^3}{2 + y_c} = 0.498$$

4. By trial and error,

$$y_c = 0.48 \text{ ft}$$

2-6. Hydraulic Jump

When rapid flow conditions are induced in liquid flowing in a channel with characteristics which promote tranquil flow, flow is unstable and a hydraulic jump will result. Attention is directed to Figure 2-5. Here,

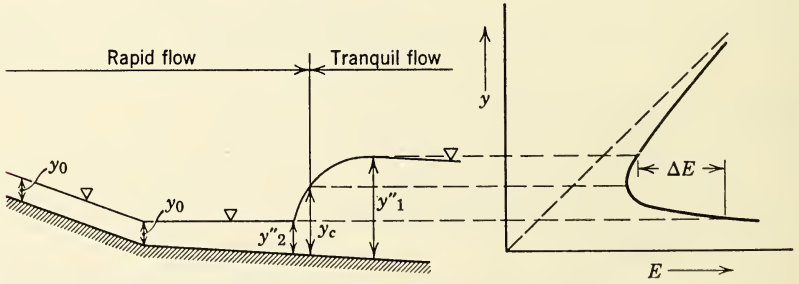

FIGURE 2-5. Specific energy relationships occurring in a hydraulic jump.

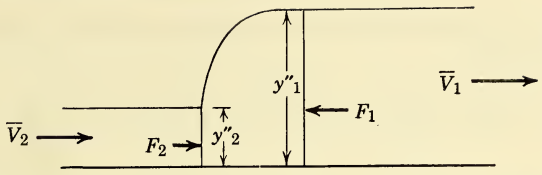

FIGURE 2-6. Hydrostatic forces acting at a hydraulic jump.

liquid flowing initially in a channel with a slope such that flow is in the rapid state flows into a second reach of channel with a slope less than critical. The flow depth increases gradually from y_0 to y''_2. At the latter depth, the depth changes abruptly to y''_1, which either is normal for the new slope or is controlled by down-channel conditions. The abrupt change is called a hydraulic jump. Flow conditions down-channel from the jump are tranquil.

The problem usually encountered in connection with the hydraulic jump is that of determining from a knowledge of the down-channel depth, or y''_1, the depth from which the jump takes off, or y''_2. The turbulence produced in a jump results in a sizable loss of energy. Consequently, a specific energy balance across the jump cannot be used. Instead, resort is made to the momentum relationships involved.

The change in the linear momentum of a liquid with respect to time is equal to the resultant force acting on the liquid. Neglecting frictional forces, the forces active over the jump are the hydrostatic forces at both ends of the liquid in the jump (Figure 2-6).

$$F_1 - F_2 = \frac{\rho q}{g_c}(\overline{V}_2 - \overline{V}_1) \tag{2-36}$$

$$\frac{g\rho b}{2g_c}(y''_1{}^2 - y''_2{}^2) = \frac{\rho q}{g_c}(\overline{V}_2 - \overline{V}_1) \tag{2-37}$$

$$\frac{y''_1{}^2}{2} - \frac{y''_2{}^2}{2} = \frac{q^2}{gb^2}\left(\frac{1}{y''_2} - \frac{1}{y''_1}\right) \tag{2-38}$$

Solving for y''_2,

$$y''_2 = \frac{y''_1}{2}\left[\left(1 + \frac{8q^2}{gb^2 y''_1{}^3}\right)^{1/2} - 1\right] \tag{2-39}$$

where y''_1 = depth downstream from jump, ft
y''_2 = depth immediately upstream from jump, ft
q = volumetric rate of flow, ft^3/sec
g = acceleration of gravity, ft/sec^2

The energy lost as the result of turbulence produced in the jump can be computed from

$$\Delta E = \left(\frac{g}{g_c} y''_2 + \frac{\overline{V}_2^2}{2g_c}\right) - \left(\frac{g}{g_c} y''_1 + \frac{\overline{V}_1^2}{2g_c}\right) \tag{2-40}$$

Surface profiles often are of interest in the solution of problems involving steady, nonuniform flow of liquids in open channels. By multiplying both sides of Equation 2-1 by $(g_c/g)L$ and rearranging terms,

$$L = \frac{[y_2 + (\overline{V}_2^2/2g)] - [y_1 + (\overline{V}_1^2/2g)]}{[(Z_1 - Z_2)/L] - (h'_f/L)} \tag{2-41}$$

where $(Z_1 - Z_2/L)$ is the slope of the channel invert. The term h'_f/L is the slope of the energy grade line and can be computed by means of the Manning equation (Equation 2-19). Starting at a known depth, the distance L is computed to a slightly different depth. If the increments of depth are small, a satisfactory profile of the liquid can be obtained.

A stepwise procedure employing Equation 2-41 can be used to locate the position of the hydraulic jump shown in Figure 2-5 relative to the point where the change of slope occurs in the channel. Both depths y_0 and y''_2 must be known, however. Another application is found in connection with the determination of the liquid surface profiles up-channel from a free discharge. Such a drop-down curve is shown in Figure 2-7. Here liquid flowing in a rectangular channel with a slope less than critical discharges freely into the atmosphere. The depth at

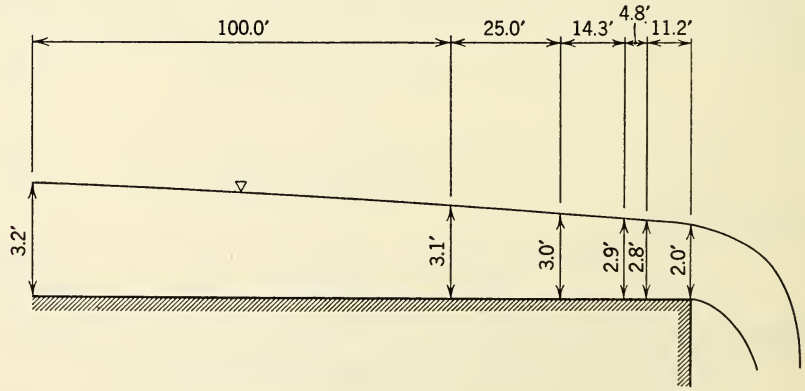

FIGURE 2-7. Drop-down curve up-channel from free discharge (Example 2-5).

the end is approximately $0.7y_c$ and the critical depth y_c has been found to occur at a distance of 3 to $4y_c$ from the end. The surface profile can be determined by starting at the discharge end and working up-channel in a series of steps, each involving a computation with Equation 2-41 (see Example 2-5).

EXAMPLE 2-4

A jump is to be induced in a rectangular channel 2 ft wide transporting 6 ft^3/sec of water. If the downstream depth is maintained at 2 ft, from what depth will the jump take off? How much energy will be lost in the jump?

Solution

1. From Equation 2-39

$$y''_2 = \frac{2}{2}\left[\left(1 + \frac{8 \times 6^2}{32.2 \times 2^2 \times 2^3}\right)^{1/2} - 1\right]$$

$$= 0.132 \text{ ft}$$

2. From Equation 2-40

$$\Delta E = \left[0.132 + \frac{(22.7)^2}{64.4}\right] - \left[2 + \frac{(1.5)^2}{64.4}\right]$$

$$= 6.11 \text{ (ft)(lb force)/(lb mass)}$$

$$P = 6.11 \times 62.4 \times 6 = 2280 \text{ (ft)(lb force)/(sec)}$$

$$= 2280(1.818 \times 10^{-3}) = 4.15 \text{ hp}$$

EXAMPLE 2-5

The rectangular channel described in Example 2-1 terminates in a free discharge. For a flow of 80 ft^3/sec, determine the coordinates of points on the drop-down curve.

Solution

1. According to Equation 2-34,

$$y_c = \left(\frac{q^2}{gb^2}\right)^{1/3} = \left(\frac{80^2}{32.2 \times 3^2}\right)^{1/3} = 2.8 \text{ ft}$$

2. Depth at discharge = $0.7y_c$ = 2.0 ft. Critical depth is $4y_c$ or 11.2 ft from discharge.

3. Compute horizontal distances between arbitrarily selected depths ranging from critical depth, 2.8 ft, to normal depth, 3.2 ft (see Table 2-2).

4. Plot coordinates and sketch in drop-down curve (see Figure 2-7).

TABLE 2-2. COMPUTATIONS FOR THE SOLUTION OF EXAMPLE 2-5

y	yb	$b + 2y$	$\frac{yb}{b+2y}$	$\overline{V}$	$\frac{\overline{V}^2}{2g}$	$y + \frac{\overline{V}}{2g}$	Average $\frac{yb}{b+2y}$	Average $\overline{V}$	$n\overline{V}$	$\frac{h'_f}{L}$	$\frac{Z_1 - Z_2}{L} - \frac{h'_f}{L}$	$-\left(y_1 + \frac{\overline{V}_1^2}{2g}\right)$	$\left(y_2 + \frac{\overline{V}_2^2}{2g}\right)$	L
2.80	8.40	8.60	0.976	9.52	1.41	4.20								
							0.983	9.36	0.1405	0.0091	−0.0021	−0.01		4.77
2.90	8.70	8.80	0.990	9.20	1.31	4.21								
							0.995	9.05	0.1360	0.0084	−0.0014	−0.02		14.30
3.00	9.00	9.00	1.000	8.90	1.23	4.23								
							1.005	8.75	0.1310	0.0078	−0.0008	−0.02		25.00
3.10	9.30	9.20	1.010	8.60	1.15	4.25								
							1.015	8.47	0.1270	0.0073	−0.0003	−0.03		100.00
3.20	9.60	9.40	1.020	8.33	1.08	4.28								

2-7. Short Weir Channels

Treatment process effluents often are collected at the surface of a vessel by means of a relatively short channel which receives the effluent along the length of the channel, laterally and over one or both sides, and discharges it at one end. In rapid sand filters such channels are called "wash-water gutters"; in settling basins they are referred to as "launders." These channels are not to be confused with "side weirs" in which the direction of flow is from the channel over the weir.

A sketch of a short weir channel is presented in Figure 2-8. The vertical scale is magnified to clarify the details of the sketch. From the standpoint of design, the most important consideration is the depth of

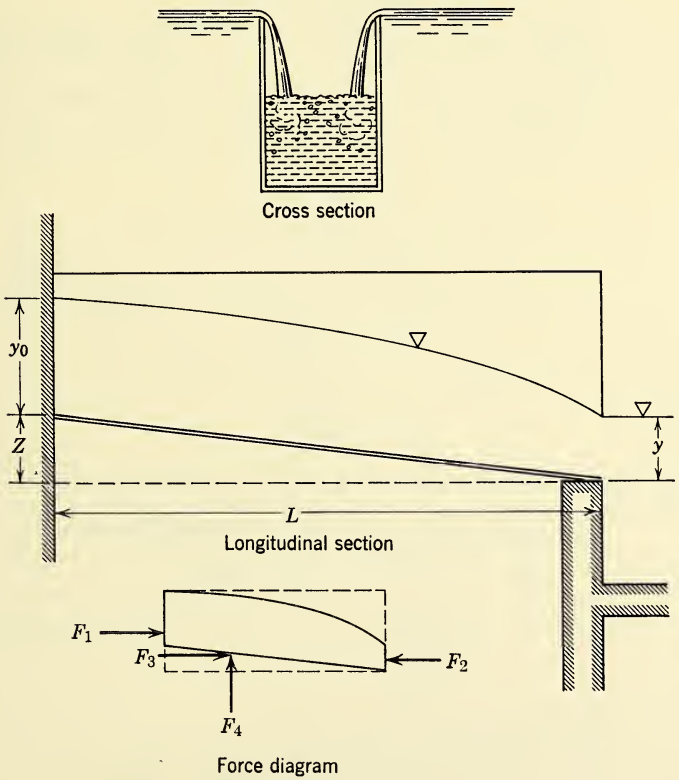

FIGURE 2-8. Flow in a short weir channel. [Adapted from Figure 6, Fair, G. M., *J. Inst. Water Engrs.*, **5**, No. 2 (March 1951).]

the liquid in the upper end of the channel, y_0. Momentum principles have been used to estimate this key dimension.[7]

The assumption is made that: (*a*) Flow inside the channel is in a horizontal direction and toward one end: (*b*) the liquid flowing over the sides of the channel imparts no momentum to the contents horizontally in the direction of discharge: (*c*) the drop-down curve describes a parabola; and (*d*) channel friction can be neglected. The change in the linear momentum of the liquid is equal to the resultant of the horizontal forces acting on the liquid.

$$\frac{\rho q}{g_c}\overline{V} = F_1 + F_3 - F_2 \tag{2-42}$$

where $\overline{V}$ = mean flow velocity at discharge end, ft/sec
q = volumetric rate of flow at discharge end, ft^3/sec
ρ = mass density of liquid, lb mass/ft^3
g_c = Newton's law conversion factor, (ft)(lb mass)/(lb force)(sec^2)
F_1, F_2, F_3 = horizontal, static forces acting on liquid in the channel, lb force

Since

$$q = by_c\overline{V}_c \tag{2-43}$$

$$\overline{V} = \frac{\overline{V}_c y_c}{y} \tag{2-44}$$

$$\overline{V}_c = \sqrt{2gy_c} \tag{2-45}$$

and

$$y_c = \left(\frac{q^2}{gb^2}\right)^{1/3} \tag{2-34}$$

The change in momentum term in Equation 2-42 becomes

$$\frac{\rho q\overline{V}}{g_c} = \frac{\rho}{g_c}(by_c\overline{V}_c)\frac{\overline{V}_c y_c}{y} = \frac{\rho}{g_c}\frac{by_c^2\overline{V}_c^2}{y} = \frac{\rho}{g_c}\frac{gby_c^3}{y} \tag{2-46}$$

where b = width of channel, ft
y_c = critical depth when flow is equal to q, ft
$\overline{V}_c$ = critical velocity when flow is equal to q, ft/sec

[7] Fair, G. M., and J. C. Geyer, *Water Supply and Waste-Water Disposal*, John Wiley and Sons, New York (1954), 690–691.

y = depth of flow at discharge end, ft
g = acceleration of gravity, ft/sec^2

The static forces acting on the liquid at ends of the channel are

$$F_1 = \frac{g\rho b y_0^2}{2g_c} \tag{2-47}$$

and

$$F_2 = \frac{g\rho b y^2}{2g_c} \tag{2-48}$$

where y_0 = depth of liquid at upper end of channel, ft.

The volume occupied by the liquid in the channel is

$$\begin{aligned} V &= (y_0 + Z)Lb - \tfrac{1}{2}ZLb - \tfrac{1}{3}(y_0 + Z - y)Lb \\ &= Lb(\tfrac{2}{3}y_0 + \tfrac{1}{6}Z + \tfrac{1}{3}y) \end{aligned} \tag{2-49}$$

where L = length of channel, ft
Z = vertical distance between upper and discharge ends of channel, ft

Accordingly, the horizontal force acting at the bottom of the channel is

$$F_3 = Zb\left(\frac{g\rho}{g_c}\right)\left(\frac{2}{3}y_0 + \frac{1}{6}Z + \frac{1}{3}y\right) \tag{2-50}$$

Substituting the above expressions in Equation 2-42

$$\frac{y_c^3}{y} = \frac{y_0^2}{2} + Z\left(\frac{2}{3}y_0 + \frac{1}{6}Z + \frac{1}{3}y\right) - \frac{y^2}{2} \tag{2-51}$$

and

$$y_0 = \left[\frac{2y_c^3}{y} + \left(y - \frac{1}{3}Z\right)^2\right]^{1/2} - \frac{2}{3}Z \tag{2-52}$$

When the discharge at the end of the channel is free, $y \simeq y_c$, and

$$y_0 = (3y_c^2 - \tfrac{2}{3}y_cZ + \tfrac{1}{9}Z^2)^{1/2} - \tfrac{2}{3}Z \tag{2-53}$$

For level inverts ($Z = 0$), Equations 2-52 and 2-53 become

$$y_0 = \left(\frac{2y_c^3}{y} + y^2\right)^{1/2} \tag{2-54}$$

and

$$y_0 = 1.73y_c \tag{2-55}$$

The foregoing equations were developed for rectangular cross sections. However, the same expressions apply to channels having V-shaped and

semicircular bottoms, provided the depths y and y_c are taken as average depths over the channel width. For such cross sections Equation 2-34 can be used to compute the critical depth.

A more precise method of analyzing flow in weir channels can be found elsewhere.[8]

EXAMPLE 2-6

A rectangular wash-water gutter, 10 ft long and 1 ft wide, is to be constructed with the discharge end 3 in. lower than the opposite end. If the gutter is to handle 2 ft^3/sec of wash-water, how deep must the gutter be at the upper end?

Solution

1. Compute the critical depth (Equation 2-34).

$$y_c = \left(\frac{2^2}{32.2 \times 1^2}\right)^{1/3} = 0.5 \text{ ft}$$

2. Compute depth at upper end (Equation 2-53).

$$y_0 = [3(0.5)^2 - \tfrac{2}{3}(0.5)0.25 + \tfrac{1}{9}(0.25)^2]^{1/2} - \tfrac{2}{3}0.25$$

$$= 0.635 \text{ ft}$$

2-8. Continuous Flow Models

Most processes and unit operations employed by the sanitary engineer are carried out in continuous-flow systems. Since all chemical and biological processes and most unit operations are time-dependent, the retention time in such systems and, hence, the mixing characteristics displayed by the systems are of prime importance. The mixing characteristics vary with the design of the system and are usually too complex to be described by precise mathematics. Consequently, use is made of simple flow models in estimating these characteristics.

Three basic models have been defined, each in terms of the behavior of the individual increments of influent material.[9] *Plug flow* is defined as that flow in which increments of influent pass through the system and are discharged in the same sequence in which they entered. No intermixing of interaction takes place; each increment is in the system for a time equal to the theoretical retention time. This type of flow would be approximated in a long tank having a relatively small cross section.

[8] Camp, T. R., "Lateral Spillway Channels," *Trans. ASCE*, **105** (1940), 606–617.

[9] Greenhalgh, R. E., R. L. Johnson, and H. D. Nott, "Mixing in Continuous Reactors," *Chem. Engr. Progr.*, **55** (1959), 44–48.

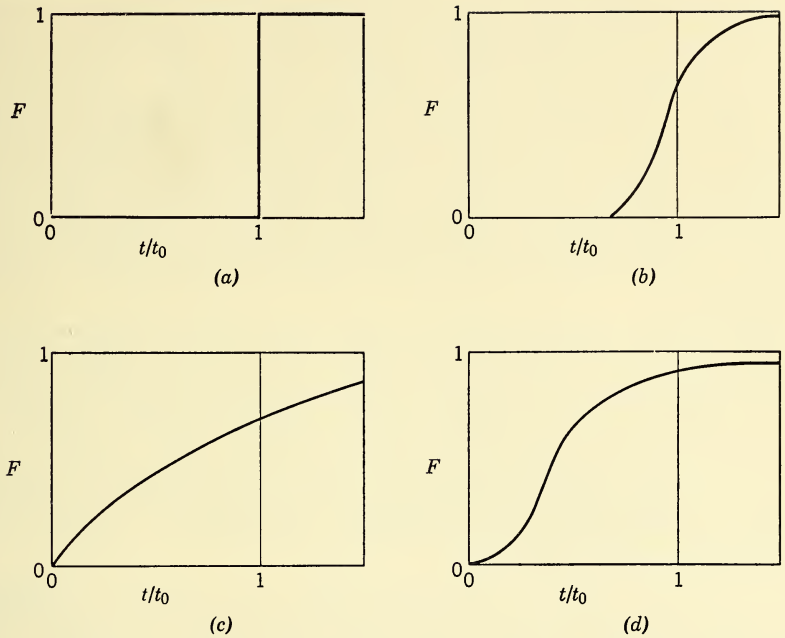

FIGURE 2-9. *F*-diagrams for continuous-flow models. (*a*) Ideal plug flow. (*b*) Plug flow with longitudinal mixing. (*c*) Complete mixing, zero intermixing. (*d*) Complete mixing, zero intermixing with stagnant pockets. [After Figure 1, Danckwerts, P. V., "Continuous Flow Systems," *Chem. Engr. Sci.*, **2**, No. 1 (1953).]

Consider a situation in which a vessel with a volume V is being fed at a constant rate q. If, beginning at time equal zero, all increments of influent are labeled in some manner or other, it is possible to identify the mixing pattern of the vessel by the time distribution of the labeled increments in the effluent. Figure 2-9*a* is a *F*-diagram giving the time-distribution relationship for ideal plug flow. The fraction of labeled increments F appearing in the effluent at time t is plotted against the dimensionless group t/t_0, where t_0 is the nominal retention time

$$t_0 = \frac{V}{q} \tag{2-56}$$

When $t = t_0$, F increases from 0 to 1.

Ideal plug flow seldom occurs, however. In most systems that are long and have small cross sections there is some longitudinal mixing. The time-distribution relationships for these systems are similar to that presented in Figure 2-9*b*.

Complete mixing with intermixing identifies the flow model in which increments of the influent intermix immediately with contents of the vessel and, thereby, lose their identity in every respect. The fluid in the vessel is completely mixed so that its properties are uniform and identical with those of the effluent. The complete mixing model is approximated in a mixing tank. Although the F-diagram for this type of system is similar to the one shown in Figure 2-9*c*, there is little significance to be attached to the distribution of labeled increments in the effluent since the increments lose their individual identity upon entering the system.

The third flow model is called *complete mixing with zero intermixing.* This model is a combination of plug flow and complete mixing. Upon entering the system, the increments are dispersed uniformly throughout the vessel but do not intermix or interact with each other. The increments retain their individual identity and appear in the effluent as a function of their statistical population. The time distribution of labeled increments in the effluent is described by the F-diagram in Figure 2-9*c*. The equation of the curve is [10]

$$F = 1 - e^{-t/t_0} \tag{2-57}$$

The F-diagram of a system of the zero-intermixing type, but one which exhibits short-circuiting characteristics due to the presence of stagnant pockets in the vessel, is presented in Figure 2-9*d*.

The results of operations and processes performed in batch systems are often used to predict the performance of continuous-flow systems. This is possible only through a consideration of the particular flow model involved. Figure 2-10 is a graphical representation of data obtained from a batch process in which a single reaction is taking place. Here the instantaneous conversion $1 - (c_t/c_0)$ is plotted as a function of time. The notations c_0 and c_t are the concentrations of a reactant at time equal 0 and t respectively. For a continuous system that displays a flow pattern conforming to the ideal plug flow model, the conversion can be estimated from the curve for a value of time equal to the theoretical retention time V/q.

It is obvious from the curve in Figure 2-10 that the rate of conversion for the particular reaction taking place in the batch system is dependent upon the concentration of one or more reactants, and will vary from some high value initially to a lower one at time equal t. Since the contents of a continuous system having a flow pattern conforming to the complete-mixing-with-intermixing model are uniform throughout, the reaction can

[10] Danckwerts, P. V., "Continuous Flow Systems," *Chem. Engr. Sci.*, **2**, No. 1 (1953).

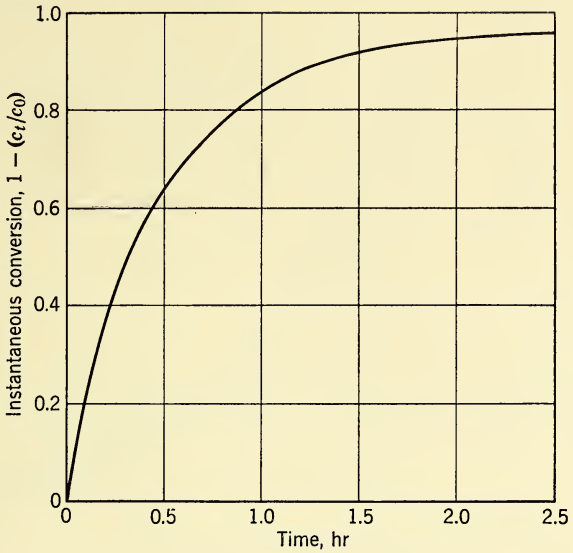

FIGURE 2-10. Batch process data. [Adapted from Figure 1, Greenhalgh, R. E., R. L. Johnson, and H. D. Nott, "Mixing in Continuous Reactors," *Chem. Engr. Progr.*, **55** (Feb. 1959) 44–48.]

proceed at one rate only: the rate corresponding to the concentration of the reactants. An equation for this model can be established on the basis of a steady-state balance of one of the reacting components,

$$q(c_0 - c_t) = V\left(\frac{dc}{dt}\right)_{c_t} \tag{2-58}$$

and

$$\frac{V}{q} = t_0 = \frac{c_0 - c_t}{(dc/dt)_{c_t}} \tag{2-59}$$

where the term $(dc/dt)_{c_t}$ is the rate of reaction at a concentration of c_t. This term can be evaluated from the slope of the batch curve at a point corresponding to c_t. The ratio V/q or t_0 gives the retention time required for the continuous system.

In reaction systems conforming to the complete-mixing-with-zero-intermixing model, the individual increments of flow behave as small batch reactors. The increments are in the vessel for different periods of time and, as a result, the effluent is a composite of increments in which the reaction has proceeded to different degrees of completion.

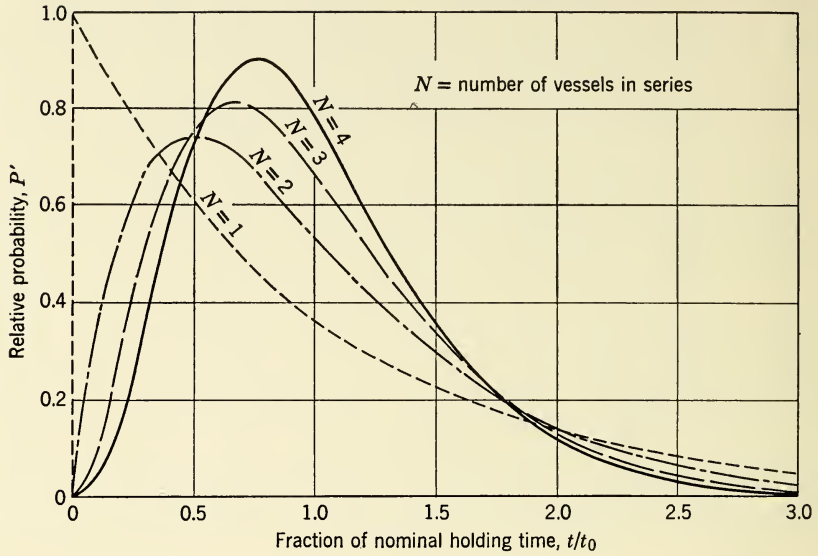

FIGURE 2-11. Probability curves for the ideal complete-mixing-with-zero-intermixing model. [After Figure 2, Camp, T. R., "Flocculation," *Trans. ASCE*, **120**, No. 8 (1955).]

The average conversion of the effluent is equal to the sum of the conversions obtained in each fraction of the effluent [11]

$$\left(1 - \frac{c_t}{c_0}\right)_{\text{ave}} = \frac{1}{t_0}\int_0^\infty P'\left(1 - \frac{c_t}{c_0}\right) dt \tag{2-60}$$

where P' = relative probability that a fraction of the influent will be retained in the system at time t and will leave before time $t + dt$.

The configuration of the F-diagram is dependent upon the relative times required by the individual portions of the influent to flow through the system, and the slope of the curve is equal to the relative probability, P'.[12]

$$P' = \frac{dF}{d(t/t_0)} \tag{2-61}$$

[11] Gilliland, E. R. and E. A. Mason, "Gas Mixing in Beds of Fluidized Solids," *Ind. Engr. Chem.*, **44**, (1952), 218.

[12] MacMullen, R. B. and M. Weber, Jr., "The Theory of Short Circuiting," *Trans. Amer. Inst. Chem. Engrs.*, **31**, (1935), 409.

Differentiation of the F-diagram for ideal zero intermixing (Figure 2-9*c*) yields the curve in Figure 2-11 labeled $N = 1$. The other curves in Figure 2-11 are for various numbers of vessels (N) in series. Similar curves can be obtained from a graphical differentiation of the F-diagrams for plug flow with longitudinal mixing (Figure 2-9*b*) and zero intermixing with stagnant pockets (Figure 2-9*d*).

A solution to Equation 2-60 is possible through an integration of batch conversion data with the relative probability function. This can be accomplished by using graphical procedures.

EXAMPLE 2-7

A process carried out in a batch system yielded time-conversion data, the plot of which is presented in Figure 2-10. What would be the conversion obtained in a continuous system having a nominal retention time of 1 hr if the flow pattern is assumed to conform to the ideal complete-mixing-with-zero intermixing model?

Solution

1. Prepare a table to facilitate the graphical solution of Equation 2-60 (see Table 2-3).

2. A curve is constructed with values in the last column of Table 2-3 plotted against time (see Figure 2-12). It appears that the curve approaches a limiting value of 0.7.

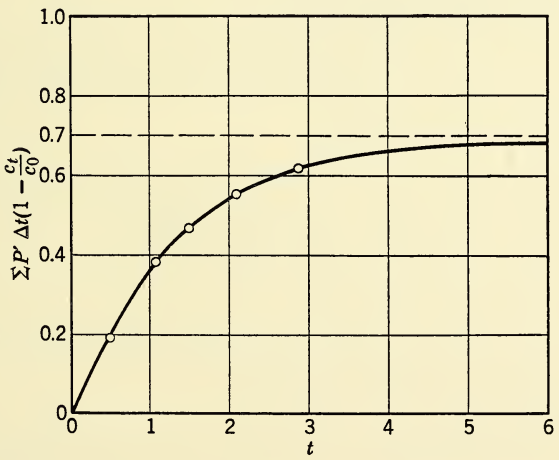

FIGURE 2-12. Estimating average conversion in effluent of continuous-flow system conforming to the ideal complete-mixing-with-zero-intermixing model (Example 2-7).

TABLE 2-3. COMPUTATIONS FOR THE SOLUTION OF EXAMPLE 2-7

t	P'	Δt	$(1 - c_t/c_0)$	$P' \Delta t(1 - c_t/c_0)$	$\Sigma P' \Delta t(1 - c_t/c_0)$
0.1	0.905	0.2	0.24	0.0435	
0.3	0.741	0.2	0.49	0.0725	0.1160
0.5	0.607	0.2	0.64	0.0775	0.1935
0.7	0.497	0.2	0.74	0.0735	0.2670
0.9	0.407	0.2	0.80	0.0650	0.3320
1.1	0.333	0.2	0.85	0.0566	0.3886
1.3	0.273	0.2	0.88	0.0480	0.4366
1.5	0.223	0.2	0.91	0.0406	0.4772
1.7	0.183	0.2	0.93	0.0341	0.5113
1.9	0.150	0.2	0.94	0.0282	0.5395
2.1	0.122	0.2	0.94	0.0229	0.5624
2.3	0.100	0.2	0.95	0.0190	0.5814
2.5	0.0821	0.2	0.95	0.0156	0.5970
2.7	0.0672	0.2	0.96	0.0129	0.6099
2.9	0.0550	0.2	0.96	0.0105	0.6204

Notations

b Width, ft; b_u, top width
c Weight concentration, lb force/ft^3; c_0 and c_t, concentrations of reactant at time equal 0 and t respectively
C Coefficient, dimensionless
D Diameter, ft; D_p, particle diameter
E Specify energy, (ft)(lb force)/(lb mass); E_c, specific energy at critical depth; ΔE, change in specific energy; E_T, total energy loss; E_s, energy dissipated by shear stresses
f Friction factor, dimensionless
F Force, lb force; F_G, gravitational force producing flow; F_R, viscous force resisting flow; F_1, F_2, and F_3, horizontal static forces acting on liquid; F_4, vertical static force acting on liquid
F Fraction of labeled increments of flow, dimensionless
g Acceleration of gravity, ft/sec^2
g_c Newton's law conversion factor, 32.17 (ft)(lb mass)/(lb force)(sec^2)
h_f Permanent head loss caused by friction, (ft)(lb force)/(lb mass); h'_f, head loss due to friction, ft of water
K Constant
L Horizontal distance, ft
n Coefficient of roughness; n', modified coefficient of roughness
N Number
N_{Re} Reynolds number, dimensionless
Δp Pressure drop, lb force/ft^2

P Power, (ft)(lb force)/(sec)

P' Relative probability, dimensionless

q Volumetric rate of flow, ft^3/sec; q', volumetric rate of flow per unit width of channel

r_H Hydraulic radius, ft; $\bar{r}_H$, mean hydraulic radius

S Cross-section area, ft^2

t Time, sec; t_0, nominal retention time

u Local velocity, ft/sec

du/dy Point velocity gradient, sec^{-1}

$\overline{V}$ Mean velocity of flow, ft/sec; $\overline{V}_1$, mean velocity at point 1; $\overline{V}_2$, mean velocity at point 2; $\overline{V}_L$, limiting mean velocity of flow; $\overline{V}_c$, mean velocity at critical depth

Δx Incremental length of channel, ft

y Depth of liquid, ft; y_1, depth at point 1; y_2, depth at point 2; $\bar{y}$, mean depth between points 1 and 2; y_c, critical depth; y'_1, conjugate depth in tranquil flow region; y'_2 conjugate depth in rapid flow region; y''_1, depth downstream from hydraulic jump; y''_2, depth immediately upstream from hydraulic jump; y_0, depth at upper end of channel; y' fluctuating depth

Z Height above arbitrary datum plane, ft; Z_1, height of channel invert at point 1; Z_2, height of channel invert at point 2

α Angle of inclination with the horizontal, degree

ϵ Absolute roughness of surface, ft

δ Thickness of laminar sublayer, ft

μ Absolute viscosity, (lb mass)/(ft)(sec)

ρ Mass density of fluid, lb mass/ft^3; ρ_s, mass density of particle

τ Shear stress, lb force/ft^2; τ_w, average shear stress along sides of channel; τ'_w, average shear stress along sides of channel at velocity where movement of deposited particles is impending

ψ Operator

ϕ Operator

3

Mixing

3-1. Introduction

The terms "mixing" and "agitation" are often used interchangeably. "Mixing," however, describes more precisely an operation in which two or more materials are intermingled to attain a desired degree of uniformity. On the other hand, "agitation" applies to those operations, the primary purpose of which is to promote turbulence in a liquid. Agitation for the purpose of promoting floc growth in suspensions is commonly called "flocculation."

Mixing and agitation find wide application in sanitary engineering treatment processes. The suspension of dissolving solids in water and sludge systems, the dispersion of gases in water systems, and the flocculation of precipitates from liquids constitute the bulk of such operations. Although mixing has been essentially an art, there is now sufficient information concerning basic principles to permit a rational development of design criteria.

3-2. Mixing Impellers

Many types of devices are used in mixing and agitation operations. These include rotating impellers, air agitators, mixing jets, and pumps. The following discussion is confined to rotating impellers, the type most commonly used in sanitary engineering.

Impellers fall into one of three groups: paddles, turbines, and propellers. Impellers in each group can be mounted one or more on a shaft, and more than one shaft may be used in a container.

Paddles

Paddle impellers range in design from a single, flat paddle on a vertical shaft to a battery of multiblade flocculators mounted on a long, horizontal shaft (Figure 3-1). Paddles turn at slow to moderate speeds (2 to 150 rpm), and are used primarily as agitators of dilute suspensions or as mixers in high-viscosity applications. The principal currents generated are radial and tangential to the rotating paddles.

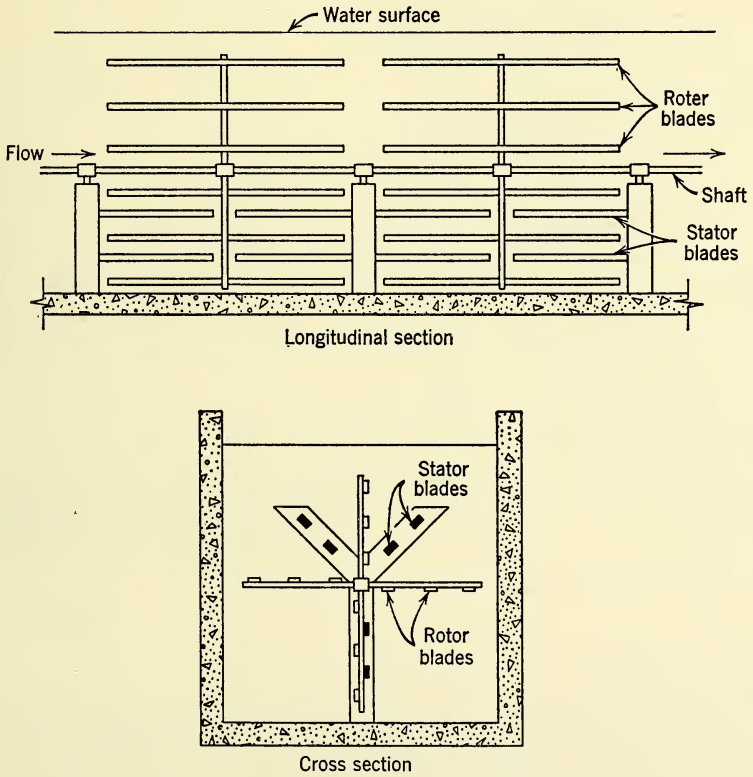

FIGURE 3-1. Flocculators. [Adapted from Figure 3, Camp, T. R., "Flocculation," *Trans. ASCE*, **120** (1955).]

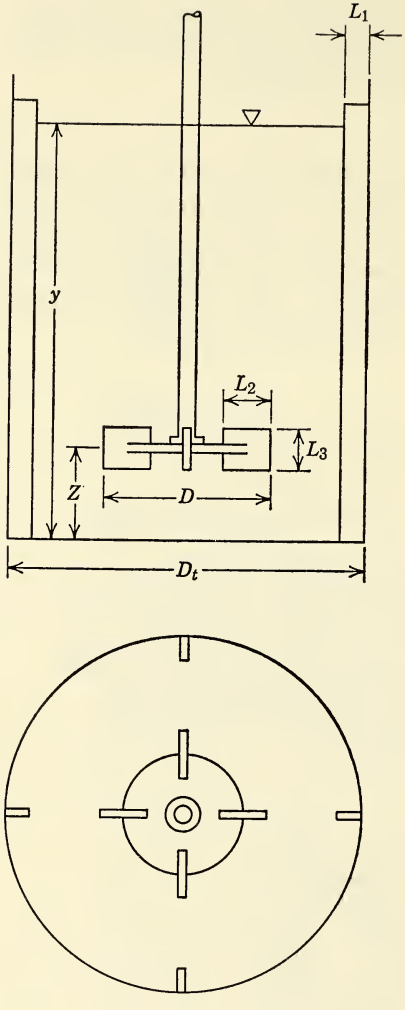

FIGURE 3-2. Turbine mixer in a baffled tank. [After Figure 6, Rushton, J. H. et al., *Chem. Engr. Progr.*, **46** (1950), 395.]

Turbines

The "turbine impeller" is a term applied to a wide variety of impeller shapes. The turbine impeller shown in Figure 3-2 is used in many mixing applications. This type of impeller consists of several straight blades mounted vertically on a flat plate. The blades of some turbine impellers are curved or tilted from the vertical. Rotation is at moderate speeds, and fluid flow is generated in a radial and tangential direction.

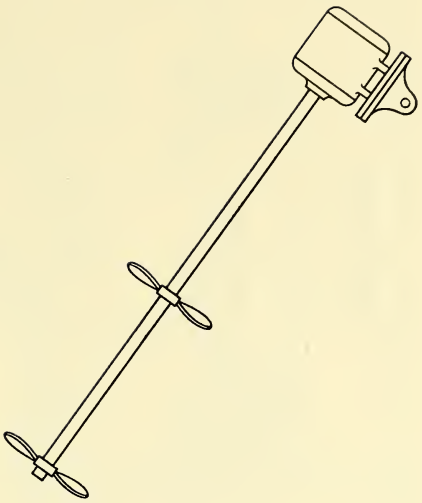

FIGURE 3-3. Propeller mixer.

Propellers

The marine-type propeller is a relatively small, high-speed impeller widely used in low-viscosity applications. It has a high rate of flow displacement and generates strong currents in an axial direction. Speed of rotation will vary from 400 rpm for large-diameter propellers to 1750 rpm for those having smaller diameters. A propeller mixer is shown in Figure 3-3.

Each impeller type has its own group of services for which it is particularly suited. Although there are situations where two impeller types will perform equally well, in general, a given service will be satisfied best by only one. Figure 3-4 can be used as a guide in making a preliminary selection of impeller type.

3-3. Baffling

The tangential component of flow induced by a rotating impeller promotes rotational movement or vortexing about the impeller shaft. Vortexing impedes the mixing operation by reducing the velocity of the impeller relative to the liquid. Furthermore, impeller power consumption is more difficult to calculate when vortexing conditions prevail.

Vortexing can be reduced by proper baffling. Vertical strips placed along the walls of the tank serve to break up rotational movement by deflecting the liquid back toward the impeller shaft. For turbine mixing operations, the width of the baffles may be as small as one-tenth to

Selection Chart				Shape relationships for turbine designs		
Service	Mixing device	Range	Criteria	Tank diameter to impeller diameter ratio	Tank height to diameter ratio	Impellers and position
Blending	Turbine Propeller Paddle		1. Volume circulation	3:1 to 6:1	Unlimited	Single or multiple
	Tank vol.	→ 1,000,000 gal				
Dispersion (immiscible systems)	Turbine Propeller Paddle		1. Drop size control 2. Recirculation	3.0:1 to 3.5:1	1:1 1:2 in staged mixers	At/or below center line of liquid charge
	Flow	→ 1,000 gal/min				
Reactions in solution (miscible systems)	Turbine Propeller Paddle		1. Intensity 2. Volume circulation	2.5:1 to 3.5:1	1:1 to 3:1	Single or multiple
	Charge vol.	→ 20,000 gal				
Dissolution	Turbine Propeller Paddle		1. Shear 2. Volume circulation	1.6:1 to 3.2:1	1:2 to 2:1	At/or below center line of liquid charge
	Charge vol.	→ 10,000 gal				

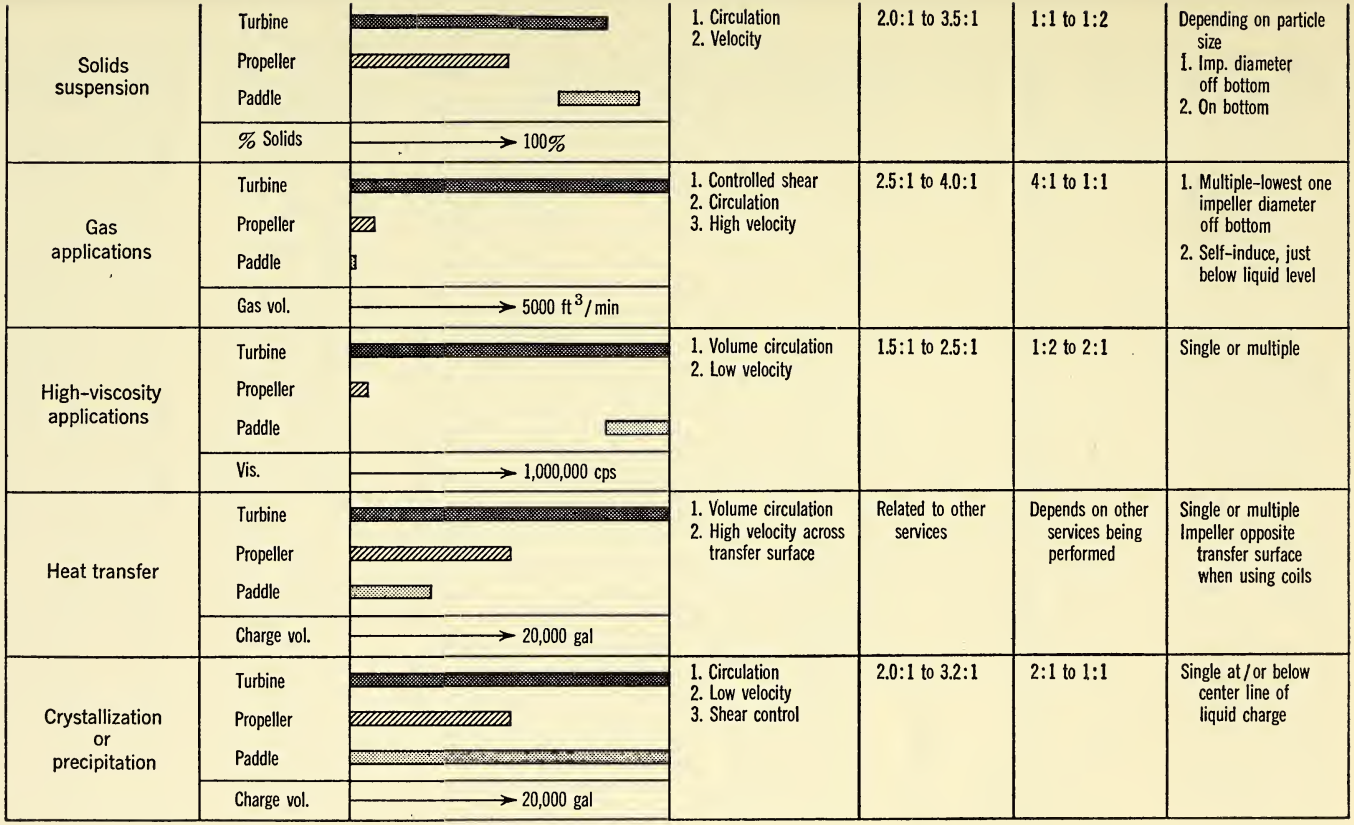

FIGURE 3-4. Impeller selection chart. [From Figure 13, Lyons, E. J., and N. H. Parker, "The Turbine as a Mixing Tool," *Chem. Engr. Progr.*, **50** (Dec. 1954).]

one-twelfth the tank diameter; for propeller operations, even smaller widths can be used. Seldom are more than four baffles necessary for these types of impellers. To reduce rotational movement in flocculation operations, stationary strips called stator blades are arranged so as to intermesh with the rotating blades of the flocculation paddles (Figure 3-1).

Where propellers are used, vortexing can be reduced by inclining the impeller shaft in some position off-center of the tank or by entering it horizontally through the side at some angle with the tank radius.

A more detailed discussion of baffling and flow patterns can be found elsewhere.[1]

3-4. Fluid Regimes

A rotating impeller establishes within a fluid mass a flow pattern governed not only by the shape, size, and speed of the impeller but also by the characteristics of the fluid container and the presence of baffling. When flow is viscous, there is no mixing within the fluid other than that due to diffusion. When flow is turbulent, however, fluid particles move in all directions, and mixing results primarily from convective displacement. The momentum transfer associated with such displacement generates strong shear stresses within the fluid. The term "fluid regime" refers to the flow pattern and the over-all summation of the mass flow-shear relationships existing in a fluid in motion.

Ordinarily, both mass flow and turbulence—or their result, fluid shear —are important in mixing operations. Most turbulence is produced as the result of high-velocity flow streams coming into contact with those of lower velocity. Flow along the sides of the container, the impeller blades, and across baffles contributes turbulence to a much lesser degree.[2]

The relative importance of mass flow and fluid shear will depend upon the application, there being a direct correlation between the fluid regime and the results desired. For this reason, the design of a mixing operation involves, first, an identification of the particular fluid regime required and, second, the synthesis of an operation for producing the regime.

A fluid regime can be identified either in terms of the relationship existing between the forces involved in sustaining and resisting the

[1] Rushton, J. H., and J. Y. Oldshue, "Mixing of Liquids," *Chem. Engr. Progress Symp. Series*, **55**, No. 25 (1959).

[2] Rushton, J. H., "Mixing of Liquids in Chemical Processing," *Ind. Engr. Chem.*, **44** (1952), 2931–2936.

regime or by some index such as power input per unit volume of liquid necessary to produce a given process result. Identification by the first method is complete in as much as the method provides for geometric, kinematic, and dynamic similarity in scaling-up operations. The second method is less complete, providing only for geometric and kinematic similarity at the most.

3-5. Power Curves

When a fluid regime is established by a rotating impeller, the major forces generated in the fluid are the inertia forces characterized by the power number, the viscous forces represented by the Reynolds number, and the gravitational forces described by the Froude number. These numbers consist of the following dimensionless groups:

$$\text{Power number} = N_P = \frac{Pg_c}{\rho n^3 D^5} \tag{3-1}$$

$$\text{Reynolds number}^{3} = N_{Re} = \frac{D^2 n\rho}{\mu} \tag{3-2}$$

$$\text{Froude number} = N_{Fr} = \frac{Dn^2}{g} \tag{3-3}$$

where P = power, (ft)(lb force)/(sec)
n = rps
D = diameter of impeller, ft
ρ = mass density of fluid, lb mass/ft^3
μ = absolute viscosity of fluid, (lb mass)/(sec)(ft)
g_c = Newton's law conversion factor, 32.17 (ft)(lb mass)/(sec^2)(lb force)
g = acceleration of gravity, ft/sec^2

The general relationship existing between the groups has been found to be [4]

$$N_P = K(N_{Re})^p(N_{Fr})^q \tag{3-4}$$

where K is a constant, and p and q are exponents, the values of which

[3] The Reynolds and Froude numbers are usually written $Du\rho/\mu$ and u^2/gD respectively. However, the term nD is proportional to u and can be substituted for the latter in these dimensionless groups.

[4] Rushton, J. H., E. W. Costich, and H. J. Evert, "Power Characteristics of Mixing Impellers, Part I," *Chem. Engr. Progress*, **46** (1950), 395–404.

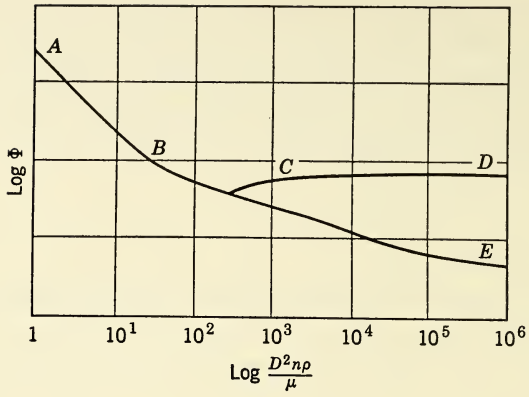

FIGURE 3-5. Power characteristics of a mixing impeller. For curve *ABCD*—no vortex present, $\Phi = Pg_c/\rho n^3 D^5$; for curve *ABE*—vortex present, $\Phi = (Pg_c/\rho n^3 D^5) \times (Dn^2/g)^{-q}$. [From Figure 1, Rushton, J. H., "The Use of Pilot Plant Mixing Data," *Chem. Engr. Progr.*, **47** (1951), 485–488.]

depend upon the mixing situation. The gravitational forces represented by the Froude number become effective only when flow is turbulent, and then only when a vortex is formed around the axis of the impeller.

A logarithmic plot of Equation 3-4 for a particular impeller is presented in Figure 3-5. Here the Reynolds number is plotted against a term Φ, called the power function. For baffled containers where no vortex is presented,

$$\Phi = N_P = \frac{Pg_c}{\rho n^3 D^5} \tag{3-5}$$

Where a vortex is formed

$$\Phi = \frac{N_P}{N_{Fr}{}^q} = \frac{Pg_c}{\rho n^3 D^5} \left(\frac{Dn^2}{g}\right)^{-q} \tag{3-6}$$

The curve *ABCD* describes the power-function–Reynolds-number relationship existing when there is no vortex formation; curve *ABE* gives the relationship when a vortex is formed. At low Reynolds numbers, the two curves coincide, indicating that the exponent q is equal to zero and

$$\Phi = N_P = K(N_{Re})^p \tag{3-7}$$

for both curves. Up to a Reynolds number of 10, the slopes of most

power curves are approximately equal to minus one. Substituting this value for p in Equation 3-7,

$$N_P = \frac{Pg_c}{\rho n^3 D^5} = K \frac{\mu}{D^2 n \rho} \tag{3-8}$$

and

$$P = \frac{K}{g_c} \mu n^2 D^3 \tag{3-9}$$

When turbulent conditions are fully developed in a container in which the vortex has been eliminated (from C to D on curve $ABCD$), the value of the exponent p is zero,

$$\Phi = N_P = K \tag{3-10}$$

and

$$P = \frac{K}{g_c} \rho n^3 D^5 \tag{3-11}$$

In such systems, turbulence is fully developed at Reynolds numbers of 100,000 or larger.

That portion of curve ABE falling in the turbulent flow region is irregular. Consequently, no equation can be conveniently established for the power input when flow is turbulent and vortex formation is permitted.

The value of the constant K depends upon the impeller shape, size, the number of baffles, and other variables not included in the power equations. Values of K are listed in Table 3-1 for different types of

TABLE 3-1. VALUES OF K FOR EQUATIONS 3-9 AND 3-11 *

Impeller †	Equation 3-9, Viscous Range	Equation 3-11, Turbulent Range
Propeller, square pitch, three blades	41.0	0.32
Propeller, pitch of two, three blades	43.5	1.00
Turbine, six flat blades	71.0	6.30
Turbine, six curved blades	70.0	4.80
Turbine, six arrowhead blades	71.0	4.00
Fan turbine, six blades	70.0	1.65
Flat paddle, two blades	36.5	1.70
Shrouded turbine, six curved blades	97.5	1.08
Shrouded turbine, with stator (no baffles)	172.5	1.12

* With four baffles at tank wall, each 10 percent tank diameter.

† Rushton, J. H., "Mixing of Liquids in Chemical Processing," *Ind. Engr. Chem.*, **44** (1952), 2931–2936.

impellers rotating at the center line of cylindrical vessels with a flat bottom, a liquid depth equal to one tank diameter, an impeller diameter one-third of the tank diameter, and with the impeller one diameter above the bottom of the tank.

The fluid regime of any system, baffled and with a given geometry, can be identified, therefore, in terms of the power and Reynolds numbers. It is believed that the former can be used to characterize the flow pattern established in the system, whereas the latter provides an expression for the turbulence or shear intensity.

EXAMPLE 3-1

A mixing operation is to be performed with a 24-in. turbine impeller with six flat blades in a tank geometrically similar to the tank for which the data in Table 3-1 were derived. The system to be mixed is aqueous and has a temperature of about 60 °F. At what speed must the impeller be rotated to ensure fully developed turbulence? What will be the power consumption at this speed?

Solution

1. For a Reynolds number of 100,000 (at which point complete turbulence is obtained), compute the speed of rotation (Equation 3-2).

$$n = \frac{\mu N_{Re}}{D^2 \rho} = \frac{1.2(6.72 \times 10^{-4})10^5}{2^2 \times 62.4} = 0.324 \text{ rps}$$

2. Compute power consumption at this speed (Equation 3-11).

$$P = \frac{K}{32.2} \times 62.4(0.324)^3 \times 2^5 = 2.1K$$

From Table 3-1, for a turbine with six flat blades rotating in turbulent range, $K = 6.3$,

$$P = 2.1 \times 6.3 = 13.2 \text{ (ft)(lb force)/sec}$$
$$= 13.2 \times 1.818 \times 10^{-3} = 0.024 \text{ hp}$$

3-6. Scale-up

Little information is available relating mixer operation with process performance. Consequently, identification of the optimum fluid regime to achieve the desired process result must be made from information derived from laboratory or pilot-plant investigations. Once the optimum regime has been identified, a method for scaling up the small scale operations can be used to design dynamically similar operations of the desired size.

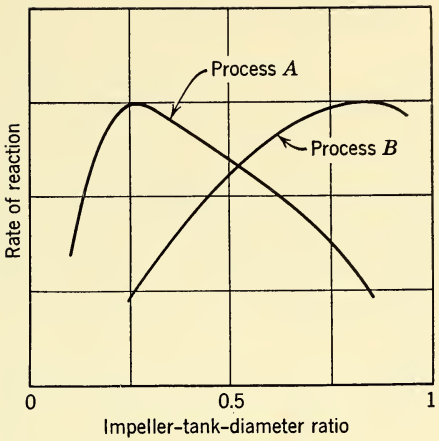

FIGURE 3-6. Effect of impeller size on reaction rate at equal power input. [Adapted from Figure 2, Rushton, J. H., "How to Make Use of Recent Mixing Developments," *Chem. Engr. Progr.*, **50** (1954), 587–589.]

Two systems are geometrically similar when the ratios of the dimensions in one system are equal to the corresponding ratios in the other. The pertinent dimensions are indicated in Figure 3-2. Two other types of similitude are important in scale-up. Kinematic similarity is achieved when the fluid motion is the same in two geometrically similar systems. Systems have dynamic similarity when, in addition to being geometrically and kinematically similar, the force ratios are equal at corresponding points in the system. As was pointed out before, precise scale-up is achieved only in systems which are dynamically similar.

For a given power expenditure, the mass-flow–shear-intensity ratio can be varied by using impellers of different sizes in what otherwise would be geometrically similar systems. Therefore, one of the first considerations at the laboratory or pilot-plant level is to determine the impeller–tank-diameter ratio giving the optimum process result. The effect of impeller size on the reaction rates of two types of processes is shown in Figure 3-6. Inasmuch as the ratio of mass flow to shear intensity can be varied at equal power input by using geometrically similar impellers of different sizes, there is little justification for experimenting with a large variety of impeller shapes.[5]

As was pointed out in Section 3-5, the Reynolds number is related to the shear intensity existing in a turbulent fluid. It is not surprising therefore, that data from reactions with rates depending upon the thickness of liquid films can be correlated with the Reynolds number. This

[5] Rushton, J. H., "How to Make Use of Recent Mixing Developments," *Chem. Engr. Progress*, **50** (1954), 587–589.

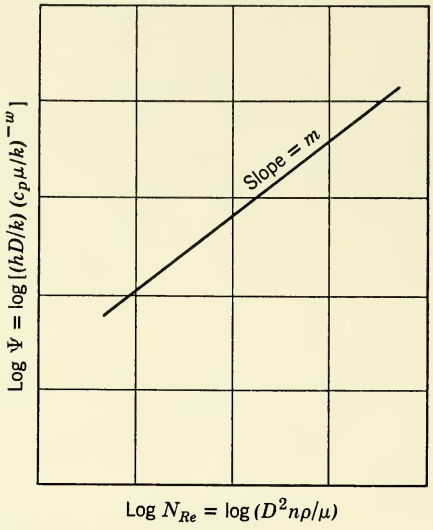

FIGURE 3-7. Correlation of rate coefficient, fluid properties, and fluid motion. Fully developed turbulence. [After Figure 2, Rushton, J. H., "The Use of Pilot Plant Mixing Data," *Chem. Engr. Progr.*, **47** (1951), 485.]

correlation, as well as its use in scaling-up operations, has been demonstrated by Rushton.[6]

Consider a circular tank fitted with a mixing impeller and baffles all of a given size, around the wall of which heating coils are arranged. Heat is to be transferred from the coils to a liquid contained in the tank. If the rate at which transfer takes place is controlled by the thickness of viscous liquid films on the outside surfaces of the heating coils, any turbulence tending to reduce film thickness will serve to increase the value of the heat transfer coefficient h.

When the impeller is rotated at different speeds in the range where flow is fully turbulent (from C to D in Figure 3-5), data are obtained to give a correlation similar to that shown in Figure 3-7. Here the Reynolds number is plotted against Ψ,

$$\Psi = \frac{hD}{k}\left(\frac{c_p\mu}{k}\right)^{-w} \tag{3-12}$$

where h = heat transfer coefficient, (Btu)/(ft^2)(hr)(°F)
k = thermal conductivity, (Btu)(ft)/(ft^2)(hr)(°F)
c_p = specific heat at constant pressure, (Btu)/(lb)(°F)
w = exponent

[6] Rushton, J. H., "The Use of Pilot Plant Mixing Data," *Chem. Engr. Progress*, **47** (1951), 485.

In equation form, the correlation is

$$\frac{hD}{k} = K' \left(\frac{D^2 n \rho}{\mu}\right)^m \left(\frac{c_p \mu}{k}\right)^w \tag{3-13}$$

where m = slope of the correlation curve.

To reproduce a given value of transfer coefficient h in a geometrically similar system of different size, a scale-up relationship may be derived by dividing the relationship in Equation 3-13 expressed in terms of one size by the relationship in terms of the other size. Since the properties of the fluid remain unchanged,

$$\frac{n_2}{n_1} = \left(\frac{D_1}{D_2}\right)^{(2m-1)/m} \tag{3-14}$$

where the subscripts 1 and 2 refer to the two different sizes.

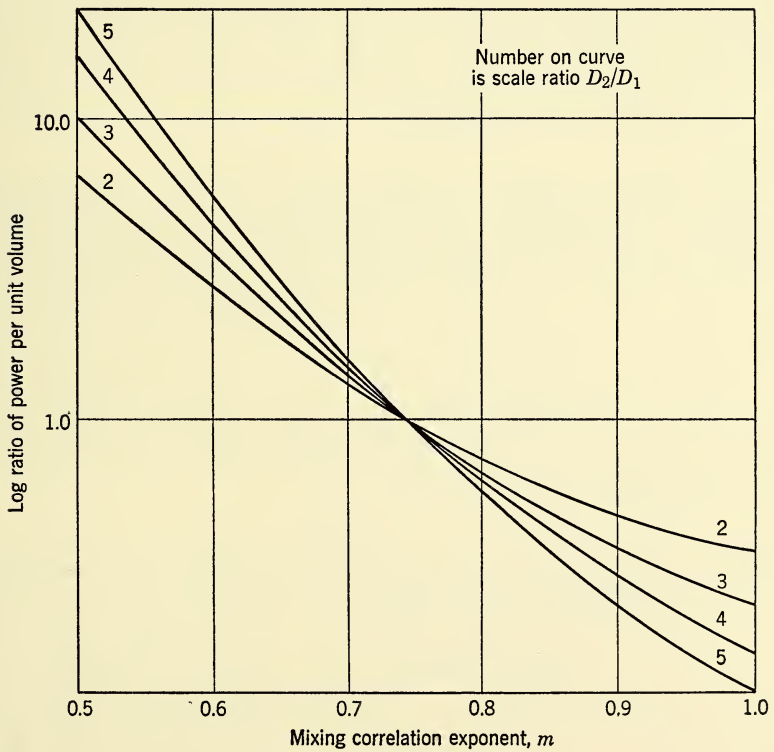

FIGURE 3-8. Power-volume-exponent-scale relationship. [After Figure 4, Rushton, J. H., "The Use of Pilot Plant Mixing Data," *Chem. Engr. Progr.*, **47** (1951), 487.]

Power requirements which must be met in the scale-up can be determined from a relationship developed by combining Equations 3-11 and 3-14.

$$\frac{P_2}{P_1} = \left(\frac{D_2}{D_1}\right)^{(3-m)/m} \tag{3-15}$$

The value of m is dependent upon the particular geometry of the tank, and the shape, size, and location of the impeller and other fittings in the tank. A plot of this exponent versus the ratio of power input per unit volume in geometrically similar systems as a function of tank size is shown in Figure 3-8. It may be seen from the curves that, with the exception of one value of m, power input per unit volume varies with scale-up. This supports the statement made in Section 3-4 to the effect that power per unit volume is an incomplete expression of the factors producing a process result. Furthermore, it is to be noted that the ratio varies with the value of m. Laboratory and pilot-plant investigations should be directed not only toward an evaluation of m but also toward determining the arrangement of tank and impeller giving the highest value of the exponent.

EXAMPLE 3-2

A heat transfer operation is to be carried out in a baffled mixing tank. Preliminary investigations revealed the optimum impeller–tank-diameter ratio at equal power input to be 0.4. Subsequent studies performed with a 6-in. impeller rotating in a tank 15 in. in diameter provided data which yield a correlation similar to that shown in Figure 3-7. The desired rate of transfer was obtained at a speed of 360 rpm and at a power input of 51.6 (ft)(lb force)/(sec). If the slope of the correlation curve is 0.7, at what speed must a 2-ft impeller rotate to reproduce the same rate of transfer in a geometrically similar tank? What will be the power consumption at this speed?

Solution

Since the larger system is to be geometrically similar to the smaller one, Equations 3-14 and 3-15 apply.

$$n = 360\left(\frac{0.5}{2}\right)^{(1.4-1)/0.7} = 163 \text{ rpm}$$

$$P = 51.6\left(\frac{2}{0.5}\right)^{(3-0.7)/0.7} = 4850 \text{ (ft)(lb force)/(sec)}$$

3-7. Gas Transfer

Gas transfer operations are often carried out in turbine mixer systems, in which the gas phase is introduced beneath the impeller, usually through a sparger ring. Little data are available on which to base the scale-up of such operations on the principles of dynamic similitude. For this reason, use is commonly made of the relationship between power input per unit volume of geometrically similar systems and process result. This procedure was shown in the preceding section to be somewhat less than precise.

In gas transfer operations, process result can be expressed in terms of K_La, the product of the mass transfer coefficient (liquid film basis) and the gas-liquid interfacial area per unit volume of the liquid. Since this group is a function of gas dispersion, bubble size, and liquid turbulence, it provides an effective measure of mixer performance.

A correlation of K_La with mixer power input per unit volume for several air flows is shown in Figure 3-9. Most transfer operations are carried out in the turbulent-flow region, and mixer power input can be computed from relationships such as those given in Figure 3-5 and Equation 3-11. However, the dispersion of gas in a liquid reduces the liquid density, and, hence, the power input. The effect is illustrated by Figure 3-10, where curves are presented relating the ratio of gassed power input to ungassed power input to the superficial gas velocity (velocity based on the tank cross section). The relationships are typical but will vary with impeller speed, impeller—tank-diameter ratio, power input per volume, and diameter of the sparger ring.

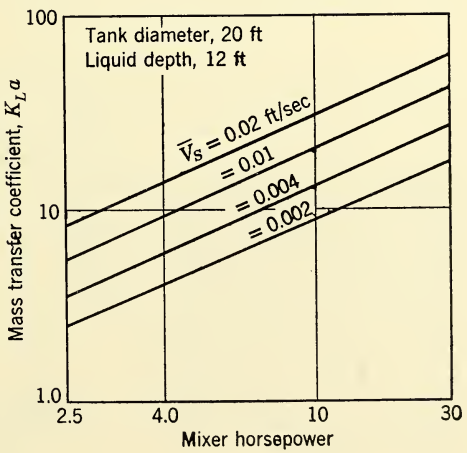

FIGURE 3-9. Mass transfer coefficient as a function of mixer horsepower and gas flow rate. [After Figure 2-58, Oldshue, V. Y., in McCabe, J., and W. W. Eckenfelder, Jr. (eds.), *Biological Treatment of Sewage and Industrial Wastes*—Vol. 1: *Aerobic Oxidation*, Reinhold Publishing Corp., New York (1956).]

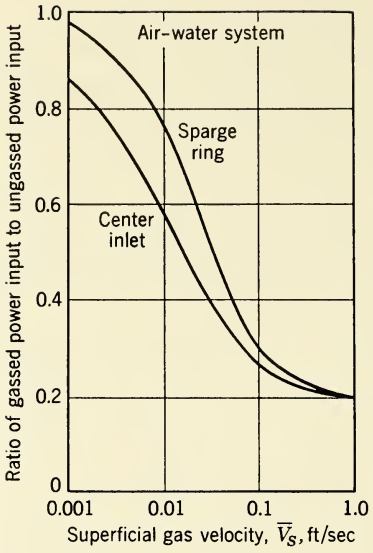

FIGURE 3-10. Effect of superficial gas velocity on power input. [After Figure 2-57, Oldshue, V. Y., in McCabe, J., and W. W. Eckenfelder, Jr. (eds.), *Biological Treatment of Sewage and Industrial Wastes*—Vol. 1: *Aerobic Oxidation*, Reinhold Publishing Corp., New York (1956).]

Curves similar to those in Figure 3-11 can be used to obtain a particular value of transfer coefficient in geometrically similar systems of different size. The relationship between mixer power input per unit volume and tank size approaches linearity when plotted on logarithmic scales. If the relationship between the variables is known for two sizes of tank, an estimate can be made of the required relationship for any other size.

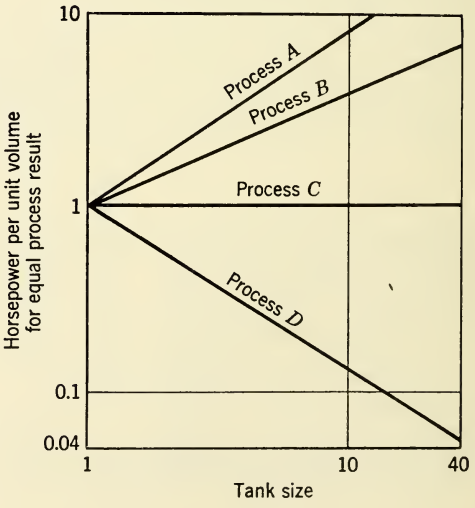

FIGURE 3-11. Power input per unit volume relationship for equal results in geometrically similar tanks of different sizes. [Adapted from Figure 2-55, Oldshue, V. Y., in McCabe, J., and W. W. Eckenfelder, Jr. (eds.), *Biological Treatment of Sewage and Industrial Wastes*—Vol. 1: *Aerobic Oxidation*, Reinhold Publishing Corp., New York (1956).]

EXAMPLE 3-3

A gas transfer operation is to be carried out with a turbine mixer in a 10-ft-diameter tank. Pilot-plant investigations performed with two systems of different sizes but geometrically similar to the 10-ft tank yielded data that plotted to form curves resembling those presented in Figure 3-9. To obtain the desired rate of gas transfer, the mixer power input to the 2-ft-diameter tank at a given gas flow rate was 1.6 hp/ft^3. At a corresponding gas flow rate, about 2.5 hp/ft^3 was required to promote the same rate of gas transfer in the 4-ft-diameter tank.

With this information, estimate the horsepower consumption in producing the same rate of transfer in the 10-ft-diameter tank.

Solution

1. Make a logarithmic plot of horsepower per unit volume versus tank size (see Figure 3-11).

2. By extrapolation along a straight line drawn through the two plotted points, a value of 4.8 hp/ft^3 is obtained for a tank 10 ft in diameter.

3-8. Flocculation

The subsidence velocity of a particle which is spherical or nearly spherical in shape will increase as the particle increases in size. Thus, when the stability of a suspension is such that coalescence of the suspended particles occurs upon contact with each other, any operation that promotes contact between particles will facilitate sedimentation. The term "flocculation" is used to describe operations of this nature. In most water treatment applications, flocculation is performed with paddle impellers.

Attention is directed to Figure 3-12. Suppose particles of two diameter sizes, D_{p1} and D_{p2}, are suspended in a liquid, the flow condition of which is viscous. In order for the particles to make contact, their centers must come within a distance $\frac{1}{2}(D_{p1} + D_{p2})$ from one another. Consequently, the number of particles of diameter D_{p2} that would come in contact with particles of diameter D_{p1} per unit of time is equal to the number of the former, N_2, per unit volume of the liquid flowing through the sphere of radius $\frac{1}{2}(D_{p1} + D_{p2})$ in unit time. For a point velocity gradient of du/dy, the volume of liquid flowing through a lamina of thickness dx in unit time is

$$dq = \left(x \frac{du}{dy}\right) [2(r^2 - x^2)^{\frac{1}{2}} dx] \tag{3-16}$$

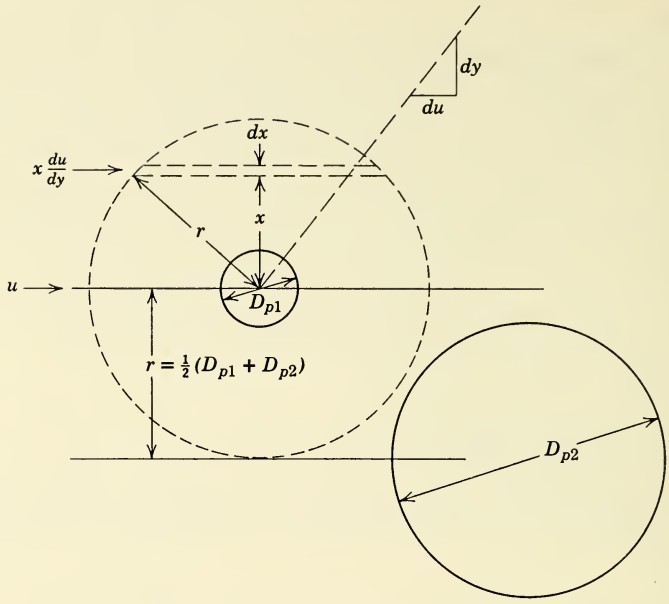

FIGURE 3-12. Definition sketch of contact opportunity in flocculation. [After Figure 7, Camp, T. R., and P. C. Stein, "Velocity Gradients and Internal Work in Fluid Motion," *J. Boston Soc. Civil Engrs.*, **30** (1943), 219–237.]

The total flow through the sphere will be

$$q = 2\int_0^r \frac{du}{dy}[2(r^2 - x^2)^{1/2}]x\,dx$$

$$= \frac{1}{6}\frac{du}{dy}(D_{p1} + D_{p2})^3 \tag{3-17}$$

Therefore, the number of contacts made by N_2 particles of diameter D_{p2} with particles of diameter D_{p1} will be

$$N' = \frac{1}{6}N_2\frac{du}{dy}(D_{p1} + D_{p2})^3 \tag{3-18}$$

For N_1 particles per unit volume of diameter D_{p1}, the total number of contacts per unit of time is

$$N'' = \frac{1}{6}N_1N_2\frac{du}{dy}(D_{p1} + D_{p2})^3 \tag{3-19}$$

and in the system as a whole

$$N = \frac{1}{6} N_1 N_2 \frac{\overline{du}}{dy} (D_{p1} + D_{p2})^3 \qquad (3\text{-}20)$$

where $\overline{du}/dy$ = mean velocity gradient in system.

According to Equation 3-20, the rate of flocculation is directly proportional to the mean velocity gradient established in the system. Also, the rate is greatest for a large concentration of particles of large size.

For different values of the velocity gradient, corresponding shear stresses are established in the liquid (see Equation 1-4). Floc particles become more fragile as they grow, and for a given value of $\overline{du}/dy$ there is a maximum size produced before the floc particle is destroyed by shear stresses. The practical limit of velocity gradient and, hence, turbulence will depend upon the size of particle desired. Scale-up of flocculation operations may be made by using a plot similar to that in Figure 3-11.

Flocculation devices commonly consist of several paddle blades revolving about either a vertical or horizontal shaft (see Figure 3-1). The use of stator blades as baffles is desirable. Where no stator blades are used, it is recommended that the area of the paddle blades be no greater than 15 to 20 percent of the cross-section area of the tank.[7] Paddles with greater blade areas will cause major rotation of the liquid. Most paddle flocculators have variable-speed drives. Under operational conditions, the peripheral speeds of paddles vary from 0.5 ft/sec to 3 ft/sec. Approximately 1 hp is lost through the transmission, stuffing boxes, and bearings, regardless of the speed. Power consumption varies from 2 to 6 kwhr/1,000,000 gal of water treated. Time of flocculation commonly ranges from 10 to 30 min.

Notations

c_p	Specific heat at constant pressure, (Btu)/(lb)(°F)
D	Impeller diameter, ft; D_o, outside diameter of pipe; D_p, particle diameter; D_t, tank diameter
g	Acceleration of gravity, ft/sec^2
g_c	Newton's law conversion factor, 32.17 (ft)(lb mass)/(lb force)(sec^2)
h	Heat transfer coefficient, Btu/(ft^2)(hr)(°F)
k	Thermal conductivity, Btu/(ft^2)(hr)(°F/ft)
K_La	Over-all, volumetric mass transfer coefficient, liquid phase basis, hr^{-1}
K, K'	Constants

[7] Bean, E. L., "Study of Physical Factors Affecting Flocculation," *Water Works Engr.*, **106** (Jan. 1953), 33.

L_1, L_2, L_3	Dimensions, ft
m	Mixing correlation exponent
n	Revolutions per second
N, N', N''	Number
N_{Fr}	Froude number, dimensionless
N_P	Power number, dimensionless
N_{Re}	Reynolds number, dimensionless
p	Exponent
P	Power, (ft)(lb force)/(sec)
q	Exponent
q	Volumetric rate of flow, ft^3/sec
r	Radius, ft
du/dy	Point velocity gradient, sec^{-1}; $\overline{du/dy}$, mean velocity gradient
$\overline{V}_S$	Superficial gas velocity, ft/sec
w	Exponent
x	Distance, ft
y	Liquid depth, ft
Z	Height above tank bottom, ft
μ	Absolute viscosity, (lb mass)/(ft)(sec)
ρ	Mass density of fluid, lb mass/ft^3
Φ	Power function, dimensionless
Ψ	Heat transfer factor, dimensionless

4

Sedimentation

4-1. Types of Sedimentation

Sedimentation, in the broad definition of the term, applies to those operations in which a suspension is separated into a clarified fluid and a more concentrated suspension. In sanitary engineering, the term has a more limited meaning and is used to describe the gravity settling of solid particles through a liquid, usually water. The terms "clarification" and "thickening" often are applied to the same operation. Clarification, however, implies a primary interest in the quality of the clarified liquid, whereas in thickening interest is commonly centered on the concentrated slurry in the underflow. The term "flotation" refers to those operations in which buoyancy is used to separate solid or liquid particles from the mother suspension. The present chapter deals primarily with gravity separation from liquid suspensions. However, many of the relationships discussed are applicable to the separation of particles from aerosols.

Particles will settle out of a suspension in one of four different ways, depending upon the concentration of the suspension and the flocculating properties of the particles. The effect of these factors on the settling regime is indicated by Figure 4-1.[1] The

[1] Fitch, E. B., in: McCabe, J., and W. W. Eckenfelder, Jr. (eds.), *Biological Treatment of Sewage and Industrial Wastes*—Vol. 2: *Anaerobic Digestion and Solids-Liquid Separation*, Reinhold Publishing Corp., New York (1958), 159–170.

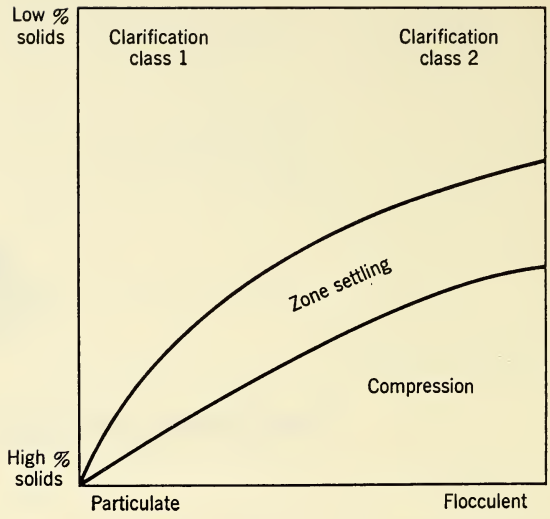

FIGURE 4-1. Paragenesis diagram. [From Figure 2-1, Fitch, E. B., in McCabe, J., and W. W. Eckenfelder, Jr. (eds.), *Biological Treatment of Sewage and Industrial Wastes*—Vol. 2: *Anaerobic Digestion and Solids-Liquid Separation*, Reinhold Publishing Corp., New York (1958), 160.]

manner in which particles having little tendency to flocculate (coalesce upon contact with each other) settle out of a dilute suspension is identified as *class-1 clarification*. If the particles flocculate, the sedimentation regime in a dilute suspension is labeled *class-2 clarification*. In flocculent suspensions of intermediate concentration, particles are close enough together to permit interparticle forces to hold the particles in a fixed position relative to each other. As a result, the mass of particles subsides as a whole in a regime described as *zone settling*. *Compression* occurs when the concentration becomes high enough so that the particles come into actual contact with each other, and the weight of particles is supported, in part, by the structure formed by the compacting mass.

4-2. Class-1 Clarification

The classical laws of sedimentation apply to the settling of discrete, nonflocculating particles in dilute suspensions. Sedimentation of a particle from such suspensions is unhindered by the presence of other settling particles and is a function only of the properties of the fluid and the particle in question.

When an external force causes a particle to move through a fluid, the resultant force on the particle is

$$F_R = F_E - F_B - F_D \tag{4-1}$$

where F_R = resultant force, lb force
F_E = external force, lb force
F_B = buoyant force, lb force
F_D = frictional or drag force, lb force

The external force can be represented by the product of the mass of the particle and the acceleration from the force.

$$F_E = \frac{ma_E}{g_c} \tag{4-2}$$

where m = particle mass, lb mass
a_E = acceleration of particle from the external force, ft/sec^2
g_c = Newton's law conversion factor, 32.17 (ft)(lb mass)/(ft)(lb force)

The buoyant force is

$$F_B = \frac{\rho}{\rho_s}\frac{ma_E}{g_c} \tag{4-3}$$

where ρ = fluid density, lb mass/ft^3
ρ_s = particle density, lb mass/ft^3

The drag force is a function of the roughness, size, shape and velocity of the particle, and of the density and viscosity of the fluid. It has been found experimentally that the relationship is

$$F_D = \frac{C_D A_p \rho u^2}{2g_c} \tag{4-4}$$

where C_D = coefficient of drag
A_p = projected area of particle, ft^2
u = linear velocity of particle, ft/sec

By substituting Equations 4-2, 4-3, and 4-4 in Equation 4-1 and expressing the resultant force in terms of mass and change in velocity with time,

$$\frac{m}{g_c}\frac{du}{dt} = \frac{ma_E}{g_c} - \frac{\rho m a_E}{\rho_s g_c} - \frac{C_D A_p \rho u^2}{2g_c} \tag{4-5}$$

and

$$\frac{du}{dt} = a_E\frac{\rho_s - \rho}{\rho_s} - \frac{C_D A_p \rho u^2}{2m} \tag{4-6}$$

where du/dt = acceleration of particle through fluid, ft/sec^2.

For spherical particles

$$\frac{A_p}{m} = \frac{(\pi D_p^2)/4}{(\pi \rho_s D_p^3)/6} = \frac{3}{2\rho_s D_p} \tag{4-7}$$

and Equation 4-7 becomes

$$\frac{du}{dt} = a_E \frac{\rho_s - \rho}{\rho_s} - \frac{3C_D \rho u^2}{4\rho_s D_p} \tag{4-8}$$

where D_p = particle diameter, ft.

If the external force causing the particle to move is gravity, a_E is equal to g, and Equation 4-8 can be rewritten as

$$\frac{du}{dt} = g \frac{\rho_s - \rho}{\rho_s} - \frac{3C_D \rho u^2}{4\rho_s D_p} \tag{4-9}$$

where g = acceleration of gravity, ft/sec^2.

A particle rising or settling through a fluid under the influence of gravity will accelerate until a velocity is reached where

$$\frac{3C_D \rho u^2}{4\rho_s D_p} = g \frac{\rho_s - \rho}{\rho_s} \tag{4-10}$$

from which point on the acceleration du/dt is zero and the velocity remains constant at a value

$$u_t = \left[\frac{4}{3} \frac{g}{C_D} \left(\frac{\rho_s - \rho}{\rho}\right) D_p\right]^{1/2} \tag{4-11}$$

where u_t = terminal settling velocity. Under normal conditions the terminal velocity is quickly reached.

The coefficient of drag C_D is a function of the Reynolds number N_{Re}. A correlation of the two is given in Figure 4-2. It is to be noted that the correlation varies with the geometric shape of the particle. The relationship between C_D and N_{Re} can be interpreted in light of the flow characteristics exhibited by a fluid passing around an immersed body.

Consider Figure 4-3. Here, a fluid in an infinite duct is flowing past a spherical particle. The solid lines, called *stream lines*, represent paths followed by fluid elements as they flow around the particle. At Reynolds numbers less than 0.1, in the region often called the Stokes' law range, the fluid will flow smoothly over the surface of the sphere, leaving no wake. Drag in this range of Reynolds numbers is composed almost entirely of *skin friction* (viscosity shear stresses). At higher values of the Reynolds number ($N_{Re} > 0.1$), the boundary layer separates from

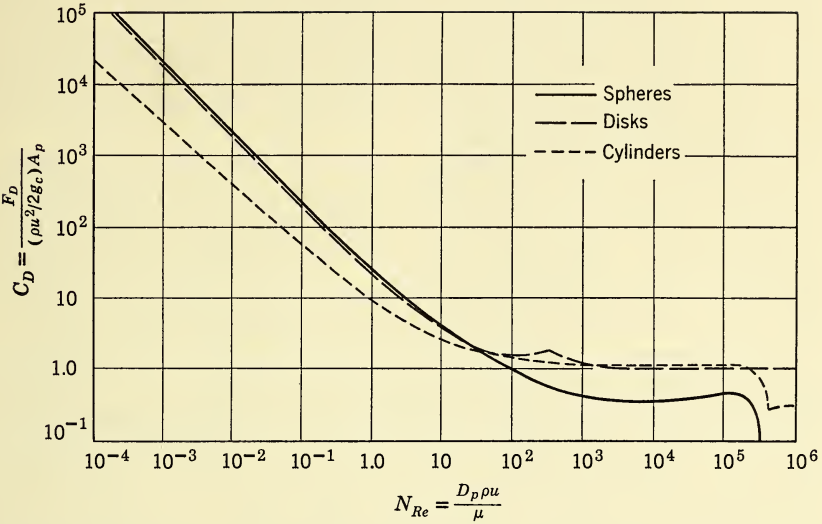

FIGURE 4-2. Drag coefficient for spheres, disks, and cylinders. [By permission from *Chemical Engineers Handbook* (J. H. Perry, ed.), by C. E. Lapple. Copyright, 1950, New York, McGraw-Hill Book Company, Inc.]

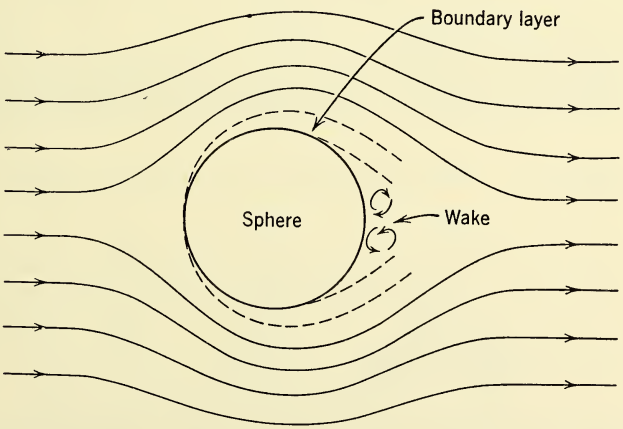

FIGURE 4-3. Fluid flow around a sphere.

the rear surface of the sphere, enclosing a relatively stable wake. A transition occurs in the region between $N_{Re} = 0.1$ and 10^3, in which *form drag* contributes more and more to the total drag on the particle. Form drag results from pressure differences caused by the acceleration of the fluid flowing around the sphere and from the high velocities of the turbulent eddies in the wake.

As the Reynolds number increases beyond 10^3, the point of boundary-layer separation moves to a position upstream from the mid-section of the sphere, and the wake becomes unstable, shedding its contents into the main stream. From $N_{Re} = 10^3$ to 2.5×10^5, in the region sometimes referred to as the Newton's law range, form drag accounts for almost all the drag on the particle, and the drag coefficient is roughly constant.

As N_{Re} increases beyond 2.5×10^5, the boundary layer becomes turbulent, first in the separated portion and then in that part which remains attached. When the boundary layer becomes completely turbulent, the point at which the boundary layer separates from the sphere shifts to a position downstream from the mid-section. The shift is accompanied by a reduction in wake, which results in a drop in drag. The sketch in Figure 4-3 represents a flow pattern that would exist in the range of $N_{Re} = 0.1$ to 10^3.

For convenience, the curve for spheres in Figure 4-2 can be divided into three divisions, each of which is represented by the relationship

$$C_D = \frac{b}{N_{Re}{}^n} \tag{4-12}$$

where b and n are constants.

The constants for Equation 4-12 have been computed [2] for spheres. These are found in Table 4-1. Note should be made that the divisions

TABLE 4-1. CONSTANTS FOR EQUATION 4-12 FOR SPHERES *

N_{Re}	b	n
<1.9	24	1
1.9 to 500	18.5	0.6
500 to 200,000	0.44	0

* After, Table 7-8, McCabe, W. L., and J. C. Smith, *Unit Operations of Chemical Engineering*, McGraw-Hill Book Co., New York (1956), 360.

[2] McCabe, W. L., and J. C. Smith, *Unit Operations of Chemical Engineering*, McGraw-Hill Book Co., New York (1956), 360.

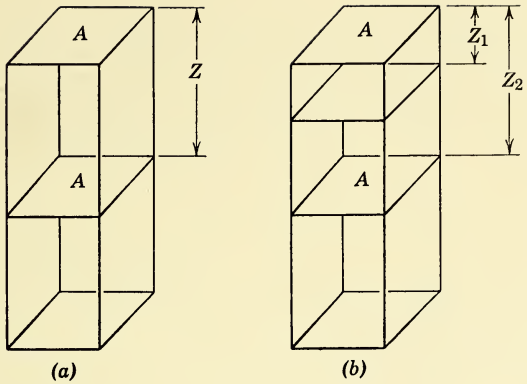

FIGURE 4-4. Rectangular volumes of suspension of nonflocculating particles settling under quiescent conditions. (*a*) Particles with uniform velocities. (*b*) Particles with two settling velocities.

do not coincide exactly with the ranges discussed above, but are established in such a way that the use of straight-line relationships introduces a minimum error.

The maximum rate at which a liquid can be clarified may be formulated as follows.

Consider the sketch in Figure 4-4*a*. Here a dilute suspension of nonflocculating particles having a uniform size and shape occupies a rectangular volume. Under quiescent conditions, the particles subside at their terminal settling velocity, and the liquid at any depth becomes clarified as soon as those particles initially at the top surface pass through it. The rate of clarification, therefore, can be computed from

$$q = \frac{Z}{t} A = u_t A \tag{4-13}$$

where q = volumetric rate of clarification, ft^3/sec
Z = distance through which particles settle in time t, ft
t = time, sec
A = cross-section area of rectangular volume in a plane perpendicular to the direction of subsidence, ft^2

From this expression, it is evident that the flow capacity of a basin in which class-1 clarification is taking place theoretically is independent of the basin depth, and is a function only of the surface area of the basin and the settling velocity of the particles.

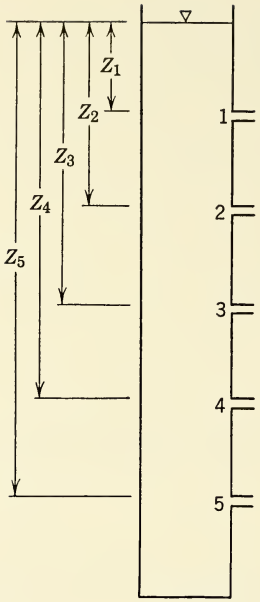

FIGURE 4-5. Column for quiescent settling analysis. [Adapted from Figure 5, Camp, T. R., "Sedimentation and the Design of Settling Tanks," *Trans. ASCE*, **111** (1946), 905.]

Consider now a situation in which liquid is withdrawn from the top of the rectangular volume at a rate q_2, computed from Equation 4-13 for a terminal settling velocity of u_{t2}. The liquid withdrawn would be free of particles having settling velocities equal to or higher than u_{t2}. From Figure 4-4*b* it is apparent that the weight-fraction removal of particles having some lower settling velocity u_{t1}, would be [3]

$$x_1 = \frac{Z_1}{Z_2} = \frac{u_{t1}}{u_{t2}} \tag{4-14}$$

At any clarification rate q_0, the over-all removal from a dilute suspension of nonflocculating particles having different settling velocities can be predicted on the basis of a settling analysis.[4] Such an analysis is performed with a column similar to the one sketched in Figure 4-5. The suspension is placed in the column and is allowed to settle under quiescent conditions. At different time intervals, samples are drawn off

[3] It is to be noted that the symbols x and x_w are commonly employed in chemical engineering literature to express concentrations in mole fraction and weight fraction respectively. To reduce the complexity of the weight fraction terms in this chapter and in Chapters 5, 6, and 9, these terms are designated by the symbol x.

[4] Camp, T. R., "Sedimentation and the Design of Settling Tanks," *Trans. ASCE*, **111** (1946), 895–936.

at a given depth and the concentration of particles in each sample is determined. Each sample contains no particles with settling velocities great enough to carry them from the surface past the sampling depth during the settling period. The maximum settling velocity of particles in each sample, therefore, is approximately

$$u_{tN} = \frac{Z_N}{t} \tag{4-15}$$

where Z_N = sampling depth, ft.

If the initial concentration is uniform throughout the column, the concentration of all the particles in a sample whose settling velocities are less than u_{tN} is the same as in the initial suspension. Hence, a settling-velocity curve such as is presented in Figure 4-6 can be plotted as a characteristic of the suspension.

For a given clarification rate q_0 where

$$q_0 = u_{t0}A \tag{4-16}$$

those particles having settling velocities $u_t \geqq u_{t0}$ will be completely removed. Such particles constitute $1 - x_0$ of the total originally in the clarified liquid. According to Equation 4-14, the weight-fraction removal of particles having velocities $u_t \leqq u_{t0}$ will be $\int_0^{x_0} (u_t/u_{t0})\, dx$. The over-all removal from the clarified liquid, therefore, will be

$$x_T = (1 - x_0) + \frac{1}{u_{t0}} \int_0^{x_0} u_t\, dx \tag{4-17}$$

The last term in Equation 4-17 can be evaluated by graphical integration of the settling-analysis curve between the limits of 0 and x_0, i.e., across the shaded area shown in Figure 4-6.

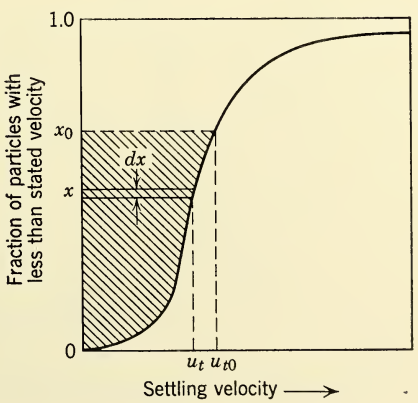

FIGURE 4-6. Settling-velocity analysis curve for suspension of nonflocculating particles. [After Figure 9, Camp, T. R., "Sedimentation and the Design of Settling Tanks," *Trans. ASCE*, **111** (1946), 909.]

EXAMPLE 4-1

A settling analysis is performed on a dilute suspension of nonflocculating particles. The following data are recorded for samples collected at the 4-ft depth.

Settling time, min	0.5	1.0	2.0	4.0	6.0	8.0
Weight fraction remaining	0.56	0.48	0.37	0.19	0.05	0.02

For a clarification rate equal to 0.08 $ft^3/sec/ft^2$, what will be the over-all removal?

Solution

1. Compute the settling velocities of particles settling 4 ft during the stated settling times. Plot the velocities as a function of the fraction of particles remaining and construct a smooth curve through the points (see Figure 4-7).

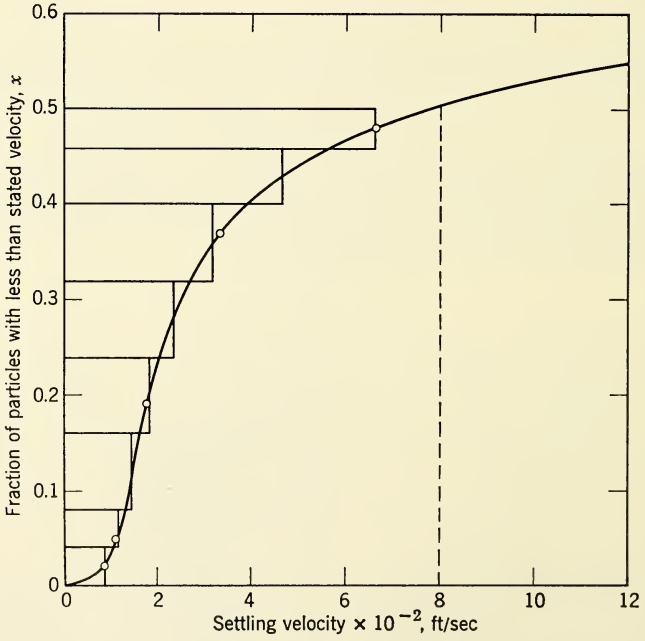

FIGURE 4-7. Graphical integration of Equation 4-17 for Example 4-1.

2. Compute the settling velocity of that size particle, 100 percent of which will just be removed when the rate of clarification is 0.08 $ft^3/sec/ft^2$ (Equation 4-16).

$$u_{t0} = \frac{q_0}{A} = 0.08 \text{ ft/sec}$$

3. From the curve it is found that 0.50 of the particles in the suspension have a velocity less than 0.08 ft/sec. The fraction of these particles that will be removed is determined by a graphical integration of the last term in Equation 4-17 between the limits of $x = 0$ and $x = 0.50$.

dx	u_t	$u_t\,dx$
0.04	0.83×10^{-2}	0.33×10^{-3}
0.04	1.18×10^{-2}	0.47×10^{-3}
0.08	1.40×10^{-2}	1.12×10^{-3}
0.08	1.80×10^{-2}	1.44×10^{-3}
0.08	2.35×10^{-2}	1.88×10^{-3}
0.08	3.20×10^{-2}	2.56×10^{-3}
0.06	4.70×10^{-2}	2.82×10^{-3}
0.04	6.70×10^{-2}	2.68×10^{-3}
		$\Sigma u_t\,dx = 13.30 \times 10^{-3}$

4. Compute over-all removal (Equation 4-17).

$$x_T = (1 - 0.50) + \frac{13.3 \times 10^{-3}}{8 \times 10^{-2}} = 0.50 + 0.17 = 0.67$$

4-3. Class-2 Clarification

The clarification of dilute suspensions of flocculating particles is a function not only of the settling properties of the particles but also of the flocculating characteristics of the suspension. Particles subsiding from such suspensions overtake and coalesce with smaller particles to form particles which settle at rates higher than did the parent particles. The greater the liquid depth, the greater will be the opportunity for contact. Therefore, class-2 clarification differs from class 1 in that removal is dependent both on the clarification rate and on depth.

The rate of flocculation has been shown to be proportional to the mean velocity gradient in the system, the concentration of particles, and particle size (Equation 3-20). However, there is no satisfactory formulation available for evaluating the flocculation effect on sedimentation,

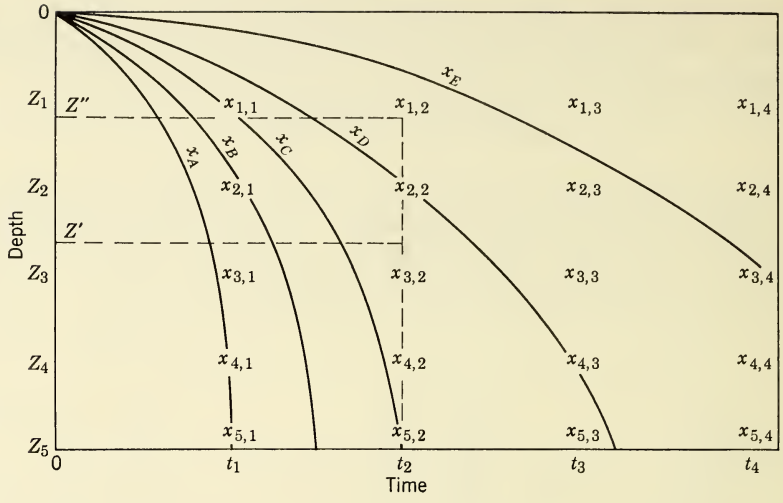

FIGURE 4-8. Fractional removal of flocculating particles as a function of time and depth. [Adapted from Figure 2-8, O'Connor, D. J., and W. W. Eckenfelder, Jr., in McCabe, J., and W. W. Eckenfelder, Jr. (eds.), *Biological Treatment of Sewage and Industrial Wastes*—Vol. 2: *Anaerobic Digestion and Solids-Liquid Separation*, Reinhold Publishing Corp., New York (1958), 173.]

and it is necessary to perform a settling-column analysis in order to measure this effect.

A suspension is placed in a column similar to the one in Figure 4-5, and is allowed to settle under quiescent conditions. Samples are withdrawn from several depths at different time intervals. The concentration of particles in each is determined, and the fraction removed (based on the initial concentration) is recorded in a plot such as is presented in Figure 4-8. The numerical value of the fraction removed is located at the coordinates identifying the time and depth of the sample. Isoconcentration lines connecting points of equal removal are then sketched in by eye, with the use of recorded values as guides.

The isoconcentration lines describe a depth-time ratio equal to the minimum average settling velocity of the fraction of particles indicated. For example, x_D of the particles in the suspension have had an average velocity greater than Z_2/t_2 by the time the depth of Z_2 is reached. By the time the depth Z_4 is reached, the same fraction of particles have had an average velocity of Z_4/t_3 or greater. The curvature of the lines reflects the flocculating nature of the suspension. Isoconcentration lines for a settling suspension of nonflocculating particles would be linear.

The over-all removal in a basin of depth Z_5 and at a clarification rate q_0, where

$$q_0 = \frac{Z_5}{t_2} A = u_{t0} A \tag{4-18}$$

is computed as follows. From Figure 4-8 it is seen that, during the time interval t_2, x_C of the particles have had an average settling velocity of Z_5/t_2 or greater. Of the remainder, $x_D - x_C$ have had an average velocity of Z'/t_2 or u'_t, and $x_E - x_D$ an average velocity of Z''/t_2 or u''_t. Thus, the over-all removal would be approximately

$$x_T = x_C + \frac{u'_t}{u_{t0}} (x_D - x_C) + \frac{u''_t}{u_{t0}} (x_E - x_D) \tag{4-19}$$

$$= x_C + \frac{Z'}{Z_5} (x_D - x_C) + \frac{Z''}{Z_5} (x_E - x_D) \tag{4-20}$$

The average settling velocity of the fraction $1 - x_E$ is so small that the removal of this fraction would be insignificant. Removal in basins of other depths and at other rates of clarification can be computed in a similar manner.

4-4. Zone Settling

The settling characteristics demonstrated by concentrated suspensions are somewhat different from those of dilute suspensions. Since the difference is more apparent for flocculating suspensions than it is for nonflocculating ones, the discussion of zone settling will be in terms of the former.

Consider a cylinder containing a dilute suspension of differently sized particles and, initially, of equal concentration throughout. The position of a particle which at $t = 0$ was at the surface of the suspension is located at different time intervals, as shown by the curve in Figure 4-9 labeled "unhindered settling." The particle will settle unhindered at its own individual velocity of subsidence. Not until point B is reached will the particle deaccelerate. Somewhere between points B and C, the particle becomes part of the deposited sludge. From C to D the position of the particle is dependent upon the compaction of the sludge deposit.

As the concentration of the suspension is increased, a concentration is reached in which the fastest settling particles form a zone and settle from then on collectively and at a reduced rate. As the concentration is increased further, this zone forms at progressively earlier periods until

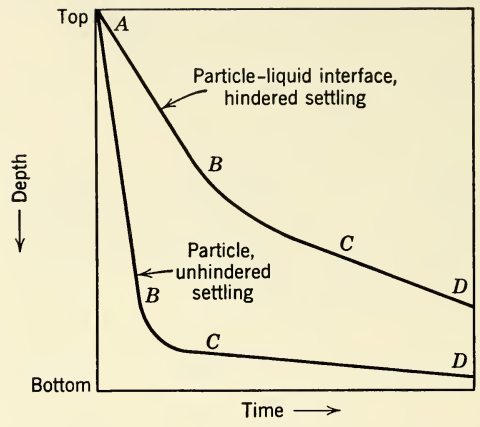

FIGURE 4-9. Position of settling particle and subsiding particle-liquid interface as a function of time.

a point is reached where initial subsidence is collective and no individual particle movement is observed. For concentrations as large as or greater than this concentration, a distinct interface is formed between the subsiding particles and the clarified liquid. The position of such an interface will vary with time in a manner similar to that described by the curve in Figure 4-9 labeled "hindered settling." It is to be noted that this curve is only a modification of the other curve.

All settling processes produce four zones, each with its own particular characteristics. Figure 4-10 is a sketch showing the relative positions of the different zones as they are formed at different time intervals in a thick, flocculent suspension. Initially, the concentration is uniform throughout the suspension. The suspension having the initial concentration is labeled B. Immediately, a solids-liquid interface develops, and a zone of clarified liquid, A, is formed. In zone B, the particles settle at a uniform velocity under conditions of hindered settling. The suspension in this zone remains constant at uniform concentration, and the magnitude of the velocity at which the suspension settles is a function of the concentration

$$u = \psi(c) \tag{4-21}$$

where u = velocity of subsidence under conditions of hindered settling
c = initial concentration of particles in suspension

Concurrent with the formation of zone A, two other zones, C and D, are formed. Zone C is a zone of transition through which the settling velocity decreases in response to an increasing concentration of solids. When the suspension becomes concentrated to the point where the solids

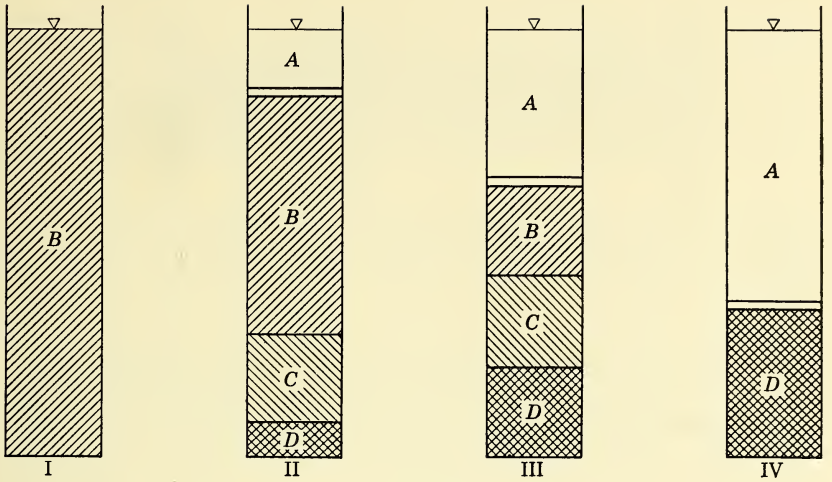

FIGURE 4-10. Zone formation in a concentrated, flocculent suspension after four different time intervals. [By permission from *Chemical Engineers Handbook* (J. H. Perry, ed.), by A. Anable. Copyright 1950, New York, McGraw-Hill Book Co., Inc.]

are supported mechanically by the solids below, they become a part of a compression zone *D*.

For continuous-flow sedimentation or thickening tanks, the surface area required to separate concentrated suspensions is based primarily on two factors: the clarification and thickening capacities. Both factors can be estimated from batch settling tests.

The *clarification capacity* can be estimated from the initial rate at which the solids-liquid interface subsides. The surface area of a continuous-flow tank must be large enough so that the rate of liquid rise (computed on the basis of liquid overflow only) is less than the subsidence velocity.

The *thickening capacity* is computed with a relationship developed from a rational analysis of the behavior of a suspension undergoing batch sedimentation.[5,6] Initially, the concentration is the same throughout the suspension, and the solids settle at a uniform velocity. Before the solids are deposited at the bottom of the settling column, they must pass through all concentrations ranging from the initial concentration to that of the deposited solids. If the solids-handling capacity at any inter-

[5] Kynch, G. J., *Trans. Faraday Soc.*, **48** (1952), 161.

[6] Talmadge, W. P., and E. B. Fitch, "Determining Thickener Unit Areas," *Ind. Engr. Chem.*, **47** (1955), 38.

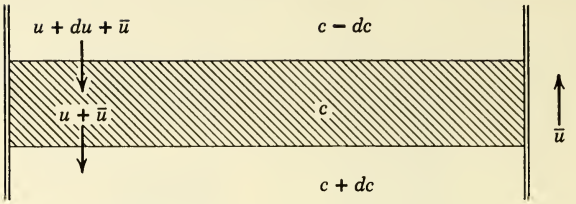

FIGURE 4-11. Definition sketch of a concentration layer rising through a settling column.

mediate concentration is less than that of the lower concentration just above it, the solids cannot pass through the concentration as rapidly as they are settling into it and, as a result, a zone of the intermediate concentration will commence building up in the column.

Consider now, at the top of such a zone, a thin layer of concentration c which was formed at the bottom of the suspension at $t = 0$, and which is rising through the column at a velocity $\bar{u}$ (see Figure 4-11). The solids settle into this layer from a layer having a concentration of $c - dc$, and at a velocity with respect to the column of $u + du$, but with respect to the layer of $u + du + \bar{u}$. The solids settle out of the layer at a velocity u with respect to the container, or $u + \bar{u}$ with respect to the layer itself. Since the layer concentration c remains constant, the quantity of solids settling into the layer perforce must equal that settling out of the layer.

$$(c - dc)At(u + du + \bar{u}) = cAt(u + \bar{u}) \tag{4-22}$$

where A = cross-section area perpendicular to direction of solids movement
t = time

By simplifying Equation 4-22 and solving for $\bar{u}$,

$$\bar{u} = c\frac{du}{dc} - u - du \tag{4-23}$$

and by dropping the infinitesimal du,

$$\bar{u} = c\frac{du}{dc} - u \tag{4-24}$$

According to Equation 4-21, the velocity of subsidence under conditions of hindered settling is a function of the concentration. Equation 4-24 then, through substitution, becomes

$$\bar{u} = c\,\psi'(c) - \psi(c) \tag{4-25}$$

The concentration of the layer under consideration remains constant. Since $\psi(c)$ and $\psi'(c)$ have fixed values, $\bar{u}$ also must remain constant. The fact that the rate $\bar{u}$ at which a layer of concentration c travels up through the suspension remains constant can be used to determine the solids concentration of the layer at the upper boundary of a settling suspension.

If a column of height Z'_0 is filled with a suspension having a uniform concentration of c_0, the total weight of solids in the suspension is equal to $c_0 Z'_0 A$. As the suspension settles, concentration layers propagate upward from the bottom. By the time any concentration layer reaches the solids-liquid interface, all the solids will have passed through it. If t_2 is the time required for a layer of concentration c_2 to reach the interface, then the quantity of solids having passed through the layer is $c_2 A t_2(u_2 + \bar{u}_2)$, which will be equal to the total weight of the solids in the column.

$$c_0 Z'_0 A = c_2 A t_2(u_2 + \bar{u}_2) \tag{4-26}$$

The rate at which any layer is propagated upward has been found to be constant. Therefore, if the interface at time t_2 is at a height Z'_2,

$$\bar{u}_2 = \frac{Z'_2}{t_2} \tag{4-27}$$

By substituting this expression into Equation 4-26 and rearranging,

$$c_2 = \frac{c_0 Z'_0}{Z'_2 + u_2 t_2} \tag{4-28}$$

A plot of the interface height as a function of time is shown in Figure 4-12. The slope at any point along the curve is equal to the velocity at which the interface at that particular point subsides. At t_2,

$$u_2 = \frac{Z'_1 - Z'_2}{t_2} \tag{4-29}$$

and

$$u_2 t_2 = Z'_1 - Z'_2 \tag{4-30}$$

Substituting the right-hand term of this expression in Equation 4-28, results in

$$c_2 Z'_1 = c_0 Z'_0 \tag{4-31}$$

The term Z'_1 can be interpreted as the height at which the sludge column would stand if all the solids in the column were at the same concentration as those in the interface. For any value of c_2, the corresponding value of Z'_1 can be calculated.

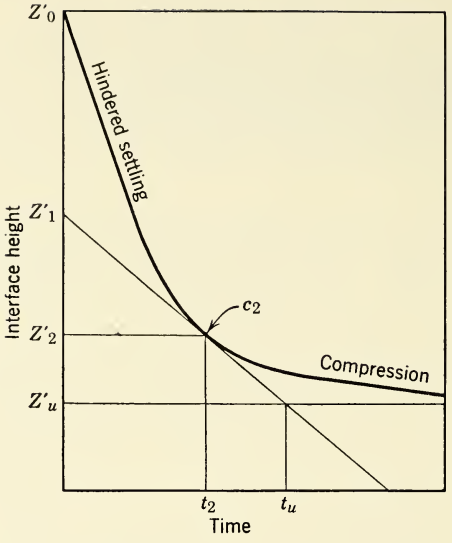

FIGURE 4-12. Graphical analysis of interface settling curve. [After Figure 1, Talmadge, W. P., and E. B. Fitch, "Determining Thickener Unit Areas," *Ind. Engr. Chem.*, **47** (1955), 38–41.]

In a continuous operation, conditions exist in which the position of the solids-liquid interface is relatively static, and the relative movement between the solids and the liquid is caused by the upward flow of the liquid. Therefore, at time t_2, the bulk rate of liquid flow past the interface having a solids concentration c_2 would be

$$q' = \frac{A(Z'_1 - Z'_2)}{t_2} \tag{4-32}$$

Not all the liquid will move through the interface. Some will accompany the solids to the underflow. The actual volume of liquid passing through the interface is equal to the volume which would be released in the concentration of the solids from the interface concentration c_2 to that of the underflow c_u. The corresponding volume of liquid in a batch analysis would be

$$V = A(Z'_1 - Z'_u) \tag{4-33}$$

where Z'_u = height of the sludge interface if all the solids in the system were at an underflow concentration of c_u

The time required for a volume of water V to flow through a layer of concentration c_2 would be

$$t = \frac{V}{q'} = \frac{A(Z'_1 - Z'_u)}{[A(Z'_1 - Z'_2)]/t_2} \tag{4-34}$$

Rearranging terms,

$$\frac{t}{Z'_1 - Z'_u} = \frac{t_2}{Z'_1 - Z'_2} \tag{4-35}$$

From Figure 4-12 it is seen that

$$t = t_u \tag{4-36}$$

The total quantity of solids in the batch analysis is $c_0 Z'_0 A$. In a continuous thickening operation, it would take time t_u for this quantity to settle past a layer with a concentration of c_2. Therefore, equating the rate of solids input with the rate at which the solids can pass through the layer,

$$qc_0 = \frac{c_0 Z'_0 A}{t_u} \tag{4-37}$$

and

$$A = \frac{qt_u}{Z'_0} \tag{4-38}$$

where A = cross section required for layer with a concentration of c_2, ft^2
q = volumetric flow rate of suspension entering thickener, ft^3/sec
t_u = time required to attain underflow concentration c_u, sec
Z'_0 = initial height of interface in settling column, ft

Values of t_u can be determined graphically from plots similar to Figure 4-12.[7] A straight line is drawn through c_2, tangent to the settling curve. The intersection of the tangent with the line representing the desired underflow concentration c_u determines t_u.

The critical concentration controlling the solids-handling capacity of the system is that concentration requiring the largest cross-section area. This concentration normally occurs in the transition zone at the point where compression begins. The compression point may be estimated by bisecting the angle formed where tangents from the hindered settling zone and the compression zone intersect.[8] The bisector cuts the settling curve near the point of compression.

When the underflow line intersects the settling curve above the compression point, the critical concentration is taken as that concentration occurring at the interface at the point of intersection. A tangent through

[7] Talmadge, W. P., and E. B. Fitch, "Determining Thickener Unit Areas," *Ind. Engr. Chem.*, **47** (1955).

[8] Eckenfelder, W. W., Jr., and N. Melbinger, "Settling and Compaction Characteristics of Biological Sludges," *Sewage and Industrial Wastes*, **29** (1957), 1114–1122.

any other concentration will intersect the underflow line at a lesser value of t_u.

The thickening capacity is generally expressed in terms of *unit area*, the units of which are square feet per ton of solids per day. Unit area may be computed from

$$\text{Unit area} = (2.32 \times 10^{-2}) \frac{t_u}{c_0 Z'_0} \tag{4-39}$$

EXAMPLE 4-2

From a batch settling analysis performed with a sludge having a solids concentration of 3000 mg/l, data were collected which plotted to give the curve in Figure 4-13. The sludge is to be settled in a continuous-flow thickener at a rate of 1 ft^3/sec. If an underflow concentration of 12,000 mg/l is desired, what will be the minimum area that the thickener can have?

Solution

1. Compute height of sludge interface if all solids in the system are at the underflow concentration $c_u = 12{,}000$ mg/l.

$$Z'_u = \frac{c_0}{c_u} Z'_0 = \frac{3000}{12{,}000} \times 40 = 10 \text{ cm}$$

Construct a horizontal line at this height.

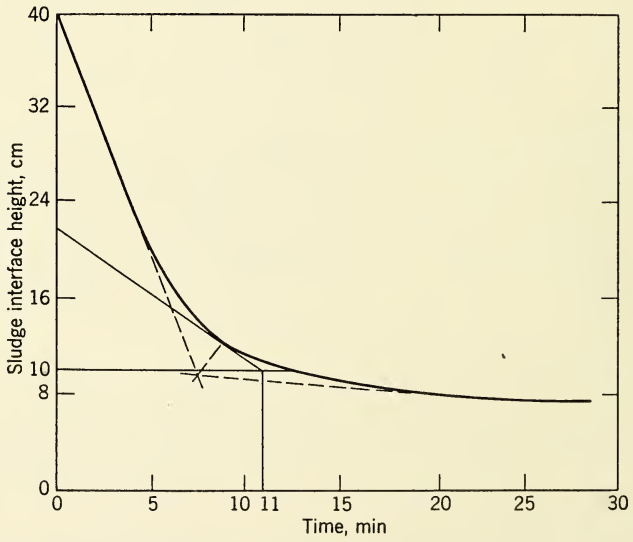

FIGURE 4-13. Interface settling curve for Example 4-2.

UNIVERSITY OF FLORIDA
GENESYS LIBRARY

2. Estimate the compression point by bisecting the angle formed by the tangents of the two end portions of the subsidence curve. Construct a straight-line tangent to the curve at the compression point. This line intersects the horizontal line representing the underflow concentration at $t_u = 11$ min.

3. Compute thickening area requirement (Equation 4-38).

$$A = \frac{qt_u}{Z'_0} = \frac{1 \times 11 \times 60}{40/30.48} = 504 \text{ ft}^2$$

4. From the hindered settling portion of the curve, the rate of subsidence is found to be

$$u = \frac{16/30.48}{4 \times 60} = 2.18 \times 10^{-3} \text{ ft/sec}$$

5. Compute the area required for clarification.

$$A = \frac{q}{u} = \frac{1(3/4)}{2.18 \times 10^{-3}} = 344 \text{ ft}^2$$

6. Thickening area requirement controls. Area of thickener must be at least 504 ft^2.

4-5. Compression

When subsiding particles pass into the zone of compression, they come into physical contact with each other and, thus, become supported by layers below. Consolidation of particles in this zone is relatively slow. The approximate rate of consolidation has been formulated as [9]

$$-\frac{dZ'}{dt} = K(Z' - Z'_\infty) \tag{4-40}$$

where Z' = height of sludge line, ft
Z'_∞ = final height of sludge line, ft
K = constant for a given suspension, sec^{-1}

[9] Coulson, J. M., and J. F. Richardson, *Chemical Engineering*, Vol. 2, McGraw-Hill Book Co., New York (1955), 515.

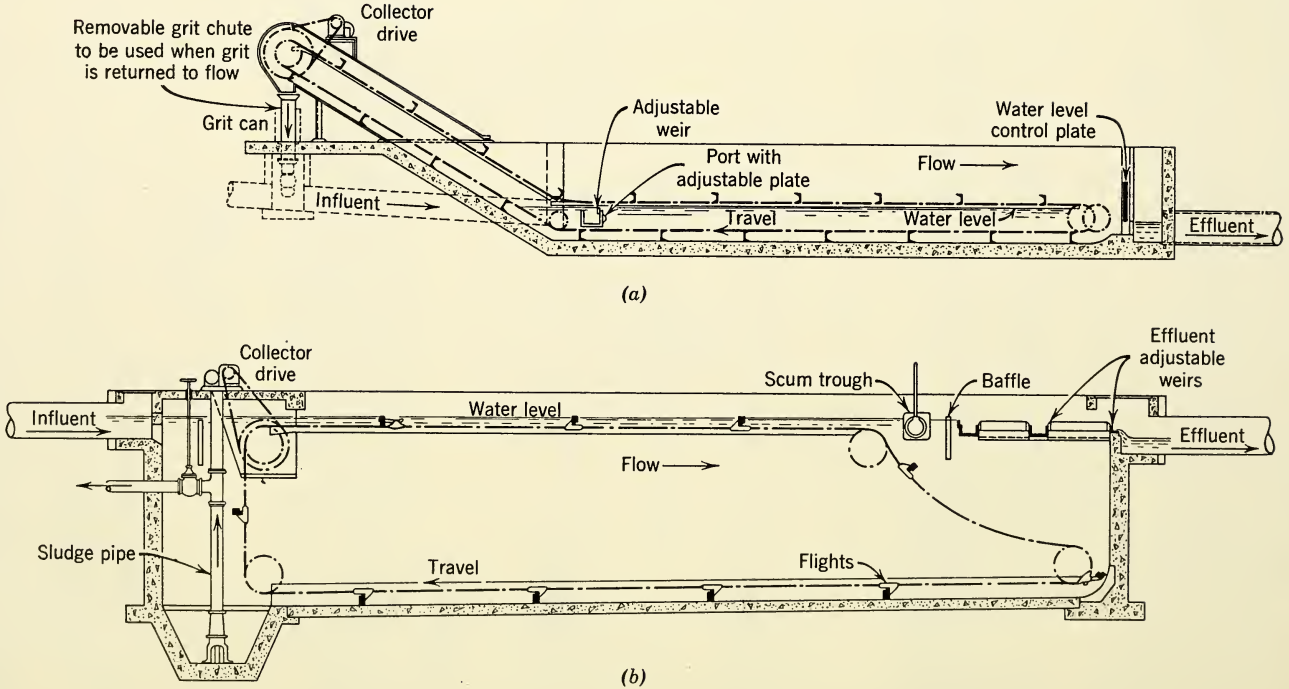
Removable grit chute
to be used when grit
is returned to flow
Collector
drive
Grit can
Adjustable
weir
Water level
control plate
Port with
adjustable plate
Flow
Influent
Travel
Water level
Effluent
(a)
Collector
drive
Effluent
adjustable
weirs
Scum trough
Baffle
Influent
Water level
Effluent
Flow
Sludge pipe
Travel
Flights
(b)

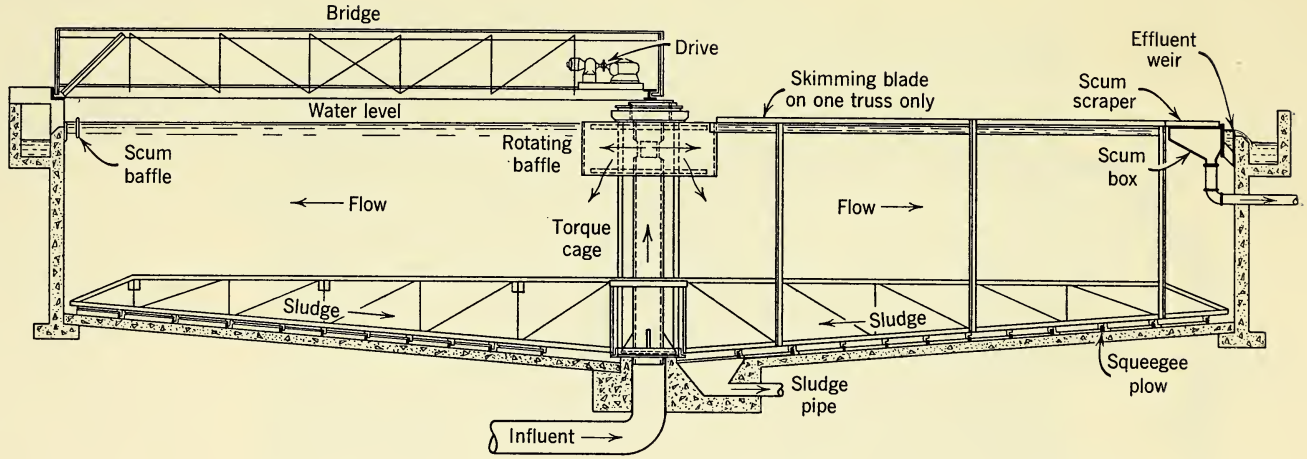

(*c*)

FIGURE 4-14. Typical horizontal-flow sedimentation basins. (*a*) Mechanically cleaned grit-removal basin. (*b*) Rectangular basin, mechanically cleaned. (*c*) Circular basin, mechanically cleaned. (From *Link-Belt Book 2617*, Link-Belt Company.)

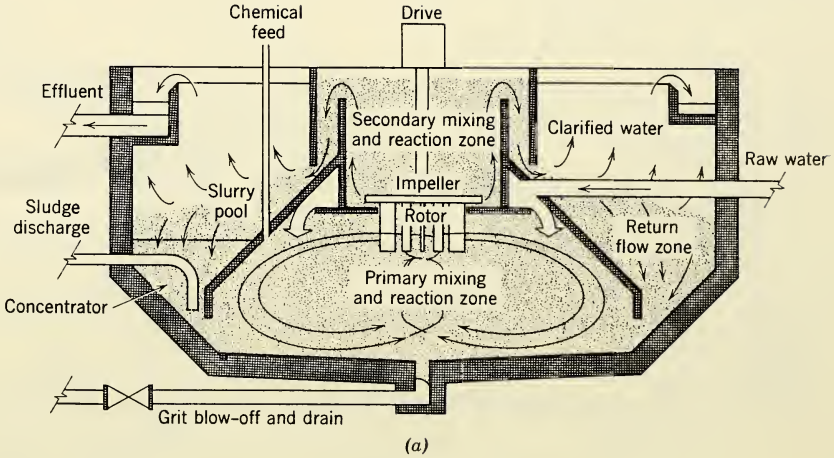

FIGURE 4-15. Typical vertical-flow sedimentation basins. (*a*) Courtesy of Infilco, Inc. (*b*) Graver Reactivator®. (Courtesy of Graver Water Conditioning Company.)

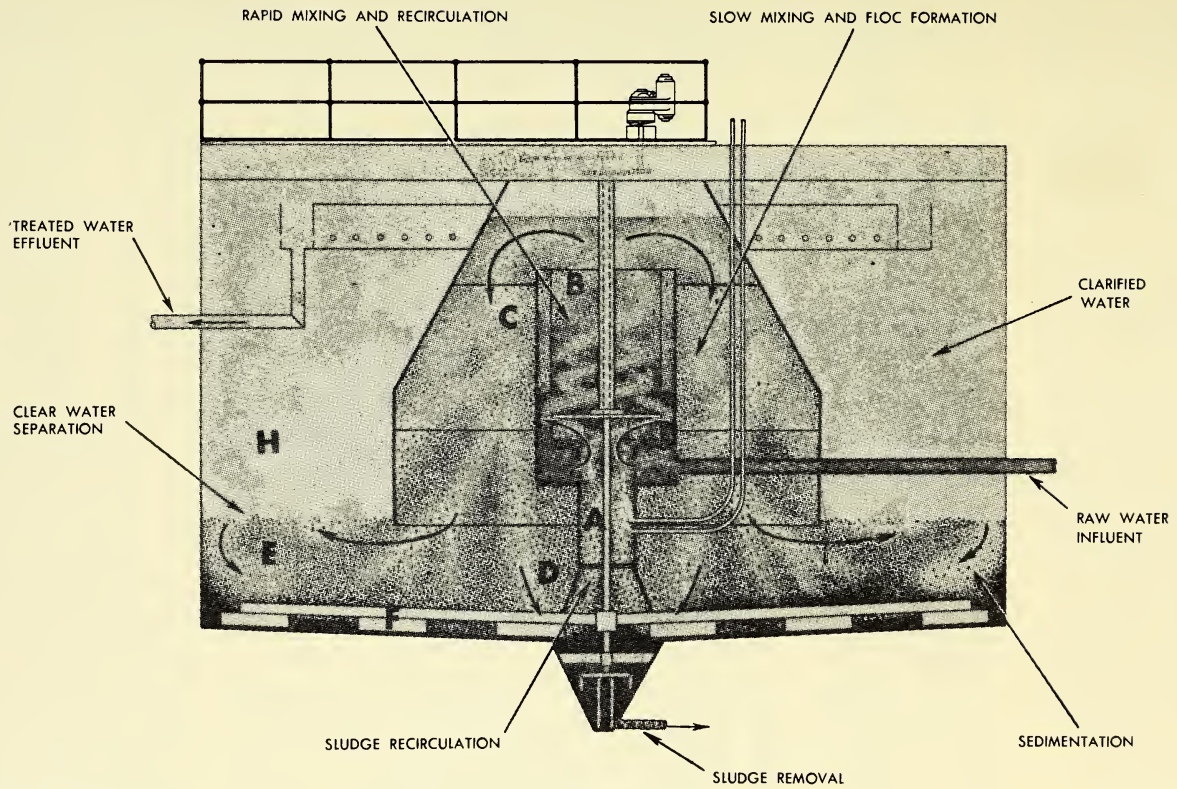
RAPID MIXING AND RECIRCULATION
SLOW MIXING AND FLOC FORMATION
TREATED WATER EFFLUENT
CLARIFIED WATER
CLEAR WATER SEPARATION
RAW WATER INFLUENT
SLUDGE RECIRCULATION
SEDIMENTATION
SLUDGE REMOVAL
A
B
C
D
E
F
H

(*b*)

Integrating Equation 4-40 between the limits of Z' at the compression point and at time t, results in

$$-\int_{Z'_c}^{Z'_t} \frac{dZ'}{Z' - Z'_\infty} = K\int_{t_c}^{t} dt$$

$$\ln \frac{Z'_c - Z'_\infty}{Z'_t - Z'_\infty} = K(t - t_c) \qquad (4\text{-}41)$$

where Z'_c = height of sludge line at the compression point, ft
Z'_t = height of sludge line at time t, ft
t_c = time sludge line is at the compression point, sec

Compaction is facilitated by gentle agitation. Such agitation commonly is provided by mechanical rakes.

4-6. Sedimentation Equipment

Continuous clarification and thickening operations in waste treatment applications are carried out in rectangular, circular, and square basins. The basin structure consists of four functional components, each with its own special problems of hydraulic and process design. Feed is introduced through an *influent structure.* Sedimentation takes place in the *settling zone.* Clarified liquid is collected by an *effluent structure,* and sludge accumulates which is withdrawn from a *sludge zone.* When sludge volumes are large, mechanical equipment is used for the continuous removal of sludge.

Both horizontal- and vertical-flow basins are used in sedimentation. Typical examples of the former are presented in Figure 4-14. In rectangular basins, feed is introduced at one end along the width of the basin and collected at the surface, either across the other end or at different points along the length of the basin. When employed, mechanical sludge-removal equipment push the settled solids down a gently sloping bottom (about 1 percent) toward a hopper at one end of the basin, where it is removed from the system. The length-to-width ratio will vary from 3:1 to 5:1, with 4:1 being the most common. With the exception of grit-removal tanks, most basins are 8 to 10 ft in depth. Some, however, are as deep as 15 ft.

Circular basins from 35 to 150 ft in diameter and 8 to 12 ft deep are currently used in water and waste treatment processes. Feed is brought into the basin through a center well. The clarified effluent is collected at weirs along the periphery of the basin. A scraper mechanism forces the settled sludge down a sloping bottom (generally 6 to 8 percent) to a central sludge hopper.

Examples of vertical-flow basins are shown in Figure 4-15. Most basins of this type are circular. Feed is applied at a point or points along the bottom, and clarified effluent is collected at the top, either at the center of the basin or along the sides. A sludge blanket is maintained in the lower part of the basin through which the suspension rises. In many cases, a portion of the basin is used for flocculation.

4-7. Continuous-Flow Operations

Preceding sections have dealt with the derivation of design criteria using either theoretical principles of sedimentation or data obtained in the laboratory from batch analyses. Although such criteria provide a basis for the design of full-scale, continuous operations, they must be modified first to take into account the actual performance characteristics of the equipment in which the operations are carried out.

The concept of an *ideal basin* can be used to relate batch sedimentation with continuous operations.[10] Imagine a hypothetical, rectangular basin through which all elements of a suspension are flowing parallel to each other, and at the same velocity. If a rectangular volume of the suspension (similar to the one depicted in Figure 4-4) with a height equal to the depth of the basin were to be observed as it moved the length of the basin, the only difference that could be noted between the settling behavior in the moving volume and that occurring in a batch analysis would be that the solids that have settled out of the suspension could be found deposited along the length of the bottom of the basin instead of at the bottom of the settling column. This relationship is brought out graphically in Figure 4-16. Similarly, a volume may be visualized in a circular, horizontal-flow basin as it moves from the center well to the wall. Here, however, the volume must change in size and shape in adjustment to the radial flow pattern. The settling behavior of dilute suspensions in such basins theoretically should conform to that in batch analyses.

The performance of actual basins departs from that of ideal basins. Such factors as density currents, wind currents, and inertial forces established by the influent and effluent structures induce short-circuiting of the contents of an actual basin. The over-all effect of short-circuiting is to reduce the effective residence time of a major portion of the flow, a factor of considerable importance in the sedimentation of flocculent suspensions. Furthermore, at flow-through velocities greater than the

[10] Camp, T. R., "Sedimentation and Design of Settling Tanks," *Trans. ASCE*, **111** (1946), 895.

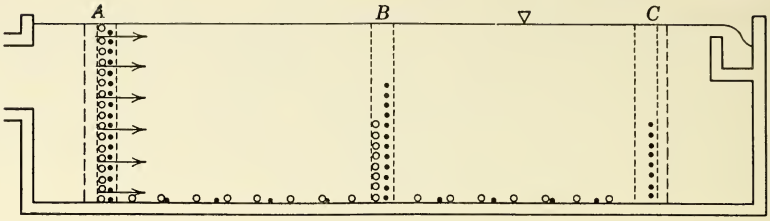

FIGURE 4-16. Relationship between continuous and batch settling. *A*—element marked at influent; *B*—element after passing part way through basin; *C*—element at effluent end of basin. [From Figure 2-2, Fitch, E. B., in McCabe, J., and W. W. Eckenfelder, Jr. (eds.), *Biological Treatment of Sewage and Industrial Wastes*—Vol. 2, Reinhold Publishing Corp., New York (1958).]

velocity of scour (see Section 2-4), eddy currents are established which radically affect performance.

Mathematical relationships have been developed for predicting basin performance.[11, 12, 13] For the most part, however, the use of such is limited to the sedimentation of nonflocculating particles. Instead, a study should be made of the flow-through characteristics in geometric scale models. Although such models for studying sedimentation are not practical because the laws of hydraulic similitude require that all dimensions, including the particle sizes, should be scaled down proportionally, they are useful in studying short-circuiting.

The net effect of all the factors that contribute toward reducing the efficiency of sedimentation in an actual basin is to decrease the clarification rate and to increase the detention time over that derived from a batch analysis. For the sedimentation of nonflocculating particles from dilute suspensions (class-1 clarification), it appears reasonable to apply a correction factor of 1 to 1.25 to both values. For the sedimentation of flocculant particles from dilute suspensions (class-2 clarification), the overflow rate generally will be decreased by a factor of 1.25 to 1.75, and the detention time will be increased by a factor of 1.50 to 2.00.[14]

In scaling-up thickening operations, a factor of 1.0 to 2.0 is applied

[11] Hazen, A., "On Sedimentation," *Trans. ASCE*, **53** (1904), 45.

[12] Camp, T. R., "Sedimentation and Design of Settling Tanks," *Trans. ASCE*, **111** (1946), 895.

[13] Ingersoll, A. C., J. E. McKee, and N. H. Brooks, "Fundamental Concepts of Rectangular Settling Tanks," *Trans. ASCE*, **121** (1956), 1179.

[14] O'Connor, D. J., and W. W. Eckenfelder, Jr., in: McCabe, J., and W. W. Eckenfelder, Jr., *Biological Treatment of Sewage and Industrial Wastes*, Vol. 2, Reinhold Publishing Co., New York (1958), 180.

to the area required for clarification (hindered settling), and a factor of 1.0 to 1.5 to that required for thickening.[15]

Notations

a_E Acceleration from an external force, ft/sec^2
A Cross-section area in plane perpendicular to direction of subsidence, ft^2
A_p Projected area, ft^2
b Constant
c Weight concentration, lb force/ft^3; c_0, initial weight concentration; c_u, weight concentration of underflow
C_D Coefficient of drag, dimensionless
D_p Particle diameter, ft
F_R Resultant force, lb force; F_E, external force; F_B, buoyant force; F_D, drag force
g Acceleration of gravity, ft/sec^2
g_c Newton's law conversion factor, 32.17 (ft)(lb mass)/(lb force)(sec^2)
K Constant
m Mass, lb mass
n Constant
N_{Re} Reynolds number, dimensionless
q Volumetric rate of clarification, ft^3/sec; q_0, rate of clarification corresponding to the volume swept by a particle subsiding at a velocity u_{t0} over a cross-section area A
t Time, sec; t_u, time required to attain underflow concentration c_u; t_c, time required for sludge interface to come to the compression point
u Linear velocity of a particle, ft/sec; $\bar{u}$, velocity at which a solids layer of concentration c travels up through a suspension; u_t, u'_t, u''_t, terminal settling velocities; u_{tN}, terminal settling velocity of particle settling Z_N distance in t seconds; u_{t0}, terminal settling velocity of smallest particle removed from suspension when the rate of clarification is q_0/ft^2 of surface area
V Volume, ft^3
x Weight fraction of particles removed; x_0, weight fraction of particles having terminal settling velocities less than u_{t0}; x_T, total removal of particles expressed in terms of weight fraction
Z Distance through which particles settle in time t, ft; Z', height of sludge interface; Z'_0, initial height of sludge interface; Z'_u, height of sludge interface if all solids in system are at an underflow concentration c_u; Z'_∞, final height of sludge line; Z'_c, height of sludge line at compression point; Z_N, sampling depth
ρ Mass density of a liquid, lb mass/ft^3; ρ_s, mass density of a particle
ψ Operator

[15] Eckenfelder, W. W., Jr., and D. J. O'Connor, *Bio-Oxidation of Organic Wastes, Theory and Design*, Manhattan College, New York (1959), 89.

5

Flotation and aerosol separation

FLOTATION

5-1. Flotation Methods

Flotation is a unit operation employed in the separation of solid and liquid particles from a liquid phase. Separation is facilitated by the presence of fine bubbles resulting from the introduction of a gas phase, usually air, to the system. The rising bubbles either adhere to or are trapped in the particle structure, thereby imparting to or increasing the buoyancy of the particles. Particles having a density even greater than that of the liquid phase can be separated by flotation. Separation by flotation does not depend so much on the size and relative density of particles being removed as it does on their surface properties.

Two methods of flotation are currently in use. In *dispersed-air flotation*, gas bubbles are generated by introducing the gas phase through a revolving impeller or through porous media. Bubble size is of the order of 1000 microns (mu) in diameter.[1] Dispersed-air flotation is used to a wide extent in the metallur-

[1] Vrablik, E. R., "Fundamental Principles of Dissolved-Air Flotation of Industrial Wastes," Paper presented at 14th *Annual Purdue Industrial Waste Conference* (1959).

gical industry. In *dissolved-air flotation,* bubbles are produced as a result of the precipitation of a gas from a solution super-saturated with the gas. The average bubble size ranges from 70 to 90 mu. This method finds wide application in the treatment of industrial wastes. Although the same principles apply in both methods, the following discussion is oriented toward dissolved-air flotation.

5-2. Gas-Particle Contact

The mechanism of contact between the gas bubbles and floated particles may be one or both of two types. The first type is predominant in the flotation of flocculent materials and involves the trapping of growing and rising gas bubbles in the growing structure of the floc particle. Here the bond between the bubble and particle is one of physical capture only.

The second type of contact is one of adhesion. Adhesion results from the intramolecular attractions that are exerted at an interface between two phases, and which give rise to interfacial tension. The extent to which adhesion will take place can be predicted from a consideration of the interfacial tensions involved in a gas-liquid-solid system.

Figure 5-1*a* shows a gas bubble in contact with a solid particle in a liquid constituting the continuous phase. The angle formed between the gas-liquid interface and the solid-liquid interface at the point where the three phases make contact is called the angle of contact α. The equilibrium existing at the point of contact between the interfacial tensions is illustrated by the force diagram in Figure 5-1*b*. Algebraically the equilibrium can be expressed as

$$\sigma_{GS} = \sigma_{SL} + \sigma_{GL} \cos \alpha \tag{5-1}$$

where σ_{GS} = interfacial tension between gas and solid phases
σ_{SL} = interfacial tension between solid and liquid phases
σ_{GL} = interfacial tension between gas and liquid phases

If σ_{GS} is equal to or less than σ_{SL}, the contact angle α is zero or cannot exist, in which case a liquid film prohibits contact between the solid and gas phases. When σ_{GS} is greater than σ_{SL}, the angle α is greater than zero and the gas bubble can adhere to the solid particle. The tendency for the gas bubble to adhere to the solid increases with size of the contact angle.

Although the adhesion mechanism has been discussed above in terms of a solid dispersed phase, the same principles apply in the case of a dispersed phase that is liquid.

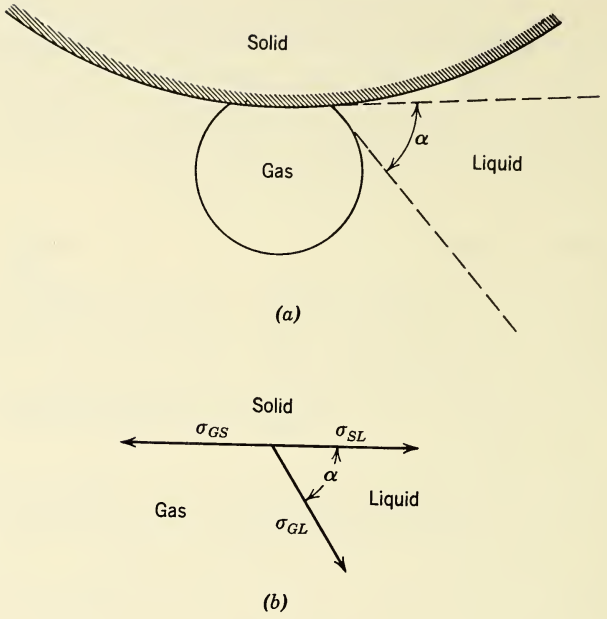

FIGURE 5-1. Interfacial tensions existing in a three-phase system.

5-3. Use of Chemical Agents

The entrapment of gas bubbles often is promoted by the use of coagulating chemicals. These chemicals, which include alum, ferric chloride, activated silica, etc., impart to or increase the flocculent structure of the floated particles, thereby facilitating the capture of gas bubbles.

Several groups of chemicals are used that aid flotation by altering the surface properties of the phases involved. *Frothers* such as the higher alcohols, pine oil, and cresylic acid serve to lower the interfacial tension between the gas and liquid, σ_{GL}. This promotes bubble formation as well as a more stable froth at the surface of the liquid. *Collectors* either reduce the interfacial tension between the solid and liquid, σ_{SL}, or increase that between the gas and solid, σ_{GS}. Both effects serve to increase the angle of contact α. Soap, fatty acids, and amines are in common use as collectors. *Activators* are a group of chemicals that improve the effect of collectors. *Depressants* prevent the flotation of certain phases without preventing the desired phase from becoming floated. Activators and depressants often are referred to as *promoters*.

5-4. Dissolved-Air Flotation

Two methods of dissolved-air flotation have been successfully used in waste treatment processes. *Vacuum flotation* is accomplished by subjecting the waste first to a short period of aeration at atmospheric pressure. This step is followed by an application of a vacuum (approximately 9 in. of mercury) which induces the precipitation of dissolved air from the saturated solution. The fact that only a limited quantity of air can be precipitated out of a solution saturated at one atmosphere limits the application of vacuum flotation.

The second method, commonly referred to as pressure flotation, involves the solution of air under an elevated pressure followed by its release at atmospheric pressure. A typical arrangement for pressure flotation is shown in Figure 5-2. Equipment components commonly include a pressurizing pump, air injection equipment, a back-pressure regulating device, and a flotation unit. Operational steps are as follows:

Air is introduced to the influent usually at the suction end of a centrifugal pump discharging into a retention tank at a pressure ranging from 25 to 50 psig. In passing through the pump, the air is sheared into fine bubbles, thereby facilitating their solution in the retention tank. The latter has a retention time of from 30 to 60 sec, and is provided with bleed lines for removing any undissolved air that separates in the unit. From the retention tank the waste flows through a back-pressure regulating device to the flotation unit.

At the flotation unit, the pressure is reduced to about 1 atm. Air bubbles released from solution float the suspended particles to the surface from where they are removed by mechanical scrapers. Clarified liquid is withdrawn at some depth below the surface while any heavier solids that do not float but settle to the bottom may be moved to the center or to one end of the tank by a conventional raking mechanism for discharge.

The flotation unit may be either rectangular or circular. Units of the latter type may be divided into two compartments: the inner compartment to be used for flotation, and the outer as a conventional clarifier.

When high-solids-to-gas ratios are permitted, only a portion of the feed or a portion of the flotation unit effluent may be aerated under pressure. The aerated portion is then mixed with the unaerated waste in the flotation unit.

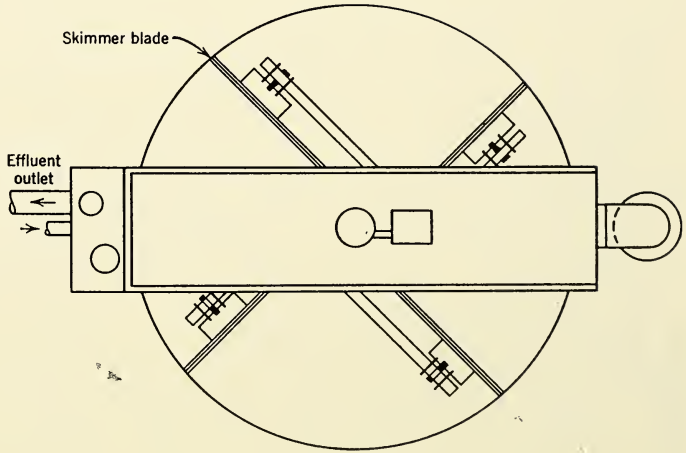

FIGURE 5-2. Pressure flotation system. (From "Sediflotor Clarifier," *Infilco Bulletin 6051.*)

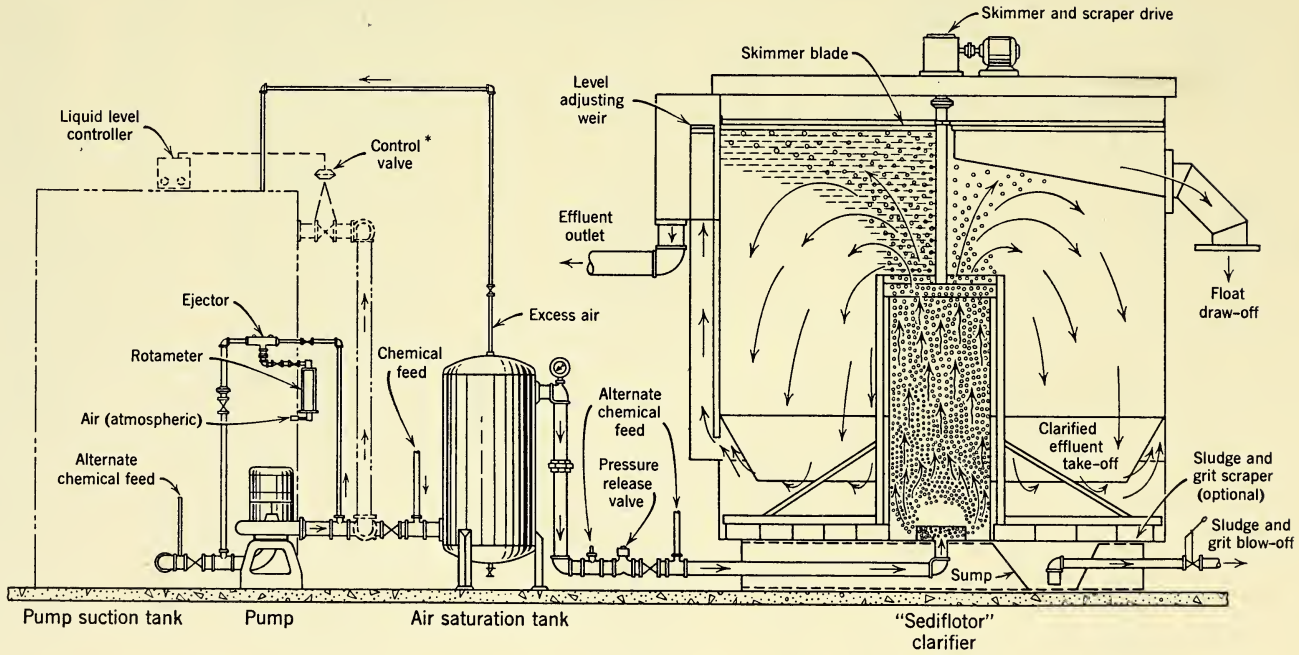
Skimmer and scraper drive
Skimmer blade
Level adjusting weir
Liquid level controller
Control * valve
Effluent outlet
Float draw-off
Ejector
Excess air
Rotameter
Chemical feed
Alternate chemical feed
Air (atmospheric)
Alternate chemical feed
Pressure release valve
Clarified effluent take-off
Sludge and grit scraper (optional)
Sludge and grit blow-off
Sump
Pump suction tank
Pump
Air saturation tank
"Sediflotor" clarifier

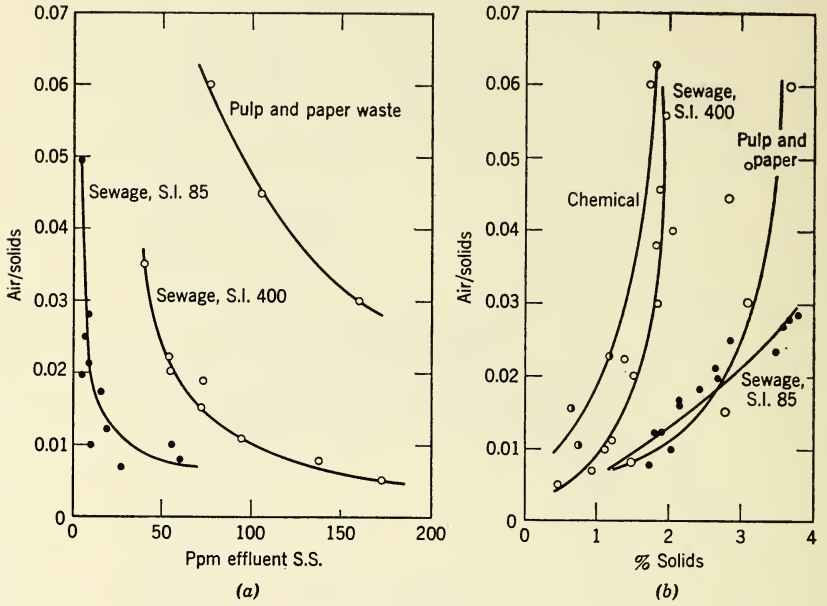

FIGURE 5-3. Relationships between the air-to-solids ratio and the effluent suspended solids and float solids concentration. [From Figures 2-55 and 2-56, McCabe, J., and W. W. Eckenfelder, Jr. (eds.), *Biological Treatment of Sewage and Industrial Wastes*—Vol. 2, Reinhold Publishing Corp., New York (1958).]

5-5. Design of Flotation Operations

The separation of suspended particles by flotation does not depend as much on the size and relative density of the particles as it does on their structure and surface properties and the quantity of air used in their flotation. For this reason, flotation operations cannot be designed on the basis of mathematical equations, and laboratory tests must be resorted to for preliminary design criteria. Test apparatus and procedures used for such tests are found elsewhere.[2,3] Final criteria should be derived from pilot-plant studies.

The factors of greatest importance in the design of a pressure flotation operation are the feed solids concentration, the quantity of air used,

[2] Rohlich, G. A., *Ind. Engr. Chem.*, **46** (1954), 304.

[3] Eckenfelder, W. W., Jr., T. F. Rooney, T. B. Burger, and J. T. Gruspier, "Studies on Dissolved Air Flotation of Biological Sludges," in: McCabe, J., and W. W. Eckenfelder, Jr. (eds.), *Biological Treatment of Sewage and Industrial Wastes*, Vol. 2, Reinhold Publishing Corp. (1958).

and the overflow rate. Retention time is important when thickening of the float is a consideration. Laboratory investigations are directed toward evaluating the effect of these variables on the float solids concentration and the suspended solids concentration in the effluent.

The feed solids concentration and the quantity of air used can be grouped together in a dimensionless ratio and correlated with effluent suspended solids and float solids concentration (Figure 5-3). From the curves presented in the figure, it is seen that no particular advantage is obtained by increasing the air-to-solids ratio beyond certain optimum values. The quantity of air used is controlled by varying either the proportion of the total flotation volume that is aerated or the pressure employed to accomplish the aeration. Pressure-saturation relationships are discussed in Section 8-4.

In most suspensions being floated, a sludge-liquid interface is formed similar, but in an inverted relationship, to that produced in a zone-settling regime (Section 4-4). The rate at which the interface rises is also a function of the air-to-solids ratio. A laboratory study of the rise rate is basic to an estimate of the overflow rate. In practice, overflow rates vary from 1 to 4 gal/ft^2/min.

As a rule, a 6-ft depth is required in the flotation unit to minimize turbulence and short-circuiting. For this depth and for the overflow rates indicated above, retention time will vary from 10 to 40 min.

EXAMPLE 5-1

A waste containing 400-ppm suspended solids and with a flow of 600 gal/min is to be treated by pressure flotation using aerated effluent recycle. Laboratory investigations revealed that an air-to-solids ratio of 0.03 is an optimum value relative to the quality of effluent and float solids concentration, and that the initial rise rate of the float interface at this ratio is 0.4 ft/min. Additional investigations showed that after the clarified effluent is saturated with air at 25 °C under a pressure of 50 psig, 5.6×10^{-4} lb of air will be released from 1 gal of effluent when the pressure is reduced to 1 atm. On the basis of this information, estimate the effluent recycle and dimensions of a flotation unit to treat the waste when the temperature of the latter is 25 °C.

Solution

1. The flow rate of the solids will be

$$600(8.34)(4 \times 10^{-4}) = 2 \text{ lb/min}$$

2. At an air-to-solids ratio of 0.03, the quantity of air required for flotation is 0.06 lb/min, and the rate of saturated effluent recycle re-

quired to furnish this air is

$$\frac{6 \times 10^{-2}}{5.6 \times 10^{-4}} = 107 \text{ gal/min}$$

However, for retention times ordinarily employed in the retention tank, the air concentration is less than saturation. Assuming that the recycle is only 50 percent saturated as it flows to the flotation unit, the rate of recycle must be twice 107 gal/min or 214 gal/min.

3. Since 214 gal/min will be recycled, the total flow through the flotation unit will be 814 gal/min. At a float solids concentration of 4 percent, only 6 gal/min of the liquid will remain with the solids. The rate of overflow of the clarified liquid from the unit will be about 800 gal/min. For a rise rate of 0.4 ft/min, the required surface area of the unit will be

$$\frac{800}{0.4(7.48)} = 266 \text{ ft}^2$$

4. Assuming a minimum depth of 6 ft, the retention time in the flotation unit would be

$$\frac{266 \times 6(7.48)}{800} = 15 \text{ min}$$

AEROSOL SEPARATION

5-6. Particle Characteristics

An aerosol is a fine suspension of particles in a gaseous medium, usually air. Particles may be either solid or liquid. Suspensions of the former are commonly referred to as *dusts*, whereas those of the latter are called *mists* or *entrainments*. Aerosol separations are employed by sanitary engineers as means for eliminating nuisances and health hazards in air-pollution control.

Mist particles are spherical in shape whereas the shapes of dust particles are usually irregular. Precise estimates of the behavior of the latter in gravitational fields are difficult to make. However, where shape irregularity is not too great, reasonable estimates can be made by considering the particles to be spheres.

A size classification of aerosol particles is presented in Figure 5-4. It is to be noted that particle diameter is measured in microns (1 mu = 3.28×10^{-6} ft). Methods employed for determining particle size are

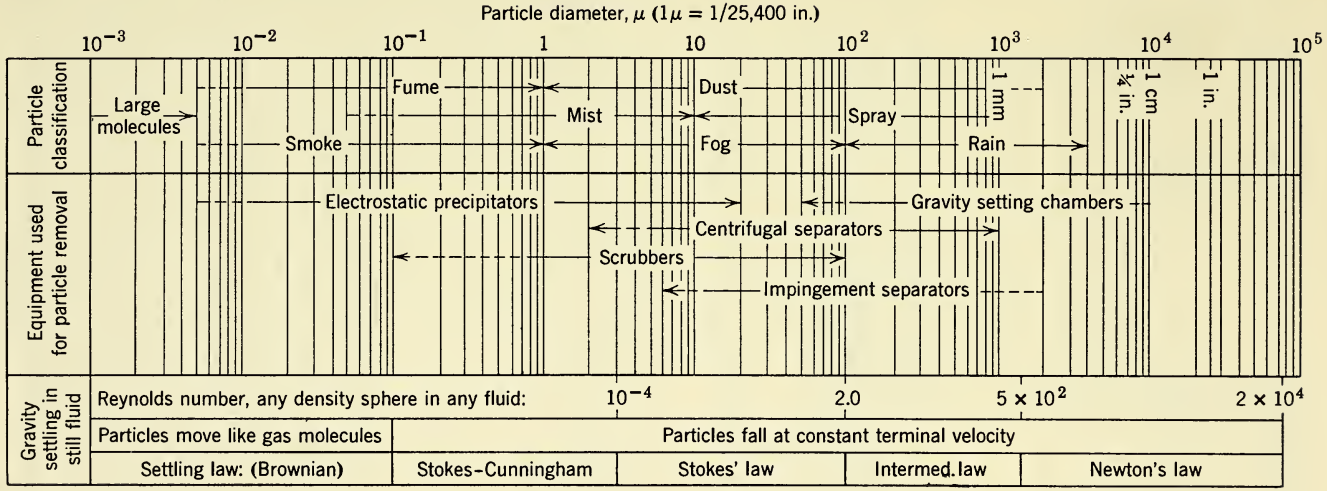

FIGURE 5-4. Size classification of aerosol particles and equipment used for particle removal. [After Figure 3, Montross, C. F., "Entrainment Separation," *Chem. Engr.*, **60** (Oct. 1953).]

Engineering and Physics Library

available.[4] Since aerosols contain particles having a wide range in size, it is necessary to express this characteristic in some form of size distribution, such as a cumulative or a frequency curve. In general, the diameters of aerosol particles follow a logarithmic normal distribution. Methods of treating size distributions are discussed elsewhere.[5]

Equipment used for aerosol separations are indicated in Figure 5-4, where specific types of equipment are correlated with ranges in particle size. Since air filters function simply as strainers, they will be omitted from the following discussion.

5-7. Gravity Settlers

The simplest device of this type consists of a long, horizontal, boxlike structure through which the aerosol flows. The cross-section area of the box is made large enough to reduce the flow velocity of the aerosol to a point where the particles can settle out under the influence of gravity (see discussion in Section 4-1). For most aerosols, this critical velocity is in the neighborhood of 10 ft/sec. In general, it is not feasible to use a box settler for removing particles with diameters of less than 40 mu.

The relationships developed for the class-1 clarification of liquid suspensions can be applied to aerosol separations. Equation 4-11 can be used to compute terminal velocities. The flow capacity of a box settler based on the complete removal of a particle of a given size may be estimated with Equation 4-16. As mentioned in the preceding section, most aerosols contain particles having a wide range in size. For such aerosols a settling analysis can be performed, and the total removal in the settler can be estimated with the use of Equation 4-17 (see Example 4-1).

The particles of many aerosols, particularly those of high concentration, flocculate as they settle. However, as a matter of convenience in designing a gravity settler, such particles are considered to behave as discrete, nonflocculating particles.

The Howard modification of the gravity settler consists of a chamber fitted with a number of horizontal plates (Figure 5-5). The flow capacity is increased in direct proportion to the increase in surface area provided by the plates. The Howard settler is practical for removing particles down to 10 mu in diameter. However, this settler is not easily cleaned, and its use is limited to aerosols of relatively low concentration.

[4] Lapple, C. E., *Heating, Piping and Air Conditioning*, **16** (1944), 580, 635; **17** (1945), 611.

[5] *Ibid.*, **18** (1946), 108.

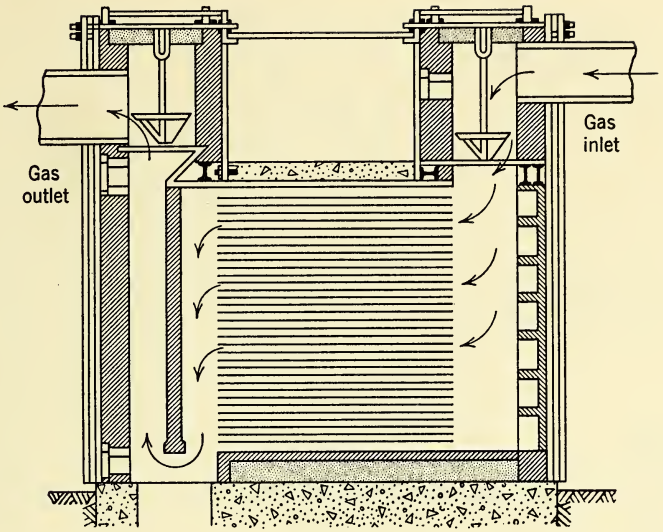

FIGURE 5-5. Howard gravity settler. [By permission from *Chemical Engineers Handbook*, by J. H. Perry (ed.). Copyright, 1950, New York, McGraw-Hill Book Company, Inc.]

The frictional head loss across a gravity settler is small, with most of the friction losses occurring at points where the gas enters and leaves the settler.

5-8. Centrifugal Separators

These devices are the most widely used of all the aerosol separators. The simplest type, called a "cyclone," consists of a vertical cylinder with a conical bottom fitted with a tangential inlet located near the top. The carrier gas flows out through a vertical pipe at the top, and the separated particulates are discharged through an outlet at the bottom (Figure 5-6). In operation, the aerosol entering the cyclone is deflected by the walls, giving it a strong rotary motion. The gas spirals downward next to the wall to the bottom of the cone. At the bottom the gas tightens its spiral and moves upward through the outer vortex to be discharged at the top. The centrifugal forces established by the circular motion in both spirals cause the aerosol particles to separate from the lighter gas and impinge on the walls of the cyclone. From there, both gravity and the vertical component of their momenta act to move the particles to the bottom of the separator.

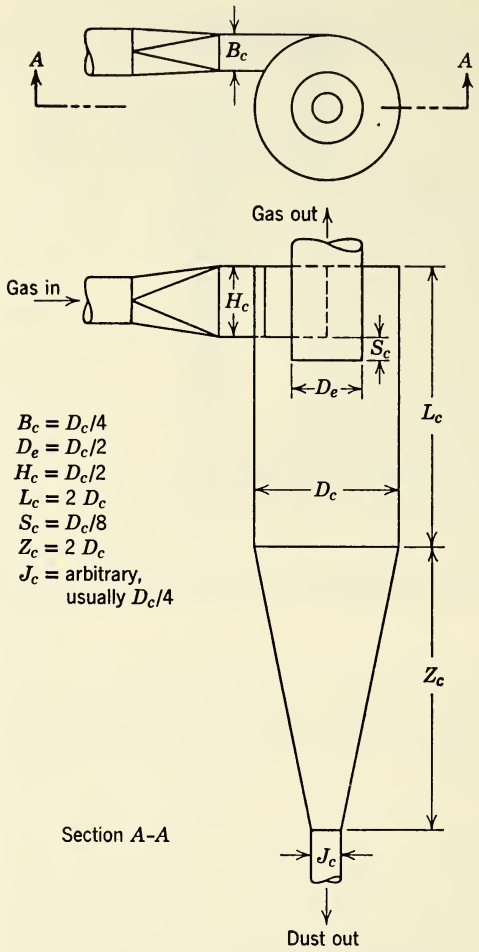

FIGURE 5-6. Cyclone separator. [By permission from *Chemical Engineers Handbook*, by J. H. Perry (ed.). Copyright, 1950, New York, McGraw-Hill Book Company, Inc.]

Although cyclones can be used to remove particles with diameters ranging from 2 to 1000 mu, in separating particles of a size greater than 200 mu, gravity settlers are usually more satisfactory. From Figure 5-4 it is seen that Stokes' law applies over a greater part of the range extending from 2 to 200 mu. It is not surprising, therefore, that the equations used for the design of cyclones are developed from Stokes' modification of Equation 4-11. By substituting the values of $24/N_{Re}$ and a_E for C_D and g in this equation,

$$u_t = \left(\frac{4}{3}\frac{a_E}{24/N_{Re}}\frac{\rho_s - \rho}{\rho}D_p\right)^{1/2} \tag{5-2}$$

$$u_t = \frac{a_E}{18} \frac{\rho_s - \rho}{\mu} D_p^2 \tag{5-3}$$

$$D_p = \left[\frac{18 u_t \mu}{a_E (\rho_s - o)} \right]^{1/2} \tag{5-4}$$

where u_t = terminal settling velocity of particle, ft/sec
D_p = particle diameter, ft
N_{Re} = Reynolds number
C_D = coefficient of drag
a_E = acceleration of particle, ft/sec^2
ρ = gas density, lb mass/ft^3
ρ_s = particle density, lb mass/ft^3
μ = absolute viscosity, (lb mass)/(ft)(sec)

Since the relationship between the velocity of the aerosol entering the cyclone and its angular velocity inside the cyclone is

$$\overline{V} = \omega r \tag{5-5}$$

where $\overline{V}$ = linear velocity of flow, ft/sec
ω = angular velocity of flow, radians/sec
r = mean radius of path, ft

the acceleration in a centrifugal field can be expressed as

$$a_E = r\omega^2 = \frac{\overline{V}^2}{r} \tag{5-6}$$

Also, since the time that the aerosol is in the cyclone is

$$t = \frac{2\pi r n_e}{\overline{V}} \tag{5-7}$$

where t = retention time of aerosol in cyclone, sec
n_e = "effective" number of revolutions made by aerosol in cyclone, dimensionless

then

$$u_t = \frac{s_r}{t} = \frac{s_r}{(2\pi r n_e)/\overline{V}} \tag{5-8}$$

where s_r = radial distance through which particle moves, ft.

Substitution of Equations 5-6 and 5-8 in Equation 5-4 gives

$$D_p = \left[\frac{9\mu s_r}{\pi \overline{V} n_e (\rho_s - \rho)} \right]^{1/2} \tag{5-9}$$

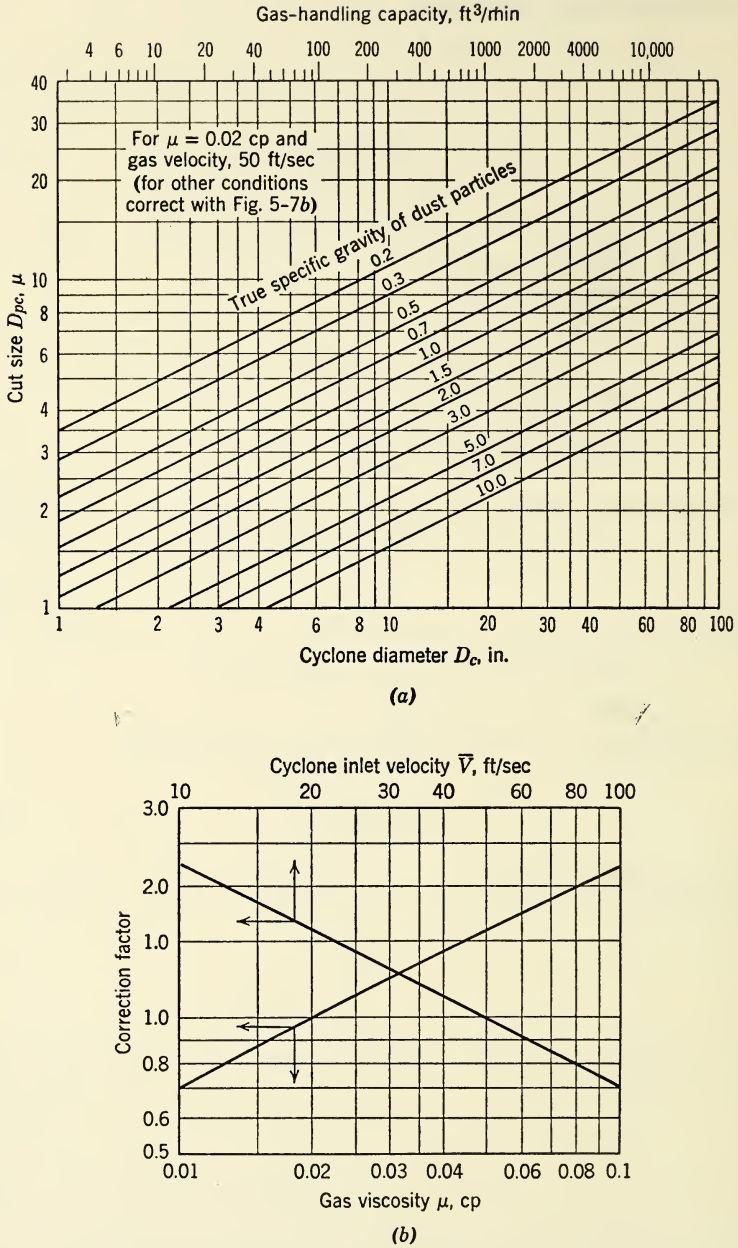
Gas-handling capacity, ft³/min
4 6 10 20 40 100 200 400 1000 2000 4000 10,000
For μ = 0.02 cp and gas velocity, 50 ft/sec (for other conditions correct with Fig. 5-7b)
True specific gravity of dust particles
0.2
0.3
0.5
0.7
1.0
1.5
2.0
3.0
5.0
7.0
10.0
Cut size D_{pc}, μ
40 30 20 10 8 6 4 3 2 1
1 2 3 4 6 8 10 20 30 40 60 80 100
Cyclone diameter D_c, in.
(a)
Cyclone inlet velocity $\overline{V}$, ft/sec
10 20 30 40 60 80 100
Correction factor
3.0 2.0 1.0 1.0 0.8 0.6 0.5
0.01 0.02 0.03 0.04 0.06 0.08 0.1
Gas viscosity μ, cp
(b)

FIGURE 5-7. Cut size for cyclones with geometric proportions the same as those in Figure 5-6. (*a*) Cut size as a function of cyclone diameter and particle specific gravity. (*b*) Viscosity and velocity correction factors for cut size. [From Figures 3*a* and 4, Lapple, C. E., *Chem. Engr.*, **58** (May 1951), 144.]

If the width of the entering aerosol stream B_c is substituted for s_r in Equation 5-9, D_p becomes the diameter of the smallest-size particles which are completely separated from the aerosol. However, the performance of a cyclone is generally specified in terms of a cut size D_{pc}. This size is defined as that diameter for which one-half of the inlet particles by weight are separated from the aerosol, the remaining 50 percent being retained.

The distance through which a particle with a diameter D_{pc} would travel before impinging on the side of the cyclone cylinder would be equal to $B_c/2$. By substituting this term for s_r in Equation 5-9, an expression is obtained for the cut size.

$$D_{pc} = \left[\frac{4.5\mu B_c}{\pi \bar{V} n_e(\rho_s - \rho)}\right]^{1/2} \tag{5-10}$$

where D_{pc} = cut size, diameter of particles of which 50 percent (by weight) are removed, ft
B_c = width of entering aerosol stream, ft (see Figure 5-6)

The term n_e is an empirical quantity which must be determined experimentally. For cyclones having the same proportions, however, the effective number of revolutions will be about the same. The value of n_e for cyclones with proportions the same as those shown in Figure 5-6 is approximately 5. The family of curves in Figure 5-7*a* provides a convenient solution of Equation 5-10 for cyclones of different diameters, but having the same proportions as those shown in Figure 5-6. These

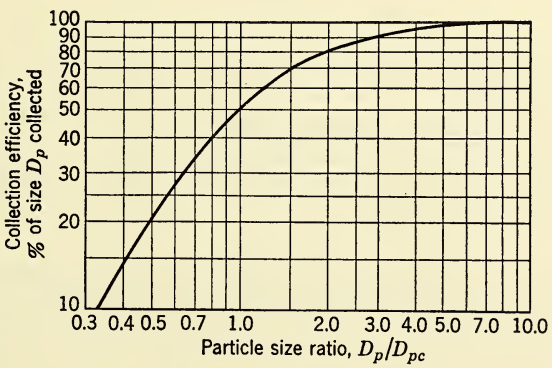

FIGURE 5-8. Removal efficiencies for cyclones with geometric proportions the same as those in Figure 5-6. [From Figure 5, Lapple, C. E., *Chem. Engr.*, **58** (May 1951), 144.]

curves have been derived on the basis of an absolute viscosity equal to 0.02 cp and a flow velocity of 50 ft/sec. For other conditions of viscosity and velocity, a correction factor obtained from Figure 5-7*b* can be applied.

Particles having diameters greater than the cut size will be removed in percentages greater than 50, whereas those with smaller diameters will be separated in smaller percentages. The curve in Figure 5-8 relates the ratio of particle size to cut size with fractional weight-removal efficiency for a cyclone having the same proportions as those shown in Figure 5-6.

The over-all removal from an aerosol containing particles of different sizes is equal to the product of the weight-removal efficiency for each size and the fraction of the total weight of the particles having that size.

$$\eta_T = \int_0^x \eta \, dx \tag{5-11}$$

where η = fractional weight-removal efficiency for each size
η_T = over-all fractional weight removal efficiency
dx = incremental fraction of total weight of particles

The integration of Equation 5-11 is conveniently performed by graphical procedures.

The pressure drop due to friction losses across a cyclone is generally expressed in terms of the velocity head of the entering gas stream,

$$\Delta p = K\rho \frac{\overline{V}^2}{2g_c} \tag{5-12}$$

where Δp = pressure drop due to friction, lb force/ft^2
K = constant
ρ = mass density of gas, lb mass/ft^3
$\overline{V}$ = velocity of entering gas stream, ft/sec
g_c = Newton's law conversion factor, 32.17 (ft)(lb mass)/(lb force)(sec^2)

The value of K will range from 1 to 20 depending upon the geometrical proportions of the cyclone. For the cyclone in Figure 5-6, K is about 8.

EXAMPLE 5-2

A cyclone 20 in. in diameter and having the proportions of the cyclone shown in Figure 5-6 is to be used to separate particulate matter (sp gr = 1.0) from air (temperature = 68 °F) at a flow rate of 830 ft^3/min.

An analysis of the aerosol particles yielded the following size distribution.

Size, mu	3.0	6.0	10.0	20.0	40.0	80.0	140.0	200.0
Weight fraction less than stated size	0.03	0.08	0.15	0.33	0.60	0.85	0.96	0.99

Estimate the over-all separation efficiency.

Solution

1. From Figure 5-7*a*, the cut size for a 20-in. cyclone (sp gr = 1.0) is about 7 mu.

2. From the proportions listed in Figure 5-6, the cross-section area at the entrance of a 20-in. cyclone is computed to be 0.347 ft. The velocity of the aerosol as it enters the cyclone will be

$$\frac{830}{60} \div 0.347 = 40 \text{ ft/sec}$$

3. From Figure 5-7*b*, the correction factor for a velocity of 40 ft/sec is about 1.15. Therefore, the adjusted cut size is

$$7 \times 1.15 = 8.05 \text{ mu}$$

4. For different ratios of particle size to cut size, the corresponding collection efficiencies are determined from Figure 5-8.

Size, D_p	Weight Fraction Less Than D_p	D_p/D_{pc}	Fractional Weight Collection Efficiency
3.0	0.03	0.37	0.12
6.0	0.08	0.74	0.37
10.0	0.15	1.24	0.60
20.0	0.33	2.48	0.85
40.0	0.60	4.97	0.95
80.0	0.85	9.95	1.00
140.0	0.96	17.40	1.00
200.0	0.99	24.80	1.00

5. The fractional weight collection efficiency is plotted against the weight fraction of particles smaller than size D_p (Figure 5-9).

6. Equation 5-11 is integrated graphically by determining the area to the left of the curve drawn through the plot in Figure 5-9.

$$\eta_T = 0.1(0.24 + 0.60 + 0.76 + 0.86 + 0.91 + 0.93 + 0.96 + 0.98 + 1.00 + 1.00) = 0.82$$

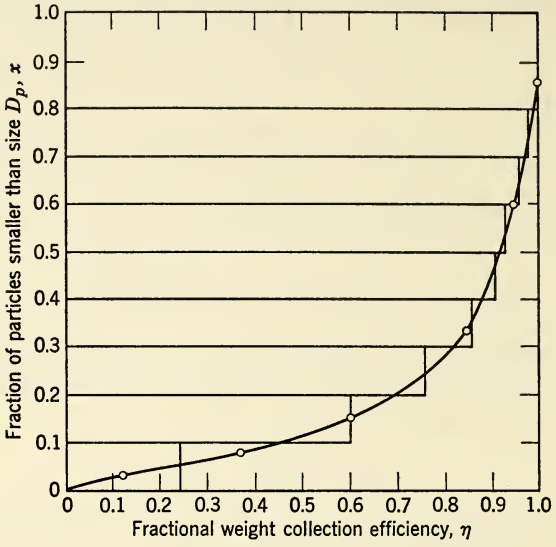

FIGURE 5-9. Graphical integration of Equation 5-11 for the solution of Example 5-2.

5-9. Impingement Separators

A wide variety of equipment is available in which particles are separated from aerosols, either partly or entirely, by impingement on surfaces placed in the aerosol stream. One of the simplest types consists only of a series of perforated plates with staggered openings through which the aerosol flows. Particles impinge and collect along the surfaces between the openings as a result of the tortuous path followed by the aerosol. Most impingement separators will remove particles down to 5 mu in diameter. No general relationship is available for estimating pressure drop due to friction through these separators. Information of this nature must be obtained from manufacturers' tests.

The theory of impingement separation is developed as follows.[6]

When an aerosol is deflected by a body placed in the flowing stream, the aerosol particles because of their inertia tend to continue moving in the original direction and impinge on the surface of the body. Attention is directed to Figure 5-10. Here, a cylinder of diameter D_b projects across an aerosol stream, causing the streamlines (solid lines) to bend around the cylinder. The particles because of their greater density and, hence, greater momenta, will follow paths represented by the dashed line. As

[6] Montross, C. F., "Entrainment Separation," *Chem. Engr.* (Oct. 1953).

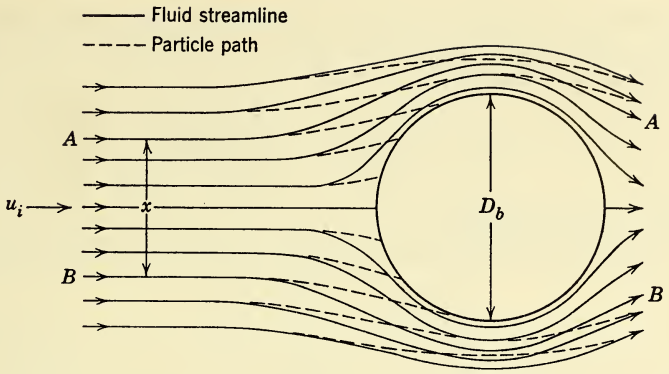

FIGURE 5-10. Impingement of aerosol particles on a cylinder. [By permission from *Chemical Engineers Handbook*, by J. H. Perry (ed.). Copyright, 1950, New York, McGraw-Hill Book Company, Inc.]

shown in the figure, all particles initially between the streamlines labeled A and B will cut across the intermediate streamlines and strike the cylinder. Those particles outside of streamlines A and B will miss the cylinder and remain suspended in the aerosol.

The distance that a particle will travel across the streamlines is called the stopping distance s. Mathematically, this distance can be written

$$s = \int_0^\infty u \, dt \tag{5-13}$$

where u = relative velocity of particle in the direction in which it is moving initially, ft/sec
t = time, sec

The drag force on the particle is given by Equation 4-4. In the Stokes' law range this equation becomes for spherical particles

$$F_D = \frac{C_D A_p \rho u^2}{2g_c} = \frac{3\pi\mu D_p u}{g_c} \tag{5-14}$$

where F_D = frictional or drag force, lb force
C_D = coefficient of drag, dimensionless
A_p = projected area of particle, ft^2
g_c = Newton's law conversion factor, 32.17 (ft)(lb mass)/(lb force)(sec^2)
ρ = fluid density, lb mass/ft^3
μ = absolute viscosity, (lb mass)/(ft)(sec)
D_p = particle diameter, ft

The drag force serves to decrease the momentum of the particle in the original direction of movement. Equating Equation 5-14 with the change in linear momentum,

$$F_D = \frac{3\pi\mu D_p u}{g_c} = -\frac{d(mu)/dt}{g_c} \tag{5-15}$$

where m = mass, lb mass.

Rearranging and integrating between the limits of time = 0 and t,

$$\int_{u_i}^{u} \frac{du}{u} = -\frac{3\pi\mu D_p}{m}\int_0^t dt \tag{5-16}$$

$$\ln\frac{u}{u_i} = -\frac{3\pi\mu D_p t}{m} \tag{5-17}$$

$$u = u_i e^{-(3\pi\mu D_p t)/m} \tag{5-18}$$

where u_i = initial relative velocity, ft/sec.

By substituting this equation in Equation 5-13 and integrating,

$$s = u_i\int_0^\infty e^{-(3\pi\mu D_p t)/m}\,dt \tag{5-19}$$

$$s = \frac{mu_i}{3\pi\mu D_p} = \frac{[u_i(\rho_s\pi {D_p}^3)]/6}{3\pi\mu D_p} = \frac{\rho_s u_i {D_p}^2}{18\mu} \tag{5-20}$$

where ρ_s = particle density, lb mass/ft^3.

The ratio of the stopping distance s and target diameter D_b (diameter of body on which the particles impinge) has been correlated with target efficiency for targets of different shapes (Figure 5-11). This efficiency

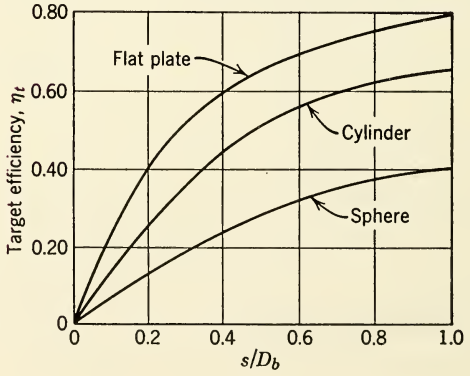

FIGURE 5-11. Target efficiency of spheres, cylinders, and plates. [From Figure 13, Montross, C. F., "Entrainment Separation," *Chem. Engr.* **60** (Oct. 1953).

is the fraction of particles that will be removed from the aerosol stream as it sweeps past the target. In Figure 5-10 the target efficiency is represented by the ratio of the distance x (distance between streamlines A and B) and the target diameter D_b. In order for the relationships in Figure 5-11 to hold, the targets must be far enough apart so that no appreciable distortion of the flow pattern will occur. Also, it should be remembered that the relationships developed in this section apply only to those particles which would settle out by gravity in conformance to Stokes' law.

EXAMPLE 5-3

A cylinder 1 in. in diameter is placed across an aerosol stream (temperature 68 °F) having a velocity of 10 ft/sec. Estimate the target efficiency for particles with diameters equal to 20 mu and a density of 100 lb/ft^3.

Solution

1. Compute the stopping distance

$$s = \frac{\rho_s u_i D_p^2}{18\mu} = \frac{100 \times 10(20 \times 3.28 \times 10^{-6})^2}{18(0.02 \times 6.72 \times 10^{-4})} = 1.78 \times 10^{-2}$$

2. The ratio s/D is equal to 0.21. From Figure 5-11, the target efficiency is about 0.28.

5-10. Electrostatic Precipitators

The operation of these separators involve the attraction and collection of charged aerosol particles on the surface of an electrode having opposite polarity. The particles are charged as a result of the attachment to their surfaces of gas ions produced by a corona discharge. Electrostatic precipitators have high removal efficiencies but are relatively expensive. Since they remove particles as small as 0.01 mu in diameter, they are generally employed when it is necessary to remove particles of a size that cannot be handled by another type of separator.

Two electrodes constitute the primary components of an electrostatic precipitator. The first, called a discharge electrode, consists of a wire or some other object with a small surface area around which is produced a high electric field called a "corona discharge." The discharge which is produced by voltages as high as 100,000 functions to ionize a portion of the gas molecules in the aerosol stream. The second electrode, the collecting electrode, has a large surface area and serves to collect the aerosol particles after they have become charged by the gas ions. Periodically, the collecting electrode is rapped to remove the accumulated deposit.

Two general classes of electrostatic precipitators are in use today. The single-stage type, sometimes referred to as a Cottrell precipitator, combines both gas ionization and particle collection in the same apparatus. This class of precipitators, which is generally used for the removal of dusts and mists from industrial discharges, is, in turn, divided into two types. The plate type consists of discharge electrodes placed between large, flat plates serving as collection electrodes. The plate type is most often used for the removal of dusts. The pipe type consists of vertical pipes serving as collecting electrodes, through the centers of which are suspended wire discharge electrodes. The latter type is normally employed for removing mists.

In the two-stage electrostatic precipitator, separate units are employed for the ionization and collection processes. The use of these precipitators is confined largely to the field of air-conditioning.

The following relationship, developed from theoretical considerations but supported by experimental evidence, can be used to evaluate the performance of a single-stage precipitator.[7]

$$\eta = 1 - e^{-u/u_0} = 1 - e^{-uK_e} \tag{5-21}$$

where η = removal efficiency, dimensionless
u = velocity at which particle migrates toward collecting electrode, ft/sec
u_0 = velocity of migration of those particles, 100 percent of which will just be removed as the aerosol leaves the precipitator, ft/sec
K_e = precipitator constant, sec/ft

The term u_0 is related to the surface area of the collecting electrode and to the aerosol flow rate by expressions similar to Equation 4-16.

Plate-type precipitators $$u_0 = \frac{q_0}{A_e} = \frac{\overline{V}B}{L}$$

Pipe-type precipitators $$u_0 = \frac{2q_0}{A_e} = \frac{2\overline{V}D}{L}$$

where q_0 = aerosol flow rate at which all particles having migration velocities equal to or greater than u_0 will be completely removed, ft^3/sec
A_e = surface area of collecting electrode, ft^2
$\overline{V}$ = average velocity of gas stream through precipitator, ft/sec

[7] Lapple, C. E., in: Perry, J. H. ,*Chemical Engineers Handbook* (3rd ed.), McGraw-Hill Book Co., New York (1950), 1040.

B = distance between discharge and collecting electrodes, ft
L = length of collecting electrodes in direction of gas flow, ft
D = inside diameter of pipe, ft

The ratio $1/u_0$ is expressed as the precipitator constant K_e. For a given precipitator, the constant should vary only with flow rate.

The velocity at which charged particles migrate in an electric field can be computed from a relationship developed as follows.

The force that pulls the particle to the collecting electrode is

$$F = \frac{Ne_pE}{13{,}850g_c} \tag{5-22}$$

where F = force, lb force
N = number of unit charges on particle
e_p = unit charge, statcoulomb
E = electrostatic field strength, statvolts/cm

In the Stokes' law range, the force resisting this movement is

$$F_D = \frac{3\pi\mu D_p u}{g_c} \tag{5-14}$$

Equating the two expressions and solving for u results in

$$u = \frac{Ne_pE}{41{,}600\pi\mu D_p} \tag{5-23}$$

It will be noted from Figure 5-4, however, that for particle sizes less than 2 mu Stokes' law no longer holds. Particles of such size tend to "slip" between the gas molecules and the gas no longer behaves as a continuous medium.

The velocity at which particles of less than 2 mu in diameter move can be estimated by multiplying the velocity as determined for particles falling in the Stokes' law range by a correction factor. Values of the correction factor for particles of different sizes moving through air at different temperatures are given in Table 5-1.

Although Equation 5-21 holds strictly for particles of a given size, it has been found to give a good approximation of the over-all removal efficiency when the velocity term u is treated as an empirical average value.

For two-stage precipitators with close spacing between plates, the removal efficiency may be expressed as [8]

$$\eta = \frac{uL}{\bar{V}B} \tag{5-24}$$

[8] G. W. Penney, *Elect. Engr.*, **56** (1937), 159.

TABLE 5-1. CORRECTION FACTOR FOR STOKES' LAW FOR AIR AT ATMOSPHERIC PRESSURE *

Particle Diameter, mu	Value of Correction Factor at Temperature		
	70 °F	212 °F	500 °F
0.1	2.8	3.61	5.14
0.25	1.682	1.952	2.528
0.5	1.325	1.446	1.711
1.0	1.160	1.217	1.338
2.5	1.064	1.087	1.133
5.0	1.032	1.043	1.067
10.0	1.016	1.022	1.033

* From Lapple, C. E., *Fluid and Particle Mechanics*, University of Delaware, Newark, Del. (1951), 285.

5-11. Scrubbers

All devices in which a liquid phase is employed in separating dusts and mists from aerosols are classed as scrubbers. Such equipment is marketed in a wide selection of types including packed towers, spray chambers, venturi scrubbers, centrifugal scrubbers, etc. In spite of the variety of types, all equipment is alike in one respect—the liquid used as the scrubbing agent is divided into thin films or drops in order to expose as much surface area as possible to the contacting aerosol. The increased surface area promotes the transfer of the aerosol particles to the liquid. In most scrubbing operations water is used as the scrubbing agent.

In each type of scrubber, one or more factors may be active in effecting particle transfer. The factors include diffusion, impingement, gravity, centrifugal force, and electrostatic attraction. Most of these factors are discussed in the preceding sections.

Notations

a_E Acceleration, ft/sec^2
A_p Projected area, ft^2
B Distance, ft; B_c, width of aerosol stream
C_D Coefficient of drag
D Inside diameter of pipe, ft
D_p Particle diameter, ft; D_{pc}, cut size

e_p Unit charge, statcoulomb
E Electrostatic field strength, statvolt/cm
F Force, lb force; F_D, drag force
g_c Newton's law conversion factor, 32.17 (ft)(lb mass)/(lb force)(sec^2)
K Constant; K_e, precipitator constant
L Length, ft
m Mass, lb mass
n_e "Effective" number of revolutions in a cyclone
N Number
N_{Re} Reynolds number
Δp Pressure drop due to friction, lb force/ft^2
q_0 Flow rate at which all particles having velocities equal to or greater than u_0 will be removed, ft^3/sec
r Mean radius of path, ft
s Stopping distance, ft; s_r, radial distance
t Time, sec
u Relative velocity of particle, ft/sec; u_i, initial relative velocity; u_0, velocity of those particles, 100 percent of which will be removed; u_t, terminal settling velocity
$\overline{V}$ Linear flow velocity, ft/sec
x Weight fraction
α Angle of contact
η Fractional weight-removal efficiency; η_T, over-all fractional weight-removal efficiency
μ Absolute viscosity, (lb mass)/(ft)(sec)
ρ Gas density, lb mass/ft^3; ρ_s, particle density
σ Interfacial tension; σ_{GS}, between gas and solid phases; σ_{SL}, between solid and liquid phases; σ_{GL}, between gas and liquid phases
ω Angular flow velocity, radians/sec

6

Flow through beds of solids

6-1. Introduction

This chapter deals primarily with gas and liquid flows through porous beds of nonconsolidated particles. Particles vary in size and shape from relatively large cylinders and rings to small, almost spherical granules. The ratio of the cross-section area of the bed to the projected area of the particles will range from the order of 10 to several thousands. The direction of flow may be either up or down. Such beds are used for a variety of purposes.

Rapid Sand Filters

The most important application of porous beds in sanitary engineering is in municipal and industrial water treatment where water is passed through beds of size-stratified sand and gravel to remove suspended matter. The hydraulic capacity of these units decreases as the suspended materials accumulate in the surface layers of the sand and, as a result, the accumulation must be removed periodically. Removal is accomplished by reversing the flow in what is called a "backwashing" operation.

Slow Sand Filters

The application of slow sand filters now is confined largely to the secondary or tertiary treatment of sewage. Settled or biologically treated sewage is passed through beds of unstratified sand and gravel. Suspended material is caught at the surface where the organic fraction is decomposed by biological agencies. The accumulation of the nondecomposable fraction necessitates periodic cleaning by scraping off the top layers of sand.

Ion Exchange Units

Water is demineralized when passed through granular beds of ion exchange materials. The units are regenerated periodically.

Adsorption Towers

The removal of odors and organic vapors from air can be accomplished by forcing the air through towers filled with activated carbon or similar adsorbents. Towers containing silica gel and activated alumina are effective in removing water vapor from air.

Contacting Towers

Columns filled with various packing materials are widely used as liquid- and gas-contacting devices.

6-2. Carman-Kozeny Equation

In the development of an expression for computing the frictional head loss through a bed of solids, it is convenient to visualize the bed as consisting of many parallel channels formed by the voids between the particles. These channels are irregular and indeterminate as far as the geometric configuration of the cross sections are concerned. To be applicable for expressing the head loss through the bed, the Darcy-Weisbach relationship (Equation 1-16) must contain for the conduit diameter D an equivalent term $4r_H$ (Equation 1-17).

$$h_f = \frac{f}{4}\frac{L}{r_H}\frac{\overline{V}^2}{2g_c} \tag{6-1}$$

where h_f = frictional head loss across bed, (ft)(lb force)/(lb mass)
f = friction factor, dimensionless
L = depth of bed, ft
r_H = hydraulic radius, ft
$\overline{V}$ = average velocity of fluid through the channels, ft/sec
g_c = Newton's law conversion factor, (ft)(lb mass)/(lb force)(sec^2)

The total channel volume can be considered to be equal to the volume occupied by the voids, or

$$\text{Channel volume} = \frac{\epsilon}{1 - \epsilon} N v_p \tag{6-2}$$

where ϵ = porosity of bed = ratio of volume of voids to the total volume, dimensionless
N = number of particles in bed
v_p = volume of a single particle, ft^3

and the total wetted surface can be considered to be equal to the surface area of the solids, or

$$\text{Wetted surface area} = N s_p \tag{6-3}$$

where s_p = surface area of a single particle, ft^2.

The hydraulic radius r_H can be computed by dividing the channel volume by the wetted surface area,

$$r_H = \frac{\epsilon}{1 - \epsilon} \frac{v_p}{s_p} \tag{6-4}$$

The ratio of the volume of a sphere to its surface area is

$$\frac{v_p}{s_p} = \frac{(\pi D_p^3)/6}{\pi D_p^2} = \frac{D_p}{6} \tag{6-5}$$

where D_p = particle diameter, ft.

For nonspherical particles, a shape factor is introduced, so that for the general case,

$$\frac{v_p}{s_p} = \phi_s \frac{D_p}{6} \tag{6-6}$$

where ϕ_s = particle shape factor, dimensionless. For spheres the particle shape factor is equal to unity.

Equation 6-6 can be used to express the relationship between the ratio v_p/s_p and some defining dimension of particles having a nonspherical or irregular shape, provided an appropriate value of the shape factor is employed.

The relationship between the average velocity at which the fluid flows through the voids and the superficial velocity at which it would flow through the empty bed is

$$\overline{V} = \frac{\overline{V}_S}{\epsilon} \tag{6-7}$$

where $\overline{V}_S$ = average superficial velocity, ft/sec.

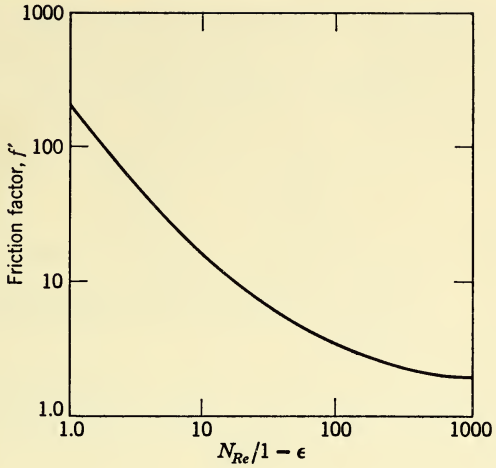

FIGURE 6-1. Friction factor for beds of solids. [From Figure 22.30, Foust, A. B. et al., *Principles of Unit Operations*, John Wiley and Sons, New York (1960).]

By combining Equations 6-1, 6-4, 6-6, and 6-7, the Carman-Kozeny relationship is obtained.[1,2]

$$h_f = f'\left(\frac{L}{\phi_s D_p}\right)\left(\frac{1-\epsilon}{\epsilon^3}\right)\left(\frac{\overline{V}_S{}^2}{g_c}\right) \tag{6-8}$$

where f' = friction factor, dimensionless.

The friction factor f' has been correlated with the Reynolds number [3]

$$f' = 150\,\frac{1-\epsilon}{N_{Re}} + 1.75 \tag{6-9}$$

where

$$N_{Re} = \frac{\phi_s D_p \overline{V}_S \rho}{\mu} \tag{6-10}$$

A correlation curve is presented in Figure 6-1.[4] This curve was established by a plot of experimental data obtained from several sources.

In the case of gas flow, the head loss through a dry, porous bed is less than that through a wet bed. This effect is primarily one of reducing

[1] Kozeny, G., *Sitzber. Akad. Wiss. Wien, Math.-naturw. Kl., Abt. IIa*, **136** (1927), 271.

[2] Carman, P. C., *Trans. Inst. Chem. Engrs. (London)*, **15** (1937), 150–166.

[3] Ergun, Sabri, *Chem. Engr. Progress*, **48** (1952), 89–94.

[4] Foust, A. S., et al., *Principles of Unit Operations*, John Wiley & Sons, New York (1960), 475.

the effective porosity and is a function of the wetness or the circulating rate of an irrigating liquid. An empirical relationship has been derived [5] for the head loss through an irrigated bed when the superficial mass velocity of the gas is below the loading point (point a in Figure 8-10).

$$h_f = \frac{mL}{10^8}(10^{nG_L/\rho_L})\left(\frac{G_G}{\rho_G}\right)^2 \tag{6-11}$$

where G_L and G_G = superficial mass velocities of liquid and gas respectively, (lb force)/(ft^2)(hr)
ρ_L and ρ_G = densities of liquid and gas respectively, lb mass/ft^3
m and n = constants

Values of the constants m and n are presented in Table 6-1 for various packing materials. The use of these values should be restricted to the ranges of G_L and $h_f\rho_G/L$ as indicated.

TABLE 6-1. VALUES OF m AND n TO BE USED IN EQUATION 6-11 FOR SEVERAL PACKING MATERIALS (FOR VALUES OF $h_f\rho_G/L$ FROM 0 TO 2.6 (LB)/(FT^2)(FT))

Packing	m	n	Range of G_L, (lb)/(hr)(ft^2)
Raschig rings:			
¾ in.	32.9	0.00450	1,800–10,800
1 in.	32.1	0.00434	360–27,000
1½ in.	12.08	0.00398	720–18,000
2 in.	11.13	0.00295	720–21,600
Berl saddles:			
½ in.	60.4	0.00340	300–14,100
1 in.	16.01	0.00295	720–28,800
1½ in.	8.01	0.00225	720–21,600

Equation 6-8 is derived on the basis of a bed particle of uniform size. Its application can be extended to beds of mixed-size particles by making the appropriate substitution for the diameter term. Equation 6-6 can be written as

$$D_p = \frac{6}{\phi_s}\frac{Nv_p}{Ns_p} = \frac{6}{\phi_s}\frac{V}{A} \tag{6-12}$$

where N = number of particles in bed
V = total volume of particles, ft^3
A = total surface area of particles, ft^2

[5] Leva, M., *Chem. Engr. Progress Symp. Ser.*, **50**(10) (1954), 51.

Substitution of this expression in Equation 6-8 gives

$$h_f = f'\left(\frac{L}{6}\right)\left(\frac{A}{V}\right)\left(\frac{1-\epsilon}{\epsilon^3}\right)\left(\frac{\overline{V}_S{}^2}{g_c}\right) \tag{6-13}$$

The area-volume term for a bed of mixed-size particles can be evaluated from

$$\left(\frac{A}{V}\right)_{\text{ave}} = \frac{6}{\phi_s}\sum_{i=1}^{i}\frac{x_i}{D_{p,i}} \tag{6-14}$$

where x_i = weight fraction of particles of size $D_{p,i}$
i = number of weight fractions in mixture

When a sieve analysis is used to determine $(A/V)_{\text{ave}}$, the term x_i represents the fraction by weight of the particles retained between adjacent sieves. The corresponding value of $D_{p,i}$ is taken as the geometric mean size of the two sieve openings.

A tabulation of shape factors for various materials is presented in Table 6-2. The values found therein are intended to serve as guide in

TABLE 6-2. SHAPE FACTORS FOR NONSPHERICAL PARTICLES *

Material	Nature of Grain	ϕ_s
Crushed glass	jagged	0.65
Pulverized coal		0.73
Natural coal dust (up to ⅜ in.)		0.65
Mica flakes		0.28
Sand, average for various types		0.75
Flint sand	jagged	0.66
Flint sand	jagged flakes	0.43
Ottawa sand	nearly spherical	0.95
Wilcox sand	jagged	0.63
Sand	rounded	0.82
Sand	angular	0.73

* Carman, P. C., "Fluid Flow Through Granular Beds," *Trans. Inst. Chem. Engrs.* (*London*), **15** (1937), 150.

the estimation of shape factors for various materials. For most geometric shapes,[6]

$$\phi_s = 4.90\frac{v_p{}^{2/3}}{s_p} \tag{6-15}$$

where v_p = volume of a single particle, ft^3
s_p = surface area of a single particle, ft^2

[6] Leva, M., et al., U.S. Bureau of Mines, *Bulletin 504* (1951).

For a reliable evaluation of the shape factor for granular materials, measurements must be taken from actual flow experiments.

For many types of particles, the porosity or void content will vary depending upon the manner and rate with which the material is introduced to the bed. The usual method of determining porosity is based on an immersion procedure in liquid. When the particles themselves are highly porous, porosity determination becomes complex.[7]

When, in the case of circular beds, the bed diameter is small relative to the diameter of the particles, there exists next to the wall a region in which the porosity is greater than that in the middle of the bed. With hollow packing, the orientation of pieces near the wall contributes heavily toward channeling effects. The wall effect becomes significant when the ratio of the bed diameter to particle diameter is less than 20. However, no correction is required if the actual porosity of the bed in question is used.

In most instances where compressible fluids flow through porous beds, the frictional pressure drop across the bed is small compared to the upstream pressure. In these cases, the fluid density may be considered as being constant through the bed. When the pressure drop due to friction is substantial, however, the effect of decreasing density should be taken into account. Equations applicable to the solution of such problems are available.[8]

EXAMPLE 6-1

Air at 60 °F and 1 atm is to be forced through a packed tower at the rate of 1000 ft^3/min. The tower is 4 ft in diameter, 20 ft high, and is filled with 1-in. Raschig rings. Estimate the frictional pressure drop across the tower: (*a*) when the packing is dry; and (*b*) when the tower is irrigated with water (60 °F) at the rate of 25 gal/min.

Solution

a. 1. Collect available data.

From Appendix 2, at 0 °C, $\rho_G = 0.0808$; at 60 °F, $\rho_G = 0.0808 \times [492/(460 + 60)] = 0.0765$ lb mass/ft^3.

From Appendix 3, $\mu = 0.0175$ cp.

From Table 8-6, $\epsilon = 0.68$, $a_V = 58$ ft^2/ft^3.

2. Determine superficial velocity.

$$\overline{V}_S = \frac{1000/60}{\pi 4^2/4} = 1.325 \text{ ft/sec}$$

[7] Ergun, Sabri, *Analyt. Chem.*, **23** (1951), 151.

[8] Leva, M., et al., U.S. Bureau of Mines, *Bulletin 504* (1951).

3. Determine $\phi_s D_p$.

$$\phi_s D_p = 6\frac{v_p}{s_p} = \frac{6(1-\epsilon)}{a_V} = \frac{6(1-0.68)}{58} = 0.0331 \text{ ft}$$

4. Compute the Reynolds number expression (Equation 6-10).

$$\frac{N_{Re}}{1-\epsilon} = \frac{0.0331 \times 1.325 \times 0.0765}{0.0175(6.72 \times 10^{-4})(1-0.68)} = 895$$

5. From Figure 6-1, $f' = 2.0$

6. Compute frictional pressure drop (Equation 6-8).

$$h_f = 2.0 \times \frac{20}{0.0331} \times \frac{1-0.68}{(0.68)^3} \times \frac{(1.325)^2}{32.2}$$

$$= 67.2 \text{ (ft)(lb force)/(lb mass)}$$

$$\Delta p = 67.2 \times 0.0765 = 5.15 \text{ lb force/ft}^2$$

b. 1. Compute superficial mass velocities.

$$G_G = \frac{1000 \times 60 \times 0.0765}{\pi 4^2/4} = 367 \text{ (lb)/(hr)(ft}^2\text{)}$$

$$G_L = \frac{25 \times 60 \times 8.33}{\pi 4^2/4} = 1000 \text{ (lb)/(hr)(ft}^2\text{)}$$

2. From Appendix 1, $\rho_L = 62.4$ lb mass/ft^3.
3. From Table 6-1, $n = 0.00434$, $m = 32.1$.
4. Compute frictional pressure drop (Equation 6-11).

$$h_f = \frac{32.1 \times 20}{10^8}(10^{(0.00434 \times 1000)/62.4})\left(\frac{367}{0.0765}\right)^2$$

$$= 174 \text{ (ft)(lb force)/(lb mass)}$$

$$\Delta p = 174 \times 0.0765 = 13.3 \text{ lb force/ft}^2$$

6-3. Rose Equation

With data obtained from experimental investigations, Rose [9] established a relationship for determining the frictional head loss through beds of spherical and nearly spherical particles of uniform size which is similar

[9] Rose, H. E., *Proc. Inst. Mech. Engrs. (London)*, **153** (1945), 141, 154; also **160** (1949), 493.

to the Carman-Kozeny equation (Equation 6-8). The Rose equation has had direct application in the hydraulics of rapid sand filters. The relationship can be expressed as

$$h_f = f'' \left(\frac{L}{\phi_s D_p}\right)\left(\frac{1}{\epsilon^4}\right)\left(\frac{\overline{V}_S{}^2}{g_c}\right) \tag{6-16}$$

where h_f = frictional head loss across bed, (ft)(lb force)/(lb mass)
f'' = friction factor, dimensionless
L = depth of bed, ft
D_p = particle diameter, ft
ϕ_s = particle shape factor, dimensionless
ϵ = porosity of bed
$\overline{V}_S$ = average superficial velocity, ft/sec
g_c = Newton's conversion factor, (ft)(lb mass)/(lb force)(sec^2)

The friction factor f'' is a function of the Reynolds number and has been found to be [10]

$$f'' = 1.067 C_D \tag{6-17}$$

where C_D = coefficient of drag, dimensionless.

The correlation of the coefficient of drag with the Reynolds number is presented in Figure 4-2. For this correlation the Reynolds number can be computed from

$$N_{Re} = \frac{\phi_s D_p \overline{V}_S \rho}{\mu} \tag{6-18}$$

When the bed is composed of particles with different sizes, an average value can be computed for the term $\phi_s D_p$ in Equation 6-16 by using the relationship found in Equation 6-14.

A bed of nonuniform size particles may be stratified hydraulically into graded layers, each layer consisting of particles of uniform size. In such cases, the larger particles are found at the bottom of the bed and the smallest at the top. If the bed porosity can be considered to be constant from top to bottom, the frictional head loss through a layer of thickness ΔL will be

$$\Delta h_f = \frac{1.067 \overline{V}_S{}^2}{g_c \phi_s \epsilon^4} \frac{C_D \, \Delta L}{D_p} \tag{6-19}$$

and the total head loss through the bed will be

$$h_f = \sum_{i=1}^{i} \Delta h_{f,i} = \frac{1.067 \overline{V}_S{}^2}{g_c \phi_s \epsilon^4} \sum_{i=1}^{i} C_{D,i} \frac{\Delta L_i}{D_{p,i}} \tag{6-20}$$

[10] Fair, G. M., and J. C. Geyer, *Water Supply and Waste-Water Disposal*, John Wiley and Sons, New York (1954), 671.

where i = number of layers in stratified bed
$C_{D,i}$ = drag coefficient for $D_{p,i}$

Since

$$\Delta L_i = x_i L \tag{6-21}$$

where x_i = weight fraction of particles in ith layer, the following relationship can be established.

$$h_f = \frac{1.067 \overline{V}_S{}^2 L}{g_c \phi_s \epsilon^4} \sum_{i=1}^{i} C_{D,i} \frac{x_i}{D_{p,i}} \tag{6-22}$$

The summation term in Equation 6-22 can be computed on the basis of a sieve analysis with a procedure similar to that used in connection with the evaluation of Equation 6-14.

EXAMPLE 6-2

A sieve analysis of a fine Ottawa sand yields the information recorded in columns 1 and 2 below. Compute the initial head loss across a stratified bed of the sand, 18 in. deep and with a porosity of 0.41, when water at 45 °F is filtered at a rate of 3 gal/min/ft^2.

Solution

Sieve Numbers, U.S. Sieve Series	Weight Fraction of Particles Retained, $\times 10^2$	Geometric Mean Diameter, $(D_p)_g$ $\times 10^4$, ft	$\frac{N_{Re}, D_p \rho \overline{V}_S}{\mu}$	C_D	$C_D \frac{x}{D_p}$
(1)	(2)	(3)	(4)	(5)	(6)
14–20	0.80	35.8	1.705	14.06	31.4
20–25	4.25	25.3	1.205	19.90	334.0
25–30	15.02	21.2	1.010	23.80	1670.0
30–35	16.65	17.8	0.850	28.20	2640.0
35–40	18.01	15.1	0.720	33.30	3980.0
40–50	18.25	11.6	0.554	43.30	6820.0
50–60	15.65	9.0	0.430	55.80	9720.0
60–70	9.30	7.5	0.358	67.10	8320.0
70–100	2.07	5.8	0.276	87.00	3110.0
					$\Sigma C_D \frac{x}{D_p} = 36{,}600$

1. Column 3: Sieve opening obtained from Appendix 7,

$$(D_p)_g = (D_{p1} \times D_{p2})^{1/2}$$

where D_{p1} and D_{p2} = size of openings in adjacent sieves.

2. Column 4: From Appendix 3, $\mu = 1.3(6.72 \times 10^{-4}) = 8.74 \times 10^{-4}$ (lb mass)/(ft)(sec); from Appendix 1, $\rho = 62.42$ lb mass/ft^3.

$$N_{Re} = \frac{\rho \overline{V}_S D_p}{\mu} = \left(\frac{62.42 \times 6.68 \times 10^{-3}}{8.74 \times 10^{-4}}\right) D_p = 477 D_p$$

3. Column 5: From Equation 4-12,

$$C_D = \frac{b}{N_{Re}{}^n} \qquad \text{for } N_{Re} < 1.9,\ b = 24,\ n = 1$$

4. From Equation 6-22,

$$h_f = \frac{1.07 \overline{V}_S{}^2 L}{g_c \epsilon^4 \phi_s} \Sigma\, C_D \frac{x}{D_p}$$

$$= \frac{1.07(6.68 \times 10^{-3})^2 \times 1.5}{32.2(0.41)^4 \times 0.95} (3.66 \times 10^4) = 3.04 \text{ ft}$$

6-4. Flow Through Expanded Beds

The Carman-Kozeny and the Rose equations predict the head loss across beds in which the voids are clear and unobstructed. In beds where materials introduced by the fluid accumulate in the pore spaces, head losses build up with time and flow capacity must be restored periodically. This is done by removing the clogged portions of the bed or by scouring out the void accumulations by fluid expansion of the bed. The following discussion is concerned with the behavior of both the bed mass and the fluid during fluid expansion.

Figure 6-2 shows a fluid flowing upward through a bed of small, uniformly sized particles. At low fluid velocities, the particles are undisturbed and the bed remains fixed. As the velocity is increased, however, a velocity is reached where the particles no longer remain stationary and in contact with one another, but are "fluidized," i.e., supported by the fluid. This critical velocity is identified in Figure 6-3 as $\overline{V}_{Sc}$.

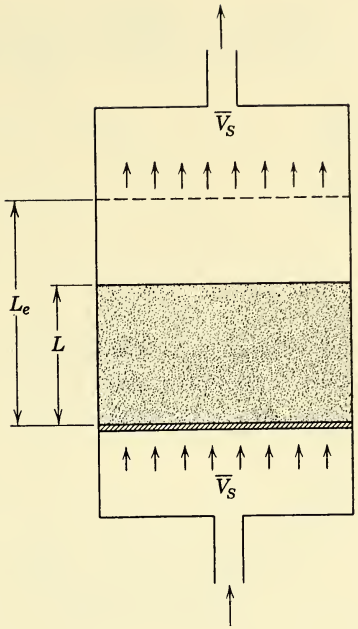

FIGURE 6-2. Flow through an expanded porous bed.

As the velocity is increased further, the particles become separated more and more, increasing the porosity and resulting in expansion of the bed. The vertical component of the velocity of the fluid between the particles is greater than the fluid velocity above the expanded bed. Finally, the velocity is increased to a value $\overline{V}'_{Sc}$ where the particles move as individuals, unhindered by the presence of other particles. The porosity at this point is almost equal to one, the bed ceases to exist as such, and the particles become transported by the fluid. When the fluid is a liquid, the velocity $\overline{V}'_{Sc}$ is approximately equal to the terminal velocity of the bed particles in a free settling situation.

The bottom curve in Figure 6-3 relates pressure drop due to friction with superficial velocity. Although the bed remains fixed, an increase in velocity is accompanied by a sizable increase in pressure drop. At the velocity where the bed becomes fluidized, $\overline{V}_{Sc}$, the pressure drop is closely equal to the effective weight of the particles in the bed. The effective weight is the maximum resistance offered by the particles to the passing fluid. Further increases in the superficial velocity result only in slight increases in pressure drop. What increases in pressure drop do develop are due primarily to the additional friction losses occurring between the fluid and the particles.

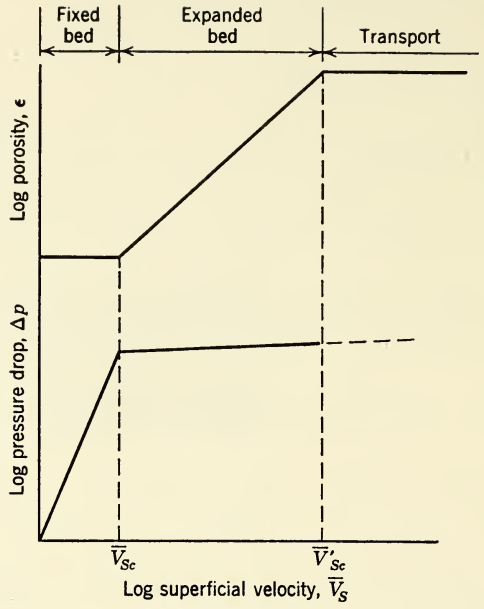

FIGURE 6-3. Variation of porosity and frictional pressure drop with superficial velocity for a fluid flowing upward through an unconsolidated, porous bed.

When a bed of uniformly sized particles reaches the point of fluidization ($\overline{V}_S = \overline{V}_{Sc}$), the effective weight of the particles (gravitational force) is just balanced by the force tending to lift the particles.

$$\Delta pS = \frac{g}{g_c} LS(1 - \epsilon)(\rho_s - \rho) \tag{6-23}$$

or

$$h_f = \frac{g}{g_c} L(1 - \epsilon)\left(\frac{\rho_s - \rho}{\rho}\right) \tag{6-24}$$

where Δp = frictional pressure drop across fluidized bed, lb force/ft^2
h_f = frictional head loss across fluidized bed, (ft)(lb force)/lb mass
S = bed cross section, ft^2
L = depth of fixed bed, ft
ρ_s = mass density of particles, lb mass/ft^3
ρ = mass density of fluid, lb mass/ft^3
ϵ = porosity of fixed bed
g = acceleration of gravity, ft/sec^2
g_c = Newton's law conversion factor, (ft)(lb mass)/(lb force)(sec^2)

A relationship between the depths and the porosities of the fixed and the expanded beds develops from the fact that the total mass of the particles remain constant.

$$LS(1 - \epsilon)\rho_s = L_e S(1 - \epsilon_e)\rho_s \tag{6-25}$$

and

$$L_e = L\frac{1 - \epsilon}{1 - \epsilon_e} \tag{6-26}$$

where L_e = depth of expanded bed, ft
ϵ_e = porosity of expanded bed

The solution of Equation 6-26 for L_e depends upon the evaluation of ϵ_e. A relationship pertinent to such evaluation has been established [11] for the hydraulic expansion of a bed of uniform sand grains,

$$\epsilon_e = \left(\frac{\overline{V}_S}{u_t}\right)^{0.22} \tag{6-27}$$

where $\overline{V}_S$ = superficial velocity based on bed cross section, ft/sec
u_t = terminal free settling velocity of particles, ft/sec

A stratified bed of nonuniform sized particles is completely fluidized when, for the largest particle,

$$\overline{V}_S = u_t\epsilon^{4.5} \tag{6-28}$$

For such beds the expanded depth can be computed with the use of a modification of Equation 6-26.

$$L_e = L(1 - \epsilon)\sum_{i=1}^{i}\frac{x_i}{(1 - \epsilon_e)_i} \tag{6-29}$$

where x_i = weight fraction of particles forming layer with porosity $\epsilon_{e,i}$
i = number of weight fractions in mixture

As indicated above, the maximum resistance that particles offer to the contacting fluid is nearly equal to their effective weight. Since the effective weight does not change with bed expansion, the pressure drop through a fluidized bed of particles of nonuniform size can be estimated with Equations 6-23 and 6-24.

EXAMPLE 6-3

The sand filter described in Example 6-2 is to be backwashed hydraulically (water temperature = 45 °F) at a rate just sufficient to fluidize the

[11] Fair, G. M., and J. C. Geyer, *Water Supply and Waste-Water Disposal*, John Wiley and Sons, New York (1954), 677.

entire bed. Compute (*a*) the backwash rate, (*b*) the head loss at this rate, and (*c*) the depth of the expanded bed.

Solution

1. Reproduce first three columns of table in Example 6-2.
2. Compute settling velocity of largest particles.

From Equation 4-11,

$$u_t = \left[\frac{4(32.2)(1.65)D_p}{3C_D}\right]^{1/2} = 8.4\left(\frac{D_p}{C_D}\right)^{1/2}$$

From Equation 4-12,

$$C_D = \frac{18.5}{[(62.4D_p u_t)/(8.74 \times 10^{-4})]^{0.6}}$$

$$= \frac{2.25 \times 10^{-2}}{D_p{}^{0.6} u_t{}^{0.6}}$$

Combining the two equations, $u_t = 315 D_p{}^{1.14}$, and for the largest particles, $u_t = 315(35.8 \times 10^{-4})^{1.14} = 0.496$ ft/sec.

Sieve Numbers, U.S. Sieve Series	Weight Fraction of Particles Retained, $\times 10^2$	Geometric Mean Diameter, $(D_p)_g$ $\times 10^4$, ft	Terminal Settling Velocity, $u_t \times 10^2$, ft/sec	Porosity of Expanded Bed, ϵ	$\frac{x}{1-\epsilon_e}$
(1)	(2)	(3)	(4)	(5)	(6)
14–20	0.80	35.8	49.6	0.410	0.0135
20–25	4.25	25.3	33.5	0.450	0.0772
25–30	15.02	21.2	27.3	0.471	0.284
30–35	16.65	17.8	22.2	0.493	0.328
35–40	18.01	15.1	18.7	0.512	0.369
40–50	18.25	11.6	14.0	0.545	0.402
50–60	15.65	9.0	10.5	0.580	0.373
60–70	9.30	7.5	8.5	0.607	0.237
70–100	2.07	5.8	6.6	0.643	0.0580
					$\Sigma \frac{x}{1-\epsilon_e} = 2.142$

3. Compute the backwash rate (Equation 6-28).

$$\overline{V}_S = 0.496(0.41)^{4.5} = 8.85 \times 10^{-3} \text{ ft/sec} = 0.53 \text{ (ft}^3\text{)/(min)(ft}^2\text{)}$$

4. Compute the head loss (Equation 6-24).

$$h_f = 1.5(1 - 0.41)1.65 = 1.46 \text{ ft}$$

5. Prepare table as follows:
   Column 4: Compute values from $u_t = 315D_p^{1.14}$.
   Column 5: Compute values from Equation 6-27.
6. Compute depth of expanded bed (Equation 6-29).

$$L_e = 1.5(1 - 0.41)2.142 = 1.9 \text{ ft}$$

6-5. Flow Through Porous Plates

Porous plates are often employed as bed supports. Besides furnishing support, porous plates serve to collect and distribute fluid evenly over the bottom of the bed. The head loss through such plates cannot be computed with equations of the Carman-Kozeny and Rose types. For this reason, the correlation of pressure drop data has been largely empirical. Typical correlations are shown in Figure 6-4. Here, head loss

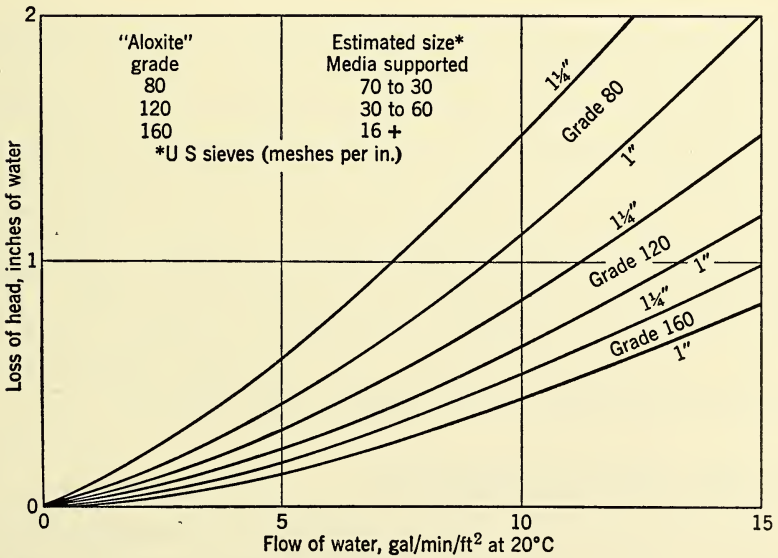

FIGURE 6-4. Head loss through zeolite and ion-exchange underdrain plates. (From Figure 20, Carborundum Company, "Porous Media.")

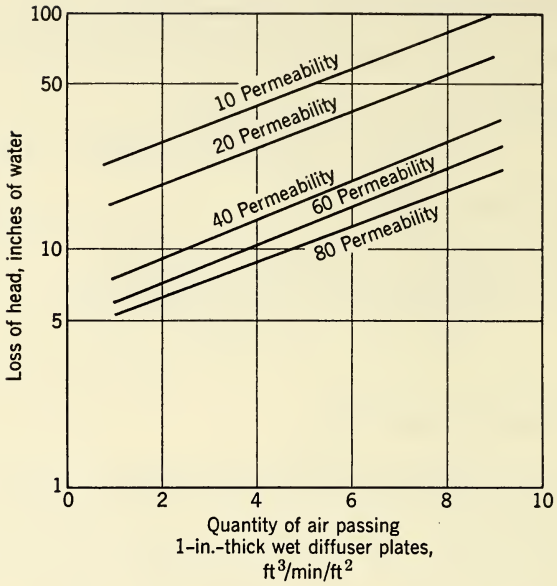

FIGURE 6-5. Estimated maximum head loss through old diffusers (submerged). (From Figure 67, Carborundum Company, "Porous Media.")

is related to flow rate for three grades of plates, each with a different pore size.

Porous plates and tubes find wide application as dispersion devices in gas transfer operations. For such a use, porous plates and tubes are characterized by a *permeability rating*. This rating is defined as the number of cubic feet per minute of air at 70 °F and 10 to 25 percent relative humidity, which will pass through 1 ft^2 of media, 1 in. in thickness, when the differential pressure across the media is 2 in. of water. Representative curves relating head loss with air flow through porous plates of different permeabilities are presented in Figure 6-5.

Most porous plates are made by bonding together grains of fused crystalline aluminum oxide with special ceramic materials.

6-6. Rapid Sand Filters—Gravity Type

Rapid sand filters employed in municipal water treatment practice are of the gravity type, and are commonly housed in concrete basins. A cutaway view of a typical filter is shown in Figure 6-6. This filter consists of a porous plate underdrain on top of which are placed 24 to

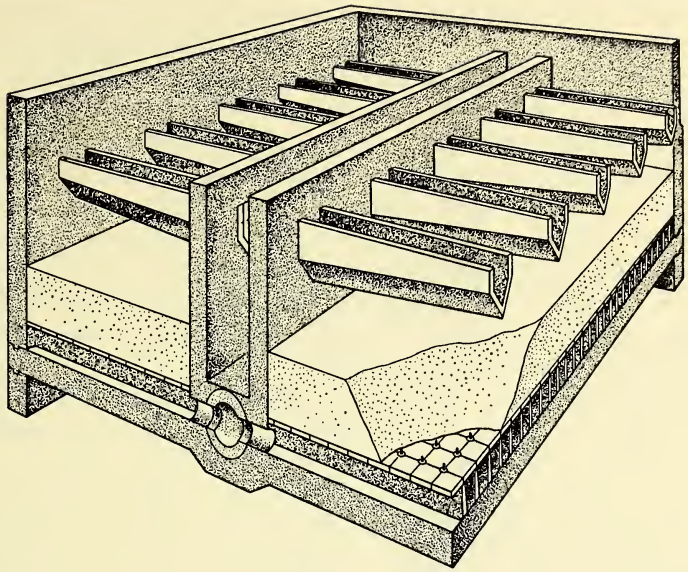

FIGURE 6-6. Cut-away view of gravity type of rapid sand filter. (From Figure 6, Carborundum Company, "Porous Media.")

30 in. of sand. In many filters the porous plate bottom is replaced by a perforated pipe or some other type of underdrainage system, covered by 18 to 24 in. of graded gravel. The sand ordinarily used has an effective size of from 0.4 to 0.55 mm, and a uniformity coefficient ranging from 1.35 to 1.75.[12] Where used to support the sand bed, gravel will vary in size from 1½ in. at the bottom to ⅛ in. at the top of the gravel layer. Filter basins are normally constructed in some even multiple or fraction of 1 mgd, and with a length-to-width ratio of approximately 1.25. Data relating to the behavior of rapid sand filters under different operating conditions are limited. For this reason, design is still based largely on empirical values.

Coagulated, settled water is applied to the filter at a rate of 2 to 4 gal/min/ft^2 of filter surface. Filtered water is collected by the underdrains and piped to a clear well. When the filter becomes clogged, it is washed by reversing the flow. Filtered water, introduced by the underdrainage system, is forced up through the bed at a rate of about

[12] Effective size is equal to the sieve size in millimeters that will pass 10 percent (by weight) of sand. Uniformity coefficient is equal to the sieve size passing 60 percent of the sand divided by that size passing 10 percent.

2 $ft^3/sec/ft^2$ of filter surface. Backwashing expands the sand bed from 20 to 60 percent above its normal depth. The suspended materials trapped in the top layers of the sand are released to the rising water. The wash water flows over the sides of the wash-water gutter and is carried to a gullet, about 2 ft wide and extending the length of the filter. From there the wash water discharges into a drain. Normally, a wash period of 4 to 5 min is sufficient to remove the materials clogging the filter. Surface sprays are often used to supplement backwashing. Perforated pipes applying water immediately above the sand surface at a rate of 4 to 6 $gal/min/ft^2$ and at a pressure of 10 psi have been found satisfactory for this purpose. Total water used for washing amounts to 1 to 4 percent of the water filtered.

Wash-water gutters of concrete or metal and of different cross sections can be used in a variety of arrangements. As a rule, the gutters are spaced 4 to 6 ft from edge to edge. The edge of the gutter is located slightly above the surface of the sand bed at maximum expansion. The bottom should clear the top of the unexpanded bed by at least 2 in.

The length of filter run usually is fixed by the head loss through the sand bed. When the bed is clean, this loss can be estimated with Equation 6-22. As a rule, 8 to 10 ft of head are available for loss through the sand and rate controller. Initially, with a clean filter, the loss through the sand will be of the order 6 to 12 in., with the remainder being taken up by the controller. As operation proceeds, losses build up in the sand until the controller is wide open. The filter must be backwashed at this point, since further increase in head loss through the sand would result in a reduction of flow through the controller. Total operating head (difference between the elevation of the water level over the filter and the maximum water level in the filtered water clear well) must be at least 10 ft.

Figure 6-7 is a sectional view of a rapid sand filter showing a typical piping arrangement and accessory equipment. At nominal plant capacity and at maximum wash rate, the velocity of flow through the pipes should not exceed the values listed in Table 6-3. For more detailed information relative to the design of rapid sand filters the reader is referred elsewhere.[13,14]

The primary objective of rapid sand filtration is the removal of suspended material from water. This material is predominately floc carryover from the sedimentation operation. Although the mechanism

[13] "Water Treatment Plant Design," *ASCE, Manual of Engineering Practice*, **19** (1940).

[14] Babbitt, H. E., and J. J. Doland, *Water Supply Engineering* (5th ed.), McGraw-Hill Book Co., New York (1955).

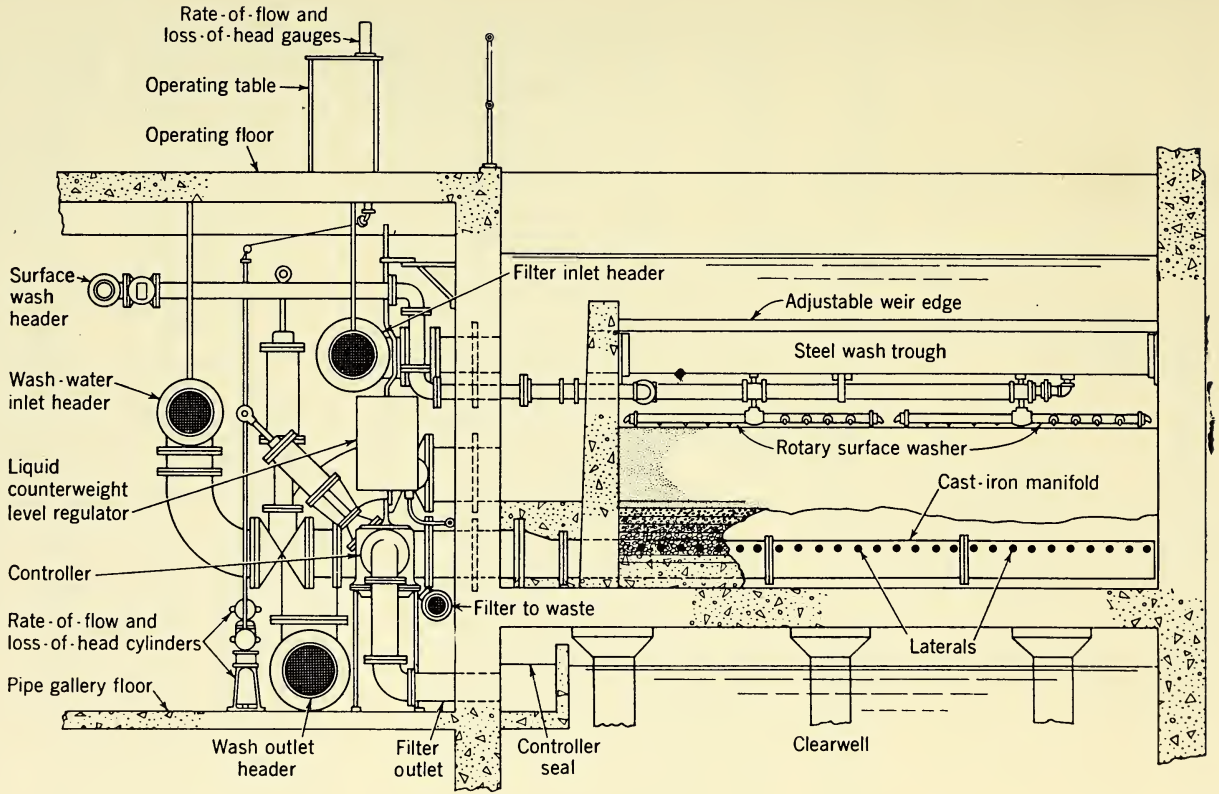

FIGURE 6-7. Piping arrangement and accessory equipment for gravity-type, rapid sand filter. (Courtesy of *The Permutit Company*, a division of *The Pfaudler Permutit Inc.*)

TABLE 6-3. MAXIMUM FLOW VELOCITIES THROUGH PIPING EXTERIOR TO RAPID SAND FILTER *

Pipe	Velocity, ft/sec
Filter influent	2
Filter effluent	5
Wash water	12
Waste water	8
Filter to waste	15

* Taken from Davis, C. V. (ed.), *Handbook of Applied Hydraulics* (2nd ed.), McGraw-Hill Book Co., New York (1952), 986.

of removal is rather obscure, it appears that the removal of small particles is accomplished by adhesion to the sand grains, whereas the larger particles are strained out by the pore constrictions.[15]

Removal efficiency is a function of filter depth. For sand filters of uniform size grains, the depth of floc penetration increases with (*a*) floc concentration, (*b*) rate of filtration, (*c*) viscosity of the water, and (*d*) size of sand grain. Penetration has been found to decrease as floc size increases. From experiments performed on the penetration of iron floc in unigranular sand beds, Stanley [16] developed an empirical relationship giving the depth of penetration for an increase of 8 ft in head loss and a temperature of 77 °F. In English units the relationship is

$$y = C' D_p^{2.46} q'^{1.56} \tag{6-30}$$

where y = penetration of iron floc, ft
D_p = diameter of sand grains, ft
q' = rate of filtration, $ft^3/sec/ft^2$
C' = coefficient = 9.3×10^9

The fact that the terminal increase in head loss is an indirect measure of the quantity of material removed from the water makes the inclusion of a loading intensity term unnecessary.

The behavior of stratified beds of nonuniform size sand defies mathematical formulation. Such behavior is illustrated by the curves pre-

[15] Camp, T. R., "Water Treatment," in: C. V. Davis (ed.), *Handbook of Applied Hydraulics* (2nd ed.), McGraw-Hill Book Co., New York (1952).

[16] Stanley, D. R., *Penetration of Floc into Sand Filters*, Thesis, Harvard University (1952).

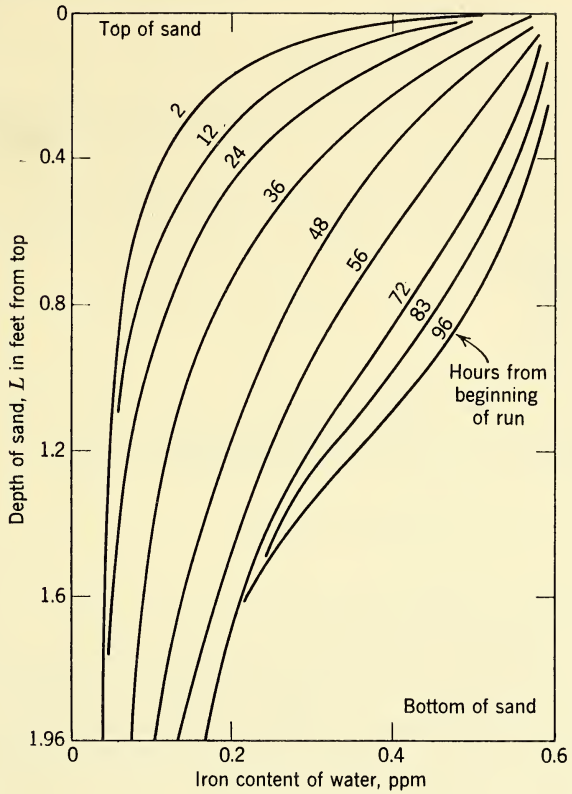

FIGURE 6-8. Floc penetration in rapid sand filter as a function of time. [Adapted from Eliassen, R., Ph.D. Thesis, MIT (1935).]

sented in Figure 6-8.[17] These curves show the penetration of iron floc in an experimental rapid sand filter. It is to be noted that removal shifts to lower layers as the top layers become clogged. For this particular filter run, total removal decreases after the run is about 25 percent complete.

Notations

a_V Surface area of dry packing per unit volume, ft^2/ft^3
A Total surface area of particles, ft^2
C' Coefficient
C_D Coefficient of drag, dimensionless

[17] Eliassen, R., Ph.D. Thesis, MIT (1935).

D_p Particle diameter, ft

f, f', f'' Friction factors, dimensionless

g Acceleration of gravity, ft/sec^2

g_c Newton's law conversion factor, (ft)(lb mass)/(lb force)(sec^2)

G_L, G_G Superficial mass velocities of a liquid and gas respectively, (lb force)/(hr)(ft^2)

h_f Frictional head loss across bed, (ft)(lb force)/(lb mass)

i Number of weight fractions in a mixture and number of layers in a stratified bed

L Depth of fixed bed, ft; L_e, depth of expanded bed

m Constant

n Constant

N Number of particles

N_{Re} Reynolds number, dimensionless

Δp Frictional pressure drop across fluidized bed, lb force/ft^2

q' Volumetric rate of filtration per unit area, ft^3/sec/ft^2

r_H Hydraulic radius, ft

s_p Surface area of a single particle, ft^2

S Bed cross section, ft^2

u_t Terminal settling velocity, ft/sec

v_p Volume of a single particle, ft^3

V Total volume of particles, ft^3

$\overline{V}$ Mean velocity of flow, ft/sec; $\overline{V}_S$, superficial velocity of flow; $\overline{V}_{Sc}$, superficial velocity of flow when fluidization is impending; $\overline{V}'_{Sc}$, superficial velocity of flow when transport is impending

x Weight fraction; x_i, weight fraction of particles of size $D_{p,i}$ and of particles in ith layer

y Depth of penetration, ft

ϵ Porosity of fixed bed, dimensionless; ϵ_e, porosity of expanded bed

μ Absolute viscosity of a fluid, (lb mass)/(ft)(sec)

ρ Mass density of a fluid, lb mass/ft^3; ρ_L, mass density of a liquid; ρ_G, mass density of a gas; ρ_s, mass density of a particle

ϕ_s Particle shape factor, dimensionless

7

Vacuum filtration

7-1. Introduction

Filtration is another unit operation for separating solids from liquids. In process engineering, filtration is performed in four different ways: by gravity, pressure, vacuum, and centrifugal force. Filtration by gravity generally is limited to the removal of solids from relatively dilute suspensions by passage through porous beds of unconsolidated media. Separations of this nature have been discussed in Chapter 6.

Vacuum filtration finds wide application in the partial separation of liquids from concentrated suspensions, sludges, and slurries. When the liquid phase is highly viscous, or when the solids are so fine that vacuum filtration is too slow, pressure filtration provides a convenient solution to the separation problem. Centrifugal filtration is used when the solids are easy to filter and a filter cake of low moisture content is desired. Although the following discussion is oriented toward vacuum filtration, the relationships developed are applicable to pressure and centrifugal filtration as well.

7-2. Rotary Drum Filters

Vacuum filtration is commonly carried out on slowly rotating drum filters in a more or less continuous operation. Such a filter consists of a cylindrical structure, the outside surface of which is covered with a filter medium. Internally, the drum

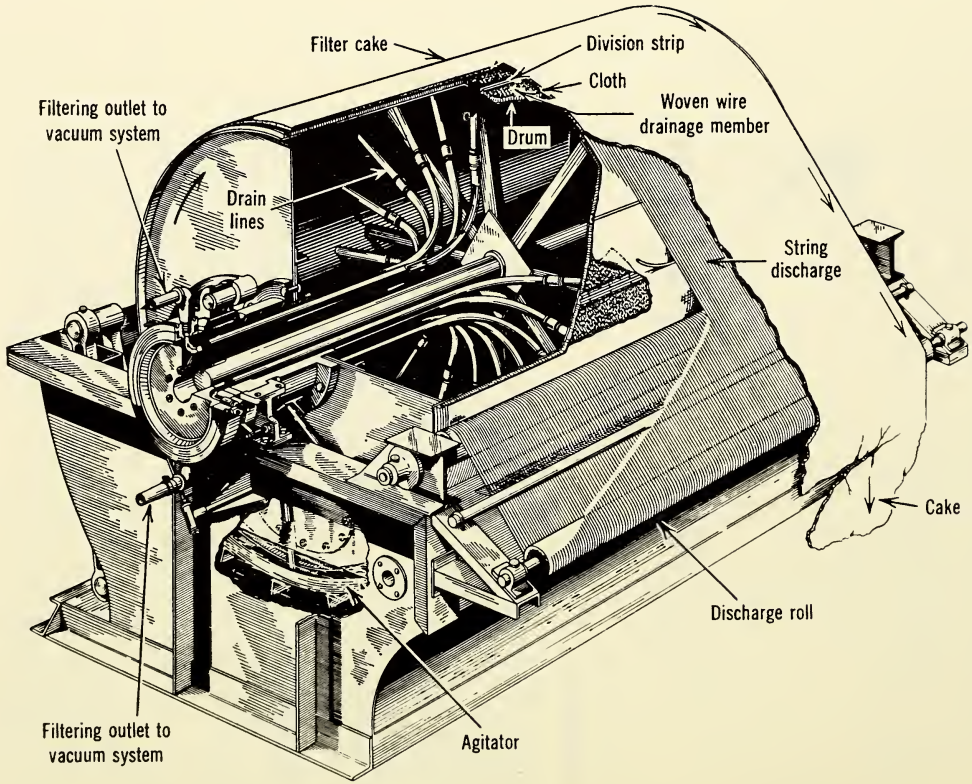

FIGURE 7-1. Rotary drum filter. (Filtration Engineers Division, *American Machine and Metals, Inc.*)

is divided into shallow drainage compartments, each of which is connected by piping to an automatic valve located at one end of the filter (Figure 7-1). Drum diameters vary from 3 to 12 ft, and lengths from as little as 1 ft to as large as 20 ft on the average.

The filter is suspended in a trough containing the sludge to be dewatered at a depth providing submergence to 20 to 40 percent of the circumferential area of the drum. As the filter is rotated, a sludge mat of ¼ in. or more in thickness is formed on the filter medium as a result of a vacuum (20 to 26 in. Hg) applied to the drainage compartments servicing the submerged portion of the drum. The vacuum is continued as the mat rises above the trough to dewater the sludge further. Just before the mat reaches the trough again, it is removed from the filter. Removal may be accomplished in several different ways. Filter speed, vacuum, and drum submergence are adjusted to meet operating conditions.

Filter media include wool, cotton, and synthetic fiber cloth as well as coil springs arranged in a two-layer pattern. Ancillary equipment typical of a vacuum-filtration system include vacuum receivers, filtrate pumps, moisture traps, and vacuum pumps (Figure 7-2).

7-3. Filter Yields

Vacuum filtration is a special case of flow through beds of solids. As such, the movement of liquid through a filter cake can be thought of as taking place inside innumerable channels with small, indeterminate cross sections. According to the Carman-Kozeny relationship, the head loss across the cake will be

$$h_f = \frac{\Delta p}{\rho} = f' \left(\frac{L}{\phi_s D_p} \right) \left(\frac{1 - \epsilon}{\epsilon^3} \right) \left(\frac{\overline{V}_S{}^2}{g_c} \right) \tag{6-5}$$

where h_f = energy head loss due to friction, (ft)(lb force)/ lb mass
Δp = permanent pressure drop due to friction, lb force/ft^2
f' = friction factor, dimensionless
L = thickness of filter cake, ft
D_p = particle diameter, ft
ϕ_s = particle shape factor, dimensionless
ϵ = porosity of bed, dimensionless
$\overline{V}_S$ = superficial velocity, ft/sec
ρ = liquid density, lb mass/ft^3
g_c = Newton's law conversion factor, (lb mass)(ft)/(lb force)(sec^2)

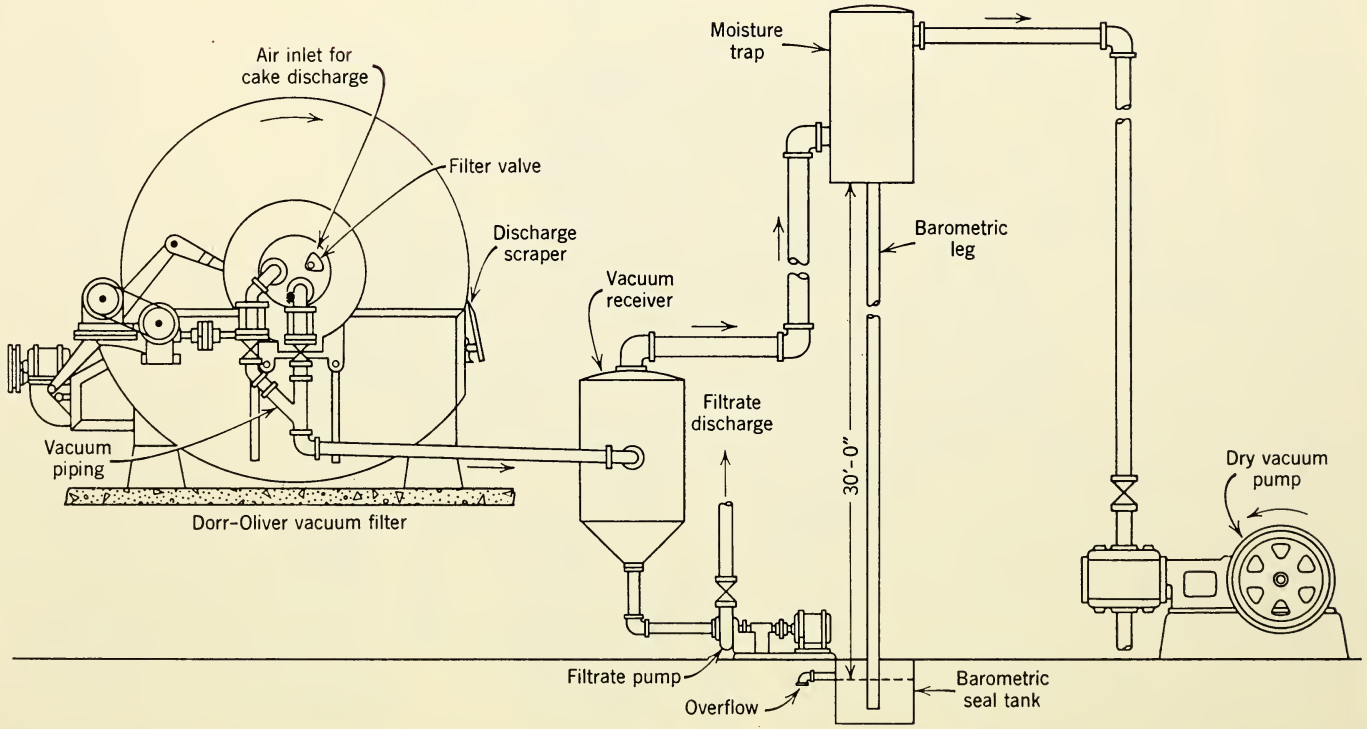

FIGURE 7-2. Ancillary equipment typical of a vacuum filtration system. (*Dorr-Oliver, Inc.*)

Since the channels are so small, the flow of liquid through them must be laminar. Examination of the curve in Figure 6-1 will reveal the inverse relationship existing between the friction factor and the Reynolds number. In the laminar flow region, the friction factor can be expressed as

$$f' = \frac{K'(1 - \epsilon)}{N_{Re}} = K' \left[\frac{\mu(1 - \epsilon)}{\phi_s D_p \overline{V}_S \rho} \right] \tag{7-1}$$

where K' = constant
N_{Re} = Reynolds number, dimensionless
μ = liquid viscosity, (lb mass)/(ft)(sec)

By substituting this relationship into Equation 6-8 and simplifying, an expression is obtained for estimating the pressure drop across a filter cake.

$$\Delta p = K' \left[\frac{(1 - \epsilon)^2}{g_c \phi_s^2 D_p^2 \epsilon^3} \right] \mu L \overline{V}_S = K' \left[\frac{(1 - \epsilon)^2}{36 g_c (v_p / s_p) \epsilon^3} \right] \mu L \overline{V}_S \tag{7-2}$$

where v_p = volume of a single particle, ft^3
s_p = surface area of a single particle, ft^2

It is to be noted that the terms enclosed in the brackets are either constants or internal properties of the filter cake.

The superficial velocity $\overline{V}_S$ at any instant can be expressed as

$$\overline{V}_S = \frac{1}{S} \frac{dV}{dt} \tag{7-3}$$

where V = volume of filtrate, ft^3
t = time, sec
S = area of filter cake, ft^2

Substituting this relationship into Equation 7-2 and combining terms,

$$\frac{dV}{dt} = \frac{KS \Delta p}{\mu L} \tag{7-4}$$

where K = permeability, (lb mass)(ft^3)/(lb force)(sec^2). Equation 7-4 provides an expression for the rate of filtration in terms of the volumetric rate at which the filtrate flows through the filter cake per unit time.[1]

Permeability is a property of the filter cake. Quantitatively, it is defined as the rate of flow of a liquid having unit viscosity across a cake

[1] The approach used herein is a reversal of historical development. The Darcy permeability relationship, defined essentially by Equation 7-4, was employed long before the works of Carman and Kozeny. The present development is offered for the purpose of identifying the factors influencing the value of K.

of unit area and thickness when the pressure drop is unity. Its value depends upon such characteristics as porosity, average specific surface area of the cake particles, and compressibility. For our purpose it is more convenient to express the effect of these properties in terms of filtration resistance where

$$R = \frac{1}{K} \tag{7-5}$$

where R = specific resistance, (lb force)(sec^2)/(lb mass)(ft^3).

Equation 7-4 becomes

$$\frac{dV}{dt} = \frac{S\,\Delta p}{\mu LR} \tag{7-6}$$

Actually, the total resistance encountered in a filtering operation is composed of two resistances in series: the resistance offered by the filter (primarily the medium) and that offered by the cake. To express the true filtration rate, therefore, Equation 7-6 must be modified,[2]

$$\frac{dV}{dt} = \frac{S\,\Delta p}{\mu(LR + R_f)} \tag{7-7}$$

where R_f = resistance of filter, (lb force)(sec^2)/(lb mass)(ft^2). Since

$$L = \frac{vV}{S} \tag{7-8}$$

where v = volume of cake deposited per unit volume of filtrate, dimensionless, then

$$\frac{dV}{dt} = \frac{S^2\,\Delta p}{\mu(vVR + SR_f)} \tag{7-9}$$

Because of the nature of compressible cakes, it is more convenient to express sludge concentration in terms of weight of dry cake solids per unit volume of filtrate than by volume of cake per unit volume of filtrate. Therefore,

$$\frac{dV}{dt} = \frac{S^2\,\Delta p}{\mu(wVR' + SR_f)} \tag{7-10}$$

where w = weight of dry cake solids per unit volume of filtrate, lb force/ft^3

R' = specific resistance, sec^2/lb mass

[2] Carman, P. C., *Trans. Inst. Chem. Engrs. (London)*, **16** (1938), 168.

In vacuum filtration, the vacuum level is kept constant during cake formation. Therefore, Equation 7-10 can be arranged and integrated in the following manner to give an expression for the time required for cake formation.

$$\int_0^t dt = \int_0^V \left(\frac{\mu w V R'}{S^2\,\Delta p} + \frac{\mu R_f}{S\,\Delta p}\right) dV \tag{7-11}$$

$$t = \frac{\mu w R'}{2S^2\,\Delta p} V^2 + \frac{\mu R_f}{S\,\Delta p} V \tag{7-12}$$

By rearranging

$$\frac{V}{S} = \left(\frac{2\,\Delta p t}{\mu w R'} - \frac{2R_f V}{w R' S}\right)^{1/2} \tag{7-13}$$

Equation 7-13 is an expression for the volume of filtrate obtained per unit of cake area during time t. A relationship can be developed for filter yield by multiplying both sides by w/t_c.

$$\frac{V}{S}\frac{w}{t_c} = B = \left(\frac{2\,\Delta p w t}{\mu R' t_c^2} - \frac{2wR_f V}{R' S t_c^2}\right)^{1/2} \tag{7-14}$$

where t_c = time required for one filter cycle, sec
B = filter yield, (lb force)/(ft^2)(sec)

The relation between the filter cycle time and the time required for the cake to be formed can be written

$$t = \gamma t_c \tag{7-15}$$

where γ = fraction of cycle time occupied by cake formation. With substitution, Equation 7-14 becomes

$$B = \left(\frac{2\,\Delta p w \gamma}{\mu R' t_c} - \frac{2wR_f V}{R' S t_c^2}\right)^{1/2} \tag{7-16}$$

When the filter resistance R_f is made negligible through the selection of a proper medium, Equation 7-16 can be reduced to

$$B = \left(\frac{2\,\Delta p w \gamma}{\mu R' t_c}\right)^{1/2} \tag{7-17}$$

The variables in Equation 7-17 can be separated into two groups: operational variables and sludge variables. Operational variables include pressure drop due to friction Δp, fraction of cycle time occupied by cake formation γ, and filter cycle time t_c. An increase in yield is promoted by increasing Δp and γ, and by decreasing t_c. As a rule, the highest vacuum

is maintained, and operational control is exerted by varying drum speed t_c and drum submergence γ. In filtering sludges that form compressible cakes, drum submergence is usually controlled by the time required to dewater the cake to the desired moisture content. Since cake thickness decreases as cycle time is reduced, drum speed is limited by the minimum thickness that can be removed conveniently from the filter.

Sludge variables include liquid (filtrate) viscosity, solids concentration,[3] and specific resistance. For a given sludge at a given temperature, filtrate viscosity is fixed. Solids concentration and specific resistance will vary, however, and are dependent upon sludge conditioning prior to filtration. As noted from Equation 7-17, increased solids concentration and decreased specific resistance operate to give increased filter yields.

EXAMPLE 7-1

Sludge containing 5 percent filterable solids is to be dewatered at a rate of 16.5 ft^3/hr on a drum filter under a vacuum of 25 in. Hg. Laboratory analyses reveal that at the same vacuum level the specific resistance of the filter cake is 6.57×10^{12} sec^2/lb mass, and a cake with 30 percent solids can be obtained with 3½ minutes dewatering. The specific gravity is approximately one and the filtration temperature of the sludge about 77 °F. Assuming a filter cycle time of 5 min, estimate the filter area required.

Solution

1. Weight of solids filtered per second,

$$\frac{Vw}{t_c} = 16.5 \times 62.2 \times 0.05(1/3600) = 1.425 \times 10^{-2} \text{ lb force/sec}$$

[3] The weight of dry cake solids per unit volume of filtrate, w, can be related to the solids concentration of the unfiltered sludge, c, by an expression derived as follows:

If wV is the total weight of filterable solids both in the filter cake and unfiltered sludge, m is the weight ratio of wet cake to dry cake, and $(mwV - wV)(g_c/\rho g)$ is the volume of liquid retained in wet filter cake, then

$$c = \frac{wV}{[(mwV - wV)(g_c/\rho g)] + V}$$

and

$$w = \frac{c}{1 - [(m - 1)(cg_c/\rho g)]}$$

or, in terms of weight fractions, it can be shown that

$$w = \frac{\rho g/g_c}{[(1 - x)/x] - [(1 - x_c)/x_c]}$$

where x = weight fraction of filterable solids in unfiltered sludge
x_c = weight fraction of filterable solids in filter cake

2. Weight of solids per unit volume of filtrate,

$$w = \frac{\rho g/g_c}{[(1 - x)/x] - [(1 - x_c)/x_c]}$$

$$= \frac{62.2}{[(1 - 0.05)/0.05] - [(1 - 0.30)/0.30]} = 3.52 \text{ lb force/ft}^3$$

3. From Equation 7-17

$$B = \left(\frac{2\,\Delta p w \gamma}{\mu R' t_c}\right)^{1/2} = \left[\frac{2(25 \times 70.75)3.52 \times 0.30}{(0.886 \times 6.72 \times 10^{-4})(6.57 \times 10^{12})300}\right]^{1/2}$$

$$= 56.2 \times 10^{-6} \text{ (lb force)/(ft}^2\text{)(sec)}$$

4. Area required,

$$S = \frac{Vw/t_c}{B} = \frac{1.425 \times 10^{-2}}{56.2 \times 10^{-6}} = 254 \text{ ft}^2$$

Note: Resistance offered by the filter medium has been considered negligible.

7-4. Specific Resistance

The specific resistance is used not only for predicting filter yields but also as a parameter for evaluating the efficacy of sludge conditioning operations. Its value may be estimated from an analysis of laboratory data.

Equation 7-12 may be written as

$$\frac{t}{V} = \frac{\mu w R'}{2S^2\,\Delta p} V + \frac{\mu R_f}{S\,\Delta p} \tag{7-18}$$

or

$$\frac{t}{V} = bV + a \tag{7-19}$$

Thus it is seen that a plot of data relating values of t/V with V will give a straight line, the slope of which is

$$b = \frac{\mu w R'}{2S^2\,\Delta p} \tag{7-20}$$

Briefly, the experimental apparatus used to obtain values of t/V and V consists of a Buchner funnel modified so that measurements can be made on the filtrate volumes at various times during filtration. Information must be obtained concerning the filter area, solids content (w or c),

filtration pressure, and the viscosity of the filtrate. Details of apparatus and experimental technique are found elsewhere.[4]

Most sludges of concern to the sanitary engineer form compressible filter cakes. For these cakes, specific resistance will vary with the vacuum level. Empirically, it has been found that the relationship is expressed satisfactorily by

$$R' = C\,\Delta p^s \tag{7-21}$$

where C = cake constant
s = coefficient of compressibility

The cake constant and coefficient of compressibility for a given sludge cake can be determined from a logarithmic plot of data relating the specific resistance with vacuum level. The slope of the straight line of best fit is equal to s while the intercept at $\Delta p = 1$ gives the value of C.

EXAMPLE 7-2

A vacuum-filtration test was performed on an aqueous sludge with the use of a modified Buchner funnel apparatus. Test conditions were as follows:

Temperature of sludge	= 25°C
Filtration vacuum	= 25 in. Hg
Filter area	= 44.2 cm^2
Weight of solids per unit volume of filtrate	= 48 mg/ml

Filtrate volumes obtained after various time intervals are recorded in the second column of the following table. Compute the specific resistance.

t, sec	V, ml	t/V, sec/ml
60	1.3	46
120	2.4	50
180	3.4	53
240	4.3	56
300	5.2	58
360	6.0	60
420	6.7	63
480	7.5	64
540	8.3	65
600	8.9	67
720	10.2	71
900	12.0	75

[4] Coakley, P., and B. R. S. Jones, "Vacuum Sludge Filtration," *Sewage and Industrial Wastes*, **28** (1956), 963.

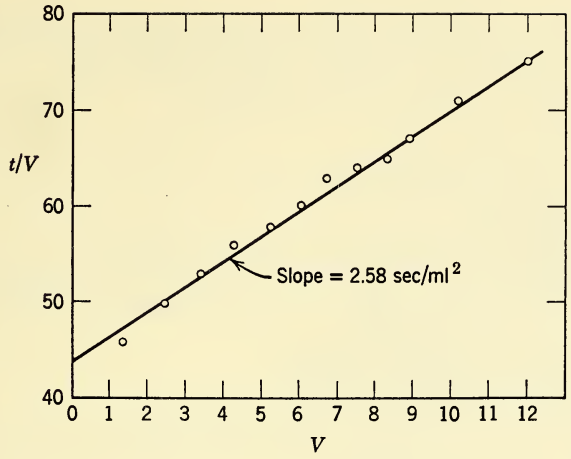

FIGURE 7-3. Plot of t/V versus V for Example 7-2.

Solution

1. Compute values of t/V for corresponding values of t and V (see column 3, p. 168).
2. Plot values of t/V versus corresponding values of V (see Figure 7-3).
3. Determine slope of straight line of best fit for the plotted data. This is found to be equal to 2.58 sec/ml^2.
4. Using Equation 7-20, determine the specific resistance.

$$R' = \frac{2bS^2\,\Delta p}{\mu w}$$

$$= \frac{2(2.58 \times 7.83 \times 10^8)(44.2 \times 1.076 \times 10^{-3})^2(25 \times 70.75)}{(0.886 \times 6.72 \times 10^{-4})(48 \times 6.25 \times 10^{-2})}$$

$$= 9.05 \times 10^{12} \text{ sec}^2/\text{lb mass}$$

Notations

a	Constant
b	Constant
B	Filter yield, (lb force)/(ft^2)(sec)
c	Concentration, lb force/ft^3
C	Cake constant
D_p	Particle diameter, ft
f'	Friction factor

g Acceleration of gravity, ft/sec^2
g_c Newton's law conversion factor, 32.17 (lb mass)(ft)/(lb force)(sec^2)
h_f Energy head loss due to friction, (ft)(lb force)/(lb mass)
K Permeability, (lb mass)(ft^3)/(lb force)(sec^2)
K' Constant
L Thickness of filter cake, ft
m Weight ratio of wet cake to dry cake
N_{Re} Reynolds number
Δp Permanent pressure drop due to friction, lb force/ft^2
R Specific resistance, (lb force)(sec^2)/(lb mass)(ft^3); R_f, resistance of filter, (lb force)(sec^2)/(lb mass)(ft^2); R', specific resistance, sec^2/lb mass
s Coefficient of compressibility
s_p Surface area of a single particle, ft^2
S Area of filter cake, ft^2
t Time, sec; t_c, time required for one filter cycle
v Volume of cake deposited per unit volume of filtrate, dimensionless
v_p Volume of a single particle, ft^3
V Volume of filtrate, ft^3
$\overline{V}_S$ Superficial velocity, ft/sec
w Weight of dry cake solids per unit of filtrate, lb force/ft^3
x Weight fraction of filterable solids in unfiltered sludge; x_c, weight fraction of filterable solids in filter cake
γ Fraction of cycle time occupied by cake formation
ϵ Porosity
μ Liquid viscosity, (lb mass)/(ft)(sec)
ρ Liquid density, lb mass/ft^3

8

Gas transfer

8-1. Mass Transfer Operations

Certain unit operations are grouped together because they involve a flow of mass between two or more phases in contact with each other. Those operations of principle interest to sanitary engineers are gas absorption and desorption in which molecules are transferred between gas and liquid phases, leaching and adsorption in which a flow of soluble materials takes place between solids and liquids, and air-water contacts and drying in which water vapor is transported between water and air.

Gas absorption and desorption have wide applications in sanitary engineering treatment processes. In water treatment, the operations are employed to remove and replace carbon dioxide, and to remove hydrogen sulfide, methane, and various volatile organic compounds responsible for tastes and odors. In waste treatment, gas absorption is used primarily to provide air for the activated sludge process.

8-2. Mechanism of Transfer

When a liquid containing dissolved gases is brought into contact with an atmosphere of gas other than that with which it is in equilibrium, an exchange of gases takes place between the atmosphere and the solution. Two theories have been advanced to explain the mechanism of the exchange. These are called the *penetration theory* and the *film theory*.

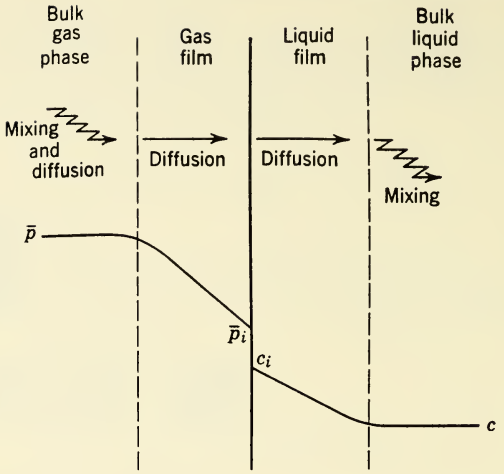

FIGURE 8-1. Schematic sketch of gas transfer mechanism.

According to the penetration theory, eddies originating in the turbulent bulk of the liquid migrate to the gas-liquid interface, where they are exposed briefly to the gas before being displaced by other eddies arriving at the interface. During their brief residence at the interface, the eddies absorb molecules from the gas. Upon return of the eddies to the liquid bulk, the molecules are distributed by turbulence. The rate of transfer is considered to be a function of the diffusivity, of a concentration gradient, and of a surface renewal factor.[1,2,3] Although the penetration theory holds considerable promise in dealing with gas transfer operations, application to present technology is limited.

The film theory, although more questionable from a theoretical standpoint, at present is of greater practical value than is the penetration theory. The film theory is based on a physical model in which two fictitious films exist at the gas-liquid interface, one liquid and one gas. These films are considered to be stagnant and furnish all resistance to gas transfer. They are thought of as persisting regardless of how much turbulence is present in the gas and liquid, the turbulence serving only to reduce the film thickness.

A schematic sketch of the imaginary transfer mechanism is shown in Figure 8-1.

[1] Higbie, Ralph, *Trans. Am. Inst. Chem. Engrs.*, **31** (1935), 365–389.
[2] Danckwerts, P. V., *Ind. Engr. Chem.*, **43** (1951), 1460–1467.
[3] Hanratty, T. J., *J. Am. Inst. Chem. Engrs.*, **2** (1956), 359–363.

Suppose, for example, gas is being transferred to a liquid which is unsaturated with respect to the gas being transferred. First, through a combined process of mixing and diffusion, the gas molecules are transported to the outer face of the gas film. The molecules then diffuse across the stagnant gas film to the gas-liquid interface where they dissolve in the liquid film. The dissolved gas then diffuses through this stagnant film to the boundary between the film and the bulk liquid phase, from where it is transported throughout the bulk liquid phase by mixing. The same mechanism in reverse prevails when gases are released from a supersaturated solution. Since transfer by diffusion is slow compared to that by mixing, the rate of transfer from one phase to another is considered to be controlled by the stagnant films.

8-3. Film Coefficients

When a concentration gradient of a given molecular species is established within a fluid, molecules of the species move in response to the gradient from regions of high concentration to those of low concentration. This behavior is called molecular diffusion. In an isolated system, diffusion ultimately results in the equalization of molecular concentrations throughout the system.

The rate at which molecules of gas A diffuse through a quiescent, nondiffusing gas of species B is given by

$$\frac{dn_A}{dt} = \frac{D_v A p}{R T_A s \bar{p}_{Bm}} (\bar{p}_{A1} - \bar{p}_{A2}) \tag{8-1}$$

where n_A = number of moles of gas A diffusing from point 1 to point 2, lb mole
t = time, hr
D_v = volumetric diffusivity, ft^2/hr
A = area across which diffusion is taking place, ft^2
p = total pressure, atm
$\bar{p}_{A1}$, $\bar{p}_{A2}$ = partial pressures of diffusing gas at points 1 and 2 respectively, atm
$\bar{p}_{Bm}$ = log mean of partial pressures of quiescent gas species over path of diffusion, atm
s = distance between points 1 and 2, ft
R = gas constant, 0.729 (ft^3)(atm)/(lb mole)(°R)
T_A = absolute temperature, °R

An analogous expression is used for molecular diffusion through quiescent liquids

$$\frac{dn_A}{dt} = \frac{D_v A c_{A+B}}{s c_{Bm}} (c_{A1} - c_{A2}) \tag{8-2}$$

where c_{A1}, c_{A2} = concentrations of diffusing molecular species at points 1 and 2 respectively, lb mole/ft^3

c_{A+B} = total number of moles of species A and B per unit volume, lb mole/ft^3

c_{Bm} = log mean of concentrations of a liquid over path of diffusion, lb mole/ft^3

The volumetric diffusivity is a function of temperature and the characteristics of both the diffusing species and the diffusion media. Values of diffusivity for ammonia, carbon dioxide, and oxygen in air and water are presented in Table 8-1.

TABLE 8-1. MASS DIFFUSIVITIES OF AMMONIA, CARBON DIOXIDE, AND OXYGEN

	In Air at 1 atm and 25 °C		In Water at 20 °C (Dilute Solutions)	
Gas	D_v, ft^2/hr	$N_{Sc}(\mu/\rho D_v)$	D_v, ft^2/hr	$N_{Sc}(\mu/\rho D_v)$
NH_3	0.890	0.67	6.83×10^{-5}	570
CO_2	0.636	0.94	6.87×10^{-5}	670
O_2	0.800	0.75	7.00×10^{-5}	558

Modifications of Equations 8-1 and 8-2 are used to express the rate at which a gas is transferred across the fictitious boundary films at a gas-liquid interface. Under steady-state conditions, there is no accumulation of diffusing molecules in either film, the molecular transport across the interface remaining constant with time.

$$N_A = \frac{dn_A}{dt} = k_G A(\bar{p}_A - \bar{p}_{Ai}) = k_L A(c_{Ai} - c_A) \tag{8-3}$$

where N_A = local rate at which component A is transferred across a gas-liquid interface, lb mole/hr

k_G, k_L = mass transfer coefficients for gas and liquid phases respectively, (lb mole)/(hr)(ft^2)(atm) and ft/hr

p_A, p_{Ai} = partial pressures of component A in the bulk gas phase and at the interface respectively, atm

c_{Ai}, c_A = concentrations of A at the interface and in the bulk liquid phase respectively, lb mole/ft^3

The terms enclosed in parentheses in Equation 8-3 can be thought of as "potential differences" that motivate transfer across the boundary films. The interfacial terms c_{Ai} and $\bar{p}_{Ai}$ are related by an equilibrium relationship since no resistance to mass transfer is assumed at the interface, and the gas and liquid phases are presumed to be in equilibrium with one another.

8-4. Equilibrium Relationships

When a gas is brought into contact with a liquid undersaturated with respect to a component of the gas, molecules of the latter will diffuse from the gas phase to the liquid phase. Concurrently, a portion of these molecules will return to the gas. The rates at which the molecules move from one phase to the other are governed by the concentrations of the diffusing component in the two phases. Ultimately, concentrations in both the liquid and gas will be such that the rate at which the molecules enter the liquid will equal that at which they leave. Thereafter, the concentrations will remain constant and the system is said to be in equilibrium.

The solubilities of gases (equilibrium concentrations) in liquids vary widely. For gases of low or moderate solubility that do not react chemically with the solvent, the quantity of gas which will dissolve at a given temperature can be determined by Henry's law

$$\bar{p} = Hx \tag{8-4}$$

where $\bar{p}$ = partial pressure of solute, atm
x = mole fraction of solute in liquid
H = Henry's law constant, atm

A mole fraction is defined as the ratio of the number of moles of a particular constituent of a phase to the number of moles of all the constituents. Equation 8-4 can be used for partial pressures up to 1 atm. Values of Henry's law constant for several gases that are slightly soluble in water are listed in Table 8-2.

The solubilities of the more soluble gases and those that react appreciably with the solvent do not behave as simple proportions of the partial pressures. Consequently, Henry's law does not express the equilibrium relationship for such gases. Instead, use must be made of experimental data in which the solubility of a gas has been determined as a function of temperature and pressure. Solubility data for ammonia and sulfur dioxide in water are presented in Appendix 8.

TABLE 8-2. HENRY'S LAW CONSTANTS FOR SEVERAL GASES SLIGHTLY SOLUBLE IN WATER

$H \times 10^{-4}$, atm/mole fraction

T, °C	Air	CO_2	CO	C_2H_6	H_2	H_2S	CH_4	NO	N_2	O_2
0	4.32	0.0728	3.52	1.26	5.79	0.0268	2.24	1.69	5.29	2.55
10	5.49	0.104	4.42	1.89	6.36	0.0367	2.97	2.18	6.68	3.27
20	6.64	0.142	5.36	2.63	6.83	0.0483	3.76	2.64	8.04	4.01
30	7.71	0.186	6.20	3.42	7.29	0.0609	4.49	3.10	9.24	4.75
40	8.70	0.233	6.96	4.23	7.51	0.0745	5.20	3.52	10.4	5.35
50	9.46	0.283	7.61	5.00	7.65	0.0884	5.77	3.90	11.3	5.88
60	10.1	0.341	8.21	5.65	7.65	0.103	6.26	4.18	12.0	6.29
70	10.5		8.45	6.23	7.61	0.119	6.66	4.38	12.5	6.63
80	10.7		8.45	6.61	7.55	0.135	6.82	4.48	12.6	6.87
90	10.8		8.46	6.87	7.51	0.144	6.92	4.52	12.6	6.99
100	10.7		8.46	6.92	7.45	0.148	7.01	4.54	12.6	7.01

From Appendix D-3, Foust, A. S., et al., *Principles of Unit Operations*, John Wiley and Sons, New York (1960).

EXAMPLE 8-1

What will be the saturation concentration of oxygen (in mg/l) in water in contact with dry air at 1 atm and 20 °C?

Solution

1. According to Dalton's law of partial pressures, the partial pressure exerted by a component of a mixture of gases is equal to the product of total pressure and the volume percentage of the component in the mixture. Since at sea level dry air contains about 21 percent oxygen

$$\bar{p} = 0.21 \text{ atm}$$

2. From Table 8-2, $H = 4.01 \times 10^4$. The mole fraction is computed to be (Equation 8-4)

$$x = \frac{\bar{p}}{H} = \frac{0.21}{4.01 \times 10^4} = 5.23 \times 10^{-6}$$

3. For 1 l of solution

$$n_{H_2O} \cong \frac{1000}{18} = 55.6 \text{ gm moles}$$

and

$$n_{O_2} = 5.23 \times 10^{-6} \times 55.6 = 2.91 \times 10^{-4} \text{ gm moles}$$

4. Weight of oxygen per liter of water $= 2.91 \times 10^{-4} \times 32 = 9.3$ mg.

8-5. Over-All Coefficients

Calculations of transfer rates based on Equation 8-3 are possible only if the interfacial partial pressure or concentration of the transferring molecules is known. In gas transfer operations this is seldom the case. Instead, equations based on determinate quantities are used. Based on concentrations in the liquid phase,

$$N_A = K_L A(c^*_A - c_A) \tag{8-5}$$

where K_L = over-all mass transfer coefficient, liquid-phase basis, ft/hr
c^*_A = equilibrium concentration corresponding to $\bar{p}_A$

A similar expression based on the partial pressures in the gas phase is

$$N_A = K_G A(\bar{p}_A - \bar{p}^*_A) \tag{8-6}$$

where K_G = over-all mass transfer coefficient, gas-phase basis, (lb mole)/(hr)(ft^2)(atm)
$\bar{p}^*_A$ = equilibrium partial pressure corresponding to c_A

The significance of the concentration and partial-pressure terms may be made more clear through a consideration of Figure 8-2. Presented therein is a curve relating the partial pressure of component A in the gas phase with the concentration of A in the liquid phase at equilibrium. It is to be noted that the curve is linear and, hence, the relationship conforms to Henry's law. The terms $\bar{p}^*_A$ and c^*_A do not exist in either phase, but simply are the equilibrium values for c_A and $\bar{p}_A$ respectively. Since equilibrium is assumed to exist at the interface, the coordinates $\bar{p}_{Ai}$ and c_{Ai} fall on the curve.

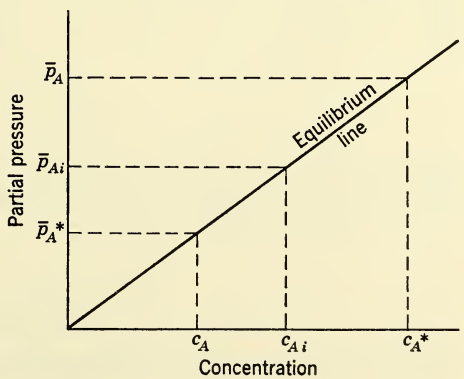

FIGURE 8-2. Equilibrium relationship conforming to Henry's law.

Equation 8-4 may be expressed in terms of molar concentration.

$$\bar{v}_i = \frac{H}{\rho_M} c_i \qquad \bar{p} = \frac{H}{\rho_M} c^* \qquad \bar{p}^* = \frac{H}{\rho_M} c \tag{8-7}$$

where ρ_M = molar density of the liquid phase.

Substitution of the first two of these terms in Equation 8-3 gives

$$N_A = \frac{k_G H}{\rho_M} A(c^*_A - c_{Ai}) \tag{8-8}$$

From Figure 8-2, it is seen that the total "driving force" between the two phases is

$$c^*_A - c_A = (c_{Ai} - c_A) + (c^*_A - c_{Ai}) \tag{8-9}$$

By substituting equivalent terms from Equations 8-3, 8-5, and 8-8 into Equation 8-9,

$$\frac{1}{K_L} = \frac{1}{k_L} + \frac{\rho_M}{H k_G} \tag{8-10}$$

Similar calculations show that

$$\frac{1}{K_G} = \frac{H}{\rho_M k_L} + \frac{1}{k_G} \tag{8-11}$$

The terms on the right side of the equality sign in each of Equations 8-10 and 8-11 are the resistances offered to transfer by the individual films, whereas the terms $1/K_L$ and $1/K_G$ are expressions of the over-all resistance. The relationships are analogous to those for series resistance in electric circuits.

When the values of the film coefficients are approximately equal, a large value for H (as would be the case for gases of low solubility) will make the last term in Equation 8-10 relatively small, and

$$\frac{1}{K_L} \cong \frac{1}{k_L} \tag{8-12}$$

indicating that the major resistance to transfer occurs in the liquid film. When H is small, i.e., the gas has a high solubility, and the film coefficients are approximately equal,

$$\frac{1}{K_G} \cong \frac{1}{k_G} \tag{8-13}$$

and the major resistance is encountered in the gas film.

The preceding expressions have been developed as representative of local or point conditions. The use of over-all coefficients in contacting equipment is strictly valid only if the equilibrium line is linear and the ratio k_L/k_G remains constant throughout the contacting device.

8-6. Equipment

A variety of equipment is used in gas absorption and desorption operations. A convenient classification of this equipment is as follows:

1. Gas dispersers.
   a. Small-orifice dispersers.
   b. Hydraulic shear dispersers.
   c. Mechanical shear dispersers.
2. Packed columns.
3. Tray columns.
4. Spray units.

Most devices employed at present in sanitary engineering operations fall into the first group. However, equipment in the other groups are continually finding wider application.

Gas Dispersers

Such equipment is used to inject gases in bubble form into a bulk of a liquid. The small-orifice dispersers include perforated pipes, porous tubes and plates, and nylon bags. As a rule, these devices are located near the bottom of a tank. When compressed gas is passed through the small-orifice dispersers, little bubbles form at the openings and grow until a size is reached where buoyancy exceeds the surface tension. At this point they break away from the disperser and rise through the liquid.

Hydraulic shear dispersers have as a characteristic feature the incipient shearing of a growing gas bubble by means of a liquid jet. Gas transfer is facilitated by the dispersal of smaller gas bubbles and increased agitation. One type of equipment, called an *impingement aerator*, consists of a relatively large orifice over which a nozzle is mounted. Compressed or blown air is released through the orifice. Liquid discharged through the nozzle under a relatively small head impinges on the orifice assembly, shearing off small gas bubbles.

The *jet aerator*, another hydraulic shear dispersing device, is essentially a venturi section with a high-velocity liquid jet mounted in a divided header. In operation, liquid from the tank is pumped at pressures from 25 to 30 psi through the jet and discharged through the venturi nozzle.

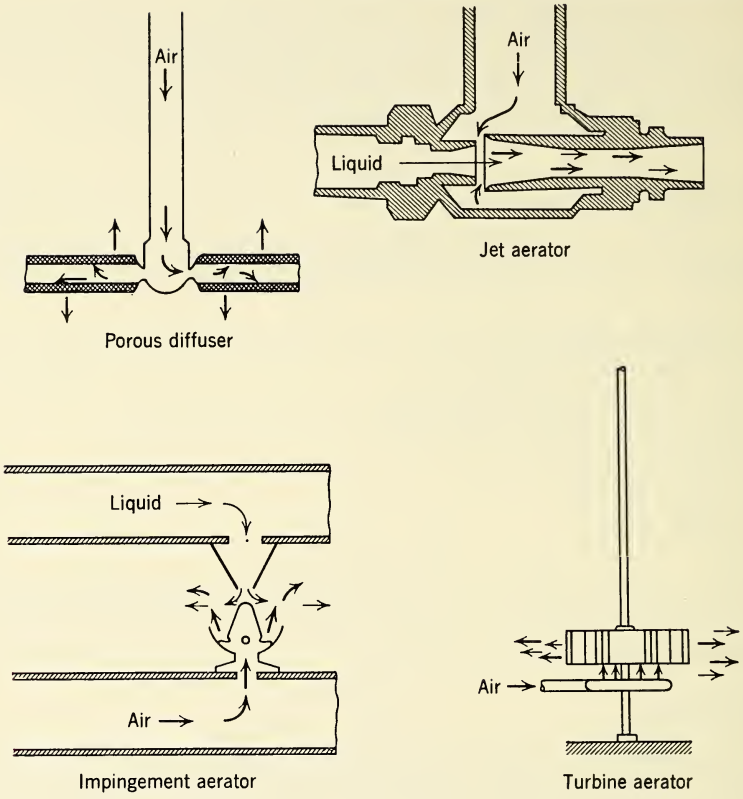

FIGURE 8-3. Schematic representation of gas dispersing devices. [From Figure 2-6, Eckenfelder, W. W., Jr., and D. J. O'Connor, *Bio-Oxidation of Organic Wastes, Theory and Design*, Civil Engineering Dept., Manhattan College, New York (1959), 56.]

Blown or aspirated air flowing in from the other compartment is entrained by the liquid jet.

The *turbine aerator*, a mechanical shear dispersing unit, consists of a turbine mixing impeller beneath which compressed air is supplied either by an open pipe or a sparger ring. Turbulence produced by the rotating impeller disperses the air into fine bubbles. Figure 8-3 is a schematic representation of several gas dispersing devices.

Packed Columns

Packed columns have had wide application as liquid-gas contacting equipment in the chemical processing industries, where they have been

employed not only as gas absorbers and desorbers but also as cooling towers. These columns consist of a vertical shell filled with packing material, dumped at random or stacked by hand. Packings sold commercially for absorption towers consist of units $\frac{3}{8}$ to 6 in. in major dimension commonly made of inert materials such as clay and porcelains. Recently, plastic and metal shapes have been employed. Occasionally, crushed rock or coke is used. Tower diameter will vary from several inches to 10 ft or more. Height will vary from a few feet to as much as 100 ft. The liquid phase is introduced at the top of the column and withdrawn from the bottom. Although the gas phase need not be in counterflow to the liquid, it is generally made to be so. Gas-liquid contact is promoted by the large surface area offered by the packing.

Tray Columns

Gas-liquid contacting equipment of this type consists of vertical towers fitted with horizontal plates or platforms spaced at even intervals throughout the height. Liquid introduced at the top cascades from one stage to another and eventually is withdrawn from the bottom of the tower. The gas phase either flows in a countercurrent direction or, in the case of open columns, in a cross-current direction to the dropping liquid.

Spray Units

Spray equipment promotes gas-liquid contacting by dispersing liquid in a gas phase. This can be performed with a variety of nozzle types spraying into either an open or enclosed system. Here, gas is the continuous phase and liquid the dispersed phase. In gas dispersion, gas is dispersed in a continuous liquid phase.

8-7. Gas Dispersers

In most gas dispersion operations, gas is transferred under conditions where the composition of both the liquid and gas phases undergoes only slight changes. Ordinarily, the gas phase is bubbled in a liquid at depths less than 15 ft. As the bubble rises through the liquid, the time of contact is relatively short, and transfer from each bubble is limited. Only the application of many bubbles makes dispersion a practical method of transfer.

In most types of gas transfer systems (or equipment), it is not possible to measure the interfacial area of contact. For this reason use is made of volumetric mass transfer coefficients which combine the interfacial area

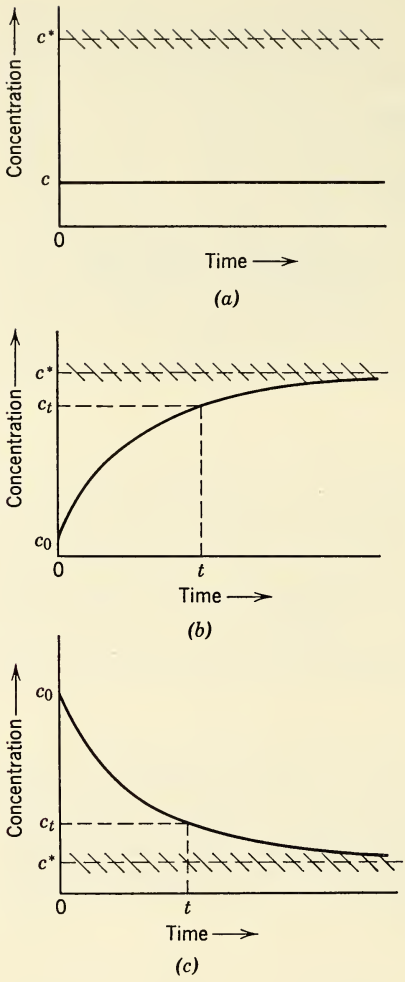

FIGURE 8-4. Gas concentration changes in a liquid as a function of time.

per unit volume of system (or equipment) with the mass transfer coefficient.

When the concentration of the solute gas in the liquid remains relatively constant during the operation (Figure 8-4*a*), transfer rates are estimated on the basis of steady-state conditions. For such conditions, Equations 8-5 and 8-6 can be written as

$$N = K_L a V(c^* - c) \tag{8-14}$$

and

$$N = K_G a V(\bar{p} - \bar{p}^*) \tag{8-15}$$

where K_La, K_Ga = over-all volumetric mass transfer coefficient, liquid- and gas-phase bases respectively, hr^{-1} and (lb mole)/(hr)(ft^3)(atm)
V = volume of system (or equipment), ft^3
N = rate at which solute gas is transferred between phases, lb mole/hr
c = concentration of solute gas in the liquid phase, lb mole/ft^3
$\bar{p}$ = partial pressure of solute gas in the gas phase, atm
c^* = equilibrium concentration corresponding to the partial pressure of the solute gas in the gas phase, lb mole/ft^3
$\bar{p}^*$ = equilibrium partial pressure corresponding to the concentration of the solute gas in the liquid phase, atm

For operations in which the solute gas concentration in the liquid changes with time (Figures 8-4*b* and *c*), a transfer rate expression can be derived by integrating the differential form of Equation 8-14 between the limits of time equal to 0 and t.

$$\frac{1}{V}\frac{dn}{dt} = \frac{dc}{dt} = K_La(c^* - c) \tag{8-16}$$

$$\int_{c_0}^{c_t} \frac{dc}{c^* - c} = K_La\int_0^t dt \tag{8-17}$$

$$\ln \frac{c^* - c_t}{c^* - c_0} = -K_La t \tag{8-18}$$

where c_0 and c_t = concentration of solute gas in liquid initially and at time t, lb mole/ft^3.

Similarly, Equation 8-6 can be integrated to give

$$\ln \frac{\bar{p}_t - \bar{p}^*}{\bar{p}_0 - \bar{p}^*} = K_GaRT_At \tag{8-19}$$

where $\bar{p}_0$ and $\bar{p}_t$ = partial pressure of solute gas in the gas phase initially and at time t, atm.

Figure 8-5*a* contains a plot of Equation 8-18 for the removal of carbon dioxide from falling drops of water supersaturated with respect to the gas. Plots for the absorption of oxygen from bubbles rising through water are shown in Figure 8-5*b*. The slopes of the curves in both Figures are equal to $-0.434K_La$.

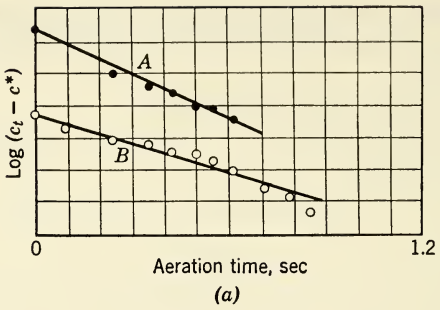

Key: A—200 drops/min at 20°C
B—300 drops/min at 16°C

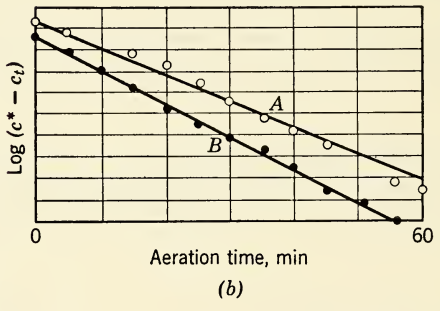

Key: A—air bubbles 1.29 mm in dia., temp. 20.6°C, 144-in. water column

B—air bubbles 1.38 mm in dia., temp. 23.8°C, 86-in. water column

FIGURE 8-5. Gas absorption and desorption in water. (*a*) Carbon dioxide removal (falling drops). (*b*) Oxygen absorption (bubbles). [From Figures 4 and 5, Haney, P.D. "Theoretical Principles of Aeration," *J. Am. Water Works Assoc.*, **46** (April 1954).]

As discussed in a previous section, spray units are used to disperse fine drops of liquid in a gas phase, an operation that is just the reverse of gas dispersion. Consequently, Equations 8-14, 8-15, 8-18, and 8-19 can be employed to evaluate the transfer characteristics of such units. The choice of equation will depend upon the specific nature of the system under consideration.

The over-all mass transfer coefficient is related to many variables. By analogy to heat transfer, the effect of a high relative velocity at an interface across which mass transfer is taking place should be proportional to the volumetric diffusivity, the Reynolds number, and the Schmidt number (the mass transfer counterpart of the Prandtl number),

$$K_L = \psi(D_v, N_{Re}, N_{Sc}) \tag{8-20}$$

For air bubbles rising through water, a relationship has been shown to exist among the Sherwood number (the mass transfer counterpart of the

Nusselt number for heat transfer), the Reynolds number, the Schmidt number, and the submergence depth of the disperser.[4]

$$N_{Sh}L^m = K'N_{Re}N_{Sc}^{1/2} \tag{8-21}$$

or

$$\left(\frac{K_L D_p}{D_v}\right) L^m = K' \left(\frac{D_p u_t \rho}{\mu}\right) \left(\frac{\mu}{\rho D_v}\right)^{1/2} \tag{8-22}$$

where K_L = over-all mass transfer coefficient, liquid-phase basis, ft/hr
D_p = diameter of air bubble, ft
D_v = volumetric diffusivity, ft^2/hr
L = submergence depth of disperser, ft
K' = constant
u_t = bubble velocity, ft/sec
ρ = mass density of liquid, lb mass/ft^3
μ = absolute viscosity, (lb mass)/(sec)(ft)
m = exponent

It can be shown that, when the depth of submergence is large (10 to 15 ft), surface aeration can be ignored. When such is the case

$$\frac{A}{V} \cong \frac{6qL}{D_p u_t V} \tag{8-23}$$

where A = total interfacial area in basin, ft^2
V = total volume of basin, ft^3
q = air flow rate, ft^3/sec

Therefore

$$K_L = K_L a \left(\frac{V}{A}\right) = K_L a \left(\frac{D_p u_t V}{6qL}\right) \tag{8-24}$$

By substituting Equation 8-24 for the coefficient term in Equation 8-22 and solving for the over-all volumetric mass transfer coefficient,

$$K_L a = \frac{K''qL^{1-m}}{D_p V(\mu/\rho D_v)^{1/2}} = \frac{K''qL^{1-m}}{D_p V N_{Sc}^{1/2}} \tag{8-25}$$

In the case of small-orifice dispersers, bubble size is a function of both orifice diameter and air flow rate. The size of bubble produced by hydraulic shear dispersers is dependent upon air flow rate and the flow rate of the recirculated liquid.

[4] Eckenfelder, W. W., Jr., "Absorption of Oxygen from Air Bubbles in Water," *Proc. Amer. Soc. Civil Engrs., J. San. Engr. Div.*, Paper 2090, **85** (July 1959).

At high air flow rates, bubble diameter is proportional to a function of the air flow rate,

$$D_p \propto q^n \tag{8-26}$$

Equations 8-25 and 8-26 combine to give an expression which can be used to characterize the performance of any small-orifice or hydraulic-shear dispersion device in a given gas-liquid system,

$$K_L aV = K''' q^{1-n} L^{1-m} \tag{8-27}$$

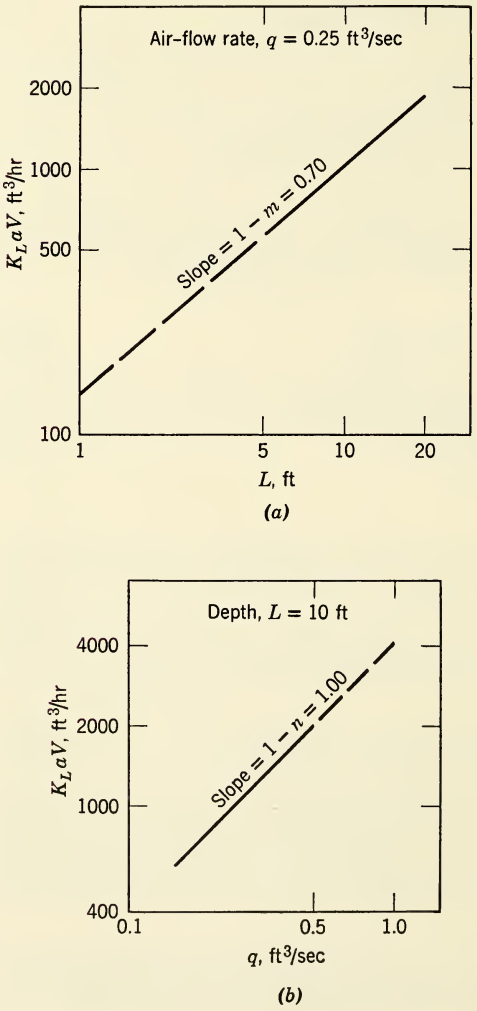

FIGURE 8-6. Oxygen transfer characteristics of a gas disperser.

The exponents $1 - n$ and $1 - m$ and the constant K''' can be evaluated with logarithmic plots similar to those presented in Figure 8-6.

For turbine aerators, the coefficient K_La can be varied either by the power input to the system (impeller speed) or by the air flow.

$$K_La \propto \overline{V}_S{}^r P^s \tag{8-28}$$

where $\overline{V}_S$ = superficial air flow velocity, based on basin cross section, ft/sec
P = power, (ft)(lb force)/(sec)
r and s = exponents

A plot of the coefficient as a function of horsepower and air flow rate is presented in Figure 3-9. For a more detailed discussion of aeration systems, the reader is referred elsewhere.[5]

EXAMPLE 8-2

The rate at which a dispersion aerator can transfer oxygen to 1000 ft^3 of sodium-sulfite-in-water solution (68 °F) is found to be 12.6 lb/hr. Assuming the equilibrium concentration of oxygen in the sulfite solution to be equal to that in pure water, compute the over-all, volumetric mass transfer coefficient on the liquid-phase basis (tank depth = 10 ft).

Solution

1. From Example 8-1 the solubility of oxygen at 20 °C and 1 atm is

$$c = 2.91 \times 10^{-4}(28.32)/454 = 18.15 \times 10^{-6} \text{ lb mole/ft}^3$$

2. The average hydrostatic pressure on the rising air bubble is assumed to be equal to the arithmetic mean of the pressure at the top and bottom of the tank.

$$p = \frac{14.7 + 19.0}{2 \times 14.7} = 1.14 \text{ atm}$$

3. The percentage of oxygen in the air bubbles will decrease as the bubbles rise through the liquid. Assuming 10 percent transfer of the oxygen, the average volume percentage will be 20 percent. Therefore,

$$c^* = 18.15 \times 10^{-6} \times 1.14 \times \tfrac{20}{21} = 19.70 \times 10^{-6} \text{ lb mole/ft}^3$$

4. As long as sodium sulfite is present in the water, the dissolved oxygen concentration c is equal to zero. From Equation 8-14,

$$K_La = \frac{N}{V(c^* - c)} = \frac{12.6/32}{1000(19.70 \times 10^{-6})} = 20 \text{ hr}^{-1}$$

[5] Eckenfelder, W. W., Jr., and D. J. O'Connor, *Bio-oxidation of Organic Wastes, Theory and Design*, Civil Engr. Dept., Manhattan College, New York (1959).

The effects of water-vapor pressure and salinity are insignificant at the conditions stated and, consequently, have been ignored.

EXAMPLE 8-3

A sodium-sulfite system is used to evaluate the oxygen transfer characteristics of a gas-dispersing device. When the air flow rate is held constant and the depth at which the disperser is submerged is varied, data are obtained which establish the correlation in Figure 8-6*a*. The curve in Figure 8-6*b* describes the effect of varying the air flow rate while the disperser is maintained at a constant depth. With this information, compute the values of the constant and the exponents in Equation 8-27.

Solution

1. The logarithmic transform of Equation 8-27 is

$$\log K_L aV = [\log K''' + (1 - n) \log q] + (1 - m) \log L$$

The slope of the curve in Figure 8-6*a* is $1 - m$ and is found to equal 0.70. The value of the expression enclosed in brackets is equal to the intercept at $L = 1$. This is found to be 140.

2. By rearranging the log transform,

$$\log K_L aV = [\log K''' + (1 - m) \log L] + (1 - n) \log q$$

The slope of the curve in Figure 8-6*b*, $1 - n$, is found to be equal to 1.00. The curve intersects $q = 1$ at 4000.

3. Solving for the constant K

$$\log K''' = \log 4000 - 0.70 \log 10$$

$$K''' = 800$$

8-8. Packed Columns

Gas transfer in packed absorption columns takes place between two streams flowing in opposite directions. As transfer proceeds, the composition of both phases are continually changing. Figure 8-7*a* shows the partial pressure of the solute in the entering gas stream to be $\bar{p}_1$. As the stream rises through the column, the partial pressure decreases as the solute is absorbed by the liquid. The partial pressure as the gas leaves the absorber is $\bar{p}_2$. The solute concentration in the liquid stream increases from c_2 at the top of the column to c_1 at the bottom where the liquid is drawn off. The curve in Figure 8-7*b* is the locus of points describing the solute partial pressure and concentration at corresponding elevations in the absorber. Such a curve is called an operating line.

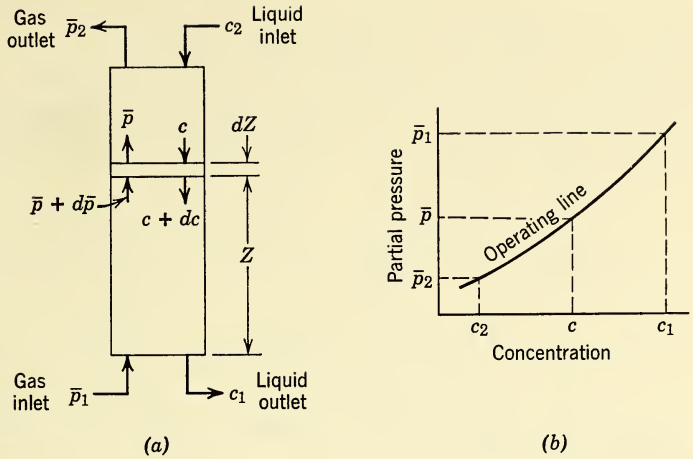

FIGURE 8-7. Schematic diagram of packed absorption column.

The equation of the operating line can be obtained by making a materials balance. The quantity of solute entering the section of the absorber below point A must be equal to that leaving the section.

$$G'_{GM}S\left(\frac{\bar{p}_1}{p - \bar{p}_1}\right) + G'_{LM}S\left(\frac{c}{\rho_M - c}\right) = G'_{GM}S\left(\frac{\bar{p}}{p - \bar{p}}\right) + G'_{LM}S\left(\frac{c_1}{\rho_M - c_1}\right) \quad (8\text{-}29)$$

where G'_{GM} = molar superficial mass velocity of the inert component of the gas phase, (lb mole)/(ft^2)(hr)
G'_{LM} = molar superficial mass velocity of the inert component of the liquid phase, (lb mole)/(ft^2)(hr)
S = cross-section area of empty column, ft^2
p = total pressure of gas phase, atm
$\bar{p}_1$ and $\bar{p}$ = partial pressures of the solute in the entering gas and at points throughout absorber respectively, atm
ρ_M = molar density of liquid phase, lb mole/ft^3
c_1 and c = concentration of solute in liquid discharge and at points throughout absorber respectively, lb mole/ft^3

Canceling and rearranging terms,

$$G'_{GM}\left(\frac{\bar{p}_1}{p - \bar{p}_1} - \frac{\bar{p}}{p - \bar{p}}\right) = G'_{LM}\left(\frac{c_1}{\rho_M - c_1} - \frac{c}{\rho_M - c}\right) \quad (8\text{-}30)$$

For a given set of terminal conditions, the operating line can be plotted from values of $\bar{p}$ computed for corresponding values of c.

Expressions for the required height of an absorption column can be derived from a consideration of the amount of absorption taking place in an incremental depth of packing. In Figure 8-7*a*, the number of moles absorbed in the depth dZ is

$$dN = G'_{LM}S\left[\frac{c + dc}{\rho_M - (c + dc)} - \frac{c}{\rho_M - c}\right] \cong G'_{LM}S\frac{dc}{\rho_M - c} \tag{8-31}$$

and

$$dN = G'_{GM}S\left[\frac{\bar{p} + d\bar{p}}{p - (\bar{p} + d\bar{p})} - \frac{\bar{p}}{p - \bar{p}}\right] \cong G'_{GM}S\frac{d\bar{p}}{p - \bar{p}} \tag{8-32}$$

The number of moles absorbed can also be expressed in terms of Equations 8-14 and 8-15.

$$dN = K_L a\, dV(c^* - c) \tag{8-33}$$

and

$$dN = K_G a\, dV(\bar{p} - \bar{p}^*) \tag{8-34}$$

Since

$$dV = S\, dZ \tag{8-35}$$

then, assuming that $K_L a$ and $K_G a$ remain constant, Equations 8-31 through 8-35 can be combined to give

$$Z = \frac{G'_{LM}}{K_L a}\int_{c_1}^{c_2}\frac{dc}{(c^* - c)(\rho_M - c)} \tag{8-36}$$

and

$$Z = \frac{G'_{GM}}{K_G a}\int_{\bar{p}_1}^{\bar{p}_2}\frac{d\bar{p}}{(\bar{p} - \bar{p}^*)(p - \bar{p})} \tag{8-37}$$

where Z = height of column, ft.

Equation 8-37 can be integrated graphically by determining the area under the curve established when $1/[(\bar{p} - \bar{p}^*)(p - \bar{p})]$ is plotted as a function of $\bar{p}$. A plot of the equilibrium and operating lines can be used to obtain corresponding values of $\bar{p}$ and $\bar{p}^*$. Equation 8-36 can be integrated in a similar fashion.

EXAMPLE 8-4

The SO_2 in a waste air stream is to be reduced from 6 percent by volume to 0.5 percent prior to discharge of the air to the atmosphere. The reduction is to be accomplished by scrubbing the air with SO_2-free water in a packed absorption tower under a pressure of 2 atm. The

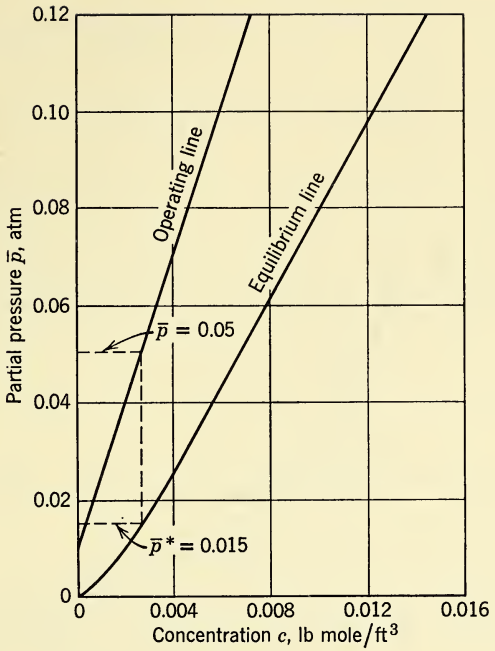

FIGURE 8-8. Equilibrium and operating lines for SO_2 in water at 20 °C and 2-atm pressure (for solution of Example 8-4).

TABLE 8-3. GRAPHICAL INTEGRATION OF EQUATION 8-37 FOR EXAMPLE 8-4

$\bar{p}$	$\bar{p}^*$	$\bar{p} - \bar{p}^*$	$p - \bar{p}$	$1/[(\bar{p} - \bar{p}^*)(p - \bar{p})]$	$\Delta\bar{p}$	Δ, Area
(1)	(2)	(3)	(4)	(5)	(6)	(7)
0.015	0.0015	0.0135	1.985	37.4	0.01	0.374
0.020	0.002	0.018	1.980	28.1		
0.025	0.004	0.021	1.975	24.1	0.01	0.241
0.030	0.006	0.024	1.970	20.7		
0.040	0.010	0.030	1.960	17.0	0.02	0.340
0.050	0.015	0.035	1.950	14.7		
0.060	0.020	0.040	1.940	12.9	0.02	0.258
0.080	0.030	0.050	1.920	10.4	0.02	0.208
0.100	0.040	0.060	1.900	8.8	0.02	0.176
0.120	0.053	0.067	1.880	7.9	0.01	0.079
					Total area =	1.676

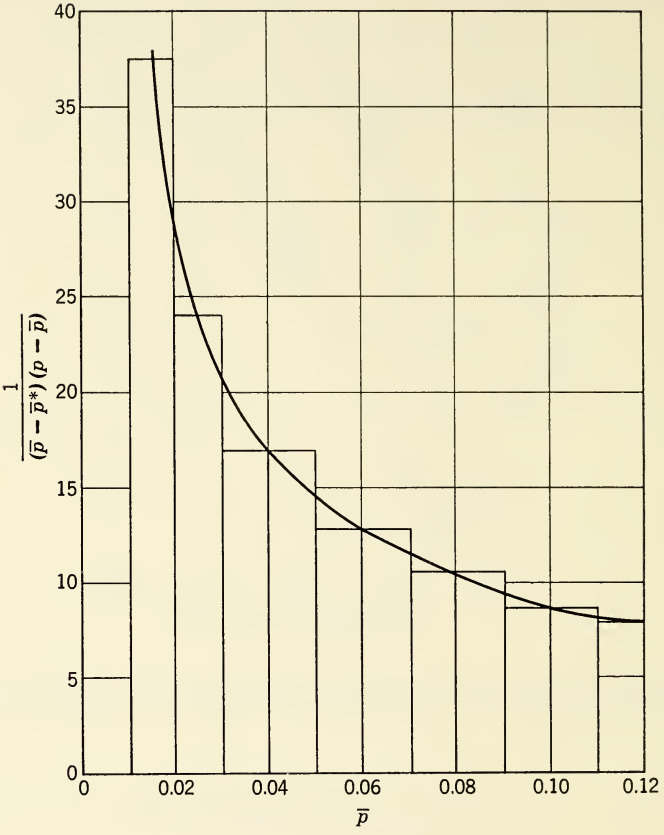

FIGURE 8-9. Graphical integration of Equation 8-37 for Example 8-4.

air flow rate on a SO_2-free basis is to be 100 lb/ft^2/hr. Water is to flow through the tower at a rate of 1800 lb/ft^2/hr and at a temperature of 20 °C. If the volumetric mass transfer coefficient K_Ga is estimated to be 0.8, how high must the tower be?

Solution

From data found in Appendix 8, an equilibrium line is constructed in Figure 8-8. Using Equation 8-30, an operating line is plotted in the same figure. These lines are used to compute the values in column 2 of Table 8-3. The values in columns 1 and 5 of Table 8-3 are plotted to give the curve shown in Figure 8-9. Graphical integration of this curve between the limits of $\bar{p}$ equal 0.01 and 0.12 atm (the partial pressure of

SO_2 in the exit and entering air streams respectively) yields a value of 1.676. From Equation 8-37

$$Z = \frac{3.45}{0.8}(1.676) = 7.25 \text{ ft}$$

8-9. Dilute Systems

For dilute systems, computations relative to the determination of the required height of an absorption column can be simplified.

When the partial pressures and concentrations are low,

$$p - \bar{p} \text{ and } p - \bar{p}_1 \cong p \tag{8-38}$$

and

$$\rho_M - c \text{ and } \rho_M - c_1 \cong \rho_M \tag{8-39}$$

In such cases, the equation for the operating line (Equation 8-30) becomes linear,

$$\frac{G'_{GM}}{p}(\bar{p}_1 - p) = \frac{G'_{LM}}{\rho_M}(c_1 - c) \tag{8-40}$$

and is readily plotted by drawing a straight line between two points.

Also, Equations 8-36 and 8-37 become

$$Z = \frac{G'_{LM}}{K_L a \rho_M} \int_{c_1}^{c_2} \frac{dc}{c^* - c} \tag{8-41}$$

and

$$Z = \frac{G'_{GM}}{K_G a p} \int_{\bar{p}_1}^{\bar{p}_2} \frac{d\bar{p}}{\bar{p} - \bar{p}^*} \tag{8-42}$$

When both the operating and equilibrium lines are straight, the integrals in Equations 8-41 and 8-42 can be evaluated from

$$\int_{c_1}^{c_2} \frac{dc}{c^* - c} = \frac{c_1 - c_2}{(c^* - c)_{\text{lm}}} \tag{8-43}$$

where

$$(c^* - c)_{\text{lm}} = \frac{(c^*_1 - c_1) - (c^*_2 - c_2)}{\ln [(c^*_1 - c_1)/(c^*_2 - c_2)]} \tag{8-44}$$

and

$$\int_{\bar{p}_1}^{\bar{p}_2} \frac{d\bar{p}}{\bar{p} - \bar{p}^*} = \frac{\bar{p}_1 - \bar{p}_2}{(\bar{p} - \bar{p}^*)_{\text{lm}}} \tag{8-45}$$

where

$$(\bar{p} - \bar{p}^*)_{\text{lm}} = \frac{(\bar{p}_1 - \bar{p}^*_1) - (\bar{p}_2 - \bar{p}^*_2)}{\ln [(\bar{p}_1 - \bar{p}^*_1)/(\bar{p}_2 - \bar{p}^*_2)]} \tag{8-46}$$

Justification for using the logarithmic mean differences, $(c^* - c)_{lm}$ and $(\bar{p} - \bar{p}^*)_{lm}$, is to be found through analogy with the logarithmic mean temperature difference discussed in Section 10-8.

EXAMPLE 8-5

How high must the absorption tower in Example 8-4 be if the equilibrium line is assumed to be straight?

Solution

1 From Equation 8-46

$$(\bar{p} - \bar{p}^*)_{lm} = \frac{(0.12 - 0.053) - (0.01 - 0)}{2.303 \log [(0.12 - 0.053)/(0.01 - 0)]} = 0.03$$

2. From Equation 8-45

$$\int_{\bar{p}_1}^{\bar{p}_2} \frac{d\bar{p}}{\bar{p} - \bar{p}^*} = \frac{0.12 - 0.01}{0.03} = 3.67$$

3. From Equation 8-42

$$Z = \frac{3.45}{0.8 \times 2} \times 3.67 = 7.90 \text{ ft}$$

8-10. Transfer Unit Method

The rate at which gas is transferred in a differential element of an absorption column can be written as

$$dN = S\, d(G_{LM}x) = G'_{LM}S\, d\frac{x}{1 - x} = G'_{LM}S\frac{dx}{(1 - x)^2} = G_{LM}S\frac{dx}{1 - x} \tag{8-47}$$

and

$$dN = S\, d(G_{GM}y) = G'_{GM}S\, d\frac{y}{1 - y} = G'_{GM}S\frac{dy}{(1 - y)^2} = G_{GM}S\frac{dy}{1 - y} \tag{8-48}$$

where G_{LM} = molar superficial mass velocity of liquid phase, (lb mole)/(ft^2)(hr)

G_{GM} = molar superficial mass velocity of gas phase, (lb mole)/(ft^2)(hr)

x = mole fraction of solute gas in liquid phase

y = mole fraction of solute gas in gas phase

Equations 8-33 and 8-34 can be expressed as follows:

$$dN = K_L a S \, dZ \rho_M (x^* - x) \tag{8-49}$$

and

$$dN = K_G a S \, dZ p (y - y^*) \tag{8-50}$$

where x^* = equilibrium mole fraction of solute gas in the liquid phase corresponding to the mole fraction y of the gas in a gas phase

y^* = equilibrium mole fraction of solute gas in the gas phase corresponding to the mole fraction x in a liquid phase

Equating these expressions and solving for dZ

$$dZ = \left(\frac{G_{LM}}{K_L a \rho_M}\right) \frac{dx}{(x^* - x)(1 - x)} \tag{8-51}$$

and

$$dZ = \left(\frac{G_{GM}}{K_G a p}\right) \frac{dy}{(y - y^*)(1 - y)} \tag{8-52}$$

Since the transfer coefficients vary directly with mass velocities, the terms in parentheses remain approximately constant. Therefore,

$$Z = \frac{G_{LM}}{K_L a \rho_M} \int_{x_1}^{x_2} \frac{dx}{(x^* - x)(1 - x)} \tag{8-53}$$

and

$$Z = \frac{G_{GM}}{K_G a p} \int_{y_1}^{y_2} \frac{dy}{(y - y^*)(1 - y)} \tag{8-54}$$

The terms in the above equations can be written

$$Z = H_{tOL} N_{tOL} \quad \text{and} \quad Z = H_{tOG} N_{tOG} \tag{8-55}$$

where

$$H_{tOL} = \frac{G_{LM}}{K_L a \rho_M}$$

$$H_{tOG} = \frac{G_{GM}}{K_G a p} \tag{8-56}$$

and

$$N_{tOL} = \int_{x_1}^{x_2} \frac{dx}{(x^* - x)(1 - x)}$$

$$N_{tOG} = \int_{y_1}^{y_2} \frac{dy}{(y - y^*)(1 - y)} \tag{8-57}$$

The magnitudes of N_{tOL} and N_{tOG} reflect the difficulty with which gas transfer takes place. Consequently, the terms conveniently provide expressions for the *number of transfer units* required to bring about a given transfer. The terms H_{tOL} and H_{tOG} are expressions for the *height of a transfer unit.* The subscripts *OL* and *OG* stand for "over-all, based on the liquid phase" and "over-all, based on the gas phase."

The rates of mass transfer in packed absorption columns are commonly reported in terms of H_{tOL} and H_{tOG}. Since the height of a transfer unit involves the ratio of flow rate to mass transfer coefficient, it is less sensitive to changes in flow rate than is the coefficient. Also, equipment efficiencies are expressed in dimensions of length, thus avoiding the multiplicity of units found in the transfer coefficient.

For low concentrations of solute gas, values of x and y are small. When such is the case

$$N_{tOL} \cong \int_{x_1}^{x_2} \frac{dx}{x^* - x}$$
$$N_{tOG} \cong \int_{y_1}^{y_2} \frac{dy}{y - y^*} \tag{8-58}$$

The relationships between the over-all height of transfer units and the phase contributions to the over-all height of transfer units can be expressed in equations similar to Equations 8-10 and 8-11.

$$H_{tOL} = H_{tL} + \frac{G_{LM}}{mG_{GM}} H_{tG} \tag{8-59}$$

and

$$H_{tOG} = H_{tG} + \frac{mG_{GM}}{G_{LM}} H_{tL} \tag{8-60}$$

where H_{tL}, H_{tG} = liquid and gas-phase height of a transfer unit respectively, ft
m = slope of equilibrium line, y^*/x or H/p

For slightly soluble gases (when Henry's law constant H is large),

$$H_{tOL} \cong H_{tL} \tag{8-61}$$

In estimating the over-all height of transfer unit for operations involving the transfer of such gases, the following empirical relationship can be used.[6]

[6] Sherwood, T. K., and F. A. L. Holloway, *Trans. Am. Inst. Chem. Engrs.*, **36** (1940), 39.

$$H_{tL} = \frac{1}{\alpha}\left(\frac{G_L}{\mu_L}\right)^n N_{ScL}{}^{0.5} = \frac{1}{\alpha}\left(\frac{G_L}{\mu_L}\right)^n \left(\frac{\mu_L}{\rho_L D_{vL}}\right)^{0.5} \tag{8-62}$$

where G_L = superficial mass velocity of liquid, (lb mass)/(hr)(ft^2)
μ_L = viscosity of liquid, (lb mass)/(ft)(hr)
ρ_L = density of liquid, lb mass/ft^3
D_{vL} = volumetric diffusivity of liquid, ft^2/hr
α, n = constants

This relationship applies for gas and liquid rates up to the loading point. Values of the constants α and n for several packing materials for liquid rates ranging from 400 to 15,000 (lb mass)/(hr)(ft^2) are presented in Table 8-4.

TABLE 8-4. VALUES OF α AND n FOR SEVERAL PACKING MATERIALS (FOR VALUES OF G_L FROM 400 TO 15,000) *

Packing	α	n
Raschig rings		
⅜ in.	550	0.46
1 in.	100	0.22
1½ in.	90	0.22
2 in.	80	0.22
Berl saddles		
½ in.	150	0.28
1 in.	170	0.28
1½ in.	160	0.28

* From Sherwood, T. K., and F. A. L. Holloway, *Trans. Am. Inst. Chem. Engrs.*, **36** (1940), 39.

When a highly soluble gas is absorbed by a liquid or when a rapid chemical reaction results between the liquid and the absorbed gas (e.g., removal of carbon dioxide with alkaline solutions), the gas phase should control the rate of transfer and

$$H_{tOG} \cong H_{tG} \tag{8-63}$$

It has been found, however, that for the majority of such cases the liquid-phase resistance remains significant and correlations for H_{tG} are not as well established as those for H_{tL}. From data obtained from the absorption of ammonia in water, the following relationship has been developed:

$$H_{tG} = \beta \frac{G_G{}^r}{G_L{}^s} N_{ScG}{}^{0.5} = \beta \frac{G_G{}^r}{G_L{}^s}\left(\frac{\mu_G}{\rho_G D_{vG}}\right)^{0.5} \tag{8-64}$$

where G_G = superficial mass velocity of gas phase, (lb mass)/(hr)(ft^2)
μ_G = viscosity of gas, (lb mass)/(ft)(hr)
ρ_G = density of gas, lb mass/ft^3
D_{vG} = volumetric diffusivity of gas, ft^2/hr
β, r, s = constants

The relationship is valid up to the loading point. Values of the constants β, r, and s, for various packings are presented in Table 8-5 along

TABLE 8-5. VALUES OF β, r, AND s FOR SEVERAL PACKING MATERIALS *

Packing	β	r	s	Range of G_G	Range of G_L
Raschig rings					
⅜ in.	2.32	0.45	0.47	200–500	500–1500
1 in.	6.41	0.32	0.51	200–600	500–4500
1½ in.	17.3	0.38	0.66	200–700	500–1500
2 in.	3.82	0.41	0.45	200–800	500–4500
Berl saddles					
½ in.	32.4	0.30	0.74	200–700	500–1500
1 in.	1.97	0.36	0.40	200–800	400–4500
1½ in.	5.05	0.32	0.45	200–1000	400–4500

* Based on data by Fellinger in: Perry, J. H., *Chemical Engineers Handbook* (3rd ed.), McGraw-Hill Book Co., New York (1950), 687–690.

with the ranges of gas and liquid flow rates for which the constants were derived.

For transfer operations in which resistances in both phases are significant, the over-all height of transfer units, H_{tOL} and H_{tOG}, can be calculated from Equations 8-59 and 8-60 using values of H_{tL} and H_{tG} computed from Equations 8-62 and 8-64. In the absence of data such as those presented in Tables 8-4 and 8-5, small pilot-plant towers can be used for the experimental determination of the over-all height of transfer units.

EXAMPLE 8-6

Hydrogen sulfide is to be removed from a waste air discharge by scrubbing it with a triethanolamine-water solution in a packed absorption tower at atmospheric pressure. At an air flow of 10 lb mole/hr/ft^2 and a solution flow rate of 40 lb mole/hr/ft^2, passage through a 10-ft-high pilot-plant tower will reduce the hydrogen sulfide in the air stream from 0.5 to 0.02 lb mole/hr/ft^2. At low concentrations, Henry's law can be applied to the hydrogen-sulfide-triethanolamine-water systems.

At the mean liquid temperature, the equilibrium relationship is found to be $y^* = 2x$.

Compute the over-all height of a transfer unit based on the gas phase.

Solution

1. Compute hydrogen sulfide absorbed.

$$0.5 - 0.02 = 0.48 \text{ lb mole/hr/ft}^2$$

2. Compute the mole fractions of hydrogen sulfide in the inflow and exit air streams.

Inflow $$y_1 = \frac{0.5}{10 + 0.5} = 0.0476$$

Exit $$y_2 = \frac{0.02}{10 + 0.02} = 0.002$$

3. Compute mole fraction of hydrogen sulfide in exit solution stream.

$$x_1 = \frac{0.48}{40 + 0.48} = 0.0118$$

4. Compute equilibrium value corresponding to x_1.

$$y^*_1 = 2 \times 0.0118 = 0.0236$$

5. Since the hydrogen sulfide systems are dilute and Henry's law can be applied, the logarithmic mean differences can be used in place of the integrals in Equation 8-58. Therefore,

$$(y - y^*)_{lm} = \frac{(y_1 - y^*_1) - (y_2 - y^*_2)}{\ln [(y_1 - y^*_1)/(y_2 - y^*_2)]}$$

$$= \frac{(0.0476 - 0.0236) - (0.002 - 0)}{2.303 \log [(0.0476 - 0.0236)/(0.002 - 0)]}$$

$$= 0.00815$$

and

$$N_{tOG} = \int_{y_1}^{y_2} \frac{dy}{y - y^*} = \frac{y_1 - y_2}{(y - y^*)_{lm}}$$

$$= \frac{0.0476 - 0.002}{0.00815} = 5.6$$

6. Since the height of the tower is 10 ft,

$$H_{tOG} = \frac{Z}{N_{tOG}} = \frac{10}{5.6} = 1.8 \text{ ft}$$

EXAMPLE 8-7

A gas mixture consisting of 5 percent ammonia and 95 percent air (by volume) is to be scrubbed with water to reduce the ammonia content to 1 percent. The gas mixture is to enter a packed tower (1-in. Raschig rings, packed at random) at a superficial mass velocity of 400 lb/hr/ft^2 and with a flow countercurrent to the water stream having an initial velocity of 500 lb/hr/ft^2. The average temperature of the gas mixture is assumed to be 25 °C and that of the water, 20 °C. Estimate the value of the over-all height of a transfer unit, based on the gas phase.

Solution

1. Compute the average superficial mass velocities through the tower.

Moles of air $\quad 17 \times \frac{5}{95} n_{\text{air}} + 29 n_{\text{air}} = 400$

$$n_{\text{air}} = 13.40$$

Moles of NH_3 $\quad 17 n_{NH_3} + 29 \times 19 n_{NH_3} = 400$

$$n_{NH_3} = 0.71$$

$$G_{GM} = 13.40 + \frac{0.71 + 0.14}{2} = 13.83 \text{ lb mole/hr/ft}^2$$

$$G_G = 13.40 \times 29 + 17 \frac{0.71 + 0.14}{2} = 396 \text{ lb mass/hr/ft}^2$$

$$G_{LM} = \frac{500}{18} + \frac{0.71 - 0.14}{2} = 28.1 \text{ lb mole/hr/ft}^2$$

$$G_L = 500 + 17 \frac{0.71 - 0.14}{2} = 504 \text{ lb mass/hr/ft}^2$$

2. Compute the gas-phase height of a transfer unit (Equation 8-64).

$$H_{tG} = 6.41 \frac{(396)^{0.32}}{(504)^{0.51}} (0.67)^{0.5} = 1.485 \text{ ft}$$

3. Compute the liquid-phase height of a transfer unit (Equation 8-62).

$$H_{tL} = 10^{-2} \left(\frac{504}{1 \times 6.72 \times 10^{-4}} \right)^{0.22} (570)^{0.5} = 4.67 \text{ ft}$$

4. Compute the over-all height of transfer unit, gas-phase basis.

From the solubility data listed in Appendix 8, the slope of the equilibrium relationship between the mole fraction of ammonia in the liquid phase

and that in the gas phase is approximately

$$m = \frac{y^*}{x} = 0.75$$

From Equation 8-60,

$$H_{tOG} = 1.48 + \frac{0.75 \times 13.83}{28.1}(4.67) = 3.2 \text{ ft}$$

8-11. Maximum Flow Rates in Packed Columns

There is for each liquid flow rate a rate of gas flow above which the liquid backs up and floods the column. This particular gas flow rate can be determined by examining the variation of pressure drop due to friction with the rate of gas flow.

Figure 8-10 shows a logarithmic plot, in which the pressure drop per unit depth of packing is correlated with the mass velocity of the gas. For dry packing, the relationship is a straight line with a slope of approximately 1.8. When the packing is irrigated with a liquid at a constant rate, the relationship is more complex. At low gas flow rates, the curve relating the two variables is a straight line. As the gas flow rate is increased, a point is reached (point *a* in the figure) where the linear relationship terminates. At this point, called the *loading point*, the liquid phase starts backing up through the column. With further

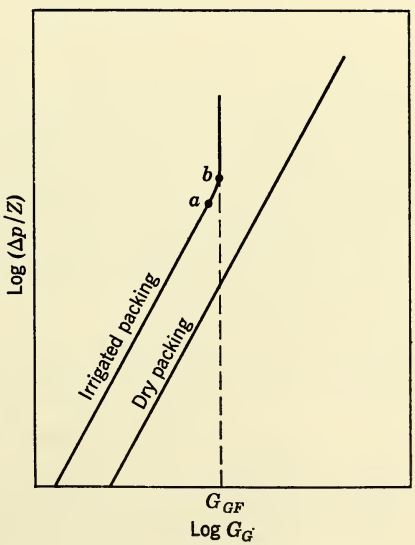

FIGURE 8-10. Frictional pressure drop through dry and irrigated packings.

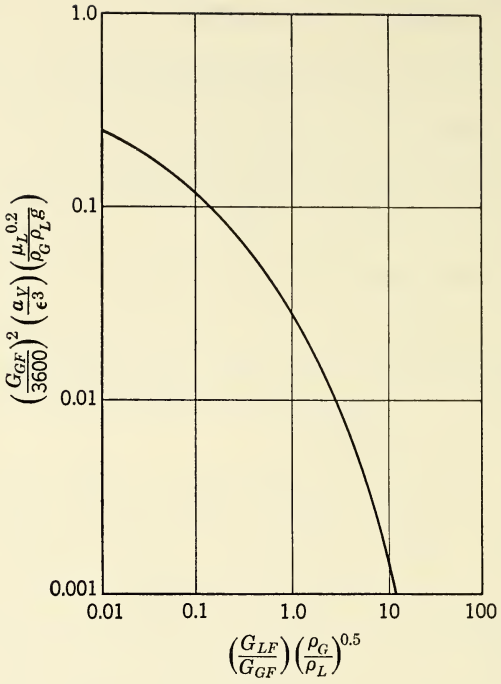

FIGURE 8-11. Correlation for flooding conditions in packed columns. [From Lobo, W. E., et al., *Trans. Am. Inst. Chem. Engrs.*, **41** (1945), 693.]

increase in gas flow rate, the flooding point is reached (point b in Figure 8-10) where the entire column is inundated. The gas flow rate at this point is called the *flooding velocity* and is represented in Figure 8-10 as G_{GF}. When the column is flooded, the liquid phase is continuous through the column, and the mechanism of gas-liquid contact is similar to that in gas dispersion. The most economical flow rate is usually at a value corresponding to about one-half of the flooding velocity.

The flooding velocity is a function of the liquid flow rate, the gas and liquid densities, the viscosity of the liquid, and the nature of the packing. These factors in dimensional groups are correlated in Figure 8-11. The notations of the terms within the groups are as follows:

G_{GF} = flooding superficial mass velocity of gas phase, (lb mass)/$(ft^2)(hr)$

G_{LF} = superficial mass velocity of liquid at G_{GF}, (lb mass)/$(ft^2)(hr)$

a_V = surface area of dry packing per unit packed volume, ft^2/ft^3

ϵ = porosity of packing
ρ_G = density of gas, lb force/ft^3
ρ_L = density of liquid, lb force/ft^3
μ'_L = viscosity of liquid, cp
g = acceleration of gravity, 32.2 ft/sec^2

Values of a_V and ϵ for different packings are found in Table 8-6.

TABLE 8-6. COMPARATIVE DATA ON STONE-WARE TOWER PACKINGS *

Packing	% Free Space ($\epsilon \times 100$)	Surface Area a_V, ft^2/ft^3	Weight, lb/ft^3	Number, units/ft^3
Berl saddles				
½ in.	68	141	45	15,000
1 in.	69	79	42	2,300
1½ in.	70	50	42	650
Raschig rings				
⅜ in.	53	148	65	26,000
½ in.	53	114	65	10,700
⅝ in.	54	80	64	5,800
¾ in.	67	72	46	3,000
1 in.	68	58	45	1,330
1¼ in.	73	44	38	670
1½ in.	68	36	45	380
2 in.	83	29	24	165

* Courtesy of Maurice A. Knight Co., Akron, Ohio.

EXAMPLE 8-8

A scrubbing operation (countercurrent flow) is to involve gas and liquid flow rates of 2000 and 7000 lb/hr respectively. The mass density of the gas is approximately 0.08 lb mass/ft^3, and the mass density and viscosity of the liquid is about 62.4 lb mass/ft^3 and 1 cp respectively. Determine the tower diameter required to prevent flooding if the packing is to consist of ¾-in. Raschig rings packed at random.

Solution

1. Compute

$$\frac{G_{LF}}{G_{GF}}\left(\frac{\rho_G}{\rho_L}\right)^{0.5} = \frac{7000}{2000}\left(\frac{0.08}{62.4}\right)^{0.5} = 0.125$$

2. From Figure 8-11, for an abscissa value of 0.125, the ordinate value is approximately 0.12.

3. Solving for the flooding velocity,

$$\left(\frac{G_{GF}}{3600}\right)^2 \left(\frac{a_V}{\epsilon^3}\right)\left(\frac{\mu_L{}^{0.2}}{\rho_G \rho_L g}\right) = 0.12$$

$$\left(\frac{G_{GF}}{3600}\right)^2 = 0.12\left(\frac{0.67^3}{72}\right)\left(\frac{0.08 \times 62.4 \times 32.2}{1^{0.2}}\right)$$

$$G_{GF} = 1020 \text{ (lb)/(hr)(ft}^2\text{)}$$

This value represents the maximum mass velocity possible without flooding the tower. In practice, to be on the safe side, this value is reduced by 50 percent.

4. Compute the required diameter.

$$S = \frac{2000}{1020/2} = 3.92 \text{ ft}^2$$

$$D = \left(\frac{4 \times 3.92}{\pi}\right)^{1/2} = 2.23 \text{ ft}$$

8-12. Tray Columns

When, in a gas transfer operation, a liquid cascades down a column of horizontal trays countercurrent to a rising gas stream, the two phases will approach at each tray an equilibrium condition with respect to the gas component being transferred. Consequently, the design of such columns is facilitated by the use of equilibrium stage calculations.

For purposes of computation, the tray column can be divided up into theoretical or equilibrium stages, the number of which can be estimated from the number of steps that can be constructed between the operating and equilibrium lines. The method is demonstrated in Figure 8-12. Presented here is a schematic diagram of a tray column consisting of n number of equilibrium stages. The column is employed in a gas transfer operation in which the operating and equilibrium lines in the lower figure apply. The liquid entering the first stage has a concentration of c_0, whereas the gas entering the same stage has a partial pressure of $\bar{p}_2$. The gas-liquid contact in the stage is assumed to be perfect to a point that equilibrium is established between the two phases. Upon leaving the first stage, therefore, the liquid has a concentration, c_1, that is in equilibrium with the partial pressure of the gas (with respect to the gaseous component being transferred) leaving the same stage, $\bar{p}_1$. The process is assumed to be repeated in each stage of the column. The

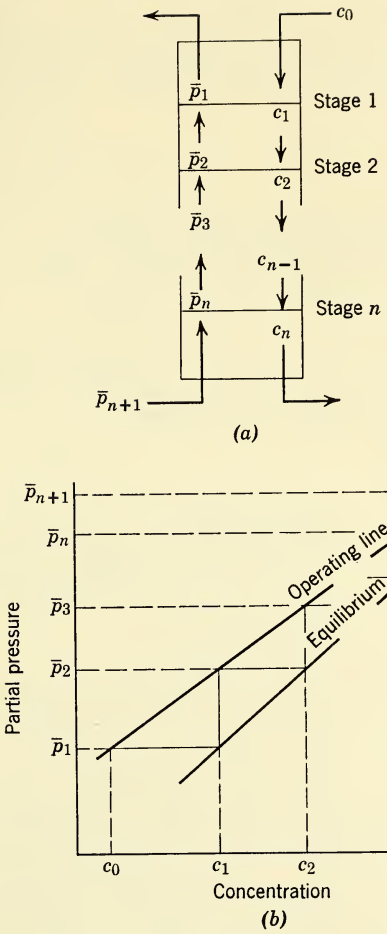

FIGURE 8-12. Schematic diagram of tray column.

equilibrium values fall along the equilibrium line at points indicated in the lower figure.

As explained in Section 8-8, points along the operating line describe the solute partial pressure and concentration at corresponding elevations in the tower. A careful consideration of Figure 8-12*b* will reveal that each step or triangle between the two lines represents an equilibrium process. The number of theoretical stages required for a particular transfer operation will be equal to the number of steps or triangles that can be constructed between the initial and terminal coordinates. When the final step does not coincide with those coordinates, it is a practice to count fractions of a stage.

Equilibrium conditions are never reached in practical operations. Hence, the number of trays that must be used is greater than the calculated number of theoretical stages. The two are related by

$$\eta_0 = \frac{N_s}{N'_s} \tag{8-65}$$

where η_0 = over-all column efficiency
N_s = theoretical number of stages
N'_s = actual number of stages

The over-all column efficiency is a function of the design details of the tray, of the flow rates of the liquid and gas, and of the chemical and physical properties of the phases.

Notations

a	Interfacial area per unit volume, ft^2/ft^3; a_V, surface area of dry packing per unit of packed volume
A	Area across which diffusion takes place, ft^2
c	Molar concentration, lb mole/ft^3; c^*, equilibrium concentration corresponding to $\bar{p}^*$
D_p	Bubble diameter, ft
D_v	Volumetric diffusivity, ft^2/hr
g	Acceleration of gravity, ft/sec^2
G_G	Mass velocity of gas phase, (lb mass)/(ft^2)(hr); G_{GF}, flooding mass velocity of gas phase
G_{GM}	Molal mass velocity of gas phase, (lb mole)/(ft^2)(hr); G'_{GM}, molal mass velocity of inert component of a gas phase
G_L	Mass velocity of liquid phase, (lb mass)/(ft^2)(hr); G_{LF}, mass velocity of liquid phase when G_G is equal to G_{GF}
G_{LM}	Molal mass velocity of liquid phase, (lb mole)/(ft^2)(hr); G'_{LM}, molal mass velocity of inert component of a liquid phase
H	Henry's law constant, atm
H_t	Height of transfer unit, ft; H_{tL} and H_{tG}, based on liquid and gas phases respectively; H_{tOL} and H_{tOG}, over-all, based on liquid and gas phases respectively
k_G	Mass transfer coefficient, gas phase, (lb mole)/(hr)(ft^2)(atm)
k_L	Mass transfer coefficient, liquid phase, ft/hr
K_G	Over-all, mass transfer coefficient, gas-phase basis, (lb mole)/(hr)(ft^2)(atm)
K_L	Over-all, mass transfer coefficient, liquid-phase basis, ft/hr
K_Ga	Over-all, volumetric mass transfer coefficient, gas-phase basis, (lb mole)/(hr)(ft^3)(atm)
K_La	Over-all, volumetric mass transfer coefficient, liquid-phase basis, hr^{-1}

K', K'', K''' Constants
L Submergence depth, ft
m Function of an exponent
m Slope of equilibrium line
n Function of an exponent
n Number of moles
N Molal rate of transfer, lb mole/hr
N_s Theoretical number of stages; N'_s, actual number of stages
N_t Number of transfer units; N_{tOL} and N_{tOG}, over-all, based on a liquid and a gas phase respectively
N_{Re} Reynolds number, dimensionless
N_{Sc} Schmidt number, dimensionless
N_{Sh} Sherwood number, dimensionless
p Total pressure, atm; $\bar{p}$, partial pressure; $\bar{p}^*$, equilibrium partial pressure corresponding to c
P Power, (ft)(lb force)/(sec)
q Gas flow rate, ft^3/sec
r Exponent
R Gas constant, 0.729 (ft^3)(atm)/(lb mole)(°R)
s Distance between two points, ft
s Exponent
S Cross-section area, ft^2
t Time, hr
T_A Absolute temperature, °R
u_t Rise velocity of bubble, ft/sec
V Volume, ft^3
$\overline{V}_S$ Superficial gas velocity, ft/sec
x Mole fraction of solute gas in liquid phase; x^*, equilibrium mole fraction of solute gas in the liquid phase corresponding to the mole fraction y of the gas in a gas phase
y Mole fraction of solute gas in gas phase; y^*, equilibrium mole fraction of solute gas in the gas phase corresponding to the mole fraction x in a liquid phase
Z Height, ft
ϵ Porosity
η_0 Over-all column efficiency
μ Absolute viscosity, (lb mass)/(sec)(ft); μ'_L, absolute viscosity of liquid, cp
ρ Mass density, lb mass/ft^3; ρ_G and ρ_L, mass density of gas and liquid respectively; ρ_M, molal mass density
ψ Operator

9

Adsorption and leaching

ADSORPTION

9-1. Definition and Types

Those operations in which a solute material is transferred from a fluid to the surface of a solid (adsorbent) upon contact with the latter, are called adsorption operations. Such operations include dehumidification of air with desiccants, removal of obnoxious components of air and water systems with activated carbon, and the exchange of ions between water solutions and ion exchange materials. Adsorption is a surface phenomenon, and good adsorbents must have both a high surface-to-volume ratio and an "active" or an "activated" surface, i.e., a surface relatively free of adsorbed materials. Many adsorbents are highly porous and filled with fine capillaries.

Three types of adsorption are recognized—physical adsorption, chemisorption, and ion exchange. Chemisorption, which takes place as a result of chemical bonds being formed between the molecules of the solute and the adsorbing solid, is highly exothermic and usually irreversible. Operations involving chemisorption have little application in sanitary engineering and, hence, will not be considered here. Physical adsorption is the result of intermolecular forces of attraction, called van der

Waal forces, whereas ion exchange results from electrostatic attraction. Both physical adsorption and ion exchange are only weakly exothermal and are generally reversible. Because so many adsorption processes are reversible, regeneration of the adsorbent plays a key role in most adsorption operations. Regeneration can be performed in a number of different ways depending upon the nature of the adsorption system concerned. Although adsorption can be carried out either in a dispersed contact operation or in a fixed bed, most sanitary engineering applications involve the fixed-bed operation.

9-2. Fixed-Bed Adsorption

Adsorption in a fixed bed involves passing the fluid phase through a stationary bed of the solid adsorbent. Periodically, the adsorbent becomes "spent" and must be regenerated or replaced. The adsorption capacity of a fixed bed is estimated from an adsorption wave such as is presented in Figure 9-1.

The curve in Figure 9-1 relates the concentration of solute in the effluent with the effluent volume. Initially, as the fluid contacts successive portions of fresh adsorbent, the solute content of the effluent is reduced almost to zero. As adsorption proceeds, the zone in which adsorption takes place moves toward the effluent end of the bed. When the adsorption zone reaches the effluent end, breakthrough occurs, and the solute concentration in the effluent increases rapidly to a value equal to that in the influent. At this point the bed is exhausted. The adsorption capacity is usually established at the point of breakthrough.

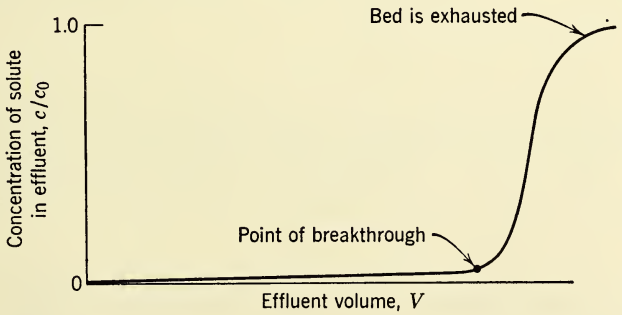

FIGURE 9-1. Adsorption wave.

LEACHING

9-3. Definition and Types

Leaching is the reverse of adsorption. The term applies to those operations in which a soluble material is transferred from a solid to a liquid. Leaching is called either solid-liquid extraction, elutriation, or washing. The elutriation of digested sludge solids to remove excessive concentrations of ions prior to chemical conditioning provides a typical example of a sanitary engineering application.

Leaching can be carried out either in fixed-bed or dispersed-contact operations. Discussion here will be confined to the latter.

9-4. Dispersed-Contact Operation

Dispersed-contact operations are carried out in stages. Each stage consists of two steps: (1) mixing the solid with the liquid to promote the transfer of solute, and (2) a partial separation of the solution from the solids. When the solute concentration in the separated liquid is the same as in the solution remaining with the solids, the stage is said to be *ideal*. *Stage efficiencies* are used to obtain the relationship between ideal and actual stages.

Mixing and separation may be carried out separately in different tanks, or they may both be carried out in the same tank. Mixing is designed to promote as intimate a contact as is possible with the expenditure of a minimum amount of power. Principles discussed in Chapter 3 are applicable to the mixing operation. In most sanitary engineering applications, the separation step is accomplished in thickeners, the design of which was discussed in Chapter 4.

Various arrangements are employed in dispersed-contact operations. Diagrams illustrating three such arrangements are shown in Figure 9-2. The simplest operation provides a single contact between the solids and liquids. This method of operation may be either batch or continuous. Assuming that equilibrium is reached, i.e., the stage is ideal, the amount of solute removed is a function only of the amount of solvent that is used.

In multistage cocurrent contact, the solid phase is brought into contact with fresh solvent in a series of two or more stages. Solute removal depends not only on the amount of solvent used but also on the number of stages in which the operation is carried out. Operation may be intermittent in the same unit or continuous in a series of units.

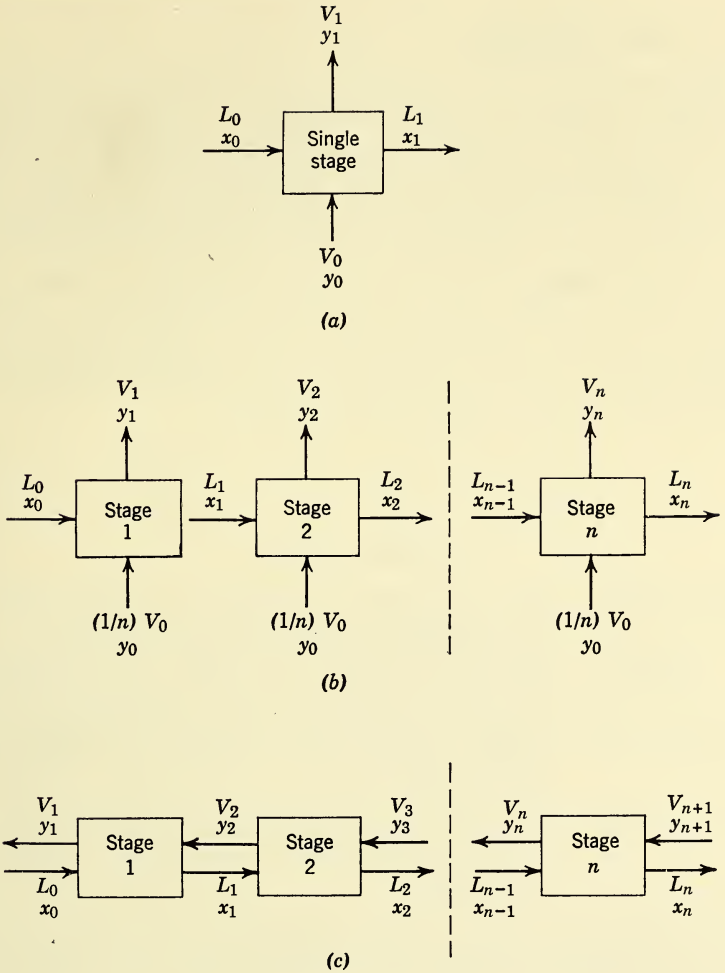

FIGURE 9-2. Flow diagrams illustrating various arrangements employed in dispersed-contact leaching operations. (*a*) Single contact. (*b*) Multistage cocurrent contact. (*c*) Multistage countercurrent contact.

In multistage countercurrent operation, the solid and solvent phases are introduced at opposite ends of a series of contact stages. Flow through the series is countercurrent, and a phase is discharged from the system at the stage where the other phase is introduced. For a given amount of solvent and a fixed number of stages, the countercurrent operation is more effective than the cocurrent operation.

9-5. Leaching Calculations

Materials balances and the concept of an equilibrium or ideal stage are used as a basis for leaching calculations. In making the computations, the solid-liquid system being extracted is considered as consisting only of three components: the solute, the solvent, and the inert solids. It is assumed that the solute is not adsorbed by the solids and is removed by a solution process rather than by a chemical reaction with the solvent. Also, the assumption is made that all the solids entering a stage will be found in the underflow stream discharged from that stage. Materials balances can be made either algebraically or by using graphical procedures.

The algebraic expressions applicable to the materials balances across a single contact extraction system are as follows:

$$L_0(x_A)_0 + V_0(y_A)_0 = L_1(x_A)_1 + V_1(y_A)_1 \tag{9-1}$$

$$L_0(x_C)_0 + V_0(y_C)_0 = L_1(x_C)_1 + V_1(y_C)_1 \tag{9-2}$$

$$L_0(x_B)_0 = L_1(x_B)_1 \tag{9-3}$$

where L_0 and L_1 = flow rates of phase containing inert solids, incoming and underflow streams respectively, lb/hr

V_0 and V_1 = flow rates of phase containing no inert solids, incoming and overflow streams respectively, lb/hr

x_A, x_B, and x_C = respectively, the weight fractions of the solute, inert solids, and the solvent in the phase containing the inert solids

y_A, y_B, and y_C = respectively, the weight fractions of the solute, inert solids, and the solvent in the phase containing no inert solids

For a multistage cocurrent contact operation, the equations for each component of the solid-liquid system (solute, solids, and solvent) can be written as

$$L_0x_0 + \left(\frac{1}{n}\right) V_0y_0 = L_1x_1 + V_1y_1 \tag{9-4}$$

$$L_1x_1 + \left(\frac{1}{n}\right) V_0y_0 = L_2x_2 + V_2y_2 \tag{9-5}$$

$$\vdots$$

$$L_{n-1}x_{n-1} + \left(\frac{1}{n}\right) V_0y_0 = L_nx_n + V_ny_n \tag{9-6}$$

where n = number of stages.

The subscripts refer to a stage number. An equation can be written for each stage in the system. These expressions apply when the solvent is added to the stages in equal increments. Their solution depends upon a prior decision as to the number of stages to be employed and a knowledge of the quantity of solvent, or solution, retained per unit quantity of inert solids in the underflow from each stage.

Equations for the materials balances for each component across a multistage countercurrent system are as follows:

$$L_0x_0 + V_{n+1}y_{n+1} = V_1y_1 + L_nx_n \tag{9-7}$$

$$L_0x_0 + V_2y_2 = L_1x_1 + V_1y_1 \tag{9-8}$$

$$L_1x_1 + V_3y_3 = L_2x_2 + V_2y_2 \tag{9-9}$$

$$\vdots$$

$$L_{n-1}x_{n-1} + V_{n+1}y_{n+1} = L_nx_n + V_ny_n \tag{9-10}$$

As indicated by the subscripts, Equation 9-7 is a balance across the entire system, and can be used for determining initial and terminal quantities. Equations 9-8, 9-9, and 9-10 apply to individual stages. Similar expressions can be written for the other stages in the system. Here again, the solution of the equations depends upon a knowledge of the ratio of the quantity of solution, or solvent, to that of the inert solids in the underflow from each stage.

The number of ideal stages required for a multistage countercurrent leaching system is determined in the following manner. An over-all materials balance is made first to establish the quantities of each component of the initial and terminal streams. The same quantities are then computed for the streams entering and leaving a stage at either end of the system. The computations are repeated for successive stages until a stage is reached from which the underflow has the desired composition. Calculations are facilitated by expressing quantities in terms of a relationship with the quantity of inert solids present in the underflow stream.

EXAMPLE 9-1

A countercurrent extraction battery is to be used to leach a soluble, radioactive salt from a waste sludge containing 13 percent inert solids, 2 percent salt, and 85 percent water. Water, initially free of the soluble salt, is to be used as a solvent in quantities equal to twice the weight of the sludge. Before the sludge can be disposed of, at least 99 percent of the salt must be removed.

Preliminary studies indicate that the underflow from the stages will contain about 6 lb solution (water plus salt)/lb inert solids.

Compute the number of ideal stages required for the leaching operation.

Solution

1. Over-all materials balance to establish terminal quantities (basis: lb/lb inert solids/hr).

Materials in			
L_0	Solids	1.0000	
	Water = $^{85}/_{13}$ =	6.5400	
	Salt = $^{2}/_{13}$ =	0.1540	
			7.6940
V_{n+1}	Water = 2 × 7.6940 =		15.3880
			23.0820
Materials out			
L_n	Solids	1.0000	
	Water = 6.0000 − 0.0015 =	5.9985	
	Salt = 0.154 × 0.01 =	0.0015	
			7.0000
V_1	Water (by difference)	15.9295	
	Salt (by difference)	0.1525	
			16.0820
			23.0820

2. Materials balance across stage 1.

Materials in			
L_0	Solids	1.0000	
	Water	6.5400	
	Salt	0.1540	
			7.6940
V_2	Water (by difference)	15.3325	
	Salt (by difference)	0.0555	
			15.3880
			23.0820

Materials out

L_1	Solids		1.0000	
	Water	$= 6.0000 - 0.0570 =$	5.9430	
	Salt	$= 6.000 \dfrac{0.1525}{16.0820} =$	0.0570	
				7.0000
V_1	Water		15.9295	
	Salt		0.1525	
				16.0820
				23.0820

3. Continue computation for successive stages until the quantity of salt in the underflow is less than 1 percent of 0.1540 lb/lb or 0.0015 lb/lb of solids. It will be noted from Table 9-1 that the quantity of salt

TABLE 9-1. SUMMARY OF QUANTITIES COMPUTED IN THE SOLUTION OF EXAMPLE 9-1

Ideal Stage Number	Materials In (lb/lb inert solids/hr)					Materials Out (lb/lb inert solids/hr)				
	Lx_A (Salt)	Lx_B (Solids)	Lx_C (Water)	Vy_A (Salt)	Vy_C (Water)	Lx_A (Salt)	Lx_B (Solids)	Lx_C (Water)	Vy_A (Salt)	Vy_C (Water)
1	0.1540	1.0000	6.5400	0.0555	15.3325	0.0570	1.0000	5.9430	0.1525	15.9295
2	0.0570	1.0000	5.9430	0.0201	15.3679	0.0216	1.0000	5.9784	0.0555	15.3325
3	0.0216	1.0000	5.9784	0.0064	15.3816	0.0079	1.0000	5.9921	0.0201	15.3679
4	0.0079	1.0000	5.9921	0.0010	15.3870	0.0025	1.0000	5.9975	0.0064	15.3816
5	0.0025	1.0000	5.9975	−(0.0011)	15.3891	0.0004	1.0000	5.9996	0.0010	15.387_0

in the underflow from stage number 5 is less than this value; hence the number of ideal stages required is 5.

9-6. Graphical Solution

The determination of the number of ideal stages in a multistage countercurrent leaching system is often facilitated by the use of the graphical method. The graphical method requires the construction of a triangular diagram, such as is shown in Figure 9-3*a*. Points on the diagram represent the composition of a three-component system. The abscissa is in terms of the weight fraction of the solute (component A), whereas the ordinate is in terms of the weight fraction of the solvent (component C). Since the total of all the weight fractions in a three-component system equals one, any set of coordinates identifies also the

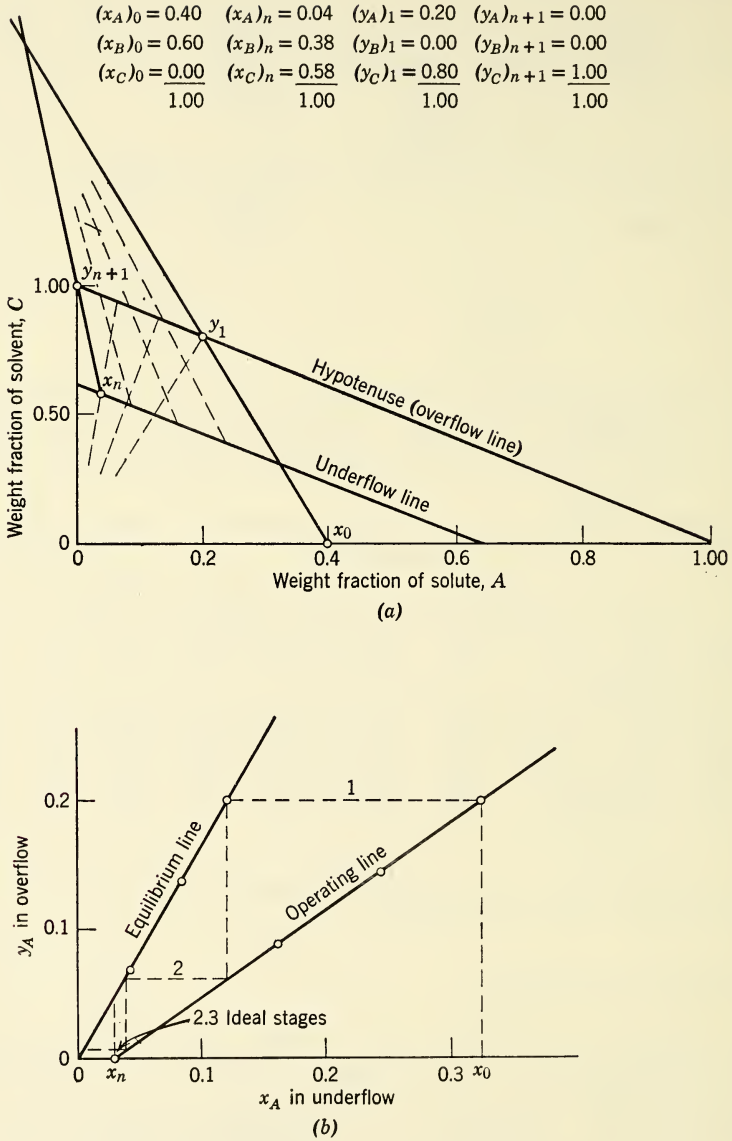

FIGURE 9-3. Graphical solution for determining number of ideal stages in a solid-liquid leaching operation. (*a*) Triangular diagram. (*b*) Operating and equilibrium lines. [Adapted from Osburn, J. O., "Find Number of Theoretical Stages," *Chem. Engr.*, **65** (July 14, 1958).]

weight fraction of the inert solids (component B). The overflow streams are considered to contain no inert solids; thus points identifying the composition of such streams are located along the hypotenuse of the triangle. If the ratio of the quantity of solution to the quantity of inert solids is the same in each underflow stream, the points identifying the composition of the underflow streams will fall along a line parallel to the hypotenuse. This line passes through the coordinates identifying the composition of the terminal underflow stream, x_n.

The underflow from a stage is a mixture of inert solids represented by the coordinates at the origin and the overflow from the stage. Therefore, equilibrium compositions are defined by straight lines passing through the origin. Intersections of the lines with the underflow line and the hypotenuse furnish coordinates with which points describing the equilibrium line in Figure 9-3*b* can be plotted.

The operating line is constructed in the following way. First, straight lines drawn through points identifying the composition of the initial and terminal streams (x_0, x_n, y_1, and y_{n+1}) are extended until they intersect. A set of lines are then drawn through the point of intersection. Intersections of the latter with the hypotenuse and underflow line provide the coordinates of points through which the operating line can be constructed.

The number of ideal stages can be determined by stepping off the stages between the equilibrium and operation lines, a procedure discussed in Chapter 8. Starting at point x_0 on the operating line, the steps are continued until the abcissa x_n is reached. In the solution presented in Figure 9-3*b*, approximately 2.3 ideal stages are required.

Notations

L_0, L_1	Flow rates of phase containing inert solids, incoming and underflow streams respectively, lb/hr
n	Number of stages
V_0, V_1	Flow rates of phase containing no inert solids, incoming and overflow streams respectively, lb/hr
x_A, x_B, x_C	Weight fractions of solute, inert solids and the solvent, respectively, in the phase containing the inert solids
y_A, y_B, y_C	Weight fractions of solute, inert solids and the solvent, respectively, in the phase containing no inert solids

10

Heat transfer

10-1. Applications

Heat transfer operations are becoming increasingly important in waste treatment. Applications include the heating of anaerobic biological processes, the evaporation of liquids, the drying of solids, and the cooling of industrial waste waters. The transfer of large quantities of heat generated by high-level radioactive wastes pose problems of a more difficult nature.

The transfer of heat may take place by conduction, convection, and radiation, either singularly or in combination with each other. This chapter discusses all three types as well as the principles of making a heat balance.

10-2. Heat Balances

A heat balance is a mathematical expression of the law of conservation of energy which states that the total amount of energy entering a system must equal that leaving plus any accumulated within the system. Heat balances along with materials balances are widely used in the determination of unknown heat quantities. Two types of heat are of importance in computing heat balances: sensible heat and latent heat.

Sensible heat is defined as that heat which when gained or lost by a body is reflected by a change in the temperature of the body. Heat of this nature is computed by multiplying the heat

capacity or specific heat of the material by its temperature above some datum.

$$Q_s = c_p W T_0 \tag{10-1}$$

where Q_s = sensible heat, Btu
c_p = specific heat at constant pressure, (Btu)/(lb)(°F)
W = weight of material, lb
T_0 = temperature of material above a datum, °F

Heat capacity is defined as the amount of heat required to raise the temperature of 1 lb of the material by 1 °F. The specific heat is the ratio of the heat capacity of the material to that of an equal weight of water at 15 °F. For ordinary calculations, the two terms are used interchangeably. Both vary with temperature. The specific heats of several common gases are listed in Appendix 9.

Latent heat is that heat required to bring about a change in state, no temperature change being involved. As most changes in state dealt with in heat balances involve a transition between a liquid and a gas, concern commonly centers around the latent heat of vaporization. Latent heat quantities may be computed from

$$Q_l = \lambda W \tag{10-2}$$

where Q_l = latent heat, Btu
λ = unit latent heat, Btu/lb
W = weight of material changing state, lb

Like heat capacity and specific heat, latent heat is a function of the temperature.

In striking a heat balance, it is necessary to consider the heat content of each component of the system. Since it is impossible to evaluate the total heat content of a material, a convenient temperature datum is selected, and the total heat is computed as the sum of the sensible and latent heat quantities above that datum. When heat is absorbed or lost from a system under constant pressure, the heat gain or loss is numerically equal to the change in enthalpy. Enthalpy data for water systems can be found in the steam tables presented in Appendixes 10 and 11. These are referenced to a datum of liquid water at 32 °F. Included also are the specific volumes of both water and steam.

EXAMPLE 10-1

Water at a rate of 1000 gal/hr is to be heated from 70 °F to 160 °F by condensing steam in a shell-and-tube heat exchanger. If saturated steam is available at 15 psig, how much per hour will be required?

Solution

Let w = rate of steam condensation.

Heat in

Enthalpy of water at 70 °F = $38.04(1000 \times 8.34)$ = 317,000
Enthalpy of saturated steam at 15 psig (250 °F) = $1164w$

Total = $317{,}000 + 1164w$ Btu/hr

Heat out

Enthalpy of water at 160 °F = $127.9(1000 \times 8.34)$ = 1,065,000
Enthalpy of condensate at 250 °F = $218.5w$

Total = $1{,}065{,}000 + 218.5w$ Btu/hr

$$317{,}000 + 1164w = 1{,}065{,}000 + 218.5w$$

$$w = 792 \text{ lb/hr}$$

10-3. Conduction

The transfer of heat by conduction involves the transmission of energy through molecular bombardment, the molecules retaining their relative position and transferring only their momentum. The flow of heat from one end of a metal bar to the other provides an example of conductive heat transfer.

The basic relationship pertaining to the flow of heat through a thermal barrier by conduction is given by Fourier's law,

$$\frac{dQ}{dt} = -kA\frac{dT}{dx} \tag{10-3}$$

where dQ/dt = instantaneous rate of heat transfer in a direction perpendicular to the surfaces of the barrier (in the x-direction), Btu/hr
k = thermal conductivity, (Btu)(ft)/(hr)(ft^2)(°F)
A = cross-section area through which the heat is transferred (area at right angles to the x-direction), ft^2
dT/dx = temperature gradient across barrier (in the x-direction), °F/ft

A definition sketch for this expression is presented in Figure 10-1.

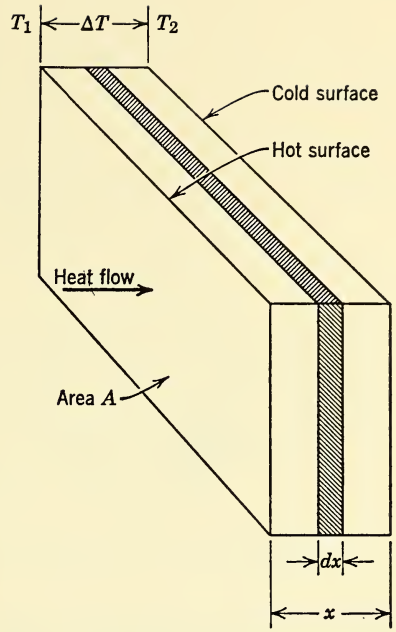

FIGURE 10-1. Definition sketch for Fourier's law.

If the temperature gradient dT/dx does not vary with time, the rate of heat transfer through the barrier remains constant, and

$$\frac{dQ}{dt} = q_h = -kA\frac{dT}{dx} \tag{10-4}$$

which upon integration becomes

$$q_h = \frac{kA}{x}(T_1 - T_2) = \frac{kA}{x}\Delta T \tag{10-5}$$

where q_h = flow of heat per unit time, Btu/hr
ΔT = temperature drop across barrier, °F

The thermal conductivity is a property of the material out of which the barrier is composed, and is found to be a function of its temperature. Values of the thermal conductivity for different materials are listed in Appendix 12. In general, the variation of conductivity is linear with temperature, hence, an arithmetic average of the conductivities at both sides of the barrier can be used in Equation 10-5.

Often the barrier through which heat transfer takes place is cylindrical. Attention is directed to Figure 10-2. It is apparent from the shaded area

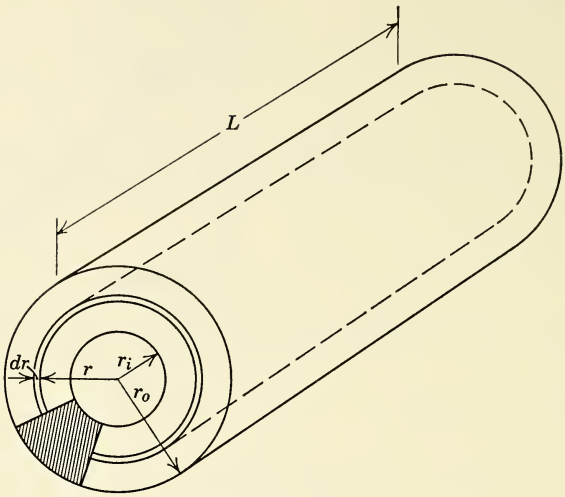

FIGURE 10-2. Heat transfer through the wall of a cylinder.

shown in the figure that, when the cylinder has thick walls, the inside area through which heat passes, when flowing in a radial direction, is considerably less than the area on the outside. The problem arises as to the proper area to be used in the transfer equation.

Consider a thin cylinder concentric with the large cylinder in Figure 10-2 and with a radius r. The thickness of the smaller cylinder dr is such that the area on the inside differs infinitesimally from the outside area. The rate at which heat will flow radially through the cylinder will be

$$q_h = -k(2\pi r L)\frac{dT}{dr} \tag{10-6}$$

where L = length of cylinder, ft.

By integrating Equation 10-6 between the limits imposed by the conditions on the inside and outside the larger cylinder,

$$\int_{r_i}^{r_o}\frac{dr}{r} = -\frac{2\pi kL}{q_h}\int_{T_i}^{T_o} dT \tag{10-7}$$

$$\ln\frac{r_o}{r_i} = \frac{2\pi kL}{q_h}(T_i - T_o) = \frac{2\pi kL}{q_h}\Delta T \tag{10-8}$$

and

$$q_h = k\left[\frac{2\pi L}{\ln (r_o/r_i)}\right]\Delta T \tag{10-9}$$

Equation 10-9 is sometimes written

$$q_h = \frac{kA_{lm}}{x} \Delta T \tag{10-10}$$

where

$$A_{lm} = 2\pi L \left[\frac{r_o - r_i}{\ln (r_o/r_i)} \right] = 2\pi L r_{lm} \tag{10-11}$$

and

$$x = r_o - r_i \tag{10-12}$$

Use of the term A_{lm} reduces the cylinder to the equivalent of a slab barrier having the same temperature drop. When the radius of the outside face of the cylinder is two times the radius of the inside face ($r_o/r_i = 2$), the error introduced in using the area based on the arithmetic mean of the radius, A_m instead of A_{lm}, is approximately 4 percent; for $r_o/r_i = 3$, the error is about 10 percent.

10-4. Compound Barriers

Figure 10-3 shows a compound barrier composed of three different thicknesses and types of materials. When heat flows by conduction from one side of the barrier to the other, it must pass through each

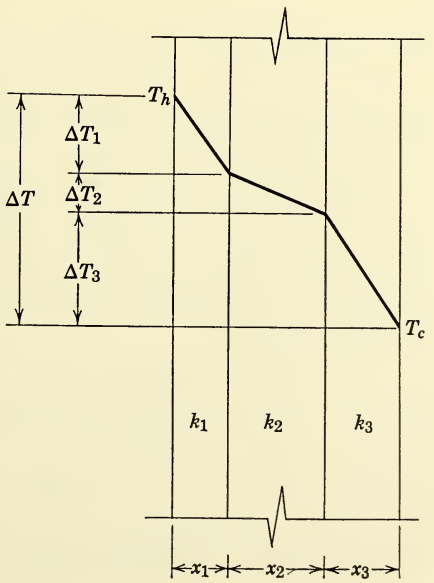

FIGURE 10-3. Temperature drop across compound barrier.

thickness. Since the rate of conduction through each thickness is equal to that through each of the other two,

$$q_h = \frac{k_1 A_1 \Delta T_1}{x_1} = \frac{k_2 A_2 \Delta T_2}{x_2} = \frac{k_3 A_3 \Delta T_3}{x_3} \tag{10-13}$$

Also, since

$$\Delta T = \Delta T_1 + \Delta T_2 + \Delta T_3 \tag{10-14}$$

it follows that

$$\Delta T = q_h \left(\frac{x_1}{k_1 A_1} + \frac{x_2}{k_2 A_2} + \frac{x_3}{k_3 A_3} \right) \tag{10-15}$$

and

$$q_h = \frac{\Delta T}{(x_1/k_1 A_1) + (x_2/k_2 A_2) + (x_3/k_3 A_3)} \tag{10-16}$$

The terms in the denominator represent the individual resistances offered to the flow of heat by the barrier materials. Since these materials are in series with respect to the heat flow, the total resistance equals the sum of the individual resistances. The temperature difference ΔT is the driving force which causes the heat to flow. An analogy can be drawn with Ohm's law governing the flow of electricity through a series of conductors.

$$\text{Current} = \frac{\text{Potential difference}}{\text{Total resistance}} = \frac{E}{R_1 + R_2 + R_3}$$

10-5. Convection

The transmission of heat by mixing or turbulence is called convection. Since the molecules of solids are relatively fixed and cannot move with respect to each other, convection is confined to fluids where it accounts for practically all of the heat transferred. Convection can be either forced or natural, depending on whether it is induced by stirring, agitation, or pumping, or by a gravitational field resulting from natural phenomena. Although natural convection has been formulated theoretically and experimentally, the following discussion will be confined to forced convection.

In Figure 10-4*a* a wall separates two fluids of different temperatures and characteristics. When flow conditions in the fluids are turbulent, there persist at the wall laminar sublayers separated from the turbulent bulks of the fluids by buffer zones. As heat flows from the hot to the cold fluid, the major portion of the temperature drop on each side of the wall occurs across the laminar sublayers and buffer zones. Because of the difficulty in estimating the individual resistances offered to heat

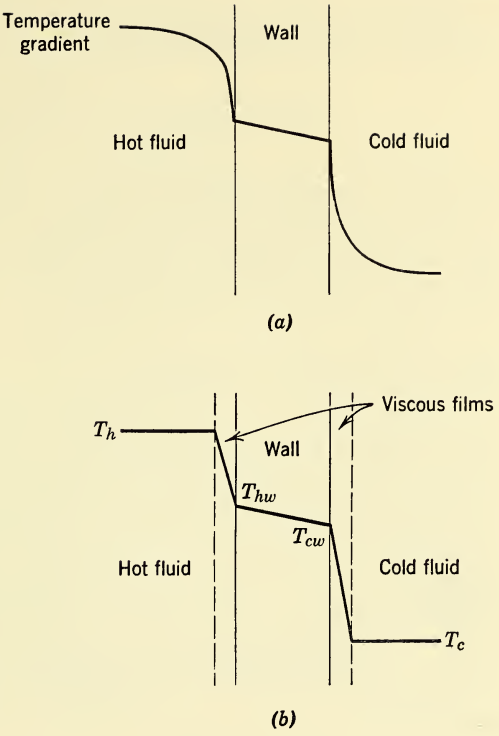

FIGURE 10-4. Temperature gradients between hot and cold fluids separated by a wall. (*a*) Temperature gradients as they exist when flow is turbulent. (*b*) Temperature gradients assumed for the film theory model when flow is turbulent.

flow by the sublayers, buffer zones, and turbulent bulks, it is convenient to make use of the film theory.

According to the film theory, a viscous film is assumed to be present on each side of the wall in which all resistance to heat transfer in the fluid is supposed to occur. The theory prescribes, for turbulent flow, that the fluid temperature is constant throughout the bulk of the hot fluid at a value of T_h, and that, at the interface between the turbulent fluid and viscous film, it drops linearly with distance to the wall temperature T_{hw}. On the other side of the wall, the temperature drops linearly across the viscous film from a wall temperature T_{cw} to the temperature of the bulk of the cold fluid T_c.

The rate at which heat is transmitted across each of the fictitious films can be computed from Newton's law of cooling.

$$q_h = hA\ \Delta T \tag{10-17}$$

where h = heat transfer coefficient, (Btu)/(hr)(ft^2)(°F)
ΔT = temperature drop across the film, °F

The rate at which heat will flow from the hot fluid to the cold fluid in Figure 10-4 can be calculated from

$$q_h = \frac{\Delta T}{(1/h_1A_1) + (x/kA_m) + (1/h_2A_2)} \tag{10-18}$$

where ΔT = total temperature drop across the system, $T_h - T_c$, °F.

It is to be noted that this expression is analogous to Equation 10-16, in which the terms in the denominator represent the individual resistances of conductors arranged in series.

10-6. Heat Transfer Coefficients

The determination of the proper film coefficient is a major difficulty in the solution of heat transfer problems. The film coefficient is a function of the properties and motion of the fluid. To assess their effect properly, the many variables involved are arranged in dimensionless groups in the correlations employed for determining the film coefficient. It is obvious that for each system specific relationships are required. Only a few will be discussed here. Relationships for other systems may be found elsewhere.[1] It should be noted that correlations of this type are established from experimental data and generally describe conditions to about ±25 percent.

Fluids in Turbulent Flow Inside Tubes

When the flow of heat is to the fluid and N_{Re} = 10,000 to 400,000 and N_{Pr} = 0.7 to 100, experimental data support the following correlation:

$$N_{Nu} = 0.023N_{Re}^{0.80}N_{Pr}^{0.40} \tag{10-19}$$

where N_{Nu} = Nusselt number = hD/k
N_{Re} = Reynolds number = DG/μ
N_{Pr} = Prandtl number = $c_p\mu/k$

The correlation, commonly referred to as the Dittus-Boelter relationship, has been found to apply for such fluids as water, oils, organic liquids, and various gases including air.

By substituting the individual terms for the dimensionless numbers in Equation 10-19 and solving for the transfer coefficient,

$$h = \frac{0.023k}{D}\left(\frac{DG}{\mu}\right)^{0.80}\left(\frac{c_p\mu}{k}\right)^{0.40} \tag{10-20}$$

[1] McAdams, W. H., *Heat Transmission*, McGraw-Hill Book Co., New York (1954).

where h = heat transfer coefficient (film coefficient), (Btu)/(hr)(ft^2)(°F)
k = thermal conductivity of the fluid, (Btu)(ft)/(hr)(ft^2)(°F)
D = inside diameter of the tube, ft
G = mass velocity of the fluid, (lb mass)/(sec)(ft^2)
μ = viscosity of fluid, (lb mass)/(ft)(sec)
c_p = specific heat of fluid at constant pressure, (Btu)/(lb)(°F)

Any system of units can be employed within the dimensionless groups as long as the units in each group are dimensionally consistent. The properties of the fluid are taken at a temperature equal to the arithmetic mean of the inlet and outlet temperatures of the bulk of the fluid.

When the flow of heat is away from the fluid, i.e., the fluid is being cooled, the exponent on the Prandtl number is changed from 0.40 to 0.30.

An analogy equation can be used to relate the transfer coefficient with fluid friction. It has been found [2] that, for fluids flowing in the turbulent region ($N_{Re} > 2000$), the transfer coefficient can be estimated from

$$\frac{f}{8} = j_H = N_{St} N_{Pr}^{2/3} \tag{10-21}$$

where f = friction factor, dimensionless (see Equation 1-16)
j_H = Colburn's j_H factor, dimensionless
N_{St} = Stanton number = h/c_pG

Through substitution and by solving for the film coefficient

$$h = \frac{f c_p G}{8} \left(\frac{c_p \mu}{k} \right)^{-2/3} \tag{10-22}$$

Fluids in Turbulent Flow through Annular Spaces

Problems often arise in which heat is transferred to or from a fluid flowing in the annular space between concentric pipes. In such cases, Equations 10-20 and 10-22 can be used to estimate the transfer coefficient, provided an equivalent diameter D_e is substituted for the diameter term in these equations.[3] The equivalent diameter is computed from Equation 1-17

$$D_e = 4r_H = \frac{D_1^2 - D_2^2}{D_1 + D_2} \tag{10-23}$$

[2] Colburn, A. P., *Trans. Am. Inst. Chem. Engrs.*, **29** (1933), 174–210.
[3] Perry, J. H., *Chemical Engineers Handbook* (3rd ed.), McGraw-Hill Book Co., New York (1950), 470.

where D_e = equivalent diameter, ft
r_H = hydraulic radius, ft
D_1 = inside diameter of the larger pipe, ft
D_2 = outside diameter of the smaller pipe, ft

Condensing Vapors Outside Tubes

When a vapor such as steam condenses on the outside surface of a tube, condensation takes place in one of two ways. The condensate either will form in an unbroken film around the tube or it will collect in drops, leaving part of the outside surface area exposed to the uncondensed vapor. The factors controlling the type of condensation are imperfectly understood. In general, it is found that vapor will condense in a film around clean tubes and in drops around those which are oily.

An expression has been developed [4] for estimating the heat transfer coefficient for film-type condensation around horizontal tubes.

$$h = 0.725 \left(\frac{k^3 \rho^2 g \lambda}{D \mu \, \Delta T_1} \right)^{1/4} \tag{10-24}$$

where ρ = density of the condensate, lb mass/ft^3
k = conductivity of condensate, (Btu)(ft)/(hr)(ft^2)(°F)
g = acceleration of gravity, (ft)/(hr)(hr)
λ = latent heat of vaporization, Btu/lb
D = outside diameter of tube, ft
μ = viscosity of condensate, (lb mass)/(ft)(hr)
ΔT_1 = difference in temperature between the saturated vapor and the outside surface of tube, °F

For cases where tubes are placed vertically, the coefficient for film-type condensation can be estimated from

$$h = 0.943 \left(\frac{k^3 \rho^2 g \lambda}{L \mu \, \Delta T_1} \right)^{1/4} \tag{10-25}$$

where L = length of tubes, ft.

In both equations, the values of the terms describing the properties of the condensate should be selected [5] at a temperature

$$T = T_v - 0.75 \, \Delta T_1 \tag{10-26}$$

where T_v = temperature of the saturated vapor, °F.

[4] Nusselt, W. Z., *Z. Ver. deut. Ing.*, **60** (1916), 541.
[5] McAdams, W. H., *Heat Transmission* (2nd ed.), McGraw-Hill Book Co, New York (1942).

10-7. Over-All Coefficients

It is often convenient to reduce the complexity of Equation 10-18 by substituting for the resistance terms in the denominator a term called an over-all coefficient. This is done by multiplying both the numerator and the denominator of the equation by one of the areas, say A_1:

$$q_h = \frac{A_1 \, \Delta T}{(1/h_1) + (A_1 x/kA_m) + (A_1/h_2 A_2)} \tag{10-27}$$

By letting

$$U_1 = \frac{1}{(1/h_1) + (A_1 x/kA_m) + (A_1/h_2 A_2)} \tag{10-28}$$

where U_1 = over-all coefficient based on area A_1, (Btu)/(hr)(ft^2)(°F)
Equation 10-27 becomes

$$q_h = U_1 A_1 \, \Delta T \tag{10-29}$$

Although the over-all coefficient can be based on any area, the area selected must be specified. Where the barrier is a thin-walled tube of large diameter, a negligible error will be introduced by using a common area A for A_1, A_m, and A_2. Since the surface area of a tubular barrier is proportional to its diameter, diameter terms may be substituted for the corresponding area terms in Equation 10-28.

EXAMPLE 10-2

Steam, saturated and at 15 psig, is to be used to heat water flowing inside of clean, horizontal, 1-in. copper tubing (Birmingham Wire Gage No. 10). If the water has an average temperature of 135 °F and flows through the pipe at a velocity of 6 ft/sec, what will be the over-all coefficient based on the inside surface?

Solution

1. Compute water film coefficient.

$$h = \frac{0.023k}{D}\left(\frac{DG}{\mu}\right)^{0.80}\left(\frac{c_p\mu}{k}\right)^{0.4}$$

From the Appendixes, the values of the properties at 135 °F:

$k = 0.376$ (Btu)(ft)/(hr)(ft^2)(°F)
$D = 0.732$ in. $= .0.061$ ft
$G = \rho\overline{V} = 61.50 \times 6 = 369$ (lb)/(ft^2)(sec)
$\mu = 0.490$ cp $\times 6.72 \times 10^{-4} = 3.29 \times 10^{-4}$ (lb)/(ft)(sec)
$c_p = 1$ Btu/lb

$$h = \left(\frac{0.023 \times 0.376}{0.061}\right)\left(\frac{0.061 \times 369}{3.29 \times 10^{-4}}\right)^{0.80}\left(\frac{1 \times 3.29 \times 10^{-4} \times 3600}{0.376}\right)^{0.40}$$

$$= 0.142(68{,}400)^{0.80}(3.15)^{0.4}$$

$$= 1670 \text{ (Btu)/(hr)(ft}^2\text{)(°F)}$$

2. Conductance through copper tubing (at 200 °F),

$$k = 218 \text{ (Btu)(ft)/(hr)(ft}^2\text{)(°F)}$$

3. Compute steam film coefficient.

$$h = 0.725\left(\frac{k^3\rho^2 g\lambda}{D\mu\,\Delta T_1}\right)^{1/4}$$

As a first approximation the temperature of the outside surface of the tube will be taken as equal to the mean of the average water temperature and the saturated steam temperature or 195 °F. Therefore, average temperature of condensate will be

$$T = T_v - 0.75\,\Delta T_1 = 250 - 0.75(250 - 195) = 210 \text{ °F}$$

The values of the properties of water at this temperature are

$k = 0.409$ (Btu)(ft)/(hr)(ft^2)(°F)
$\rho = 59.88$ lb/ft^3
$g = 4.18 \times 10^8$ (ft)/(hr)(hr)
$\lambda = 972$ Btu/lb
$D = 1.000$ in. $= 0.0833$ ft
$\mu = 0.260$ cp $\times\ 2.42 = 0.630$ (lb)/(ft)(hr)
$\Delta T_1 = 250 - 195 = 55$ °F

$$h = 0.725\left[\frac{(0.409)^3(59.88)^2(4.18 \times 10^8)972}{0.0833 \times 0.630 \times 55}\right]^{1/4}$$

$$= 1750 \text{ (Btu)/(hr)(ft}^2\text{)(°F)}$$

4. Compute resistance.

$$\text{Steam film} = \frac{1}{h_1 D_1} = \frac{1}{1750 \times 0.0833} = 6.85 \times 10^{-3}$$

$$\text{Copper wall} = \frac{x}{kD_m} = \frac{0.01116}{218 \times 0.0722} = 0.71 \times 10^{-3}$$

$$\text{Water film} = \frac{1}{h_2 D_2} = \frac{1}{1670 \times 0.061} = \frac{9.82 \times 10^{-3}}{17.38 \times 10^{-3}}$$

5. Compute temperature drop across steam film.

$$\Delta T_1 = (250 - 135)\frac{6.85 \times 10^{-3}}{17.38 \times 10^{-3}} = 45\ ^\circ\text{F}$$

$$\text{Surface of metal} = 250 - 45 = 205\ ^\circ\text{F}$$

6. Recompute steam film coefficient. Average temperature of condensate will be

$$T = 250 - 0.75(250 - 205) = 216\ ^\circ\text{F}$$

Values of properties at 216 °F are:

$k = 0.413$ (Btu)(ft)/(hr)(ft^2)(°F)
$\rho = 59.70$ lb/ft^3
$\lambda = 968$ Btu/lb
$\mu = 0.605$ (lb)/(ft)(hr)
$\Delta T_1 = 45$ °F

$$h = 0.725\left[\frac{(0.413)^3(59.7)^2(4.18 \times 10^8)968}{0.0833 \times 0.605 \times 45}\right]^{1/4}$$

$$= 1870\ \text{(Btu)/(hr)(ft}^2\text{)(°F)}$$

7. Recompute resistances.

$$\text{Steam film} = \frac{1}{1870 \times 0.0833} = 6.42 \times 10^{-3}$$

$$\text{Copper wall} = \frac{0.01116}{218 \times 0.0722} = 0.71 \times 10^{-3}$$

$$\text{Water film} = \frac{1}{1670 \times 0.061} = \frac{9.82 \times 10^{-3}}{16.95 \times 10^{-3}}$$

8. Recompute temperature drop across steam film.

$$\Delta T_1 = (250 - 135)\frac{6.42 \times 10^{-3}}{16.95 \times 10^{-3}} = 43.5\ ^\circ\text{F}$$

9. Compute over-all coefficient based on inside surface.

$$U_2 = \frac{1}{(D_2/h_1D_1) + (D_2x/D_mk) + (1/h_2)}$$

$$= \frac{1}{(3.91 \times 10^{-4}) + (0.43 \times 10^{-4}) + (6.00 \times 10^{-4})}$$

$$= 966\ \text{(Btu)/(hr)(ft}^2\text{)(°F)}$$

10-8. Variable Temperature Gradient

In many heat exchange devices the flow of hot and cold fluids to each other is either parallel or countercurrent. Temperature-length curves for both types of flow are shown in Figure 10-5. From these curves it is seen that the temperature difference between the two fluids varies from point to point in the exchanger. If Equation 10-29 is to be used, then the value selected for the term ΔT must be such that the quantitative relationship expressed by the equation remains valid.

At any point along the length of the exchanger,

$$dq_h = U\,\Delta T\,dA \tag{10-30}$$

and

$$dq_h = -(c_p)_h w_h\,dT_h = (c_p)_c w_c\,dT_c \tag{10-31}$$

where $(c_p)_h$ and $(c_p)_c$ = specific heat of hot and cold fluids, Btu/lb
w_h and w_c = mass rate of flow of hot and cold fluids, lb/hr
dT_h and dT_c = differential change in temperature of hot and cold fluids, °F

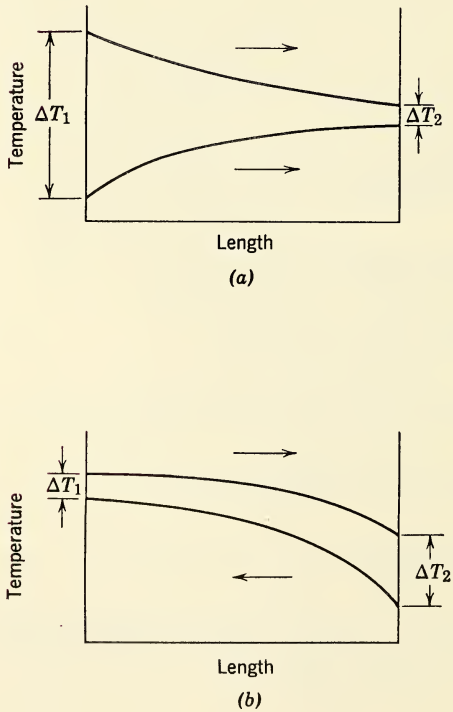

FIGURE 10-5. Temperature-length curves. (*a*) Parallel flow. (*b*) Countercurrent flow.

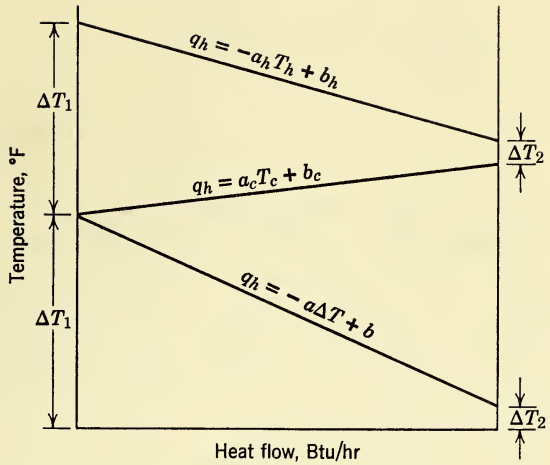

FIGURE 10-6. Relationships between temperature and rate of heat transmission when flow is parallel.

By assuming that the terms $(c_p)_h w_h$ and $(c_p)_c w_c$ remain constant, both dT_h and dT_c can be treated as straight-line functions of dq_h, and

$$q_h = -a_h T_h + b_h = a_c T_c + b_c \tag{10-32}$$

where a_h, b_h, a_c, and b_c are constants. From the curves in Figure 10-6, it is seen that, if T_h and T_c vary linearly with q_h, so must ΔT. The slope of the bottom curve is

$$-\frac{d(\Delta T)}{dq_h} = \frac{\Delta T_1 - \Delta T_2}{q_h} \tag{10-33}$$

This expression combined with Equation 10-30 gives

$$-\frac{d(\Delta T)}{\Delta T} = \frac{U(\Delta T_1 - \Delta T_2)}{q_h} dA \tag{10-34}$$

If the over-all coefficient U is assumed to remain constant throughout the heat exchanger, Equation 10-34 when integrated over the entire surface area becomes

$$\int_{\Delta T_2}^{\Delta T_1} \frac{d(\Delta T)}{\Delta T} = \frac{U(\Delta T_1 - \Delta T_2)}{q_h} \int_0^A dA \tag{10-35}$$

$$\ln \frac{\Delta T_1}{\Delta T_2} = \frac{U(\Delta T_1 - \Delta T_2)A}{q_h} \tag{10-36}$$

$$q_h = UA \left[\frac{\Delta T_1 - \Delta T_2}{\ln (\Delta T_1 / \Delta T_2)} \right] = UA\ \Delta T_{\text{lm}} \tag{10-37}$$

where ΔT_{lm} = logarithmic mean temperature difference.

Actually, the value of the over-all coefficient will vary over the length of the exchanger. Where temperature variations are not too great, the over-all coefficient can be estimated by using film coefficients based on the arithmetic means of the inlet and exit temperatures of the fluids. In the case of countercurrent flow, the temperature differences ΔT_1 and ΔT_2 are usually close enough together to permit the use of the arithmetic mean temperature difference for ΔT_{lm}.

Where the heating medium is a condensing vapor, such as steam, entering the exchanger with little superheat, the temperature of the vapor can be considered as remaining constant at the boiling point, and the logarithmic mean temperature difference can be used for parallel, countercurrent, and cross-flow conditions in both single- and multipass exchangers. If a vapor with considerable superheat is to be used in parallel or counterflow with the second fluid in a single-pass unit, it is advisable to divide the exchange process into two regions: one region in which heat is exchanged during the loss of the vapor's sensible heat, and the other in which condensation is taking place. The total surface area requirement in such a case would be equal to the sum of the areas required in each region as computed with the use of the logarithmic mean temperature difference. The logarithmic mean temperature difference does not apply in multipass and cross-flow exchangers where the temperatures of both fluids change. The design of these units may be found elsewhere.[6]

10-9. Heat Exchangers

Many types of heat exchangers are currently in use, their design being highly specialized and dependent upon the specific application. The following discussion will be limited to two general types.

The double-pipe exchanger shown in Figure 10-7*a* is one of the simplest types of exchanger employed. This exchanger consists of units of two pipes, one inside of another, arranged in vertical banks. One fluid flows through the inner pipe parallel with or countercurrent to the other fluid

[6] McAdams, W. H., in: Perry, J. H., *Chemical Engineers Handbook* (3rd ed.), McGraw-Hill Book Co., New York (1950).

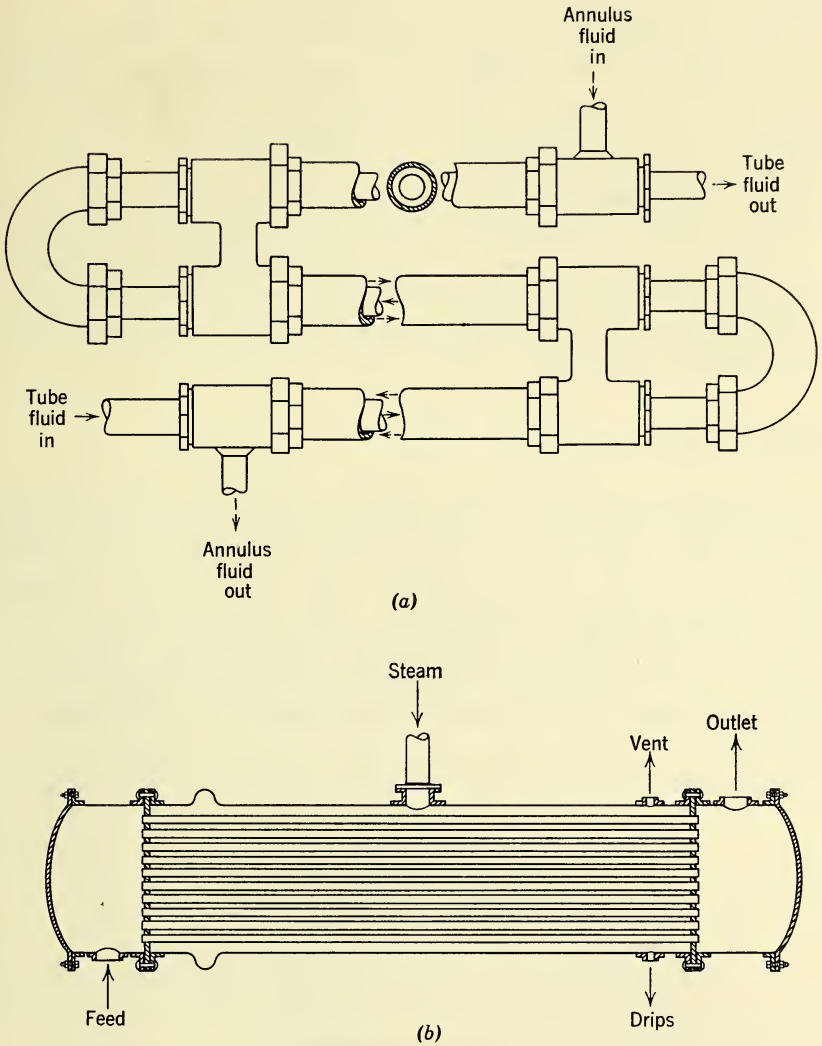

FIGURE 10-7. Typical heat exchangers. (*a*) Double-pipe exchanger. [From Figure 15.1, Foust, A. S., et al., *Principles of Unit Operations*, John Wiley and Sons, New York (1960).] (*b*) Single-pass, cross-flow shell-and-tube exchanger. (By permission from *Elements of Chemical Engineering*, by Badger, W. L. and W. L. McCabe. Copyright 1936, New York, McGraw-Hill Book Company, Inc.)

flowing through the annular space between the two pipes. Both fluids are usually liquids.

The shell-and-tube exchangers constitute the most popular type of heat exchanger in use. Figure 10-7*b* shows a single-pass, cross-flow shell-and-tube exchanger. This particular exchanger consists of two heads connected by a tube bundle. Cold fluid entering the exchanger at one end flows through the tube bundle and out the other end of the exchanger. Steam fills the space between the tubes and condenses on the outside surfaces. Condensate is removed from the bottom of the shell. In multipass units, the heads are baffled so that the fluid being heated passes the shell-side fluid several times before it is discharged. By increasing the fluid velocity, this arrangement increases the value of the heat transfer coefficient.

10-10. Radiation

All materials at temperatures above absolute zero emit energy as electromagnetic radiation. The radiation, consisting of wavelengths predominately in the infrared region of the spectrum, travels in straight lines until it strikes other materials. Substances receiving radiation either reflect, transmit, or absorb it. That portion of the radiation absorbed is converted to thermal energy. Concurrently, the radiated body is emitting radiation of its own to materials it can "see." A continuous interchange of radiation exists between all bodies in sight of each other.

The energy emitted by a plane surface is given by the expression

$$q_h = A\epsilon\sigma T_A^4 \tag{10-38}$$

where q_h = rate at which energy is radiated, Btu/hr
A = area of surface, ft^2
ϵ = emissivity
σ = Stefan-Boltzman constant = 1730×10^{-12} $(Btu)/(ft^2)(hr)(°R^4)$
T_A = absolute temperature of the body, °R

The emissivity ϵ is the ratio of the energy emitted by the surface in question to that emitted by the surface of a "black body," a hypothetical material which absorbs 100 percent of the incident radiation. Since the value of q_h is proportional to the fourth power of the absolute temperature, a small increase in surface temperature greatly increases the amount of radiation emitted.

The net loss or gain in energy by a surface is equal to the difference

between the energy emitted by the surface and that absorbed from the radiation emitted by other surfaces. For the case where a large plane surface with an area A_1 and a temperature T_{A1} is parallel to another large, plane surface at temperature T_{A2}, the rate at which heat is radiated from the first surface to the second is closely

$$q_{h1} = A_1\sigma\epsilon_1 {T_{A1}}^4 - A_1\sigma\alpha_1 {T_{A2}}^4 \qquad (10\text{-}39)$$

where α_1 = absorptivity. By assuming that the absorptivity is independent of the wavelength composition of the incident radiation, α_1 may be considered as being equal to ϵ_1.

Equation 10-39 applies only to surfaces that completely "see" each other. In practical applications, the equation must be modified for the particular geometrical relationship existing between the two surfaces.

$$q_{h1} = 0.173\epsilon_1 A_1 \left[\left(\frac{T_{A1}}{100}\right)^4 - \left(\frac{T_{A2}}{100}\right)^4\right] F \qquad (10\text{-}40)$$

where F = geometric factor. Values of F for several geometric relationships may be found elsewhere.[7]

Notations

A	Cross-section area, ft^2; A_{lm}, $\log_e$ mean area; A_m, arithmetic mean
c_p	Specific heat at constant pressure, (Btu)/(lb force)(°F)
D	Diameter, ft; D_e, equivalent diameter
f	Friction factor, dimensionless
F	Geometric factor, dimensionless
g	Acceleration of gravity, ft/hr^2
G	Mass velocity, (lb mass)/(sec)(ft^2)
h	Heat transfer coefficient, (Btu)/(ft^2)(hr)(°F)
j_H	Colburn's j_H factor, dimensionless
k	Thermal conductivity, (Btu)(ft)/(hr)(ft^2)(°F)
L	Length, ft
N_{Nu}	Nusselt number, dimensionless
N_{Re}	Reynolds number, dimensionless
N_{Pr}	Prandtl number, dimensionless
N_{St}	Stanton number, dimensionless
q_h	Rate of heat flow, Btu/hr
Q	Quantity of heat, Btu; Q_s, sensible heat; Q_l, latent heat
r	Radius, ft; r_i, inside radius; r_o, outside radius
r_H	Hydraulic radius, ft
T	Temperature, °F; T_0, temperature above a datum; ΔT, temperature drop
T_A	Absolute temperature, °R

[7] Perry, J. H., *Chemical Engineers Handbook* (3rd ed.), McGraw-Hill Book Co., New York (1950).

U Over-all heat transfer coefficient, (Btu)/(hr)(ft^2)(°F)
w Mass rate of flow, lb/hr
W Weight, lb force
x Thickness, ft
α Absorptivity, dimensionless
ϵ Emissivity, dimensionless
λ Unit latent heat, Btu/lb force
μ Viscosity, (lb mass)/(ft)(sec)
ρ Mass density, lb mass/ft^3
σ Stefan-Boltzman constant, 1730×10^{-12} (Btu)/(ft^2)(hr)(°R^4)

11

Evaporation

11-1. Introduction

The concentration of solutions of nonvolatile solutes through heat-induced vaporization of the solvent (generally water) is called evaporation. Evaporation is a relatively expensive operation, and its application in waste treatment is limited primarily to the recovery of valuable by-products from waste liquids and to the treatment of wastes where no alternate methods are available.

Essentially, evaporation involves the addition of heat to a boiling solution held in a container which is vented to permit the continuous removal of vapor collecting over the liquid. Heat must be supplied in quantities sufficient to raise the temperature of the solution to its boiling point and to furnish the latent heat required by the fraction of the solvent that vaporizes. Although hot gases, solar irradiation, and direct fire are sometimes used to meet these requirements, as a rule indirect steam is employed.

Evaporation is often carried out at pressures less than atmospheric. Operation under a vacuum establishes a larger temperature difference between the heat source and the boiling liquid. This, in turn, increases the rate of evaporation. Furthermore, reduced boiling temperatures serve to protect any organic fraction of the evaporating solution from thermal decomposition. Evaporators may be employed in batches or in a continuous operation.

11-2. Evaporators

The following discussion will be confined to steam-heated, tubular evaporators. These are the most common type where large quantities of water are to be evaporated.

The horizontal-tube evaporator is heated by passing steam inside a bank of horizontal tubes located close to the bottom of the vessel (Figure 11-1*a*). No provision is made for forced circulation; consequently, the heat transfer coefficients are low, and the use of this type of evaporator is limited primarily to nonviscous, nonfoaming solutions. However, it has a relatively low first cost.

The standard, vertical-tube evaporator has a wide application in "run-of-the-mill" evaporation operations. It consists of a cylindrical shell, in the bottom section of which are fitted two tube sheets supporting a number of small vertical tubes arranged around one large central tube (Figure 11-1*b*). Steam introduced between the tube sheets makes contact with the outside of the tubes, heating the liquid on the inside. Circula-

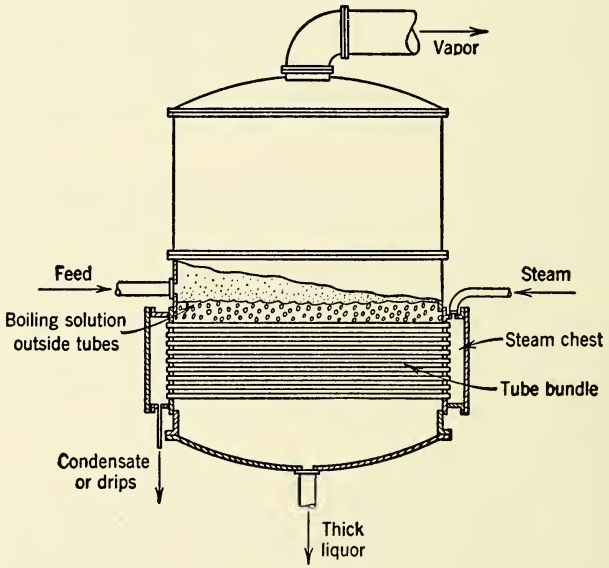

(*a*)

FIGURE 11-1. Typical evaporator types. (*a*) Horizontal-tube evaporator. (*b*) Standard, vertical-tube evaporator. (*c*) Long-tube evaporator. (*d*) Forced-circulation evaporator. (*Swenson Evaporator Co.*)

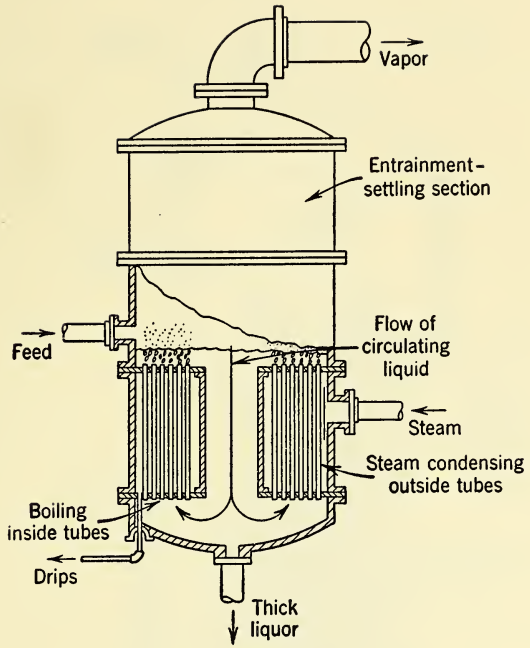

(*b*)

FIGURE 11-1. (*Continued*)

tion is established in which the heated solution travels up through the small tubes and then down the large draft tube at the center of the tube bundle. In as much as the tubes are not arranged conveniently for cleaning and replacement, this type of evaporator is not suitable for corrosive solutions.

The basket-type evaporator is similar to the standard type except for the circulation scheme. The steam chamber of the basket type is without a central draft tube, and the circulation downward is through an annular space between the chamber and the vessel wall. The chamber or "basket" has a removable tube section, making it more desirable for use in evaporating corrosive solutions.

The long-tube evaporator is a vertical-tube type with tubes ranging in length up to 20 ft or more (Figure 11-1*c*). The high velocities of liquid movement induced by the long-tube design result in heat transfer rates greater than those occurring in most evaporator types. Consequently, the fraction of liquid evaporated per pass is relatively high. Operation may involve one pass only, with the concentrated solution being with-

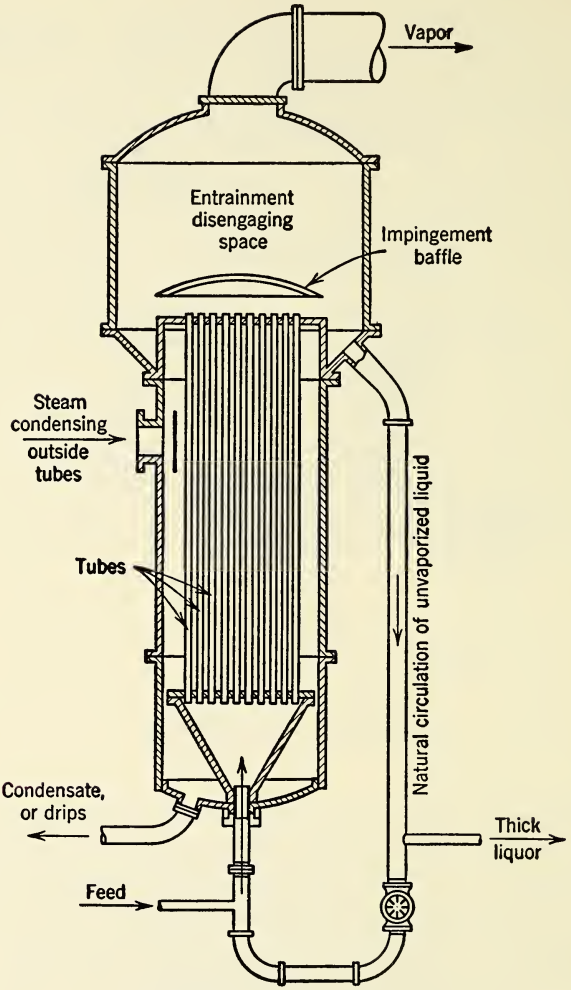

(*c*)

FIGURE 11-1. (*Continued*)

drawn from the top section of the evaporator. A modification of this type of evaporator is constructed with the heating element arranged externally to the vessel proper. The long-tube evaporator is suited to the concentration of foamy solutions. However, it is not particularly satisfactory for the evaporation of solutions which are either salting or scaling.

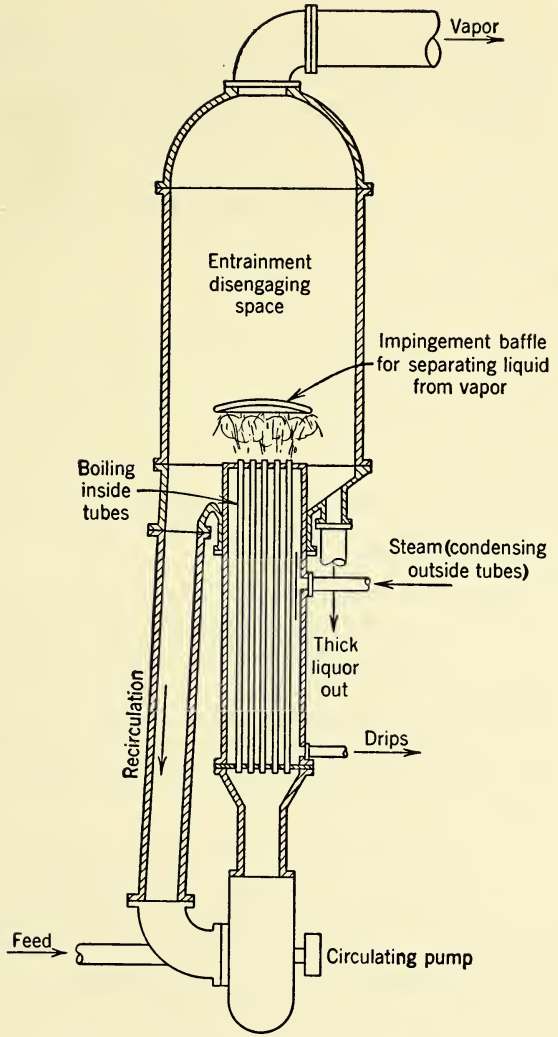

(*d*)

FIGURE 11-1. (*Continued*)

Forced-circulation evaporators are particularly adapted to the concentration of salting or scaling solutions (Figure 11-1*d*). Centrifugal pumps or, in the case of very viscous solutions, positive displacement pumps are employed to circulate the liquid at high velocities through the tube section. The discharge from the tubes impinges against a baffle

and the concentrated solution is recirculated back through the pump. Feed is introduced at the suction end of the pump. Here, again, an external arrangement of the tube section is sometimes employed to facilitate cleaning and replacement. This type also is suited for viscous and foaming liquids.

Formerly, evaporators were constructed of cast iron. Now, most evaporators are being built of mild steel plate with welded construction.

11-3. Ancillary Equipment

When evaporation is carried out under a vacuum, water vapor and noncondensable gases must be removed as quickly as they are formed. Vacuum pumps and steam-jet ejectors are used for this purpose. However, the pumping load is reduced first by condensing the vapor either in a surface condenser of conventional tube-and-shell design or in a contact condenser. A contact condenser consists of a chamber in which the vapor is condensed by bringing it into direct contact with fine sprays or cascading sheets of cooling water.

The condensate, the noncondensable gases, and, in systems where contact condensers are employed, the cooling water are removed from the condenser either together by means of a "wet" vacuum pump or the noncondensables are removed separately with a "dry" vacuum pump or a steam-jet ejector. In such cases, the water phase is discharged through a water pump or a "barometric leg." The latter is a vertical pipe at least 34 ft long, the bottom end of which is sealed with a small tank of water.

For continuous operation under atmospheric pressure, pumps are required both on the feed and on the concentrated-liquid ends of the system. When a vacuum is employed, however, the feed pump may be omitted. Centrifugal separators or baffles may be installed to trap droplets of solution entrained in the vapor. Steam traps are used for the removal of condensate forming in the steam chests.

11-4. Evaporator Capacity

It would be desirable to consider the heat transfer characteristics of evaporators in terms of the individual film resistances. Unfortunately, little information is available relative to the film coefficients applicable under operating conditions. Consequently, evaporator capacities are determined by the expression

$$q_h = UA\,\Delta T \tag{11-1}$$

where q_h = rate of heat transfer, Btu/hr
A = heating surface, ft^2
U = over-all transfer coefficient, (Btu)/(hr)(ft^2)(°F)
ΔT = mean temperature difference between the heating medium and the boiling solution, °F

The heating surface is fixed by the design of the evaporator, and is referenced with respect to the over-all coefficient. As a rule, the resistance offered by the liquid film is greater than that on the steam side, and A is the surface area on the liquid side of the tubes.

The mean temperature difference between the steam and the boiling solution, ΔT, ordinarily is determined with the use of steam tables on the basis of pressures existing in the steam chest and in the vapor space above the boiling solution. When determined in this manner, the difference is called the *apparent temperature drop*. Many solutions, however, have boiling temperatures significantly higher than that of water. If the true boiling temperature is known and is used to compute the mean temperature difference, the latter is known as the *net temperature drop*.

The determination of the true boiling temperatures of solutions is facilitated through the use of Dühring's rule. In effect, this rule states that, within the range of pressures ordinarily encountered in evaporation operations, the boiling temperatures of a solution of constant composition at different pressures vary in a straight-line relationship with the boiling temperatures of water at the same pressures. Therefore, if the boiling point of a solution is known at two different pressures, it can be estimated for any other pressure. Most concentrated solutions of salts and caustic have significant boiling point elevations, whereas the elevations of solutions containing colloidal material usually are negligible.

The quantity of heat required to evaporate water from solution is the sum of: (*a*) the sensible heat to bring the feed to the boiling temperature; (*b*) the latent heat of vaporization; (*c*) the heat of concentration; (*d*) the heat of crystallization of any products formed; and (*e*) the convective and other heat losses. The latent heat of vaporization is the largest component of the total heat requirement. Data relating to the heats of concentration and crystallization are relatively scarce. Fortunately, these heats can safely be ignored in most evaporation calculations. With adequate insulation around the evaporator, the convective losses are minor and can be disregarded also.

The latent heat of vaporization of solutions with boiling temperatures close to that of water may be considered as equal to that of water. Solutions with boiling temperatures significantly higher have latent heats greater than the latent heat of water.

The latent heats of vaporization of solutions with boiling point elevations are greater than that of water. If the boiling point elevation is small, the difference is insignificant and the latent heat of water can be used. If the elevation is considerable, then calculations should be based on the actual latent heat of the solution. When dealing with a solution for which such data are unavailable (the usual case), the latent heat can be approximated either by taking that of water at the pressure (rather than the temperature) at which the evaporation takes place or by making use of the following expression:[1]

$$\lambda' = \lambda \left(\frac{T'^2}{T^2}\right)\left(\frac{dT}{dT'}\right) \tag{11-2}$$

where λ' = latent heat of vaporization of 1 lb of water at a temperature T', from a solution whose boiling point is T'

λ = latent heat of vaporization of water for a temperature T

T' and T = boiling points of solution and of water, respectively, at the same pressure

dT/dT' = slope of the Dühring line

Specific heat, likewise, is a function of the dissolved solids concentration. When the specific heat of a solution is unknown (again, the usual case), it is generally assumed to be equal to the specific heat of water.

In most calculations, any superheat of the steam as well as the temperatures of the incoming feed and the condensate discharged from the steam chest is ignored in the determination of the mean temperature difference.

The over-all coefficient U is primarily a function of evaporator design. The value of the coefficient will depend upon which temperature difference is employed in its determination. The coefficient, when computed with the use of the apparent temperature drop, is called the *apparent coefficient;* when the net temperature drop is used, it is known as the *coefficient corrected for rise in boiling point.*

The over-all coefficient will vary also with the temperature drop and the properties of the evaporating solution. Figure 11-2 illustrates the relationship existing between the boiling point, the apparent temperature drop, and the apparent coefficient when pure water is evaporated in a basket-type, vertical tube evaporator.[2] Note is to be made of the increase in the coefficient as the temperature drop becomes larger. The larger temperature gradients induce greater heat flow across the tube surface which, in turn, promotes more turbulence on the liquid side of

[1] Badger, W. L., in: Perry, J. H., *Chemical Engineers Handbook* (3rd ed.), McGraw-Hill Book Co., New York (1950), 501.

[2] Badger, W. L., and P. W. Shepard, *Trans. Am. Inst. Chem. Engrs.*, **13,** No. I (1920), 101–137.

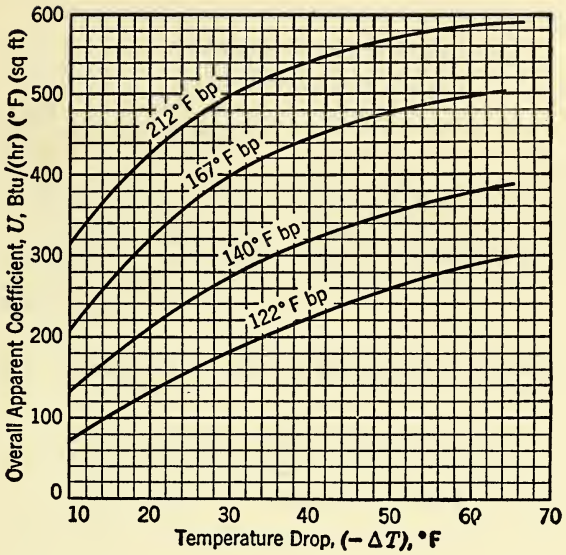

FIGURE 11-2. Relationship between boiling point, temperature drop, and heat transfer coefficient in a vertical-tube evaporator. [From Figure 465, Brown, G. G., et al., *Unit Operations*, John Wiley and Sons, New York (1950).]

the tube. This reduces the liquid film thickness and results in a drop in total resistance to the flow of heat. The increase in coefficient with increased boiling temperatures is attributed to the decrease in liquid viscosity at higher temperatures.

EXAMPLE 11-1

An engineer plans to use an idle evaporator with 500 ft^2 of heating surface to concentrate a colloidal waste from 10 to 30 percent solids. Dry steam at 10 psig is available and a vacuum of 26 in. of Hg (gage) can be established in the vapor space. The unconcentrated waste has a boiling temperature close to that of water. The temperature of the waste as it is fed to the evaporator will be 125 °F, while that of the condensate leaving the evaporator is assumed to be 180 °F. The operating conditions are such that an over-all coefficient of 600 Btu/hr/ft^2/°F is anticipated. (*a*) At what rate can the waste be concentrated with single-effect operation? (*b*) At what rate must steam be available?

Solution

(*a*) The solution requires first a materials balance over the liquid side of the evaporator.

Materials in

Water in feed = $0.90w$
Solids in feed = $0.10w$

$1.00w$ lb/hr

Materials out

Solids in liquor discharge = $0.10w$
Water in liquor discharge = $0.10w\frac{70}{30} = 0.233w$
Water in vapor = $0.90w - 0.233w = 0.667w$

$1.00w$ lb/hr

For the conditions stated in the problem, the capacity of the evaporator will be

$$q_h = 500 \times 600(240 - 125) = 34.5 \times 10^6 \text{ Btu/hr}$$

At equilibrium, the heat transferred will equal that required for the vaporization of $0.667w$ lb/hr of water at 125 °F. Therefore,

$$0.667w \times 1022 = 34.5 \times 10^6$$

and

$$w = 50{,}400 \text{ lb/hr}$$

(*b*) From the steam tables, the enthalpy of dry steam at 10 psig (24.7 psia) is found to be 1160 Btu/lb and that of the condensate at 180 °F is found to be 145 Btu/lb. The rate at which steam must be furnished, therefore, will be

$$w = \frac{34.5 \times 10^6}{1160 - 145} = 34{,}050 \text{ lb/hr}$$

11-5. Multiple-Effect Evaporation

Evaporation can be carried out in several steps with evaporator units arranged in series. Such operation, known as multiple-effect evaporation, affords an economy of steam through the reuse of heat which is commonly lost in the vapor phase of single-effect operation. Figure 11-3 illustrates a flow diagram of a triple-effect forward-feed evaporator. Both feed and steam enter the system at the first effect. The vapor from the first effect is used to heat the solution in the second, and the vapor from the second furnishes heat to the third. Vapor from the third effect is withdrawn from the system. Feed introduced at the first effect is concentrated as it passes through successive effects, and is discharged from the third with the concentration desired.

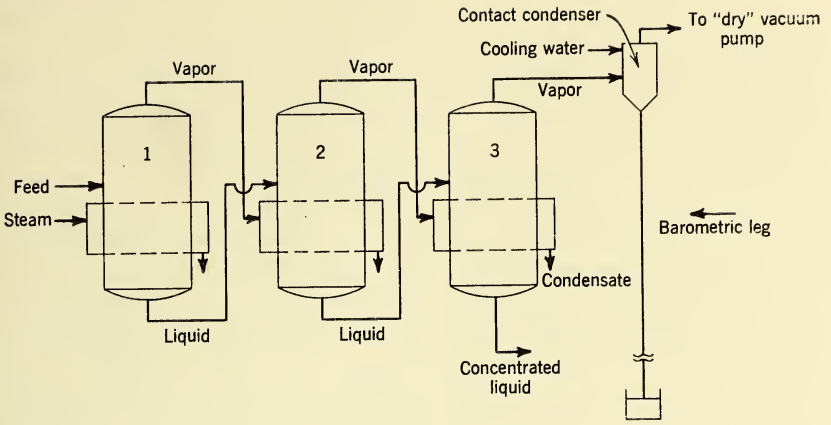

FIGURE 11-3. Triple-effect forward-feed evaporator.

When a forward-feed arrangement is employed in multiple-effect evaporation, a pump at the discharge end and, as a rule, one at the feed end are required. The flow of concentrated solution between effects is induced by the difference in pressure between the first and last effects.

In the case of unusually cold or viscous solutions, it is often desirable to introduce the feed at the third effect and withdraw the liquid from the first, a countercurrent arrangement known as backward feed. Backward feed requires pumps between each effect, an operational disadvantage as well as a factor increasing the initial cost.

One pound of steam in triple-effect evaporation accomplishes roughly three times as much evaporation as is possible in single-effect operation. The latent heat introduced to the system by the steam passes from evaporator to evaporator. It would appear on first consideration that an infinite economy would result from the use of an infinite number of effects. Actually, however, several factors limit the number of effects practicable in a system.

Each effect of a multiple-effect evaporator operates only on a fraction of the total temperature drop across the system. Since the total drop is seldom larger than that employed in single-effect evaporation, the capacity per unit area of heating surface is reduced proportionately. It is evident then, that, although a savings in operational costs may be realized through multiple-effect operation, equipment costs are greater. For a given total capacity, each effect of a multiple-effect evaporator will cost approximately the same as a single-effect system.

An increase in boiling temperature by dissolved solids is another

factor that limits the number of effects practicable in multiple-effect evaporators.

If a solution in the first effect has a boiling point elevation, the water vapor leaving the first effect will be superheated to the extent of the boiling point elevation. The superheat, being sensible heat, is but a small fraction of the total heat transmitted by the vapor. The vapor entering the second effect quickly loses its superheat and comes into contact with most of the heating surface at the boiling temperature of the water. The solution evaporating in the second effect must have, therefore, a temperature lower than that of the first effect by an amount equal to the boiling point elevation of the solution in the first effect plus the temperature drop across the heating surface of the second effect. If the boiling point elevations are large, the reduction in the effective temperature drop across the entire system is sizeable, and the number of effects is limited.

For any multiple-effect operation, the number of effects should be determined on the basis of the economics specific to that operation. In most cases, no more than three or four effects are found to be economical.

EXAMPLE 11-2

An aqueous waste with a dissolved solids concentration of 10 percent is to be concentrated to 40 percent solids by triple-effect, forward-feed evaporation. Steam at 25 psig and a vacuum of 26 in. of Hg are available for the operation. Investigations reveal that the waste has the following boiling temperatures.

Solids, %	Boiling Temperatures at Atmospheric Pressure, °F
10	216
20	224
30	238
40	260

For the operating conditions anticipated, over-all coefficients of 700, 600, and 500 Btu/hr will be assumed for effects 1, 2, and 3 respectively. The temperature of the feed entering the system is 200 °F and the effects are to be of equal size. What must be the area of heating surface in each effect if the system is to concentrate 50,000 lb of the waste per hour?

Solution

1. As a first approximation, assume evaporation in each effect to be equal. On the basis of this assumption, estimate the concentration of the solution discharged from each effect.

(*a*) Water content of feed,

$$0.90 \times 50{,}000 = 45{,}000 \text{ lb/hr}$$

Solids content of feed,

$$0.10 \times 50{,}000 = 5000 \text{ lb/hr}$$

Water content of concentrated liquid, leaving system,

$$5000 \times \frac{0.60}{0.40} = 7500 \text{ lb/hr}$$

Water evaporated in each effect,

$$\frac{45{,}000 - 7500}{3} = \frac{37{,}500}{3} = 12{,}500 \text{ lb/hr}$$

(*b*) Concentration of discharge from first effect,

$$\frac{5000}{45{,}000 - 12{,}500 + 5000} = 13.3 \text{ percent}$$

Concentration of discharge from second effect,

$$\frac{5000}{45{,}000 - 25{,}000 + 5000} = 20.0 \text{ percent}$$

Concentration of discharge from third effect is 40.0 percent.

2. Estimate the boiling point elevations for the solutions in each effect, add them together and subtract the sum from the total temperature drop across the system.

(*a*) Estimated boiling point elevations,

$$\begin{aligned} \text{Elevation in effect 1} &= 6° \\ \text{Elevation in effect 2} &= 12° \\ \text{Elevation in effect 3} &= 48° \\ \text{Total} &= 66° \end{aligned}$$

(*b*) Total temperature drop across system (25 psig = 266 °F and 26 in. of Hg = 125 °F) is 266° − 125° = 141°.

(*c*) Total effective temperature drop is 141° − 66° = 75°.

3. Assume temperature drop across each effect by distributing the total effective drop in inverse proportion to the over-all coefficients.

$$\frac{q_h}{A} = U_1 \Delta T_1 = U_2 \Delta T_2 = U_3 \Delta T_3$$

$$= 700 \Delta T_1 = 600 \Delta T_2 = 500 \Delta T_3$$

and

$$\Delta T_1 + \Delta T_2 + \Delta T_3 = 75°$$

Therefore,

$$\Delta T_1 = 21 \text{ °F} \qquad \Delta T_2 = 25 \text{ °F} \qquad \Delta T_3 = 29 \text{ °F}$$

4. Based on estimated boiling point elevations and temperature drops, establish temperature conditions throughout system.

	Effect 1	Effect 2	Effect 3	Condenser
Vapor, °F	245	214	173	125
Solution, °F	245	214	173	
Heating medium, °F	266	239	202	

5. Strike a heat balance around each effect. Four equations are obtained with four unknowns. By solving these equations, the following quantities are obtained.

Steam required = 13,600 lb/hr
Evaporation from effect 1 = 11,020 lb/hr
Evaporation from effect 2 = 12,040 lb/hr
Evaporation from effect 3 = 14,296 lb/hr

6. Based on the quantities determined in the preceding step, compute the required heating surface area for each effect.

$$A_1 = \frac{13{,}600 \times 934}{700 \times 21} = 865 \text{ ft}^2$$

$$A_2 = \frac{11{,}020 \times 952}{600 \times 25} = 700 \text{ ft}^2$$

$$A_3 = \frac{12{,}040 \times 976}{500 \times 29} = 810 \text{ ft}^2$$

7. Re-estimate the concentration of solution discharged from each effect on the basis of the evaporation quantities estimated in step 5.

Concentration of discharge from effect 1 = 12.8 percent
Concentration of discharge from effect 2 = 19.2 percent
Concentration of discharge from effect 3 = 38.5 percent

Since the revised concentrations are so close to those assumed in the first trial, the boiling point elevations are assumed to remain the same.

8. The temperature drop across each effect is adjusted for the second trial by multiplying by the ratio of the area of heating surface computed for the effect in the first trial to the average of the three areas.

$$\Delta T_1 = 21 \times \frac{865}{792} = 23\ ^\circ\text{F}$$

$$\Delta T_2 = 25 \times \frac{700}{792} = 22\ ^\circ\text{F}$$

$$\Delta T_3 = 29 \times \frac{810}{792} = 30\ ^\circ\text{F}$$

9. Based on estimated boiling point elevations and revised temperature drops, re-establish temperature conditions throughout system.

	Effect 1	Effect 2	Effect 3	Condenser
Vapor, °F	243	215	173	125
Solution, °F	243	215	173	
Heating medium, °F	266	237	203	

10. Following the procedure outline in trial 1, strike a new heat balance across each effect, compute evaporation quantities, and determine required heating surface areas.

$$A_1 = 790\ \text{ft}^2$$

$$A_2 = 800\ \text{ft}^2$$

$$A_3 = 780\ \text{ft}^2$$

$$\bar{A} = 790\ \text{ft}^2$$

Notations

A Heating surface, ft^2; $\bar{A}$, average heating surface
q_h Rate of heat transfer, Btu/hr
T Temperature, °F; T, boiling point of water; T', boiling point of solution; ΔT, mean temperature difference
U Over-all heat transfer coefficient, (Btu)/(hr)(ft^2)(°F)
w Mass flow rate, lb/hr
λ Unit latent heat, Btu/lb force; λ, latent heat of water at boiling point of water; λ', latent heat of water at boiling point of solution

12

Psychrometry and humidification

12-1. Psychrometry

For present purposes, psychrometry is defined as the systematized knowledge of the properties and behavior of mixtures of water vapor and air.

Psychrometry has a wide application in sanitary engineering. It is used in the regulation of air temperature and humidity for physiological comfort, which is an important facet of environmental control. In the sewage and industrial waste field, psychrometric principles are employed in the design of drying and water-cooling operations.

12-2. Definitions

The *absolute humidity* H is the weight of water vapor carried by a unit weight of dry air. The absolute humidity is related to the partial pressure of the water vapor in the air by

$$H = \frac{M_v}{M_a}\left(\frac{\bar{p}}{p - \bar{p}}\right) = \frac{18}{29}\left(\frac{\bar{p}}{p - \bar{p}}\right) \qquad (12\text{-}1)$$

where H = absolute humidity, lb water vapor/lb dry air
M_v = molecular weight of water, lb force/lb mole
M_a = molecular weight of air, lb force/lb mole
$\bar{p}$ = partial pressure of the water vapor in the air, atm
p = total pressure of the air-water vapor mixture, atm

When the air is saturated with water vapor the absolute humidity is also the *saturation humidity* H_s.

The *relative humidity* H_R is the ratio of the partial pressure of the water vapor to the vapor pressure of water at the air temperature. On a percentage basis,

$$H_R = 100 \frac{\bar{p}}{\bar{p}_s} \tag{12-2}$$

where $\bar{p}_s$ = vapor pressure of water.

The *percentage humidity* or *relative saturation* H_p is the ratio of the absolute humidity to the saturation humidity at the air temperature, or

$$H_p = 100 \frac{H}{H_s} = 100 \left[\frac{\bar{p}/(p - \bar{p})}{\bar{p}_s/(p - \bar{p}_s)} \right] \tag{12-3}$$

The *dry volume* v or *specific volume* is the volume occupied by a unit weight of dry air. The *humid volume* v_H is the total volume of a unit weight of dry air and the water vapor it contains. When the air is saturated, the humid volume becomes the *saturated volume* v_s. For one pound of air,

$$v = \frac{V_M{}^0}{M_a p} \frac{T_A}{492} = \frac{359}{29p} \frac{T_A}{492} = 0.0252 \frac{T_A}{p} \tag{12-4}$$

and

$$v_H = v + \frac{V_M{}^0 H}{M_v p} \frac{T_A}{492} = v + \frac{359H}{18p} \frac{T_A}{492} = v + 0.0406H \frac{T_A}{p} \tag{12-5}$$

where v = dry volume, ft^3/lb dry air
v_H = humid volume, ft^3/lb dry air
$V_M{}^0$ = volume of gas per mole at standard conditions, ft^3/lb mole
T_A = absolute temperature, °R
p = pressure, atm

The *humid heat* c_s is the quantity of heat required to raise the temperature of a unit weight of dry air and its accompanying water vapor one degree. Assuming the specific heats of dry air and water vapor to be constant over the range of temperature normally encountered,

$$c_s = (c_p)_{\text{air}} + H(c_p)_{\text{water vapor}} = 0.24 + 0.45H \tag{12-6}$$

where c_s = humid heat, Btu/lb dry air
c_p = specific heat at constant pressure, (Btu)/(lb)(°F)

The *enthalpy* of an air-water vapor mixture is the sum of the relative enthalpies of the dry air and the water vapor in the mixture. The total enthalpy can be determined from

$$i = (c_p)_{\text{air}}(T - T_0) + H[\lambda_0 + (c_p)_{\text{water vapor}}(T - T_0)]$$

$$= c_s(T - T_0) + H\lambda_0 \qquad (12\text{-}7)$$

where i = enthalpy, Btu/lb dry air
T_0 = base temperature, °F
λ_0 = latent heat of vaporization at base temperature

The *dew point* T_{dp} is the temperature to which air with a given absolute humidity must be cooled in order to become saturated.

The *dry-bulb temperature* T_a is that temperature obtained by placing a dry bulb of a thermometer in contact with a mixture of air and water vapor and allowing it to come to thermal equilibrium.

The *wet-bulb temperature* T_w can be defined as the steady-state temperature reached by a small mass of water with a surface exposed to air in such a manner that the heat carried away by evaporation is balanced by the heat transferred from the air to the water. The wet-bulb temperature can be obtained by passing air rapidly over a thermometer bulb covered with an absorbent wick saturated with water.

12-3. Psychrometric Charts

Psychrometric calculations are facilitated through the use of a chart such as is shown in Figure 12-1. Use of this chart is illustrated in Figure 12-2.

A sample of air with properties locating it at point A would have a dry-bulb temperature of T_a, an absolute humidity of H, and a relative saturation of 20 percent. If the air is cooled at constant humidity, its dew point will be reached at T_{dp}. The humid heat of the sample is found to be c_s. The volume of dry air in the sample (at T_a) is v, whereas the volume of the same air if it were saturated with moisture would be v_s. If the air is cooled adiabatically from its initial condition at A, the dry-bulb temperature-humidity relationship will follow the adiabatic saturation line to the 100 percent relative saturation line. The temperature at this point, T_s, is called the *adiabatic saturation temperature.*

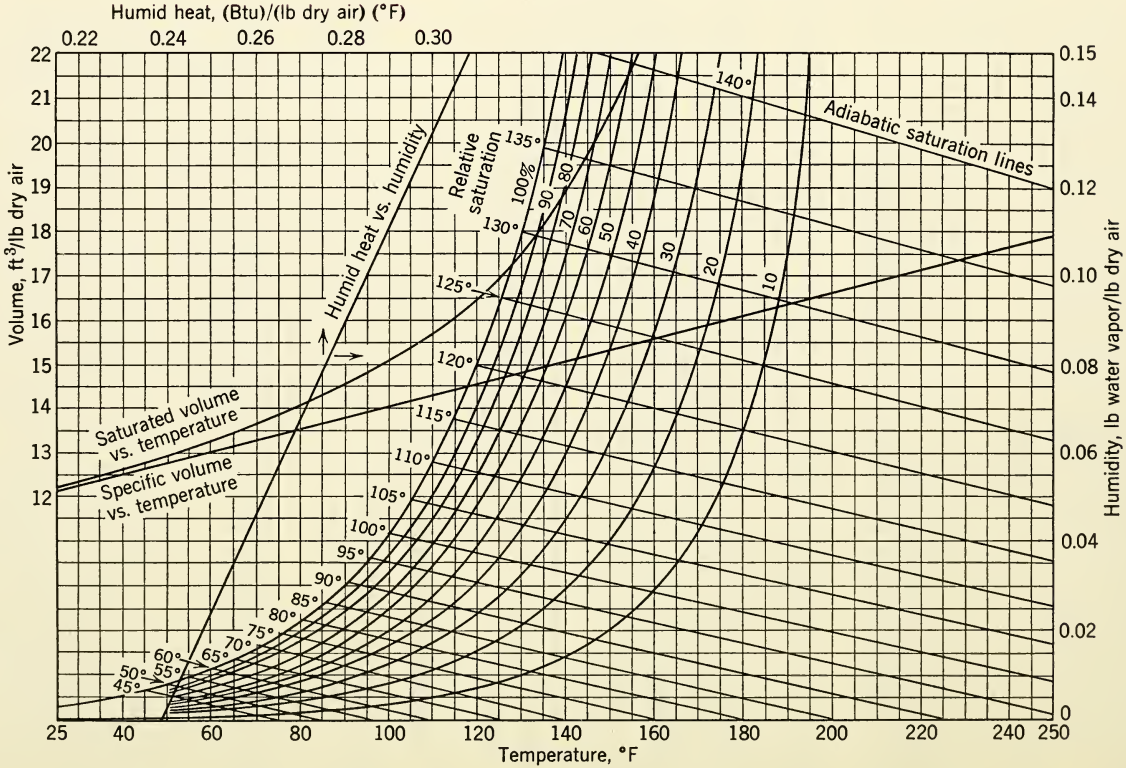

FIGURE 12-1. Psychrometric chart for the air-water vapor system at a pressure of 1 atm. [From Grosvenor, W. M., *Trans. Am. Inst. Chem. Engrs.*, **1** (1908), 184.]

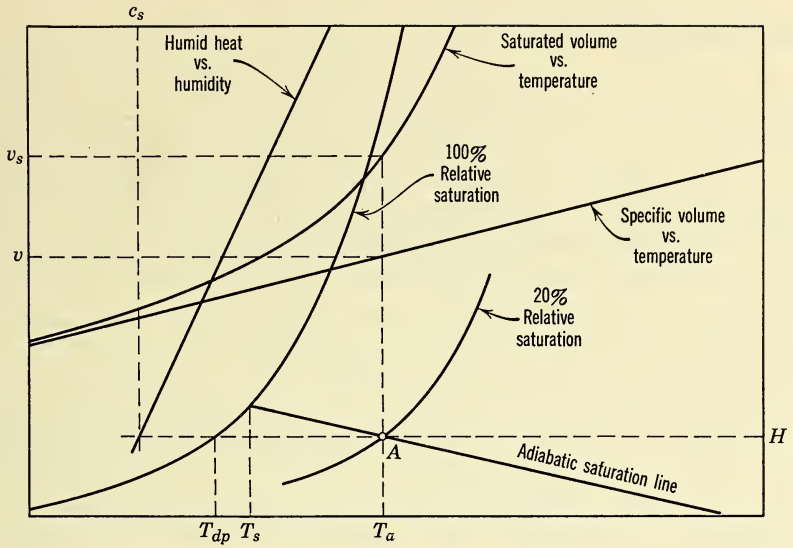

FIGURE 12-2. Illustration showing use of psychrometric chart.

EXAMPLE 12-1

A sample of air has a dry-bulb temperature of 110 °F and an absolute humidity of 0.02 lb water vapor/lb dry air. Determine (*a*) the relative saturation, (*b*) the dew point, and (*c*) the temperature and humidity reached should the air be cooled adiabatically to its saturation point.

Solution

(*a*) On the psychrometric chart the temperature line $T_a = 110$ °F and the absolute humidity line $H = 0.02$ intersect at a point between the 30 and 40 percent relative saturation lines. By interpolating, the relative saturation is found to be about 33 percent.

(*b*) Reading to the left along the humidity line $H = 0.02$, the relative saturation line of 100 percent is intersected at $T = 75$ °F. This is the dew point.

(*c*) As the air is cooled adiabatically, the temperature-humidity characteristics move left along a line parallel to the adiabatic saturation lines. The air becomes 100 percent saturated at a temperature of about 84 °F. The absolute humidity at this point is approximately 0.025 lb water vapor/lb dry air.

12-4. Wet-Bulb Theory

The relationship between humidity and the wet- and dry-bulb temperatures of the air can be derived from a consideration of what happens when air is constantly being passed over a thermometer bulb covered by a wick continually wetted by water. Figure 12-3 illustrates how undersaturated air is being replaced continually across a limited water surface by more air, the air temperature and humidity being constant. The water surface, assumed to be at air temperature at the beginning, represents the free moisture held by the wick.

Initially, evaporation reduces the sensible heat of the water. At the same time, the resulting difference between the temperature of the air and that of the water causes heat to flow from the air to the water. As evaporation proceeds, the temperature difference becomes larger and larger until a gradient is reached where the flow of heat from the air equals that which is released from the water through vaporization. The temperature, called the wet-bulb temperature, from there on will remain constant.

Under steady-state conditions the rate at which heat is removed through evaporation can be found from

$$q_h = w\lambda_{T_w} \tag{12-8}$$

where q_h = rate of heat transfer, Btu/hr
w = weight of water evaporated per unit of time, lb/hr
λ_{T_w} = latent heat of vaporization at the wet-bulb temperature, Btu/lb

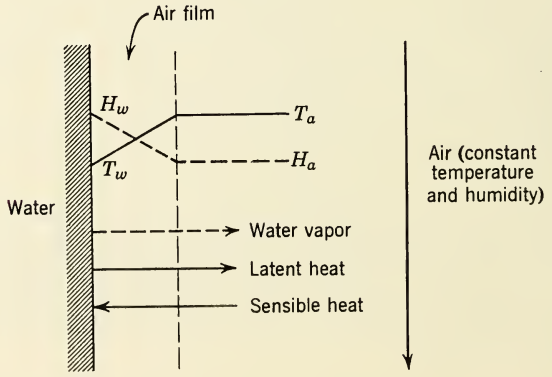

FIGURE 12-3. Conditions assumed in the development of wet-bulb theory.

The rate at which water is evaporated can be determined from an expression for the rate of diffusion of water vapor across the stationary air film at the air-water interface,

$$w = k_G A M_v(\bar{p}_w - \bar{p}_a) \tag{12-9}$$

where A = interfacial area, ft^2
k_G = mass transfer coefficient, gas phase, (lb mole)/(hr)(ft^2)(atm)
$\bar{p}_w$ = vapor pressure of water at the wet-bulb temperature, atm
$\bar{p}_a$ = partial pressure of the water vapor in the air, atm

Substituting Equation 12-9 for w in Equation 12-8

$$q_h = k_G A M_v \lambda_{Tw}(\bar{p}_w - \bar{p}_a) \tag{12-10}$$

Since $\bar{p}$ is generally small in comparison with the total pressure p, Equation 12-1 may be modified,

$$H = \frac{M_v}{M_a}\left(\frac{\bar{p}}{p - \bar{p}}\right) \cong \frac{M_v}{M_a}\frac{\bar{p}}{p}$$

and

$$\bar{p} = \left(\frac{M_a p}{M_v}\right) H \tag{12-11}$$

Equation 12-10 can be written as

$$q_h = M_a p k_G A \lambda_{Tw}(H_w - H_a) \tag{12-12}$$

where H_a = humidity of the bulk air
H_w = saturation humidity at temperature T_w

The rate at which heat flows from the air to the water surface can be expressed as

$$q_h = h_G A(T_a - T_w) \tag{12-13}$$

where h_G = heat transfer film coefficient, gas phase, (Btu)/(hr)(ft^2)(°F). At steady state, the removal of heat through evaporation equals the transfer of heat from the air to the water surface.

Equating Equations 12-12 and 12-13,

$$h_G A(T_a - T_w) = M_a p k_G A \lambda_{Tw}(H_w - H_a)$$

and

$$H_w - H_a = \frac{h_G}{M_a p k_G}\left(\frac{T_a - T_w}{\lambda_{Tw}}\right) = \frac{h_G}{k_Y}\left(\frac{T_a - T_w}{\lambda_{Tw}}\right) \tag{12-14}$$

where $k_Y = M_a p k_G$ = mass transfer coefficient, gas phase, (lb mass)/(hr)(ft^2)(ΔH).

The film coefficient k_Y is commonly used in humidification operations. Since this coefficient is computed directly from ΔH values, the necessity for making the assumption of Equation 12-11 may be foregone. The latter relationship may be poor for high temperatures and humidities.

With Equation 12-14, the absolute humidity of an air sample can be determined from a knowledge of the wet- and dry-bulb temperatures, the saturation humidity at the wet-bulb temperature, and the value of h_G/k_Y. As long as the air flow conditions surrounding the bulb are turbulent, the ratio h_G/k_Y is independent of the air velocity. For air-water systems under a total pressure of 1 atm, the value of h_G/k_Y is approximately equal to 0.24.[1]

12-5. Adiabatic Cooling

Frequently, the engineer is concerned with the change in the temperature and humidity of a quantity of air as the air undergoes prolonged contact with a free water surface under adiabatic conditions.

Consider an adiabatic operation in which undersaturated air is brought into intimate contact with recirculated water. If the temperature of the water initially is the same as that of the incoming air, the former will drop as evaporation takes place. At the same time, sensible heat will flow from the air to the water in response to the temperature difference developing across the stationary air film at the air-water interface. Ultimately there is established a steady state wherein the water is at the adiabatic saturation temperature T_s. If the contact between the water and air is sufficiently long, the temperature of the exit air will be close to T_s and its humidity close to saturation.

For such conditions, a heat balance can be struck for the air component. Using T_s as a datum,

$$G_G c_s(T_a - T_s) + G_G H_a \lambda_s = G H_s \lambda_s \qquad (12\text{-}15)$$

where G_G = mass velocity of dry air, (lb mass)/(ft^2)(hr)
c_s = humid heat of entering air on a dry basis, Btu/lb mass
T_a = dry-bulb temperature of entering air, °F
H_a = humidity of entering air
λ_s = latent heat of vaporization at the adiabatic saturation temperature, Btu/lb
H_s = saturation humidity at the adiabatic saturation temperature

Rearranging,

$$H_s - H_a = \frac{c_s(T_a - T_s)}{\lambda_s} \qquad (12\text{-}16)$$

[1] Treybal, R. E., *Mass Transfer Operations*, McGraw-Hill Book Co., New York (1955), 169.

Equation 12-16 is the mathematical expression of the family of adiabatic saturation lines shown in Figure 12-1.

By dividing Equation 12-14 by Equation 12-16,

$$\left(\frac{H_w - H_a}{H_s - H_a}\right)\left(\frac{T_a - T_s}{T_a - T_w}\right)\left(\frac{\lambda_s}{\lambda_{Tw}}\right) = \frac{h_G}{k_Y c_s} \tag{12-17}$$

where $h_G/k_Y c_s$ = psychrometric ratio.

For air-water systems, the psychrometric ratio is approximately unity. This fortuitous coincidence makes the adiabatic saturation temperature and the wet-bulb temperature closely identical and permits the use of adiabatic cooling lines as wet-bulb curves for such systems.

EXAMPLE 12-2

A sample of air has a dry-bulb temperature of 120 °F and a wet-bulb temperature of 90 °F. Determine the absolute humidity of the sample by (*a*) using Equation 12-11 and (*b*) using Figure 12-1 alone.

Solution

(*a*) From Figure 12-1, the saturation humidity H_w at 90 °F is found to be 0.031. From Appendix 10, λ_{Tw} is 1042.

$$0.031 - H_a = 0.24 \times \frac{120 - 90}{1042}$$

and

$$H_a = 0.024$$

(*b*) Following the 90 °F adiabatic saturation line on Figure 12-1 to an intersection with the 120 °F temperature line, an absolute humidity of 0.024 is obtained.

12-6. Water Coolers

In Figure 12-4*a*, hot water is being cooled by contacting it with air in a counterflow arrangement in a cooling apparatus. Figure 12-4*b* is a schematic diagram depicting conditions as they are assumed to exist at an air-water interface at the top of the apparatus. It is to be noted that both heat and mass transfers are taking place between the phases. Sensible heat is transferred to the air as the result of the temperature difference existing between the interface and the bulk air. The rate at which it is transferred per unit cross section in a differential length of apparatus is

$$G_G c_s dT_a = h_G a(T_i - T_a)\, dZ \cong k_Y a c_s (T_i - T_a)\, dZ \tag{12-18}$$

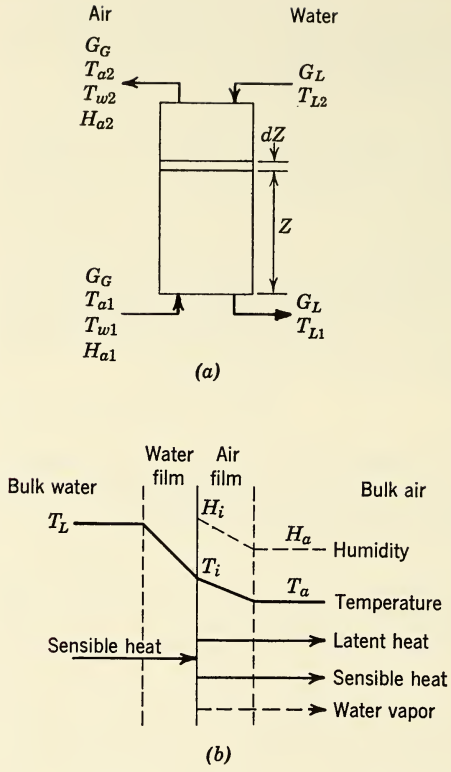

FIGURE 12-4. Water cooling. (*a*) Counterflow cooling apparatus. (*b*) Conditions assumed to exist at an air-water interface at top of apparatus.

where G_G = superficial mass velocity of dry air, (lb mass)/(hr)(ft^2)
c_s = humid heat, (Btu)/(lb dry air)(°F)
h_G = heat transfer film coefficient, gas phase, (Btu)/(hr)(ft^2)(°F)
a = interfacial surface area per unit volume of apparatus, ft^2/ft^3
k_Y = mass transfer film coefficient, gas phase, (lb mass)/(hr)(ft^2)(ΔH)
Z = height of apparatus, ft
T_i, T_a = temperature at the interface and of the bulk air respectively, °F

Also, the rate at which water vapor is being transferred in the same differential length of apparatus is

$$G_G\, dH = k_Y a(H_i - H_a)\, dZ \qquad (12\text{-}19)$$

where H_i, H_a = absolute humidity at the interface and in the bulk air respectively.

By multiplying both sides of Equation 12-19 by the latent heat of vaporization at the base temperature, λ_0, and adding this equation to Equation 12-18,

$$G_G c_s \, dT_a + G_G \lambda_0 \, dH = k_Y a c_s (T_i - T_a) \, dZ + k_Y a \lambda_0 (H_i - H_a) \, dZ \tag{12-20}$$

If the change in enthalpy taking place in the differential length of apparatus is

$$di_a = c_s \, dT_a + \lambda_0 \, dH \tag{12-21}$$

and if

$$i_i = c_s (T_i - T_0) + \lambda_0 H_i \tag{12-22}$$

$$i_a = c_s (T_a - T_0) + \lambda_0 H_a \tag{12-23}$$

then Equation 12-20 can be written as

$$G_G \, di_a = k_Y a (i_i - i_a) \, dZ \tag{12-24}$$

where i_i, i_a = enthalpy of the air at the interface and in the bulk air respectively, Btu/lb dry air.

The temperature and, hence, the enthalpy at the interface are indeterminate. For this reason use is made of an enthalpy term based on a determinate temperature.[2]

$$G_G \, di_a = K_Y a (i^* - i_a) \, dZ \tag{12-25}$$

where $K_Y a$ = over-all volumetric mass transfer coefficient, (lb mass)/(hr)(ft^3)(ΔH)

i^* = enthalpy of a saturated air-water mixture in equilibrium with the bulk of the water (at T_L), Btu/lb dry air

Assuming that the ratio $G_G/K_Y a$ remains constant through the apparatus, Equation 12-25 is integrated over the length of the apparatus to give

$$Z = \frac{G_G}{K_Y a} \int_{i_{a1}}^{i_{a2}} \frac{di_a}{i^* - i_a} = H_{tOG} N_{tOG} \tag{12-26}$$

It is apparent that the design of a water cooler can be based on the transfer unit method (see Section 8-10). The over-all number of transfer units N_{tOG} can be determined by graphical integration. The equilibrium curve relates the enthalpy of saturated air to water temperature. Points for plotting the equilibrium curve can be computed with Equation 12-7,

[2] See Section 8-5 for a discussion of an analogous treatment given to concentrations and partial pressures.

using the saturation humidity H_s for the humidity term. The operating curve can be established from an enthalpy balance.

An enthalpy balance over a differential length of apparatus may be written as

$$G_L c_p \, dT_L = G_G \, di_a \tag{12-27}$$

where G_L = mass velocity of the water, (lb mass)/(hr)(ft^2)
c_p = specific heat at constant pressure, (Btu)/(lb mass)(°F)
T_L = bulk liquid temperature, °F

Although the mass velocity of the water will change as evaporation proceeds in the apparatus, the change will be small compared to the mass velocity of the entering water, and can be considered as equaling the latter.

Integrating Equation 12-27 between the limits imposed by the terminal conditions,

$$\begin{gathered} G_L c_p \int_{T_{L1}}^{T_{L2}} dT_L = G_G \int_{i_{a1}}^{i_{a2}} di_a \\ G_L c_p (T_{L2} - T_{L1}) = G_G (i_{a2} - i_{a1}) \end{gathered} \tag{12-28}$$

A plot of Equation 12-28 (water temperature versus enthalpy of the air-water vapor mixture) establishes a straight line which is the operating curve.

When both the operating and equilibrium lines are straight over the operating range of water temperature, the number of transfer units can be determined from

$$N_{tOG} = \frac{i_{a2} - i_{a1}}{(i^* - i_a)_{\text{lm}}} \tag{12-29}$$

where

$$(i^* - i_a)_{\text{lm}} = \frac{(i^* - i_{a1}) - (i^* - i_{a2})}{\ln [(i^* - i_{a1})/(i^* - i_{a2})]} \tag{12-30}$$

For design purposes, the difference between the exit liquid temperature and the wet-bulb temperature of the entering air, $T_{L1} - T_{w1}$, ordinarily is chosen to be from 5 to 10 °F.

When warm, humid air is contacted with water at such a temperature that the humidity at the air-water interface H_i is less than that of the warm air H_a, water vapor will diffuse from the air to the interface, thereby dehumidifying the air. For such operations, the design of apparatus capacity can be made with the use of Equation 12-26. However, in the case of dehumidification, the operating line falls above the equilibrium line, and the force motivating mass transfer is represented by $i_a - i^*$ rather than by $i^* - i_a$.

Water-cooling operations can be carried out in a variety of contacting equipment. Packed towers and tray towers of the types ordinarily used in gas transfer can be employed for such operations. Of more popular use, however, are cooling towers constructed of tiers of horizontal wood slats. The tiers are arranged in such a manner that the water is intercepted repeatedly by the slats as it drops through the tower. Air circulation can be either natural or forced. In towers having natural circulation, the flow of air is either horizontal across the tower or vertical, induced by the rise of warm air from the top of the tower.

EXAMPLE 12-3

A 6-ft-square tower consisting of $\frac{3}{8}$-in. $\times$ 2-in. wood slats arranged horizontally in tiers, 12 in. apart, is to be used to air-cool an aqueous waste prior to its discharge into a small trout stream. The air with a dry-bulb temperature of 70 °F and a wet-bulb temperature of 60 °F is to be blown into the bottom of the tower at a rate of 30,000 lb dry air/hr. The liquid waste with a temperature of 130 °F is introduced at the top of the tower at a rate of 25,000 lb/hr. At the flow rates to be used, the over-all volumetric mass transfer coefficient applicable to the design of such a tower is reported to be

$$K_Y a = 0.286 G_L^{0.4} G_G^{0.5}$$

If the waste is to be cooled to 70 °F prior to discharge, how high must be the tower?

Solution

1. From the psychrometric chart (Figure 12-1), air with dry-bulb and wet-bulb temperatures of 70 °F and 60 °F respectively has an absolute humidity of 0.009 and a humid heat of 0.242 (Btu)/(lb dry air) (°F).

2. Using a base temperature of 32 °F, the enthalpy of the entering air is computed from Equation 12-7.

$$i_{a1} = 0.242(70 - 32) + 0.009 \times 1076 = 20 \text{ Btu/lb dry air}$$

3. The enthalpy of the exiting air is computed from Equation 12-28.

$$\frac{25{,}000}{36} (130° - 70°) = \frac{30{,}000}{36} (i_{a2} - 20)$$

$$i_{a2} = 70 \text{ Btu/lb dry air}$$

4. Construct an operating line on a plot of enthalpy versus liquid temperature by drawing a straight line between terminal conditions (see Figure 12-5).

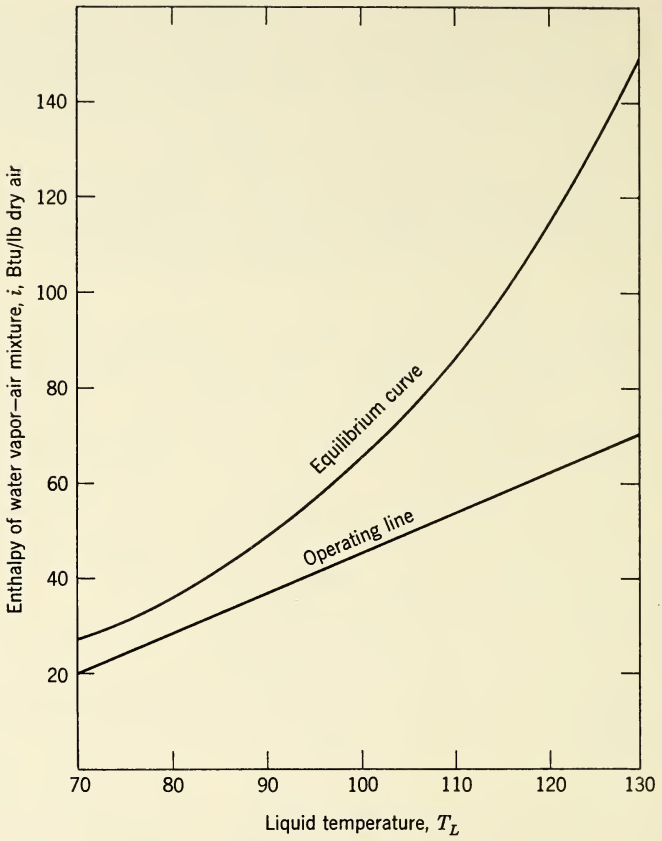

FIGURE 12-5. Operating and equilibrium curves used in the solution of Example 12-3.

5. Construct an equilibrium curve with enthalpy values computed with Equation 12-7, using the saturation humidity H_s for the humidity term (see Figure 12-5).

6. Solve for the over-all number of transfer units by a graphical integration of the term $di_a/(i^* - i_a)$. As the first step, Table 12-1 is prepared with the use of enthalpy values obtained from the curves in Figure 12-5. The second step involves the construction of a curve from values found in the last two columns of Table 12-1 (see Figure 12-6). As the third step, the curve thus constructed is integrated graphically between the terminal enthalpy conditions $i_a = 20$ and $i_a = 70$. From the graphical integration performed in Figure 12-6,

$$N_{tOG} = \int_{20}^{70} \frac{di_a}{i^* - i_a} = 3.25$$

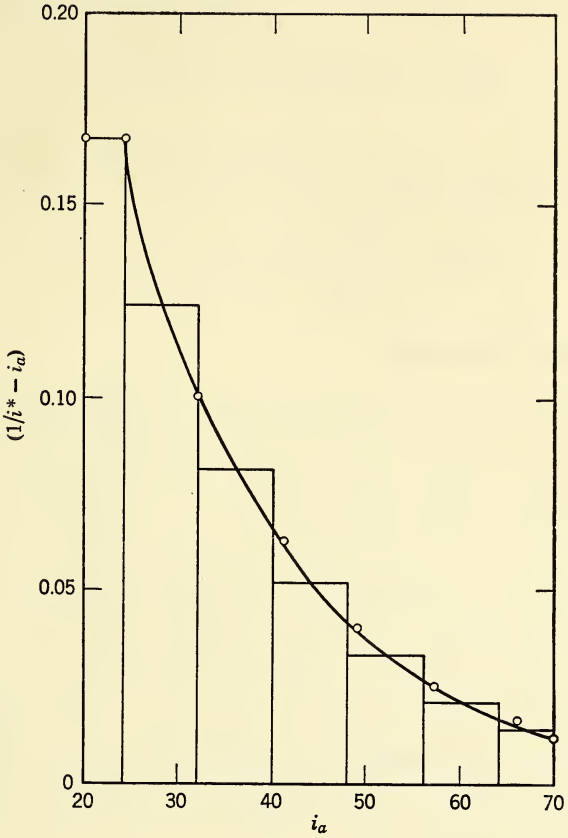

FIGURE 12-6. Graphical integration performed for the solution of Example 12-3.

TABLE 12-1. TABULATED VALUES USED FOR PLOTTING CURVE IN FIGURE 12-6

T_L, °F	i^* (Equilibrium Curve)	i_a (Operating Line)	$1/i^* - i_a$
70	26	20	0.167
75	30	24	0.167
85	42	32	0.100
95	57	41	0.063
105	74	49	0.040
115	98	57	0.024
125	130	66	0.016
130	148	70	0.013

7. The over-all volumetric mass transfer coefficient is computed to be

$$K_Y a = 0.286 \left(\frac{25{,}000}{36}\right)^{0.4} \left(\frac{30{,}000}{36}\right)^{0.5}$$

$$= 113 \text{ (lb mass)/(hr)(ft}^3\text{)}(\Delta H)$$

8. Solve Equation 12-26 for height of tower.

$$Z = \frac{30{,}000/36}{113} \times 3.25 = 24 \text{ ft}$$

12-7. Adiabatic Humidifiers

Frequently, air with a certain temperature and humidity is required. Such air can be produced by the series of operations indicated in Figure 12-7*a*. Here, air with a temperature T''_a and humidity H_{a2} is prepared from air initially with a temperature T'_a and humidity H_{a1}. After first heating the air to a temperature T_{a1}, it is cooled adiabatically by bringing it into close contact with a water surface. The air is cooled to a temperature T_{a2} at which point the desired humidity is reached. A final heating imparts the required temperature to the air.

Adiabatic humidification is commonly carried out in a horizontal chamber, baffled at both ends and fitted with centrifugal spray nozzles. Water collected at the bottom is recirculated. As a rule, make-up water is used with a temperature such that the water temperature in the humidifier remains close to the adiabatic saturation temperature. The heating operations are accomplished by passing the air over heated coils or banks of finned tubes.

Figures 12-7*b* and *c* will be of assistance in following the development of expressions relating to humidifier capacity.

If air is humidified in a spray chamber of length Z, the rate at which water vapor is transferred across the air film at the air-water interface present in a differential length of chamber is

$$G_G \, dH_a = k_Y a (H_s - H_a) \, dZ \tag{12-31}$$

where H_s = saturation humidity at the adiabatic saturation temperature.

Integrating Equation 12-31 over the length of the chamber,

$$\int_{H_{a1}}^{H_{a2}} \frac{dH_a}{H_s - H_a} = \frac{k_Y a}{G_G} \int_0^Z dZ$$

$$\ln \frac{H_s - H_{a1}}{H_s - H_{a2}} = \frac{k_Y a}{G_G} Z \tag{12-32}$$

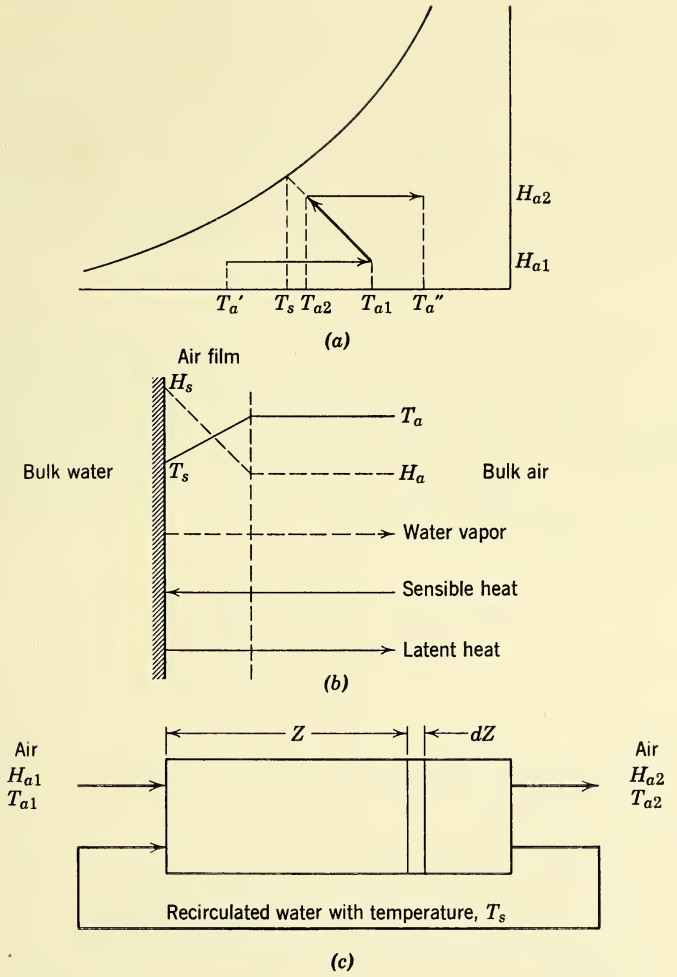

FIGURE 12-7. Adiabatic humidification. (*a*) Psychrometric relationship. (*b*) Heat and mass transfer. (*c*) Diagram of spray chamber.

Or, in terms that are used in the transfer unit method,

$$Z = \frac{k_Y a}{G_G}\left(\ln \frac{H_s - H_{a1}}{H_s - H_{a2}}\right) = H_{tG}N_{tG} \tag{12-33}$$

The terms $k_Y a/G$ and H_{tG} can be evaluated for any specific type of spray chamber.

EXAMPLE 12-4

Air initially with a percentage humidity of 40 percent and a temperature of 60 °F is to be heated to 175 °F and then humidified adiabatically in a spray chamber having a cross section of 16 ft^2, a length of 5 ft, and, at an air flow rate of G_G = 1000 (lb)/(hr)(ft^2), a volumetric mass transfer film coefficient $k_Y a$ equal to 400 (lb mass)/(hr)(ft^2)(ΔH_a). What will be the absolute humidity of the air leaving the chamber when the flow rate G_G is 1000 (lb)/(hr)(ft^2)?

Solution

1. Locate on the psychrometric chart the point representing the initial conditions. The absolute humidity H_{a1} corresponding to this point is found to be 0.005. Moving right along the 0.005 humidity line, the temperature line at 175 °F is intersected at a point through which the 84 °F adiabatic cooling line would pass. The saturation humidity at the adiabatic saturation temperature (84 °F) is found to be 0.026.

2. Solving Equation 12-32 for H_{a2}

$$\ln \frac{0.026 - 0.005}{0.026 - H_{a2}} = \frac{400}{100} \times 5$$

$$H_{a2} = 0.023$$

Notations

a	Area of air-water interface per unit volume, ft^2/ft^3
A	Interfacial area, ft^2
c_p	Specific heat at constant pressure, (Btu)/(lb)(°F)
c_s	Humid heat, Btu/lb dry air
G_G	Superficial mass velocity of dry air, (lb mass)/(ft^2)(sec)
G_L	Superficial mass velocity of water, (lb mass)/(ft^2)(hr)
h_G	Heat transfer film coefficient, gas phase, (Btu)/(hr)(ft^2)(°F)
H	Absolute humidity, lb water vapor/lb dry air; H_a, humidity of entering air; H_s, saturation humidity; H_w, saturation humidity at T_w; H_R, relative humidity; H_p, percentage humidity
H_{tOG}	Over-all height of a transfer unit, gas phase, ft
i	Enthalpy, Btu/lb dry air; i^*, enthalpy of a saturated air-water mixture in equilibrium with the bulk of the water (at T_L)
k_G	Mass transfer coefficient, gas phase, (lb mole)/(hr)(ft^2)(atm)
k_Y	Mass transfer coefficient, gas phase, (lb mass)/(hr)(ft^2)(ΔH)
$K_Y a$	Over-all volumetric mass transfer coefficient, (lb mass)/(hr)(ft^3)(ΔH)
M	Molecular weight, lb force/mole; M_v, molecular weight of water; M_a, molecular weight of air
N_{tOG}	Over-all number of transfer units, gas phase, dimensionless
p	Total pressure, atm

$\bar{p}$ Partial pressure, atm; $\bar{p}_w$, vapor pressure of water at the wet-bulb temperature; $\bar{p}_a$, partial pressure of the water vapor in the air; $\bar{p}_s$, vapor pressure of water

q_h Rate of heat transfer, Btu/hr

T Temperature, °F; T_{dp}, dew point; T_a, dry-bulb temperature; T_w, wet-bulb temperature; T_s, adiabatic saturation temperature; T_0, base temperature

T_A Absolute temperature ($T + 460$), °R

v Dry or specific volume, ft^3/lb dry air

v_H Humid volume, ft^3/lb dry air

v_s Saturated volume, ft^3/lb dry air

$V_M{}^0$ Volume of gas per mole at standard conditions, ft^3/lb mole

w Mass flow rate, lb force/hr

λ Latent heat of vaporization, Btu/lb force; λ_{Tw}, latent heat of vaporization at the wet-bulb temperature; λ_s, latent heat at the adiabatic saturation temperature; λ_0, latent heat of vaporization at base temperature T_0

13

Drying

13-1. Introduction

Drying can be defined as the reduction of the liquid content (usually water) of solids or nearly solid materials. Moisture reduction can be accomplished through heating the solids by conduction or radiation, or by bringing the wet material into contact with unsaturated hot air or gases. Some drying operations involve only the exposure of solids to unsaturated air at normal temperature.

In waste treatment, drying is applied as a terminal dewatering operation, being preceded by one or a combination of operations such as settling, thickening, evaporation, and filtration. Heat drying is expensive and is most often used where the dried material is of commercial value. In general, air drying is employed to facilitate the disposal of worthless sludge.

13-2. Heat Dryers

A wide selection of equipment is available for heat-drying operations. The drying equipment employed by the sanitary engineer, however, is confined largely to two types: the rotary and the flash dryer.

Most rotary dryers consist of cylinders slightly inclined from the horizontal and equipped with lifting flights. When the dryer is rotated, the material being dried moves by gravity

from one end to the other. The dryer is called a direct rotary type if the material being dried comes into direct contact with the drying medium. If only indirect contact is made, the dryer is known as an indirect rotary type. Direct-indirect rotary dryers incorporate features of both.

In direct rotary dryers the flow of the air or gases constituting the heating medium can be either parallel or countercurrent to the drying charge. Parallel flow offers marked advantages for most drying operations. These include higher thermal efficiencies due to rapid cooling of the heating medium near the feed end with consequent lower radiation losses, a minimum of heat loss due to lower temperatures of the material discharged, and a higher evaporative capacity when handling heat-sensitive materials. As a rule, countercurrent flow is employed only when the material being dried is subject to case hardening or when a very low residual moisture is desired. Figure 13-1*a* is a flow sheet for a sludge-drying system which includes a direct rotary dryer.

Many direct rotary dryers have lifting flights fixed to the interior wall for carrying the charge to the top of the shell as the dryer rotates. Material carried to the top is released and falls through the air or gas stream, thereby promoting maximum contact between the material and the drying medium. This feature limits the use of the direct rotary type to materials which are not too dusty upon being dried. Nevertheless, the direct rotary dryer enjoys a wide application. Its relative simplicity makes it inexpensive and easy to operate.

Indirect rotary dryers are commonly employed where the material being dried is extremely dusty or when contact between the material and the drying medium is undesirable. In this type of dryer the material being dried is heated by metal surfaces, which, in turn, are heated by hot gases or steam. The heating medium flows through an insulated casing along the outside of the cylinder and/or passes through tubes located on the inside of the drying chamber.

Essentially, the direct-indirect rotary dryer is similar to the indirect dryers employing hot air or gases as a heating medium. In the former, however, an arrangement is provided whereby the heating medium is recirculated to flow in direct contact with the drying charge. The direct-indirect type is more expensive than the direct but is more efficient and has a higher capacity.

The rotary louver dryer consists of a horizontal, rotating cylinder, on the inside of which are louvers arranged in such a manner that they overlap each other to divide the cylinder into an inner and outer compartment. The drying medium enters the dryer at the feed end, passes through the outer compartment, and then flows between the louvers and

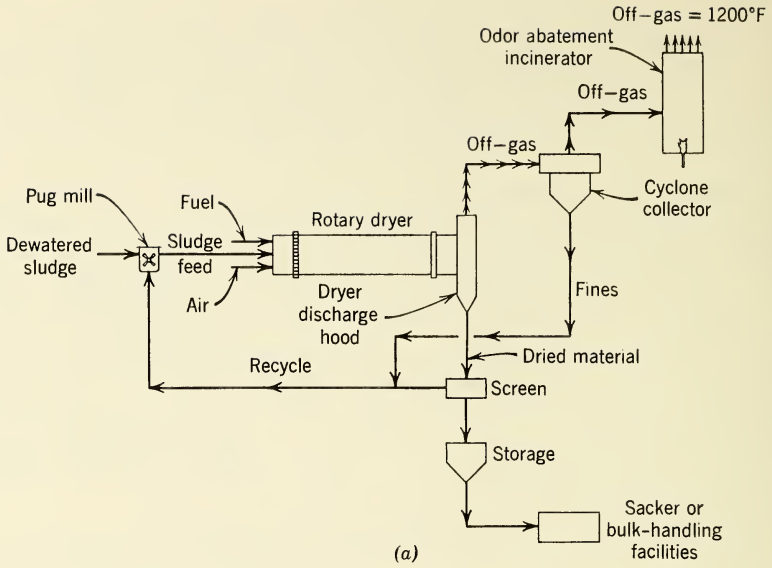
Off–gas = 1200°F
Odor abatement incinerator
Off–gas
Off–gas
Cyclone collector
Pug mill
Fuel
Rotary dryer
Dewatered sludge
Sludge feed
Air
Dryer discharge hood
Fines
Dried material
Recycle
Screen
Storage
Sacker or bulk-handling facilities

(a)

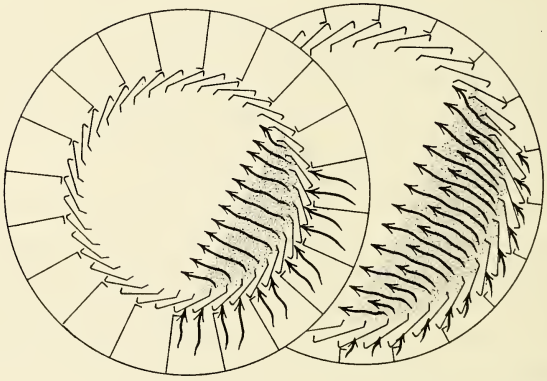

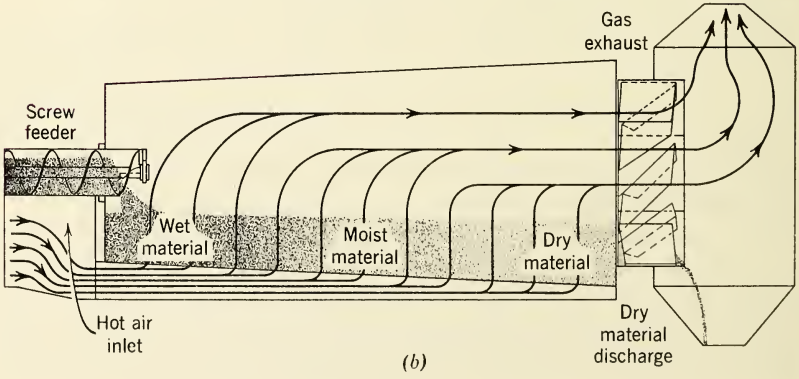
Gas exhaust
Screw feeder
Wet material
Moist material
Dry material
Hot air inlet
Dry material discharge

(b)

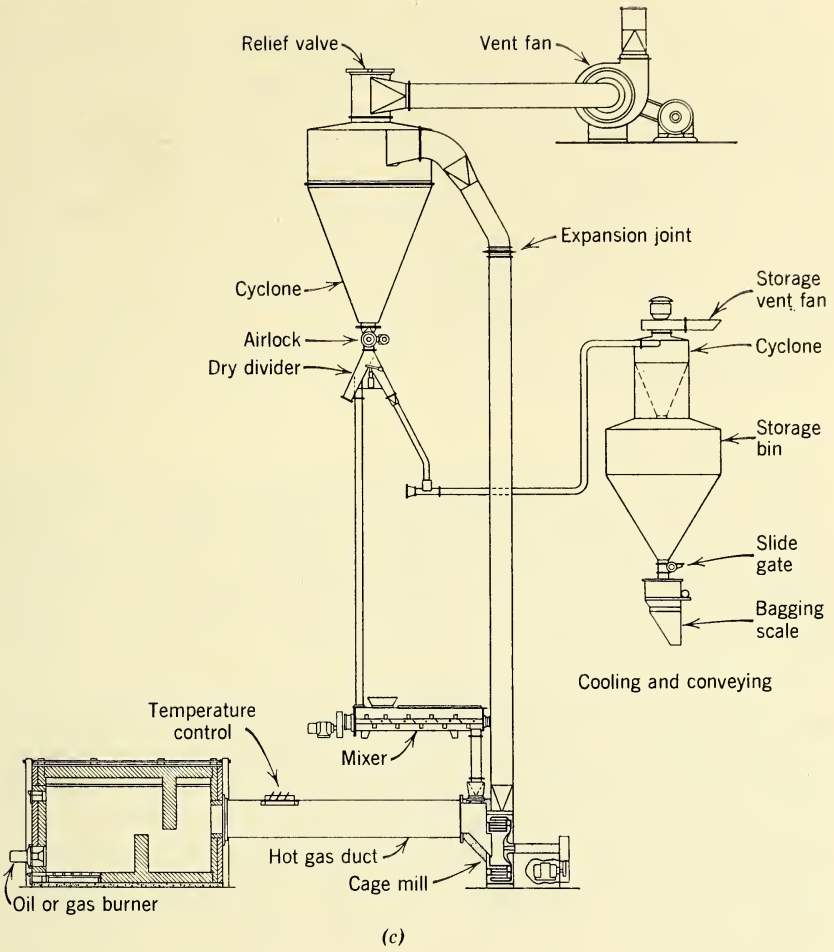

FIGURE 13-1. Dryer types. (*a*) Direct rotary dryer (*Standard Steel Corporation*). (*b*) Rotary louver dryer (*Link-Belt Company*). (*c*) Flash dryer (*Combustion Engineering Company*).

up through a bed of drying material into the inner compartment. Unlike most rotary dryers, the material being dried does not cascade throughout the cylinder volume. Instead, the material moves down the cylinder as a bed, subjected only to a gentle stirring action caused by the rotation of the cylinder. The latter feature minimizes dusting and particle breakage. Since drying is accomplished primarily through convective heat transfer, the louver dryer is a direct type. A schematic diagram of a rotary louver dryer is shown in Figure 13-1*b*.

Flash dryers derive their name from the fact that wet particles are dried in suspension in a stream of hot gases, providing an instantaneous removal of moisture. Reference to the flash dryer in Figure 13-1*c* will be helpful in understanding the operation of the system. A blend of wet and dry material is fed to a cage mill, where particles of the material are dispersed throughout a stream of hot gases. Gas-borne particles pass to a cyclone separator where the dried material is removed from the moisture-laden gases. A part of the dried material is automatically returned to the mixer for blending with incoming wet cake or sludge. This type of dryer is particularly applicable when size reduction as well as drying is desirable, or when the feed is a heat-sensitive material with low internal moisture.

13-3. Rates of Drying

Heat for drying may be supplied through either conduction, radiation, or convection. Some commercial dryers utilize all three forms of heat transfer. However, heat that is either primarily or entirely convective is used in the vast majority of waste treatment applications. For this reason the following discussion will be limited to drying with heated air.

Drying with heated air involves both heat and mass transfers. When air, warm and unsaturated, flows across a wet material, vaporization of the moisture occurs, and water vapor is transferred to the air in response to the humidity gradient across the air film. Initially, vaporization may occur at the expense of the sensible heat of the wet material. After steady-state conditions have been established, the latent heat requirements are met by the transfer of heat from the air to the vaporizing surface. Conditions existing at the steady state are illustrated in Figure 12-3.

An understanding of the mechanism of drying is facilitated by a study of drying rates. Consider a slab of wet solids being dried by a stream of air of constant inlet temperature, velocity, and humidity. If the temperature of the wet solids initially is at the wet-bulb temperature of the air, the drying rates when plotted as a function of solids moisture may describe a curve similar to the one in Figure 13-2. The curve for the drying operation indicates two separate periods: the constant-rate and falling-rate periods.

During the constant-rate period, the movement of liquid from the interior to the surface of the slab keeps pace with evaporation. Both heat and mass transfers are considered to be controlled by the resistance offered by an air film. The temperature of the wet material remains

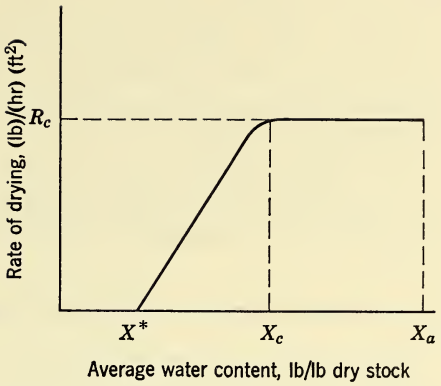

FIGURE 13-2. Rate-of-drying curve.

constant at the wet-bulb temperature of the air. The moisture content is reduced from the initial value X_a to the critical moisture content X_c.

After the critical moisture content has been reached, the movement of liquid through the slab can no longer keep up with evaporation. The plane of vaporization recedes from the exterior surface and, as a result, a zone is established in the slab which offers additional resistance to the transfer of heat and vapor. As the thickness of this zone increases, the rate at which drying proceeds decreases. If the material being dried is composed of nonporous, granular particles, the curve during the falling-rate period may be approximately straight, and drying will cease shortly after the plane of vaporization has passed through the slab. The falling-rate curve for porous and/or hygroscopic materials may vary considerably from a straight line. In either case, no further drying takes place after the equilibrium moisture content X^* is reached. The average temperature of the material increases during the falling-rate period and tends toward equilibrium with the temperature of the drying medium.

The critical moisture content is a function not only of the physical and chemical characteristics of the material itself but also depends on the drying rate and the thickness of the drying slab. Critical moisture conditions are reached at a higher moisture content when the drying rate is high and the slab thickness is large. The critical moisture content for a given material being dried under a given set of conditions may be determined through drying tests.

The equilibrium moisture content also is a function of the properties of the material and the conditions under which drying takes place. For any material in contact with air of a given temperature and humidity, there is an equilibrium moisture content below which moisture cannot be removed. At this moisture content, the vapor pressure of the bound

water is in balance with the humidity of the air. Nonporous, granular materials, even when in contact with air of high humidity, have an equilibrium moisture close to zero. On the other hand, the equilibrium moisture of hygroscopic materials in contact with high humidity air may be 30 percent or more.

The difference between the initial moisture and the equilibrium moisture is called the free moisture. It is the free moisture which is amenable to removal under the applied drying conditions.

13-4. Drying Equations—Constant Drying Conditions

The drying-rate curve in Figure 13-2 can be used to develop theoretical relationships from which an estimate can be made of the time required to accomplish drying under a given set of operating conditions.

For constant drying conditions, i.e., constant temperature of drying material and constant temperature, humidity, and velocity of the drying medium, the rate of drying during the constant-rate period is given by a modification of Equation 12-9.

$$w = \frac{W_1 - W_2}{t} = k_Y A(H_w - H_a) \tag{13-1}$$

where w = rate of drying, lb mass/hr
W_1, W_2 = initial and final mass of water in material, lb mass
t = drying time, hr
k_Y = mass transfer coefficient, gas phase, (lb mass)/(hr)(ft^2)(ΔH)
A = area of wetted surface exposed to drying medium, ft^2
H_w = saturation humidity at the wet-bulb temperature, lb water vapor/lb dry air
H_a = humidity of the air bulk, lb water vapor/lb dry air

The rate at which heat is required to vaporize w pounds of liquid water per hour is

$$q_h = w\lambda_{Tw} = k_Y A\lambda_{Tw}(H_w - H_a) \tag{13-2}$$

where λ_{Tw} = latent heat of vaporization at the wet-bulb temperature, Btu/lb mass.

When drying takes place under adiabatic conditions, the latent heat of vaporization is furnished only by the transfer of heat from the air. The rate at which the transfer of heat takes place is expressed by Equation 12-13,

$$q_h = h_G A(T_a - T_w) \tag{12-13}$$

where h_G = heat transfer film coefficient, gas phase, (Btu)/(hr)(ft^2)(°F)
T_a = dry-bulb temperature of the bulk air, °F
T_w = wet-bulb temperature of the air, °F

Through substitution and rearrangement of terms in Equations 13-1, 13-2, and 12-13,

$$q_h = h_G A(T_a - T_w) = k_Y A \lambda_{Tw}(H_w - H_a) = \frac{W_1 - W_2}{t}\lambda_{Tw} \tag{13-3}$$

and

$$t = \frac{\lambda_{Tw}}{h_G A}\left(\frac{W_1 - W_2}{T_a - T_w}\right) \tag{13-4}$$

Equation 13-4 can be used to compute the drying time for the constant-rate period.

As pointed out in Section 13-3, the drying curve during the falling-rate period may or may not be straight. In cases where the curve approaches a straight line, the rate of drying during this period is

$$-\frac{dW}{A\,dt} = \frac{R_c}{X_c - X^*}(X - X^*) = \frac{R_c}{\overline{X}_c}\overline{X} \tag{13-5}$$

where R_c = rate of drying during the falling-rate period, (lb mass)/(hr)(ft^2)
X = moisture content, lb water/lb dry solids
X_c = critical moisture content, lb water/lb dry solids
X^* = equilibrium moisture content, lb water/lb dry solids
$\overline{X}$ = free moisture content, lb water/lb dry solids
$\overline{X}_c$ = free moisture content at the critical point, lb water/lb dry solids

The change in moisture of the drying material can be expressed as

$$dW = W_d\,d\overline{X} \tag{13-6}$$

where W_d = mass of dry material, lb mass.

Through substitution and rearrangement, Equation 13-5 can be modified to give

$$dt = -\left(\frac{W_d\overline{X}_c}{AR_c}\right)\frac{d\overline{X}}{\overline{X}} \tag{13-7}$$

which upon integration becomes

$$t = -\frac{W_d\overline{X}_c}{AR_c}\int_{\overline{X}_1}^{\overline{X}_2}\frac{d\overline{X}}{\overline{X}} = \frac{W_d\overline{X}_c}{AR_c}\ln\frac{\overline{X}_1}{\overline{X}_2} \tag{13-8}$$

where $\overline{X}_1$ and $\overline{X}_2$ = initial and final free moisture content, lb water/lb dry solids.

Also, from Equation 13-3,

$$R_c = \frac{w}{A} = \frac{h_G}{\lambda_{Tw}} (T_a - T_w) \tag{13-9}$$

By substituting this expression into Equation 13-8

$$t = \frac{\lambda_{Tw} W_d \overline{X}_c}{h_G A (T_a - T_w)} \ln \frac{\overline{X}_1}{\overline{X}_2} \tag{13-10}$$

In most waste treatment applications, drying is performed on porous, hygroscopic materials. The falling-rate curves exhibited by such materials may vary considerably from a straight line. When this is the case, the curve may be expressed by

$$-\frac{dW}{A\,dt} = \psi(\overline{X}) \tag{13-11}$$

After substituting Equation 13-6 for dW, rearranging and integrating, the expression becomes

$$t = \frac{W_d}{A} \int_{\overline{X}_2}^{\overline{X}_1} \frac{d\overline{X}}{\psi(\overline{X})} \tag{13-12}$$

The drying time during the falling-rate period may be determined by a graphical integration of Equation 13-12.

The influence of air velocity on drying time can be expressed by velocity effects on the heat transfer coefficient. When air flow is parallel to the drying plane, it has been found that [1]

$$h_G = 0.0128 G_G^{0.8} \tag{13-13}$$

where G_G = mass velocity of dry air, (lb mass)/(ft^2)(hr).

For air flow normal to the drying plane [2]

$$h_G = 0.37 G_G^{0.37} \tag{13-14}$$

Equations 13-10 and 13-12 will apply only to situations where the thickness of the drying material is essentially the same as that for which the free moisture terms have been evaluated.

[1] Shepherd, C. B., C. Hadlock, and R. C. Brewer, *Ind. Eng. Chem.*, **30** (1938), 388.

[2] Molstad, N. C., P. Farevaag, and V. A. Farrell, *ibid.*, 1131.

13-5. Design of Continuous, Direct Rotary Dryers

Most drying operations are carried out under conditions in which the temperature and humidity of the drying medium change during the course of the operation. Such conditions as well as the mode of contact between the hot gases and drying material depend upon the particular features of the equipment employed. Consequently, the use of mathematical equations for design purposes is limited. Drying tests and previous experience must be relied on for the proper design of most dryers.

The direct rotary dryer is one type for which a reasonable mathematical analysis can be applied to a preliminary design.[3] The volume requirement of this type of dryer can be computed from the heat transfer expression

$$q_h = UaV(\Delta T)_m \tag{13-15}$$

where q_h = total heat transferred, Btu/hr
Ua = volumetric heat transfer coefficient, (Btu)/(hr)(°F)(ft^3 of dryer volume)
V = volume of dryer, ft^3
$(\Delta T)_m$ = over-all mean temperature difference between the drying medium and the material, °F

Temperature-length curves for a continuous, parallel-flow, direct rotary dryer are shown in Figure 13-3. Here, hot air or gases entering the dryer at a temperature T_{a1} exit at some cooler temperature T_{a2}. The feed, initially at temperature T_1, is heated by the drying medium until, at some distance L_1 from the feed end, the wet-bulb temperature of the drying medium is reached. From L_1 to L_2 the material dries at a constant rate, and the temperature remains constant at some value close to the wet-bulb temperature. At L_2, drying proceeds into the falling-rate period, and the temperature of the material increases until it is discharged at some temperature close to the exit temperature of the drying medium. It is apparent, therefore, that the dryer can be divided into three zones: the initial zone wherein the temperature of the feed is brought to the wet-bulb temperature of the drying medium; a second zone in which the temperature of the material remains essentially constant; and a final zone wherein the temperature of the material increases until the material is finally discharged from the dryer. The total heat

[3] Perry, J. H., *Chemical Engineers Handbook* (3rd ed.), McGraw-Hill Book Co., New York (1950), 831.

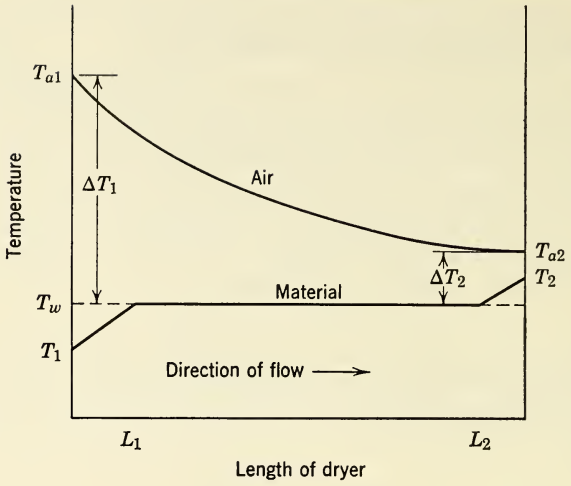

FIGURE 13-3. Temperature-length curves for a continuous, parallel-flow, direct rotary dryer.

transferred in the dryer will equal the sum of the heat transferred in each zone, or

$$q_h = q'_h + q''_h + q'''_h \tag{13-16}$$

In cases where considerable moisture is removed, the total heat transferred is approximately equal to that transferred in the second, or constant temperature, zone.

$$q_h \cong q''_h \tag{13-17}$$

and

$$(\Delta T)_m \cong \Delta T'' \tag{13-18}$$

where $\Delta T''$ = mean temperature difference between the drying medium and material in the constant temperature zone, °F.

The mean temperature difference in the constant temperature zone and, hence, the over-all mean temperature difference in the dryer can be approximated by the logarithmic mean difference between the wet-bulb temperature and the inlet and exit air temperatures. Frequently, allowance is made for radiation effects by assuming that the temperature of the material will remain constant at a value somewhat above the wet-bulb temperature.

The inlet temperature of the drying medium is generally fixed by the method by which it is heated. When steam coils are used, the air entering the dryer ranges in temperature from 250° to 300 °F. Gases

heated in gas or oil burners will have an initial temperature of 1000 °F or more. The selection of the proper exit temperature of the drying medium is based on economical considerations. It has been found that rotary dryers operate most economically when the following relationship holds [4]

$$1.5 < \frac{T_{a1} - T_{a2}}{(\Delta T)_m} < 2.0 \tag{13-19}$$

The value of the volumetric coefficient depends not only upon the equipment design and the air and feed rates employed in operation but also on the physical characteristics of the material being dried. It has been found [5] that the coefficient can be estimated with the expression

$$Ua = \frac{10 G_G^{0.16}}{D} \tag{13-20}$$

where G_G = mass velocity of air, (lb mass)/(ft^2)(hr)
D = diameter of dryer, ft

An accurate value of the coefficient can be obtained only from an analysis of pilot-plant data.

The mass velocity at which the drying medium is passed through direct rotary dryers varies from 200 to 10,000 lb/hr/ft^2. As a rule, the value employed is the highest that can be used without serious dusting of the drying material. For any given material, the value should be determined by tests.

Equation 13-15 can be used to estimate the volume requirements of a direct rotary dryer. The diameter of this type of dryer ranges from 1 to 10 ft and the length-to-diameter ratio from 4 to 10.

EXAMPLE 13-1

A continuous, parallel-flow, direct rotary dryer is to be designed to reduce the moisture content of a filter cake of material primarily organic from 50 to 10 percent. The drying medium is to be hot air with dry- and wet-bulb temperatures of 300 °F and 115 °F respectively. The feed rate will be 1000 lb/hr of dry solids, and the temperature of the cake as it enters the dryer will be 50 °F. Tests on the dried material reveal that a mass velocity as high as 450 lb/ft^2/hr can be used without excessive dusting. Determine the required length and diameter of the dryer.

[4] Perry, J. H., *Chemical Engineers Handbook* (3rd ed.), McGraw-Hill Book Co., New York (1950), 831.

[5] Friedman, S. J., and W. R. Marshall, *Chem. Engr. Progress*, **45** (1949), 482, 573.

Solution

1. To correct for radiation effects, it is assumed that during the constant-rate drying period the temperature of the material will remain constant at 5 °F above the wet-bulb temperature of the air, and that the heat transferred during the constant-rate period approximately will be equal to the total heat transferred. Therefore,

$$(\Delta T)_m \cong \frac{\Delta T_1 - \Delta T_2}{\ln (\Delta T_1/\Delta T_2)} = \frac{180 - (T_{a2} - 120)}{\ln [180/(T_{a2} - 120)]}$$

Assuming further that the following relationship holds,

$$\frac{T_{a1} - T_{a2}}{(\Delta T)_m} = \frac{300 - T_{a2}}{(\Delta T)_m} = 2$$

By substitution

$$\frac{300 - T_{a2}}{2} = \frac{300 - T_{a2}}{\ln [180/(T_{a2} - 120)]}$$

and

$$T_{a2} = 144 \text{ °F}$$

Therefore

$$(\Delta T)_m = \frac{300 - 144}{2} = 78 \text{ °F}$$

2. Assuming that the specific heat of the material being dried is 0.4, and the temperature of the material as it leaves the dryer is 140 °F, the heat transferred in the dryer will be:

Heat to remove moisture. For raising temperature of liquid to 120 °F = 889(120 − 50)	=	62,100 Btu/hr
Latent heat of vaporization = 889(1025)	=	910,000 Btu/hr
For superheat of vapor = 889[(0.45)(144 − 120)]	=	9,600 Btu/hr
Heat to solids = 1000[(0.4)(140 − 50)]	=	36,000 Btu/hr
	q_h =	1,017,700 Btu/hr

3. The mass velocity of air required for drying will be

$$G_G = \frac{1{,}020{,}000}{0.24(300 - 144)S} = \frac{27{,}200}{S} \text{ (lb)/(ft}^2\text{)(hr)}$$

Since a mass velocity of 450 lb/(ft^2)(hr) can be used,

$$S = \frac{27{,}200}{450} = 60.5 \text{ ft}^2$$

and the required diameter will be

$$D = 9 \text{ ft}$$

4. The volumetric heat transfer coefficient is estimated to be

$$Ua = \frac{10G_G^{0.16}}{D} = \frac{10(450)^{0.16}}{9} = 2.95 \text{ (Btu)/(hr)(°F)(ft}^3\text{)}$$

5. Dryer volume required will be

$$V = \frac{q_h}{Ua(\Delta T)_m} = \frac{1{,}020{,}000}{2.95 \times 78} = 4440 \text{ ft}^3$$

and the length will be

$$L = \frac{4440}{63.5} = 70 \text{ ft}$$

6. Since

$$\frac{L}{D} = \frac{70}{9} \cong 8$$

and

$$4 < 8 < 10$$

the dimensions are satisfactory.

Notations

A	Area of wetted surface, ft^2
D	Diameter, ft
G_G	Mass velocity of air, (lb mass)/(hr)(ft^2)
h_G	Heat transfer film coefficient, gas phase, (Btu)/(hr)(ft^2)(°F)
H	Humidity, lb water vapor/lb dry air; H_a, humidity of air bulk; H_w, saturation humidity at the wet-bulb temperature
k_Y	Mass transfer coefficient, gas phase, (lb mass)/(hr)(ft^2)(ΔH)
q_h	Heat flow, Btu/hr
R_c	Rate of drying during the falling-rate period, (lb mass)/(hr)(ft^2)
S	Cross-section area, ft^2
t	Drying time, hr
T	Temperature, °F; T_a, dry-bulb temperature of the bulk air; T_w, wet-bulb temperature of the air; $(\Delta T)_m$, over-all mean temperature difference between the drying medium and the material, °F
Ua	Volumetric heat transfer coefficient, (Btu)/(hr)(°F)(ft^3)
V	Volume, ft^3
w	Rate of drying, lb mass/hr
W	Mass of water, lb mass; W_d, mass of dry material

X Moisture content, lb water/lb dry solids; X_c, critical moisture content; X^*, equilibrium moisture content; $\overline{X}$, free moisture content; $\overline{X}_c$, free moisture content at the critical point

λ_{Tw} Latent heat of vaporization at the wet-bulb temperature, (Btu)/(hr)(ft^2)(°F)

ψ Operator

Appendix 1

DENSITY OF WATER AS A FUNCTION OF TEMPERATURE

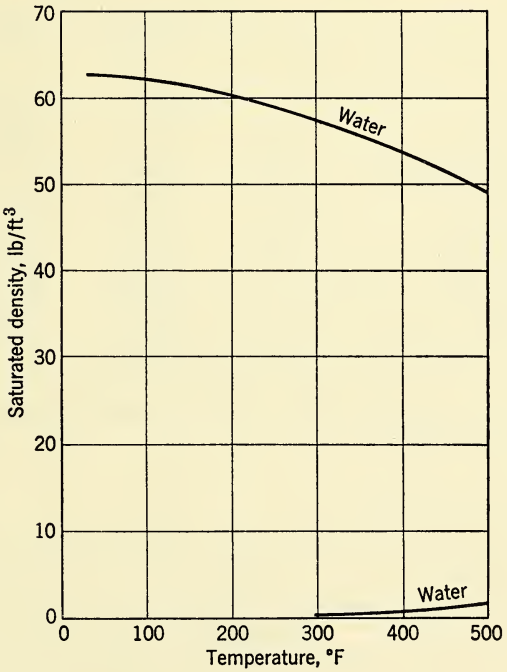

After Figure 544, Appendix, Brown, G. G., et al., *Unit Operations*, John Wiley and Sons, New York (1950).

Appendix 2

DENSITIES OF GASES AT 1 ATM AND 0 °C

Gas	Formula	Molecular Weight	Density, lb/ft^3
Air	—	29*	0.0808
Ammonia	NH_3	17.03	0.0482
Carbon dioxide	CO_2	44.00	0.1235
Chlorine	Cl_2	70.91	0.2011
Hydrogen	H_2	2.016	0.0056
Methane	CH_4	16.03	0.0448
Nitrogen	N_2	28.022	0.0782
Oxygen	O_2	32.00	0.0892
Sulfur dioxide	SO_2	64.06	0.1828

* The volumetric weighted average of the molecular weights of the normal gaseous constituents of air.

Appendix 3

VISCOSITY OF WATER AND OF VARIOUS GASES AS A FUNCTION OF TEMPERATURE AT 1 ATM

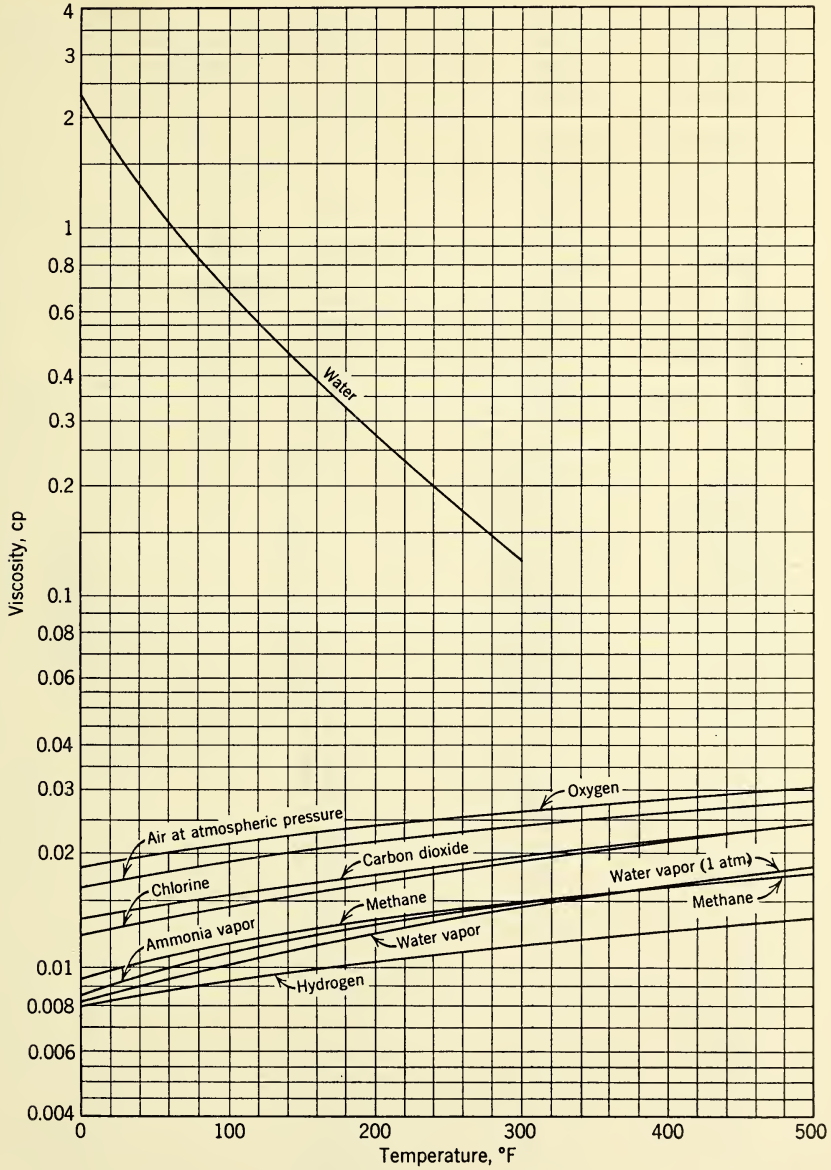

Adapted from Appendix D-9, Foust, A. S., et al., *Principles of Unit Operations*, John Wiley and Sons, New York (1960).

Appendix 4

NOMOGRAPH FOR THE SOLUTION OF HAZEN-WILLIAMS EXPRESSION WHEN $C = 100$

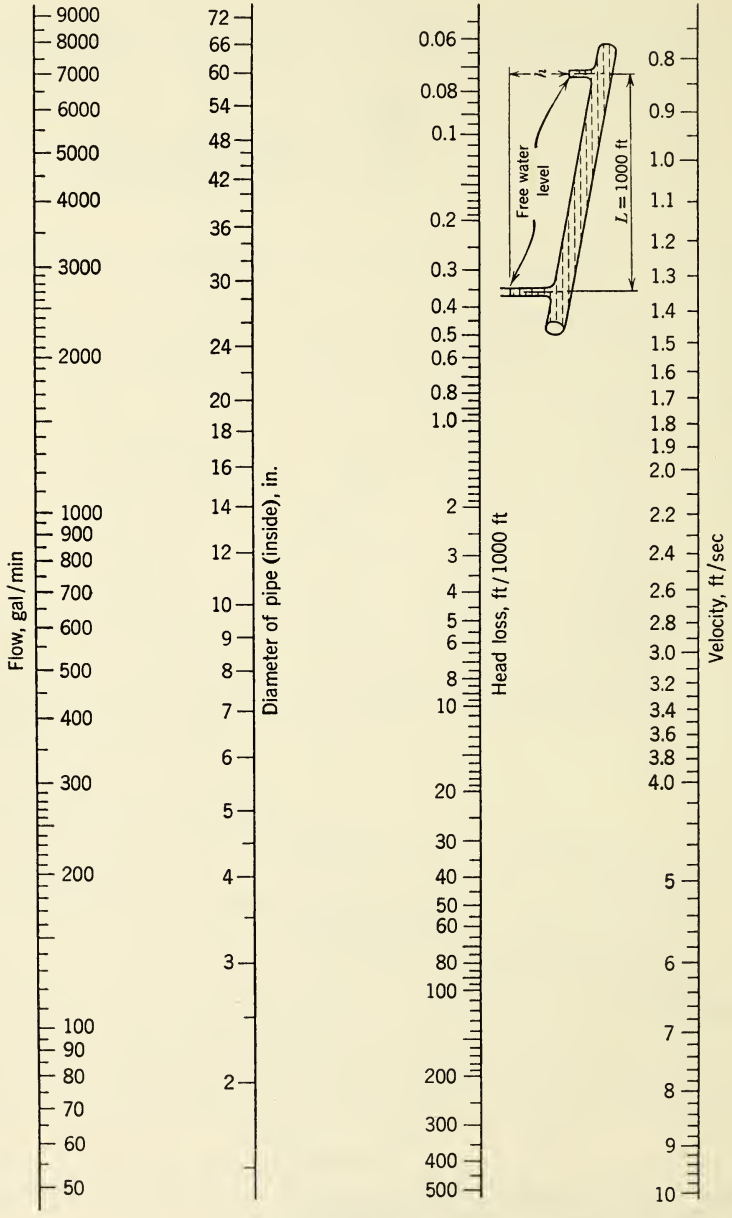

Appendix 5

NOMOGRAPH FOR THE SOLUTION OF THE MANNING FORMULA ($n = 0.013$)

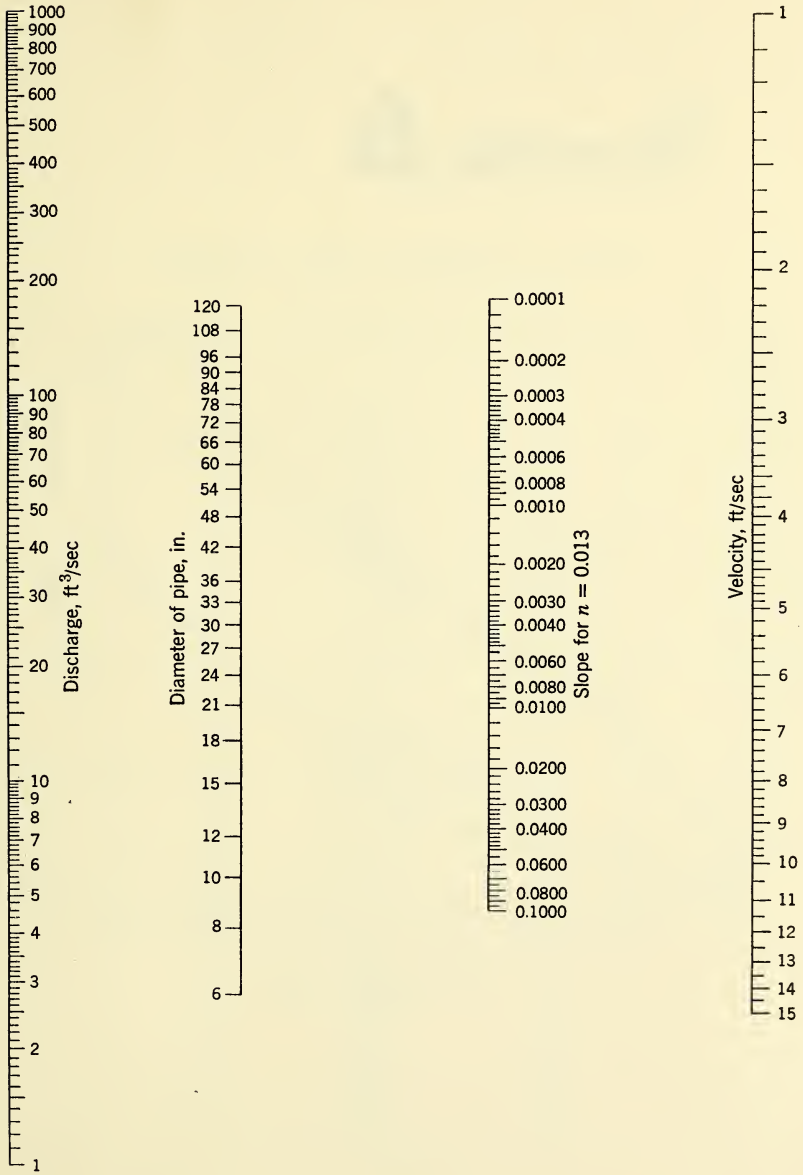

Appendix 6

HYDRAULIC ELEMENTS OF CIRCULAR SECTIONS

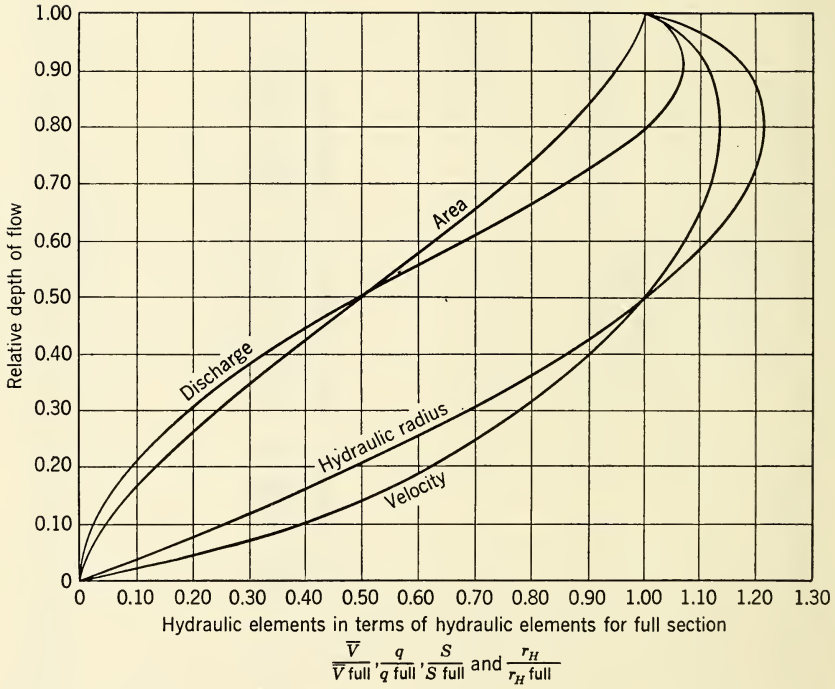

Appendix 7

U.S. SIEVE SERIES

Sieve No.	Sieve Opening, in.	Sieve Opening, mm
4	0.187	4.76
5	0.157	4.00
6	0.132	3.36
7	0.111	2.83
8	0.0937	2.38
10	0.0787	2.00
12	0.0661	1.68
14	0.0555	1.41
16	0.0469	1.19
18	0.0394	1.00
20	0.0331	0.84
25	0.0280	0.71
30	0.0232	0.59
35	0.0197	0.50
40	0.0165	0.42
45	0.0138	0.35
50	0.0117	0.297
60	0.0098	0.250
70	0.0083	0.210
80	0.0070	0.177
100	0.0059	0.149
120	0.0049	0.125
140	0.0041	0.105
170	0.0035	0.088
200	0.0029	0.074

Appendix 8

SOLUBILITY DATA FOR AMMONIA AND SULFUR DIOXIDE IN WATER

Ammonia

Mass NH_3 per 100 Masses H_2O	Partial Pressure NH_3, mm Hg						
	0 °C	10 °C	20 °C	30 °C	40 °C	50 °C	60 °C
100	947						
90	785						
80	636	987					
70	500	780					
60	380	600	945				
50	275	439	686				
40	190	301	470	719			
30	119	190	298	454	692		
25	89.5	144	227	352	534	825	
20	64	103.5	166	260	395	596	834
15	42.7	70.1	114	179	273	405	583
10	25.1	41.8	69.6	110	167	247	361
7.5	17.7	29.9	50.0	79.7	120	179	261
5	11.2	19.1	31.7	51.0	76.5	115	165
4		16.1	24.9	40.1	60.8	91.1	129.2
3		11.3	18.2	29.6	45.0	67.1	94.3
2			12.0	19.3	30.0	44.5	61.0
1					15.4	22.2	30.2

SOLUBILITY DATA FOR AMMONIA AND SULFUR DIOXIDE IN WATER (*Continued*)

Sulfur Dioxide

Mass SO_2 per 100 Masses H_2O	Partial Pressure of SO_2, mm Hg							
	0 °C	7 °C	10 °C	15 °C	20 °C	30 °C	40 °C	50° C
20	646	657						
15	474	637	726					
10	308	417	474	567	698			
7.5	228	307	349	419	517	688		
5.0	148	198	226	270	336	452	665	
2.5	69	92	105	127	161	216	322	458
1.5	38	51	59	71	92	125	186	266
1.0	23.3	31	37	44	59	79	121	172
0.7	15.2	20.6	23.6	28.0	39.0	52	87	116
0.5	9.9	13.5	15.6	19.3	26.0	36	57	82
0.3	5.1	6.9	7.9	10.0	14.1	19.7		
0.1	1.2	1.5	1.75	2.2	3.2	4.7	7.5	12.0
0.05	0.6	0.7	0.75	0.8	1.2	1.7	2.8	4.7
0.02	0.25	0.3	0.3	0.3	0.5	0.6	0.8	1.3

From Sherwood, T. K., *Ind. Eng. Chem.*, **17** (1925), 745.

Appendix 9

SPECIFIC HEATS OF GASES, (BTU)/(LB)(°F)

Temperature, °F.	Air	H_2	O_2	N_2	CO	CO_2	H_2O Vapor
0	0.239	3.364	0.218	0.248	0.248	0.190	0.443
32	0.240	3.390	0.218	0.248	0.248	0.195	0.444
50	0.240	3.395	0.219	0.248	0.248	0.197	0.445
100	0.240	3.425	0.220	0.248	0.249	0.205	0.446
150	0.241	3.437	0.221	0.248	0.249	0.211	0.448
200	0.241	3.449	0.222	0.249	0.249	0.217	0.450
250	0.242	3.455	0.224	0.249	0.250	0.222	0.454
300	0.243	3.461	0.226	0.250	0.251	0.228	0.457
350	0.244	3.464	0.228	0.250	0.252	0.233	0.460
400	0.245	3.466	0.230	0.251	0.253	0.238	0.464
450	0.246	3.468	0.232	0.252	0.254	0.243	0.468
500	0.247	3.469	0.234	0.254	0.256	0.247	0.471

From *Natl. Bur. Standards Circular 461C* (1947), 298. Figures for air calculated from Table 2.10, *NBS-NACA Tables of Thermal Properties of Gases* (1949).

Appendix 10

DRY SATURATED STEAM: TEMPERATURE TABLE

Temperature T, °F.	Absolute Pressure p, lb/in.^{2}	Specific Volume, ft^3/lb: Saturated Liquid, v_f	Specific Volume, ft^3/lb: Evaporation, v_{fg}	Specific Volume, ft^3/lb: Saturated Vapor, v_g	Enthalpy, Btu/lb: Saturated Liquid, i_f	Enthalpy, Btu/lb: Evaporation, i_{fg}	Enthalpy, Btu/lb: Saturated Vapor, i_g
32	0.08854	0.01602	3306	3306	0.00	1075.8	1075.8
35	0.09995	0.01602	2947	2947	3.02	1074.1	1077.1
40	0.12170	0.01602	2444	2444	8.05	1071.3	1079.3
45	0.14752	0.01602	2036.4	2036.4	13.06	1068.4	1081.5
50	0.17811	0.01603	1703.2	1703.2	18.07	1065.6	1083.7
60	0.2563	0.01604	1206.6	1206.7	28.06	1059.9	1088.0
70	0.3631	0.01606	867.8	867.9	38.04	1054.3	1092.3
80	0.5069	0.01608	633.1	633.1	48.02	1048.6	1096.6
90	0.6982	0.01610	468.0	468.0	57.99	1042.9	1100.9
100	0.9492	0.01613	350.3	350.4	67.97	1037.2	1105.2
110	1.2748	0.01617	265.3	265.4	77.94	1031.6	1109.5
120	1.6924	0.01620	203.25	203.27	87.92	1025.8	1113.7
130	2.2225	0.01625	157.32	157.34	97.90	1020.0	1117.9
140	2.8886	0.01629	122.99	123.01	107.89	1014.1	1122.0
150	3.718	0.01634	97.06	97.07	117.89	1008.2	1126.1
160	4.741	0.01639	77.27	77.29	127.89	1002.3	1130.2
170	5.992	0.01645	62.04	62.06	137.90	996.3	1134.2
180	7.510	0.01651	50.21	50.23	147.92	990.2	1138.1
190	9.339	0.01657	40.94	40.96	157.95	984.1	1142.0
200	11.526	0.01663	33.62	33.64	167.99	977.9	1145.9
210	14.123	0.01670	27.80	27.82	178.05	971.6	1149.7
212	14.696	0.01672	26.78	26.80	180.07	970.3	1150.4
220	17.186	0.01677	23.13	23.15	188.13	965.2	1153.4
230	20.780	0.01684	19.365	19.382	198.23	958.8	1157.0
240	24.969	0.01692	16.306	16.323	208.34	952.2	1160.5
250	29.825	0.01700	13.804	13.821	218.48	945.5	1164.0
260	35.429	0.01709	11.746	11.763	228.64	938.7	1167.3
270	41.858	0.01717	10.044	10.061	238.84	931.8	1170.6
280	49.203	0.01726	8.628	8.645	249.06	924.7	1173.8
290	57.556	0.01735	7.444	7.461	259.31	917.5	1176.8
300	67.013	0.01745	6.449	6.466	269.59	910.1	1179.7
310	77.68	0.01755	5.609	5.626	279.92	902.6	1182.5
320	89.66	0.01765	4.896	4.914	290.28	894.9	1185.2
330	103.06	0.01776	4.289	4.307	300.68	887.0	1187.7
340	118.01	0.01787	3.770	3.788	311.13	879.0	1190.1
350	134.63	0.01799	3.324	3.342	321.63	870.7	1192.3
360	153.04	0.01811	2.939	2.957	332.18	862.2	1194.4
370	173.37	0.01823	2.606	2.625	342.79	853.5	1196.3
380	195.77	0.01836	2.317	2.335	353.45	844.6	1198.1
390	220.37	0.01850	2.0651	2.0836	364.17	835.4	1199.6
400	247.31	0.01864	1.8447	1.8633	374.97	826.0	1201.0
410	276.75	0.01878	1.6512	1.6700	385.83	816.3	1202.1
420	308.83	0.01894	1.4811	1.5000	396.77	806.3	1203.1
430	343.72	0.01910	1.3308	1.3499	407.79	796.0	1203.8
440	381.59	0.01926	1.1979	1.2171	418.90	785.4	1204.3
450	422.6	0.0194	1.0799	1.0993	430.1	774.5	1204.6
460	466.9	0.0196	0.9748	0.9944	441.4	763.2	1204.6
470	514.7	0.0198	0.8811	0.9009	452.8	751.5	1204.3
480	566.1	0.0200	0.7972	0.8172	464.4	739.4	1203.7
490	621.4	0.0202	0.7221	0.7423	476.0	726.8	1202.8
500	680.8	0.0204	0.6545	0.6749	487.8	713.9	1201.7
520	812.4	0.0209	0.5385	0.5594	511.9	686.4	1198.2
540	962.5	0.0215	0.4434	0.4649	536.6	656.6	1193.2
560	1133.1	0.0221	0.3647	0.3868	562.2	624.2	1186.4
580	1325.8	0.0228	0.2989	0.3217	588.9	588.4	1177.3
600	1542.9	0.0236	0.2432	0.2668	617.0	548.5	1165.5
620	1786.6	0.0247	0.1955	0.2201	646.7	503.6	1150.3
640	2059.7	0.0260	0.1538	0.1798	678.6	452.0	1130.5
660	2365.4	0.0278	0.1165	0.1442	714.2	390.2	1104.4
680	2708.1	0.0305	0.0810	0.1115	757.3	309.9	1067.2
700	3093.7	0.0369	0.0392	0.0761	823.3	172.1	995.4
705.4	3206.2	0.0503	0	0.0503	902.7	0	902.7

Adapted from Keenan, J. H., and F. G. Keyes, *Thermodynamic Properties of Steam*, John Wiley and Sons, New York (1936).

Appendix 11

DRY SATURATED STEAM: PRESSURE TABLE

Absolute Pressure p, lb/in.^{2}	Temperature T, °F.	Specific Volume, ft^3/lb		Enthalpy, Btu/lb		
		Saturated Liquid, v_f	Saturated Vapor, v_g	Saturated Liquid, i_f	Evaporation, i_{fg}	Saturated Vapor, i_g
0.491	79.03	0.01608	652.3	47.05	1049.2	1096.3
0.736	91.72	0.01611	444.9	59.71	1042.0	1101.7
0.982	101.14	0.01614	339.2	69.10	1036.6	1105.7
1.227	108.71	0.01616	274.9	76.65	1032.3	1108.9
1.473	115.06	0.01618	231.6	82.99	1028.6	1111.6
1.964	125.43	0.01622	176.7	93.34	1022.7	1116.0
2.455	133.76	0.01626	143.25	101.66	1017.7	1119.4
5	162.24	0.01640	73.52	130.13	1001.0	1131.1
10	193.21	0.01659	38.42	161.17	982.1	1143.3
14.696	212.0	0.01672	26.80	180.07	970.3	1150.4
15	213.03	0.01672	26.29	181.11	969.7	1150.8
16	216.32	0.01674	24.75	184.42	967.6	1152.0
18	222.41	0.01679	22.17	190.56	963.6	1154.2
20	227.96	0.01683	20.089	196.16	960.1	1156.3
25	240.07	0.01692	16.303	208.42	952.1	1160.6
30	250.33	0.01701	13.746	218.82	945.3	1164.1
35	259.28	0.01708	11.898	227.91	939.2	1167.1
40	267.25	0.01715	10.498	236.03	933.7	1169.7
45	274.44	0.01721	9.401	243.36	928.6	1172.0
50	281.01	0.01727	8.515	250.09	924.0	1174.1
55	287.07	0.01732	7.787	256.30	919.6	1175.9
60	292.71	0.01738	7.175	262.09	915.5	1177.6
65	297.97	0.01743	6.655	267.50	911.6	1179.1
70	302.92	0.01748	6.206	272.61	907.9	1180.6
75	307.60	0.01753	5.816	277.43	904.5	1181.9
80	312.03	0.01757	5.472	282.02	901.1	1183.1
85	316.25	0.01761	5.168	286.39	897.8	1184.2
90	320.27	0.01766	4.896	290.56	894.7	1185.3
100	327.81	0.01774	4.432	298.40	888.8	1187.2
110	334.77	0.01782	4.049	305.66	883.2	1188.9
120	341.25	0.01789	3.728	312.44	877.9	1190.4
130	347.32	0.01796	3.455	318.81	872.9	1191.7
140	353.02	0.01802	3.220	324.82	868.2	1193.0
150	358.42	0.01809	3.015	330.51	863.6	1194.1
160	363.53	0.01815	2.834	335.93	859.2	1195.1
170	368.41	0.01822	2.675	341.09	854.9	1196.0
180	373.06	0.01827	2.532	346.03	850.8	1196.9
190	377.51	0.01833	2.404	350.79	846.8	1197.6
200	381.79	0.01839	2.288	355.36	843.0	1198.4
250	400.95	0.01865	1.8438	376.00	825.1	1201.1
300	417.33	0.01890	1.5433	393.84	809.0	1202.8
350	431.72	0.01913	1.3260	409.69	794.2	1203.9
400	444.59	0.0193	1.1613	424.0	780.5	1204.5
450	456.28	0.0195	1.0320	437.2	767.4	1204.6
500	467.01	0.0197	0.9278	449.4	755.0	1204.4
550	476.94	0.0199	0.8424	460.8	743.1	1203.9
600	486.21	0.0201	0.7698	471.6	731.6	1230.2
650	494.90	0.0203	0.7083	481.8	720.5	1202.3
700	503.10	0.0205	0.6554	491.5	709.7	1201.2
750	510.86	0.0207	0.6092	500.8	699.2	1200.0
800	518.23	0.0209	0.5687	509.7	688.9	1198.6
850	525.26	0.0210	0.5327	518.3	678.8	1197.1
900	531.98	0.0212	0.5006	526.6	668.8	1195.4
950	538.43	0.0214	0.4717	534.6	659.1	1193.7
1000	544.61	0.0216	0.4456	542.4	649.4	1191.8
1100	556.31	0.0220	0.4001	557.4	630.4	1187.8
1200	567.22	0.0223	0.3619	571.7	611.7	1183.4
1300	577.46	0.0227	0.3293	585.4	593.2	1178.6
1400	587.10	0.0231	0.3012	598.7	574.7	1173.4
1500	596.23	0.0235	0.2765	611.6	556.3	1167.9
2000	635.82	0.0257	0.1878	671.7	463.4	1135.1
2500	668.13	0.0287	0.1307	730.6	360.5	1091.1
3000	695.36	0.0346	0.0858	802.5	217.8	1020.3
3206.2	705.40	0.0503	0.0503	902.7	0	902.7

Adapted from Keenan, J. H., and F. G. Keyes, *Thermodynamic Properties of Steam*, John Wiley and Sons, New York (1936).

Appendix 12

THERMAL CONDUCTIVITIES

	Temperature, °F.							
	−200°	−100°	0°	100°	200°	300°	400°	500°
Metals								
Copper	245	228	224	220	218	215	212	210
Aluminum		112	114	117	119	122	128	130
Brass (70-30)		54	56	57.2	59	61	63	65
Nickel		37.6	36.5	35.4	34.5	34.0	33.0	32.0
Mild steel		27.0	26.6	26.2	26.0	25.7	25.5	25.2
Stainless steel (304)		7.7	8.1	8.55	9.0	9.5	10.0	10.4
Insulating Materials								
Fir plywood								
17% moisture		0.062	0.069	0.076	0.083			
0% moisture		0.047	0.053	0.060	0.067			
Cork board								
12.2 lb/ft^3		0.021	0.0235	0.026	0.0285			
6.5 lb/ft^3		0.018	0.020	0.022	0.024			
Asbestos fiber, 36 lb/ft^3			0.082	0.097	0.11	0.115	0.12	0.125
Glass fiber								
9 lb/ft^3			0.010	0.011	0.020	0.023	0.031	0.043
3 lb/ft^3			0.013	0.015	0.025	0.035	0.047	0.065
Cellular Glass								
Density, 10 lb/ft^3		0.019	0.028	0.038	0.042	0.046	0.050	0.055
Mineral wool (Zerolite)								
Density, 15 lb/ft^3		0.016	0.021	0.024	0.028	0.032	0.035	0.038
Magnesia (85%)			0.036	0.039	0.041	0.043	0.046	0.049
Equivalent conductivity of 1-in. air gap								
Between materials of ordinary emissivity		0.052	0.078	0.104	0.130			
With aluminum on warm side		0.037	0.038	0.039	0.041			

THERMAL CONDUCTIVITIES (*Continued*)

	Temperature, °F.							
	−200°	−100°	0°	100°	200°	300°	400°	500°
Liquids								
Water (liquid)			0.298	0.350	0.402	0.470		
Ammonia (liquid)			0.290	0.290	0.290			
Carbon tetrachloride			0.098	0.086	0.074			
Acetone			0.108	0.103	0.0975			
Gasoline			0.091	0.089	0.085	0.082	0.080	
37° API distillate			0.082	0.079	0.076	0.075	0.072	
SAE 10 lube oil (21° API)			0.074	0.071	0.068	0.066	0.064	
Ethylalcohol (100%)			0.109	0.103	0.0983			
Benzene			0.10	0.09	0.08			
n-Pentane			0.083	0.0775	0.072			
Gases								
Air	0.006	0.0089	0.0108	0.0141	0.0162	0.0181	0.0197	0.0211
Ammonia		0.0088	0.0118	0.0150	0.0185	0.0215	0.025	0.029
Carbon dioxide		0.0057	0.007	0.0085	0.01	0.0126	0.0135	0.0156
Chlorine				0.0049	0.0061	0.0075		
Hydrogen		0.072	0.095	0.113	0.127	0.14	0.153	0.168
Methane	0.0080	0.0125	0.0165	0.0205	0.025	0.0295	0.0347	0.0398
Oxygen	0.0074	0.011	0.0126	0.0149	0.0171	0.019	0.0206	0.0221
Propane			0.0076	0.0105	0.0146	0.0190	0.024	0.029
n-Pentane			0.0066	0.0093	0.0125	0.0160	0.0198	0.024
Water vapor				0.0115	0.0140	0.0165	0.0192	0.0225

Refractory and Insulating Materials	Density, lb/ft^3	0°	500°	1000°	1500°	2000°
Brick						
30% Chromia	200	0.56	0.70	0.81	0.89	0.96
Fire brick	125–130	0.47	0.55	0.66	0.76	0.86
Missouri fire clay			0.64	0.82	0.91	0.97
Castable refractory						
Aluminum silicate base	110	0.24	0.28	0.31	0.34	0.38
Lightweight silicate base	75	0.13	0.13	0.15	0.15	0.16
Diatomaceous earth						
Molded brick	40	0.13	0.14	0.16	0.18	0.19
Natural brick	28	0.07	0.08	0.10	0.11	0.12
Powder	17	0.035	0.05	0.06	0.07	0.08

From Brown, G. G., *Unit Operations*, John Wiley and Sons, New York (1950).

Appendix 13

CHARACTERISTICS OF TUBING

OD Tubing, in.	Thickness: Birmingham Wire Gage	Thickness: In.	Internal Transverse Area, in.^{2}	External Surface, ft^2/ft length	Internal Surface, ft^2/ft length	Brass, lb/ft length	Copper, lb/ft length	Steel, lb/ft length	ID Tubing, in.	Constant, C *	$\frac{OD}{ID}$	Metal Area (Transverse Metal Area), in.^{2}
3/8	16	0.065	0.0471	0.0982	0.0641	0.233	0.245	0.218	0.2450	74	1.530	0.063
3/8	20	0.035	0.0731	0.0982	0.0799	0.149	0.156	0.139	0.3050	114	1.230	0.040
9/16	21	0.032	0.1952	0.1473	0.1304	0.196	0.206	0.183	0.4985	305	1.128	0.053
5/8	12	0.109	0.130	0.1636	0.107	0.649	0.683	0.605	0.407	202	1.53	0.177
5/8	16	0.065	0.1924	0.1636	0.1295	0.420	0.44	0.39	0.495	300	1.26	0.114
5/8	20	0.035	0.2419	0.1636	0.146	0.238	0.25	0.22	0.555	377	1.13	0.0649
3/4	12	0.109	0.223	0.1963	0.14	0.807	0.845	0.75	0.532	348	1.41	0.219
3/4	16	0.065	0.302	0.1963	0.163	0.514	0.54	0.48	0.620	471	1.21	0.140
3/4	20	0.035	0.3632	0.1963	0.179	0.289	0.306	0.267	0.680	567	1.10	0.0786
7/8	10	0.134	0.2890	0.2297	0.158	1.134	1.24	1.06	0.607	451	1.44	0.312
7/8	14	0.083	0.394	0.2297	0.186	0.759	0.798	0.702	0.709	615	1.23	0.207
7/8	18	0.049	0.474	0.2297	0.2034	0.467	0.49	0.432	0.777	740	1.12	0.127
1	10	0.134	0.421	0.2618	0.192	1.34	1.41	1.24	0.732	657	1.37	0.364
1	14	0.083	0.5463	0.2618	0.2183	0.88	0.923	0.813	0.834	852	1.20	0.239
1	18	0.049	0.639	0.2618	0.236	0.54	0.568	0.50	0.902	997	1.11	0.146
1 1/4	10	0.134	0.757	0.3272	0.258	1.73	1.83	1.597	0.982	1180	1.27	0.470
1 1/4	14	0.083	0.923	0.3272	0.284	1.12	1.173	1.04	1.084	1440	1.15	0.304
1 1/4	20	0.035	1.092	0.3272	0.308	0.498	0.521	0.454	1.180	1704	1.06	0.135
1 1/2	10	0.134	1.192	0.3927	0.322	2.12	2.23	1.98	1.232	1860	1.22	0.575
1 1/2	12	0.109	1.291	0.3927	0.335	1.76	1.85	1.64	1.282	2020	1.17	0.476
1 1/2	16	0.065	1.474	0.3927	0.359	1.08	1.13	0.996	1.37	2300	1.10	0.293
2	11	0.12	2.433	0.5236	0.460	2.62	2.76	2.45	1.76	3780	1.14	0.709
2	13	0.095	2.573	0.5236	0.474	2.09	2.20	1.933	1.81	4015	1.10	0.569
2 1/2	9	0.148	3.80	0.654	0.575	4.09	4.30	3.82	2.20	5930	1.14	1.109

Condensed from a table published by the Tubular Exchanger Manufacturers' Association.

* Liquid velocity $= \frac{\text{Pounds/tube/hr}}{C \times \text{sp gr of liquid}}$ ft/sec (sp gr of water at 60 °F = 1.0).

Index

Absolute humidity, 255
Absolute viscosity, 4
Absorption, *see* Gas transfer
Activators, 112
Adiabatic compression exponent, 16
Adiabatic saturation temperature, 257
Adsorption, 208, 209
  towers, 137
Aerator, jet, 179, 180
Aerosols, classification, 119
  equipment for removal, 120–134
  particle characteristics, 118–120
Agitators, *see* Mixing impellers
Air-water contacts, *see* Psychrometry
Ammonia solubility in water, 296
Angle of contact, 111
Annular space, heat transfer in, 227, 228
Apparent coefficient, 246
Apparent temperature drop, 246

Backwashing, *see* Expanded beds
Baffles, 63, 66
Barometric leg, 244
Bernoulli equation, *see* Mechanical energy equation
Black body, 236
Boiling point, effect on heat transfer coefficient, 246, 247
Boundary layer, 3
  around spheres, 85, 86

Carman-Kozeny equation, 137–143
Centimeter-gram-second system, 2
Centrifugal filtration, 159
Centrifugal separators, 121–128
  cut-size, 124, 125
  proportions, 122
  removal efficiencies, 125, 126
Chemisorption, 208
Clarification, definition, 81
  see also Sedimentation
Coefficient, of compressibility, 168
  drag, 83–86
  rigidity, 5–7, 19
Colburn's j_H factor, 227
Collectors, 112
Conduction, *see* Thermal conduction
Contact condensers, 244
Continuous flow models, 52–57
Convection, *see* Thermal convection
Cooling towers, 263–270
Cottrell precipitators, 132
Critical moisture content, 279
Critical velocity, 42, 43
Cyclone separator, *see* Centrifugal separators
Cylinders, heat flow through, 222
  shearing stresses on, 16–18
  target efficiencies for, 130

Dalton's law, 176
Darcy-Weisbach equation, 11–16

Dehumidification, 266
Density, *see* Mass density
Depressants, 112
Depth, conjugate, 43
  critical, 43
Dew point, 257
Diffusivity, 173, 174
Dilatant fluids, 4, 6
Dispensers, gas, 179–188
Dittus-Boelter equation, 226
Double-pipe heat exchanger, 235
Drag coefficient, 83–86
Drag form, 86
Driving force, in gas transfer, 175
  in heat flow, 224
Drum, filters, 159–161
  dryers, 274–277
Dry-bulb temperature, 257
Dry volume, 256
Drying, 274–288
  definition, 274
  design of operations, 283–285
  equipment used in, 274–278
  rates, 278–282
Dühring's rule, 245
Dusts, 118, 119

Eddy viscosity, 9
Effective size of sand grains, 153
Electrostatic precipitators, 131–134
Elutriation, 210
Enthalpy, 219
Entrainments, 118, 119
Equilibrium, lines, 177
  moisture content, 279
  stage, 204–206
Equivalent diameter, 227
Equivalent lengths of valves and fittings, 14, 15
Evaporation, 239–254
Evaporators, ancillary equipment, 244
  capacity requirements, 244–247
  multiple-effect, 248–250
  types, 240–244
Expanded beds, flow through, 146–149
Extraction, solid-liquid, 210

F-diagrams, 53–57
Fanning equation, 11
Film theory, 171–173, 225
Filters, air, 120
Filters, drum, *see* Vacuum filtration
  sand, *see* Sand filters
Filtration, centrifugal, 159
  gravity, 159
  pressure, 157
  vacuum, *see* Vacuum filtration
Flash dryers, 274–278
Floc penetration in sand filters, 157
Flocculation, 77–79
Flocculators, 61, 79
Flotation, 110–117
  chemical agents used in, 112
  design of operations, 116, 117
  dissolved-air, 113
  gas-particle contact, 111
  methods, 110, 111
Flow equalization, 26–29
Flow, in open channels, 32–59
  in pipes, 1–31
Fluid classification, 4
  regimes, 66, 67
Foot-pound-second system, 2
Force-units, 2
Form drag, 86
Fourier's law, 220, 221
Friction factor, for beds of solids, 139, 144
  correlation with heat transfer coefficient, 227
  in open channel flow, 35
  in pipe flow, 11–15
  in vacuum filtration, 163
Friction losses, in beds of dry solids, 139–145
  in beds of irrigated solids, 140
  for compressible fluids, 15, 16
  through expanded beds of solids, 148
  in open channels, 33–37
  in pipes, 11–22, 26–29
  for plastic liquids, 18–20
  through porous plates, 151, 152
  through vacuum filters, 163
Frothers, 112
Froude number, 24
  in mixing, 67–69

Gas transfer, 171–207
  with dispersers, 179–188
  equilibrium relationships in, 175, 176
  equipment used in, 179–181
  film coefficients, 173

Gas transfer, mechanism, 171
over-all coefficients, 177–179
in packed columns, 188–204
in tray columns, 204–206
with turbine mixers, 75
Gravity settlers, 120, 121
Groups, dimensionless, 184, 185, 226

Hagen-Poiseuille equation, 16–20
Hazen-Williams equation, 20–22
nomograph for, 292
Heat capacity, 219
Heat exchangers, 234–236
Heat transfer, 218–238
applications, 218
coefficients, 72, 226–229
across compound barriers, 223, 224
by conduction, 220–223
by convection, 224–226
heat balances, 218, 219
by radiation, 236, 237
variable temperature gradients, 232–234
Height of transfer unit, 196
Henry's law, 175
Hindered settling, 98
Howard settler, 120, 121
Humid heat, 256
Humid volume, 256
Humidification, 263–273
in adiabatic humidifiers, 270, 271
in water coolers, 263–267
Humidity, *see* Absolute humidity
Hydraulic elements, chart of, 294
Hydraulic jump, 44–47
Hydraulic radius, 15

Ideal contact stages, 210
Impellers, *see* Mixing impellers
Impingement, aerator, 179, 180
separators, 128–131
target efficiencies for, 130
Ion exchange, 208
units for, 137

j_H factor, Colburn's, 227
Jet aerator, 179, 180

Kinematic eddy viscosity, 9
Kozeny equation, *see* Carman-Kozeny equation

Laminar flow, in open channels, 33–35
in pipes, 3–7
Laminar sublayer, 3, 4, 224
Latent heat, 219
Launders, 49
Leaching, 210–217
calculations, 212, 213
definition, 210
dispersed contact, 210, 211
graphical solution for, 215–217
Limiting moisture content, 6
Limiting velocities, in open channels, 38–40
in pipes, 23–25
Logarithmic mean temperature difference, 233, 234

Manning equation, 37
coefficients for, 37
nomograph for, 293
Mass density, 2
of gases, 290
of suspensions, 24
of water, 289
Mass transfer coefficients, 75, 174–178, 261–265, 280, 281
over-all, 182–187, 265
Mass transfer operations, 171
Mechanical energy equation, for closed conduits, 10
for open channels, 32
Mists, 118, 119
Mixing, 60–80
baffles, 63–66
definition of, 60
flocculation, 77–79
fluid regimes in, 66, 67
gas transfer by, 75, 76
impellers, 60–63
Moisture, in drying, 278–280
Mole fraction, 175
Moody diagram, 11, 12

Newtonian fluids, 4, 5
Newton's law, 2, 86, 225
conversion factor, 2
Nonuniform flow, 32
Nusselt number, 226

Operating lines, 188–190
Over-all coefficients, *see* Heat transfer co-

efficients; Mass transfer coefficients, over-all

Packed columns, 188–204
flooding velocities in, 201–203
friction losses in, 201–203
operating lines for, 188–190
packing in, 203
transfer unit for, 194–198
Paddles, *see* Mixing impellers
Paragenesis diagram, 82
Penetration theory, 171, 172
Percentage humidity, 256
Permeability, 163
rating, 152
Plastic fluids, 4–6
Plug flow model, 52–57
Poiseuille, *see* Hagen-Poiseuille equation
Porosity, 138, 148, 149
Porous plates, 152, 153
permeability rating of, 152
Poundals, 2
Power curves, 67–70
Power number, 67–69
Prandtl, boundary layer, 3
mixing length, 9
number, 226, 227
Pressure drop, *see* Friction losses
Probability curves, 56
Promoters, 112
Propellers, *see* Mixing impellers
Pseudoplastic fluids, 4, 6
Psychrometric ratio, 263
Psychrometry, 255–263
adiabatic cooling, 262, 263
definition, 255
wet-bulb theory, 260–262

Radiation, *see* Thermal radiation
Rapid flow, 41
Rapid sand filters, *see* Sand filters
Relative humidity, 256
Reynolds number, in mixing, 67–69
in pipe flow, 11
Reynolds number correlation, with drag coefficient, 85, 144
with friction factor, 139, 163
with heat transfer coefficients, 72, 226
with mass transfer coefficient, 184, 185
with power function, 68
Rheology, 5–7
Rheopectic fluids, 7
Rose equation, 143–146
Rotary dryers, 274–277
Roughness, absolute, 15
coefficients, 37
relative, 13, 15

Sand filters, floc penetration in, 157
piping arrangement for, 155, 156
rapid, 136, 152–157
slow, 137
wash water gutters in, 154
Saturation humidity, 256
Saturated volume, 256
Scale-up, in mixing operations, 70–74
Schmidt number, 184, 185
Scrubbers, 134
Sedimentation, 81–109
class-1, 82–89
class-2, 91–93
compression, 101, 106
continuous flow in, 107, 108
definition, 81
equipment, 102–107
in ideal basins, 107, 108
types, 81, 82
Sensible heat, 218, 219
Settling, analyses, 88–92
regimes, 81, 82
Shape factors, 141
Shear stresses, in open channels, 36
in pipes, 3–5, 8, 9
Sherwood number, 184, 185
Short weir channels, 49–52
Sieve openings, 295
Similitude, 71
Skin friction, 84
Sludge compression, 101, 106
Solubility in water, of ammonia, 296
of sulfur dioxide, 297
Specific energy, 40–44
Specific gravity, 2
of sewage sludges, 19
Specific heat, 219
of gases, 298
Specific resistance, 164–168
Specific volume, 256
Specific weight, 2
Spray units, 170, 171, 181, 184

Stanton number, 227
Steady flow, 32
Steam tables, 299, 300
Stefan-Boltzman constant, 236
Stokes law, 84–86
  correction factors for, 134
Sulfur dioxide solubility in water, 297
Superficial gas velocity, 76
Surface profiles, 46, 47

Target efficiencies, 130
Temperature drops, 245
Temperature-length curves, 232
Thermal, conduction, 220–223
  conductivities, 301, 302
  convection, 224–226
  radiation, 236, 237
Thickening, capacity, 95–100
  definition, 81
Thixotropic fluids, 7
Transfer unit, 194–198
Tranquil flow, 41
Tray columns, 204–206
Tubing characteristics, 303
Turbines, 62, 180

Uniform flow, 32
Uniformity coefficient, 153
Unit area, 100
Universal constant, 9
Unsteady flow, 32

Vacuum filtration, 159–169
  equipment in, 159–162
  yields in, 161–166
Vacuum flotation, 113
Velocity, critical, 42, 43
  gradients, 3, 4
  limiting, *see* Limiting velocities
  profiles, 3
  terminal, 84
Viscosity, 4
  of water and gases, 291

Wash-water gutter, 49, 154
Water, properties of, 290, 291
Water coolers, 263–270
Wet-bulb temperature, 257

Yield stress, 5, 6, 19
  variation with moisture, 6

03514

Date Due

Due	Returned	Due	Returned
JUN 12 1970	JUN 10 '70		
APR 19 '71			
MAY 10 '71	MAY 11 '71		
NOV 25 '76	NOV 30 '76		
DEC 10 '76	DEC 8 '76		
NOV 21 '77	NOV 21 '77		

UNIVERSITY OF FLORIDA
GENESYS LIBRARY

628
R498un

Engineering
& Physics
Library

Unit operations of sanitar UGE
628 R498un

3 1262 01109 6707

Date Due

DUE	RETURNED	DUE	RETURNED

KEEP CARD IN POCKET